Dynamics of CD8+, CD4+ T cells, and Myeloid-Derived Suppressor Cells in Late-Stage Melanoma Patients

Dissertation

der Mathematisch-Naturwissenschaftlichen Fakultät

der Eberhard Karls Universität Tübingen

zur Erlangung des Grades eines

Doktors der Naturwissenschaften

(Dr. rer. nat.)

vorgelegt von

M.Sc. Andrea Gaißler

aus Ellwangen (Jagst)

Tübingen

2024

Gedruckt mit Genehmigung der Mathematisch-Naturwissenschaftlichen Fakultät der Eberhard Karls Universität Tübingen.

Tag der mündlichen Qualifikation:	03.07.2024
Dekan:	Prof. Dr. Thilo Stehle
1. Berichterstatter/-in:	PD Dr. Kilian Wistuba-Hamprecht
2. Berichterstatter/-in:	Prof. Dr. Hans-Georg Rammensee

Acknowledgments

I am extremely grateful for the opportunity to write a dissertation and obtain a doctorate. First and foremost, I would like to thank Kilian Wistuba-Hamprecht for giving me the chance to gain my doctorate in his group and to obtain more knowledge in the field of immunology and cancer research. Thank you for your great advice, expertise, and patience.

Special thanks to my colleagues Nicola Herold, Janine Spreuer, and Jonas Bochem, for all the great input, thoughts, support and laughter. Without you, this experience would not be the same and less memorable.

Then I would like to thank Graham Pawelec and Manfred Claassen for their advice and expertise throughout this thesis and manuscript preparation and Hans-Georg Rammensee for being my second advisor.

Last but not least, I would like to thank my friends and family for staying with me and supporting me throughout the whole time. Especially to Maiky & Moni: You make my days even brighter - without you, I wouldn’t have made it.

Table of Contents

1. Abbreviations

AJCC	American joint committee on cancer
APC	Antigen-presenting cell
CD	Cluster of differentiation
CNS	Central nervous system
CTA	Cancer testis antigen
CTLA	Cytotoxic T-lymphocyte–associated antigen
DC	Dendritic cell
DNA	Desoxy ribonucleic acid
E-MDSC	Early MDSC
Eo-MDSC	Eosinophilic MDSC
FDA	Food and Drug Administration
F-MDSC	Fibrocytic MDSC
FOXP3	Forkhead-Box-Protein
GM-CSF	Granulocyte-macrophage colony-stimulating factor
HLA	Human lymphocyte antigen
ICB	Immune checkpoint blockade
IL	Interleukin
IFN	Interferon
LAG-3	Lymphocyte activation gene
LAMP-1	Lysosomal-associated membrane protein-1
LDH	Lactate dehydrogenase
MAE	Melanoma-associated epitope
MAGE	Melanoma Antigen Gene
MDSC	Myeloid-derived suppressor cells
MHC	Major histocompatibility complex
mm	Millimeter
M-MDSC	Monocytic MDSC
MO	Microorganism
NK	Natural killer
NLR	Neutrophil-lymphocyte ratio
NO	Nitric oxide
OS	Overall survival
PD-1	Programmed death receptor
PD-L	Programmed death receptor ligand
PFS	Progression-free survival
pMHC	Peptide-loaded major histocompatibility complex
PMN-MDSC	Polymorphonuclear MDSC
RNA	Ribonucleic acid

ROS	Reactive oxygen species
STEAP	Six transmembrane epithelial antigen of the prostate
TAA	Tumor-associated antigen
TAP	Transporter associated with antigen processing
TCR	T cell receptor
TGF	Tumor growth factor
TIL	Tumor-infiltrating lymphocytes
TIM-3	T cell immunoglobulin and mucin domain 3
TME	Tumor microenvironment
TNF	Tumor necrosis factor
TNM	Thickness, Nodes, Metastases
TRP	Tyrosinase Related Protein

2. Abstract

Melanoma is the most fatal form of skin cancer with a continuously rising incidence. Melanomas have a high mutational load and therefore immune checkpoint blockade (ICB) is particularly suitable as a therapy. Although the approval of ICB has helped many patients and prolonged their lives approximately 50% still die of their cancer. ICB comprises monoclonal antagonistic antibodies against the immune checkpoint PD-1 and CTLA-4. The potential binding of these antibodies to exhausted T cells aims to prevent inhibition of the T cell response after antigen recognition.

This thesis addresses multiple aspects in three studies. The first two studies cover the dynamics and specificities of melanoma-associated peripheral CD8+ T cells and the dynamics and functionality of melanoma-associated antigen-reactive peripheral CD4+ T cells in melanoma patients under therapy. It was shown that the disappearance of 3 melanoma-associated epitope-specific CD8+ T cell populations early under PD-1 inhibition correlated with short overall survival. In contrast, the disappearance of multifunctional CD4+ T cells correlated with longer survival, compared with patients who showed an increase or stable detection of these populations. The results of these two studies deliver complementary insights into cancer rejection under ICB. This leads to the assumption that not all melanoma-associated T cells that are present are functionally active and that different T cell populations might work together in a complex network.

The third study of this thesis investigated M-MDSC frequencies in melanoma patients under ICB, as they are known to inhibit T cell response and thereby promote tumor growth. To thee best of our knowledge for the first time we reported, that a decreasing M-MDSC frequency under therapy correlated with longer survival compared to an increasing or stable frequency. M-MDSCs are discussed as a potential biomarker. Our

research shows, that some patients still benefit from ICB, even though they were previously classified as poor survivors.

The results of this thesis could aid in finding new therapeutic targets, for example in new vaccination strategies or M-MDSC targeted therapies.

3. Zusammenfassung

Das Melanom ist die tödlichste Form von Hautkrebs, Inzidenz steigend. Melanome weisen eine hohe Mutationslast auf, weshalb sich die Immun-Checkpoint-Blockade (ICB) besonders gut als Therapie eignet. Obwohl die Zulassung von ICB vielen Patienten und Patientinnen geholfen, ihr Leben verlängert hat sterben noch immer etwa 50 % der Patienten und Patientinnen an Krebs und dessen folgen. ICB umfasst unter anderem, monoklonalen antagonistischen Antikörpern gegen die Immun-Checkpoints PD-1 und CTLA-4. Diese Antikörper zielen mutmaßlich darauf ab, in erschöpften T-Zellen die Inhibierung der T-Zell-Antwort nach der Antigenerkennung zu verhindern.

In dieser Doktorarbeit werden mehrere Aspekte in drei Studien behandelt. Die ersten beiden Studien befassen sich mit den Dynamiken und der Spezifität von Melanom-assoziierten peripheren CD8+ T-Zellen sowie mit den Dynamiken und Funktionalitäten von Melanom-assoziierten Antigen-reaktiven peripheren CD4+ T-Zellen bei Melanom Patienten unter Immun-Checkpoint-Blockade. Es konnte gezeigt werden, dass das Verschwinden von 3 Melanom-assoziierten antigenspezifischen CD8+ T-Zell Populationen unter PD-1-Inhibierung frühzeitig mit einem kurzen Gesamtüberleben korreliert. Im Gegensatz dazu korrelierte das Verschwinden von bestimmten multifunktionalen CD4+ T-Zellen mit einem längeren Überleben, verglichen mit Patienten und Patientinnen, die eine Zunahme oder ein stabiles Vorhandensein dieser Populationen zeigten. Die Ergebnisse dieser beiden Studien liefern ergänzende Erkenntnisse über die Krebsabwehr unter ICB. Dies führt zu der Annahme, dass nicht alle vorhandenen Melanom-assoziierten T-Zellen funktionell aktiv sind und dass

verschiedene T-Zell-Populationen in einem komplexen Netzwerk zusammenarbeiten könnten.

Der dritte Teil dieser Doktorarbeit untersuchte M-MDSC-Frequenzen in Melanom-Patienten unter ICB da sie bekanntermaßen die T-Zell-Antwort hemmen und dadurch das Tumorwachstum fördern. Nach bestem Wissen wird zum ersten Mal berichtet, dass eine abnehmende M-MDSC-Frequenz unter Therapie mit einem längeren Überleben korreliert, im Vergleich zu Patienten und Patientinnen mit einer gleichbleibenden oder zunehmenden Frequenz. M-MDSC werden als potenzieller Biomarker diskutiert. Unsere Forschung zeigt, dass einige Patienten von der ICB profitieren, obwohl sie zuvor als schlechte Überlebende eingestuft wurden.
Die Ergebnisse dieser Arbeit könnten dazu beitragen, neue therapeutische Ziele zu finden, z. B. neue Impfstrategien mit Melanom-assoziierten Antigenen oder gezielte M-MDSC-Therapien.

4. List of Publications with contributions

1. **Gaißler A**, Meldgaard TS, Heeke C, Babaei S, Tvingsholm SA, Bochem J, Spreuer J, Amaral T, Wagner NB, Klein R, Meier F, Garbe C, Eigentler TK, Pawelec G, Claassen M, Weide B, Hadrup SR and Wistuba-Hamprecht K. **Dynamics of Melanoma-Associated Epitope-Specific CD8+ T Cells in the Blood Correlate With Clinical Outcome Under PD-1 Blockade.** Front. Immunol. 13:906352 (2022); doi: 10.3389/fimmu.2022.906352

2. **Gaißler A**, Babaei S, Bochem J, Spreuer J, Amaral T, Wagner N B, Claassen M, Weide B, Pawelec G, Eigentler K and Wistuba-Hamprecht K. **Early disappearance of blood derived, multifunctional MAGE-A10 and TRP-2-reactive CD4+ T cells in melanoma under anti-PD-1 checkpoint blockade associate with improved survival.** (Unsubmitted Manuscript)

3. **Gaißler A***, Bochem J*, Spreuer J, Ottman S, Martens A, Amaral T, Wagner N B, Claassen M, Meier F, Terheyden P, Garbe C, Eigentler T, Weide B, Pawelec G and Wistuba-Hamprecht K. **Early decrease of blood myeloid-derived suppressor cells during checkpoint inhibition is a favorable biomarker in metastatic melanoma.** Journal for ImmunoTherapy of Cancer; 11:e006802 2023. doi:10.1136/jitc-2023-006802. * shared authorship

Nr.	**Accepted publication yes/no**	Position of candidate in list of authors	Scientific ideas by the candidate (%)	Data generation by the candidate (%)	Analysis and Interpretation by the candidate (%)	Paper writing done by the candidate (%)
1	yes	1	40	70	80	80
2	no	1	70	85	90	85
3	yes	1*	50	50	60	40

Publications not embedded in this thesis:

1. Bochem J, Zelba H, Spreuer J, Amaral T, **Gaissler A**, Pop O, T, Thiel K, Yurttas C, Soffel D, Forchhammer S, Sinnberg T, Niessner H, Meier F, Terheyden P, Konigsrainer A, Garbe C, Flatz L, Pawelec G, Eigentler T, K, Loffler M, W, Weide B, Wistuba-Hamprecht K. Early disappearance of tumor antigenreactive T cells from peripheral blood correlates with superior clinical outcomes in melanoma under anti-PD-1 therapy. Journal for ImmunoTherapy of Cancer 2021;9:e003439. doi:10.1136/jitc-2021-003439

2. Herold N, Schöllhorn A, Feile A, **Gaißler A**, Mohrholz A, Pawelec G, Löffler MW, Dimitrov S, Gouttefangeas C, Wistuba-Hamprecht K. Integrin activation enables rapid detection of functional Vδ1+ and Vδ2+ γδ T cells (2022). European Journal of Immunology 52(5): 730-736. PMID: 35133647.

6. Introduction

The human body is constantly exposed to environmental influences (e.g. UV exposure) and pathogens. The immune system helps to protect the body from such influences and pathogens. When the immune system is defective and can't eliminate damaged cells, serious chronic diseases such as cancer might manifest. The immune system is usually categorized by the type of detected structures. Innate immunity recognizes conserved structures and patterns, for example on the surface of bacteria. Adaptive immunity "learns" to recognize new or adapted pathogens as well as malfunctioning cells via various mechanisms. Subsequently, it "remembers" previous interactions – resulting in a long-lasting immunity. This enables the body to protect itself against new dangers in the form of pathogens in a flexible manner. Furthermore, the adaptive immune system is able to recognize malfunctioning cells before a tumor develops. If malignant cells develop escape mechanisms or if the immune system is weakened or defective, a tumor can develop from degenerate cells. In this thesis, T cells, an essential compartment of adaptive immunity were studied in more detail, in the first paper of this thesis (chapter 8.1) MHC-I bound peptides, that could be recognized by CD8+ T cells were explored. The second paper of this thesis (chapter 8.2) investigated the (multi-)functionality of tumor-associated antigen (TAA) reactive CD4+ T cells. Additionally, the third paper of this thesis (chapter 8.3) investigated inhibitory cell populations such as myeloid-derived suppressor cells (MDSC) were investigated in melanoma patients under PD-1 checkpoint blockade.

6.1. Peripheral T cells and their regulators

6.1.1. (Tumor-associated) T cells

The αβ T cells are part of the adaptive immune system and detect (tissue) foreign, overexpressed, or mutated peptides through their T cell receptor (TCR). The TCR consists of two chains, α and β. These chains are expressed on the surface of T cells. αβ T cells can be divided into two major subsets, defined by their accessory molecules: CD4+ and CD8+ T cells. TCRs can bind peptide-loaded major histocompatibility complex (MHC) molecules on the surface of the target cell. CD8 dimers bind to MHC-I and CD4 monomers to MHC-II molecules. Human MHC molecules are encoded by the human leucocyte antigen (HLA) genes and these genes are highly polymorphic[1].

CD4+ T cells are often referred to as “T-helper cells” (T_h) because, upon TCR stimulation they produce and secrete cytokines that interact with other cells, for example, B-cells or dendritic cells (DC)[2]. CD4+ T cells can differentiate into several different effector subsets (e. g. T_h1, T_h2, T_h17, Tregs, or T_{FH})[3], depending on the signals of the microenvironment e.g. cytokines. Furthermore, the release of cytokines like interferon (IFN)-γ, tumor necrosis factor (TNF)-α, or granzyme B show target-eliminating properties, similar to CD8+ T cells[3 4]. CD8+ T cells, commonly referred to as “cytotoxic T cells”, produce effector molecules like perforin, granzyme B, and TNF-α to directly eliminate infected or mutated cells. In the cancer setting, mostly CD8+ T cells are investigated, because most tumors do not express MHC-II and thereby direct recognition by CD4+ T cells is not possible[4 5]. However, CD4+ T cells can act through cross-presentation to stromal cells like macrophages and monocytes and thereby enhance CD8+ T cell recognition and response[4 5]. A second T cell population is the γδ T cells. They are less abundant in peripheral blood and their TCR is composed of a γ and a δ chain. γδ T cells recognize their target cells in an MHC-independent

manner and the different subtypes of γδ T cells recognize their targets via different molecules[6].

In the cancer setting, antigens are mainly categorized into two large groups, neo-antigens, and shared antigens. Shared tumor antigens are not tumor-specific and can be further divided into three main subgroups: overexpressed, cancer-testis antigens (CTA), and differentiation antigens[7]. The cancer testis antigen New York Esophageal cancer (NY-ESO-1) and the differentiation antigen Melan-A have been investigated intensively in the past and the presence of functionally active, peripheral T cells correlated with the survival of melanoma patients[8-10]. Neo-antigens develop from tumor mutations and while some can be shared across patients, others might be patient-specific[11].

Epitope-spreading is the diversification of TCR clonotypes[12]. These epitopes are non-cross-reactive and different from the epitope that was targeted originally[12 13]. Epitope-spreading occurs when (tumor) cells die and/ or release intracellular proteins, that are taken up and then presented by APCs[12]. It was shown that vaccination induced epitope-spreading in cancer patients[14]. Mouse models have shown epitope-spreading under immune checkpoint blockade (chapter 6.1.3), even of sub-dominant clones of the same protein[15 16].

The diversity and amount of antigens, expressed by the tumors are predominantly unique for each patient, therefore further characterization of the antigen recognition by T cells is urgently needed. As tumor recognizing T cells, can also be found in peripheral blood[17 18], allowing an easy non-invasive opportunity to investigate them in (cancer) patients.

The MHC-dependency of T cell recognition can be exploited to determine their specificity, using fluorescent-labelled-peptide loaded-MHC-I multimers. One such approach applies “dextramers”. These are DNA-barcoded multimers with on dextrane backbone and with a DNA sequence specific for each pMHC, that enables the detection of T cells specific for up to 1000 different peptides in one sample[19]. Compared to other pMHC multimer approaches, for example, “tetramers”, dextramers also enable the detection of low-affinity TCRs[19].

6.1.2. αβ T cell activation

T cells are primed and activated in secondary lymphoid tissues (e.g. lymph nodes) through antigen-specific stimulation. After stimulation of T cells through their TCR, specific T cells expand, and activated CD8+ T cells are then trafficking via peripheral blood to the target site and are in principle ready to kill their target cells. Most T cells after antigen clearance die but about 5% differentiate into memory T cells[20]. Other research suggests that T cell differentiation might also be driven through TCR signal strength and is therefore determined from the beginning of T cell development[21]. Through repeated antigen stimulation, these T cells become terminally differentiated, with only little effector function[20].

Cytokines released by activated T cells, e.g., IFN-γ, TNF-α or interleukin (IL)-2, or other proteins, might act against the target cell like perforin or granzyme B. IFN-γ for example is mainly produced by CD4+ Th1 and CD8+ T cells, but it might also be produced by NK cells, B cells or professional antigen-presenting cells (APC). IFN-γ promotes cytotoxicity by upregulation of MHC-I and MHC-II antigen-presenting pathways in tumor cells while inhibiting IL-4 production in Th2 cells which might inhibit the T cell response[22]. TNF-α is also produced by various cells of the immune system including

T cells, natural killer (NK) cells, and macrophages. The release of TNF-α triggers further production of TNF-α as well as the production of other cytokines like GM-CSF and IL-8 which leads to recruitment and activation of macrophages and T cells at the target site, but also activate endothelial cells and eventually might promote angiogenesis[23]. Other effector molecules are granzymes and perforin, which directly interact with the target cell, leading to its apoptosis[24].

To examine the T cell activation status, these effector molecules can be detected in flow cytometry experiments. Additional molecules that might be upregulated upon stimulation in T cells are CD107a (lysosomal-associated membrane protein-1 (LAMP-1)) or CD154 (CD40L)[25 26]. CD107a is a highly glycosylated protein, that lines the inside of the membrane of granules in cytotoxic T and NK cells and is responsible for maintaining the lysosomal integrity, catabolism, and pH during the production of cytotoxic effector molecules[27 28]. Therefore, it is a marker for degranulation. CD154 is the ligand of CD40 and is predominantly expressed by CD4 T cells[29]. CD40 is expressed by macrophages, B cells, and other cell types and is part of the TNF-receptor family. Interaction of CD154 with its receptor CD40 mediates the formation of germinal centers, B cell proliferation, Ig production, class switching, and the generation of B memory cells[26]. Furthermore, it was shown that CD154 expression enhances the immunogenicity of tumor cells through enhanced (Transporter associated with antigen processing) TAP expression and mediates apoptosis through increased TRAF3 in tumor cells[26].

6.1.3. Immune checkpoint blockade

In patients with chronic infection or cancer, T cells are often repeatedly stimulated and therefore most of them terminally differentiate, exhaust or become senescent. Upon

TCR stimulation T cells express increased levels of (co)-inhibitory molecules such as cytotoxic T-lymphocyte–associated antigen (CTLA)-4, lymphocyte activation gene (LAG)-3, T cell immunoglobulin and mucin domain 3 (TIM-3) and programmed death receptor (PD)-1[30 31]. They are also often referred to as checkpoint receptors. Each of these molecules has a distinct function. CTLA-4 prevents T cell activation by competing with CD28 for CD80/CD86. CD80 and CD86 are co-stimulatory molecules on the surface of antigen-presenting cells (APC)[32 33]. LAG-3 is a regulator of T cell proliferation, it inhibits signal transduction by crosslinking with CD3 - then CD3 can't transduce TCR signals anymore[34]. TIM-3 is suggested to regulate type 1 immunity because it is mostly found on IFN-γ producing cells[34]. Furthermore, TIM-3 was found to suppress the immune response through interaction with immune suppressive cells like myeloid derived suppressor cells (MDSC) in mice[34]. PD-1 inhibits T cell proliferation by, prevention of phosphorylation of TCR signal intermediates, after binding to one of its ligands programmed death receptor ligand (PD-L)-1 or -2[32]. The expression of these molecules on T cells is linked to a rather exhausted state with low to no capability to produce effector molecules such as IFN-γ[34]. Upon TCR stimulation, PD-1 and CTLA-4 are upregulated and CTLA-4 now binds CD80/CD86 with a higher affinity as compared to CD28 and thereby dampens the T cell response[33]. The inhibition of these mechanisms is exploited as a therapeutical approach in the Immune checkpoint blockade (ICB).

ICB is an antibody-based therapeutic strategy targeting checkpoints and preventing the binding of these checkpoints to their ligands. Currently, ICB includes but is not limited to antagonistic antibodies against PD-1 alone or combined with antibodies against CTLA-4.

Because CTLA-4 expression and negative regulation are linked to CD28 co-stimulation, CTLA-4 primarily acts at sites of T cell priming such as lymph nodes. PD-

1 on the other hand, binds to for example PD-L1 on the surface of tumor cells and inhibits T cell response and proliferation. PD-L1 is upregulated in (tumor) cells through IFN-γ signaling[35]. Antibodies against PD-1 or CTLA-4 bind to their target and prevent binding of inhibitory molecules and therefore invigorate T cell response[33 36 37]. Other inhibitory cells, like MDSC, might also express PD-L1 (see section 6.1.4.2) to inhibit T cell responses. Because PD-L1 is mainly expressed by nonlymphoid tissue, PD-1 inhibition takes place mostly in the periphery[33].

6.1.4. Regulatory cells

6.1.4.1. Regulatory T cells

In addition to inhibitory co-receptors on the T cell surface, regulation of their functionality can be performed by various cell types. Such a negative (or suppressive) regulation of an immune response can for example be performed by regulatory T cells (Tregs)[38]. Tregs express TCRs with an intermediate affinity and are essential to maintain immunological self-tolerance[39]. Treg pre-cursor cells are positively selected in the thymus and consequently driven into differentiation, thereby becoming functionally competent regulatory T cells[39]. This process is driven by IL-2 receptor signals, which do not play a role in the differentiation of conventional T cells[39]. Additionally, differentiation into Tregs can be induced in secondary lymphoid tissue from naïve, conventional CD4+ T cells, through retinoic acid, produced by APCs[38 40]. The main function of induced Tregs is to prevent immune reaction against the microflora in the gut[39]. Tregs are commonly characterized through the expression of the transcription factor Forkhead-Box-Protein P3 (FOXP3)[38]. Furthermore, they express the IL-2 receptor (CD25)[38 41], phenotyped by the α-chain, and low levels to

none of the IL-7 receptor (CD127)[38]. Tregs inhibit T cell function through different mechanisms. For example, the secretion of inhibitory cytokines like IL-10, which inhibits the production of pro-inflammatory cytokines by antigen-presenting cells (APC) or tumor growth factor (TGF)-β that inhibits T cell proliferation or expression of suppressive molecules, such as CTLA-4. Tregs with high CTLA-4 expression compete with other T cells for B7 on the APC surface– preventing T cell stimulation[38]. Furthermore, through constitutive expression of CD25, Tregs bind IL-2 thereby lowering IL-2 concentration and thus prevent CD8+ T cell activation[42].

Loss of function or low levels of Tregs causes a variety of autoimmune diseases, inflammatory diseases and allergies. In the cancer setting, it is debated whether high Treg levels are beneficial for tumor rejection or not: some studies show that high Treg levels are correlated with poorer prognosis across cancer types[42], including melanoma[43]. However other studies showed that high levels of Treg correlated with longer OS in CRC patients[44]. This highlights the complex role of regulatory T cells in cancer rejection and will be discussed later in this thesis.

6.1.4.2. Myeloid-derived suppressor cells

Another type of cell that influences T cell activity are myeloid-derived suppressor cells (MDSCs), these are not fully differentiated cells of the myeloid lineage[45-47]. They evolve from common myeloid progenitor cells, which under normal conditions develop either into neutrophils, dendritic cells or monocytes[48]. MDSCs accumulate as a response to inflammations, infections or tumors[45]. In healthy individuals, they are therefore present at low frequencies in the circulation and participate in the modulation of immune responses and tissue repair[45]. Tumors for example disrupt developmental processes by the release of different colony-stimulating factors[48]. These factors regulate normal

myeloid development, but when the composition of these growth factors is imbalanced, the development of a part of myeloid cells stops and MDSCs accumulate[48].

MDSC generation is a two-step process: 1) accumulation, terminal differentiation of immature myeloid cells is blocked and 2) activation, mediated by persistent cytokine secretion like IL-6, IL-10, IL-1β, IFN-γ as well as toll-like receptor (TLR) ligands, through the tumor[48,49].

In vitro experiments have shown that MDSC subsets can differentiate into inflammatory or suppressive macrophages in the presence of TLR agonists Resiquimod (R848) or Pam3CSK4, respectively[50]. Furthermore, the differentiation of MDSC into macrophages could be driven by cytokines such as IL-10, TNF-α or IFN-γ[50].

MDSC can be categorized into three main groups: monocytic (M-)MDSCs which fail to differentiate into monocytes or dendritic cells, polymorphonuclear (PMN-)MDSCs which fail to differentiate into neutrophils and early (E-)MDSCs, resembling an early differentiation state of MDSCs[48 49]. These subsets are phenotypically distinct and can in humans be distinguished through their expression of CD14 and CD15. The suggested markers to identify the phenotypes of the three main MDSC subsets are depicted in Table 1.

Table 1: Immunological markers to identify the three main MDSC phenotypes in humans: M-MDSC, PMN-MDSC and E-MDSC in humans. Adapted from Bronte et al.[51] and Ostrand-Rosenberg et al.[52]

Marker	M-MDSC	PMN-MDSC	E-MDSC
CD3CD19CD56	-	-	-
CD11b	+	+	?
CD33	+	+	+
CD14	+	-	-
CD15	-	+	-
HLA-DR	low/-	-	-
CD66b	-	+	-
IL-4Rα	+	-	-

Some research suggests additional investigation of the CD123 expression to distinguish E-MDSCs from basophils (CD123high)[53]. Recent reports also mention other subtypes of MDSC like eosinophilic (Eo-)MDSCs that develop during *Staphylococcus aureus* infection in mice as well as fibrocytic (F-)MDSCs in mice[54]. However, for these two subpopulations, there is so far no consensus phenotype described. MDSC can precede various functions, during pregnancy PMN-MDSCs accumulate in the mothers' blood to increase tolerance of the mother against the fetus and accumulation of MDSCs is found to prevent diabetes in mice[52 55] and humans[55]. They also may exceed various pro-tumor functions. For example, vascular endothelial growth factor or matrix metalloproteases released by MDSCs promote angiogenesis, metastasis and tumor invasion[52]. Furthermore, they can inhibit T cell function. PMN-MDSC inhibit T cell function through the release of reactive oxygen species (ROS), peroxynitrite, and prostaglandin[49]. Free radicals like ROS or peroxynitrite not only inhibit T cell function by decreasing the expression of the TCR ζ-chain and thereby

inhibiting T cell proliferation[48]. Free radicals also stimulate VEGF expression, recruiting more MDSC to the TME[48]. An upregulation of arginase-1 causes depletion of L-arginine from the TME, therefore L-arginine is no longer available as a substrate for T cells. M-MDSC mainly act through nitric oxide (NO) production and the expression of immune suppressive cytokines (like IL-10 and TGF-β) as well as the expression of negative immune regulatory molecules, for example PD-L1[49]. Binding of PD-L1 to PD-1 on the T cell surface causes anergy of T cells, the release of immune suppressive cytokines like IL-10 induces immune suppressive cells like M2 macrophages (promoting tumor growth) and IL-10 and IFN-γ induces Tregs (inhibiting T cell function)[48].

6.2. Melanoma

6.2.1. Biology of melanoma

Melanoma is with roughly 3000 deaths in 2019 in Germany[56] with a worldwide increasing incidence[57] the most fatal form of skin cancer. Melanomas develop when melanocytes mutate and escape the before described elimination by the immune system[58]. Melanocytes are skin cells that produce the pigment melatonin which is responsible for skin color[57]. Mutations are often caused by exposure to ultraviolet radiation of the sunlight, resulting in a comparably high mutational burden and thereby in uncontrolled tumor growth[59]. When detected at early stages, the tumor can be removed surgically, and chances to cure patients are high.

Melanomas are usually classified using the guidelines established by the American Joint Committee on Cancer (AJCC), which employs the lesion thickness, metastatic nodes, and sites of metastasis (TNM) system and is revised on a regular basis[60 61]. Patients in stages 0-II are classified solely by the thickness of the lesion, as they have not spread into lymph nodes or other organs[60 61]. Stage 0 melanomas are confined to the upper layer of the epidermis and Stage I is a localized tumor but confined to the skin and maximal 2 mm thick. Stage II melanomas are with up to 4 mm, thicker than stage I and start spreading into the dermis[60], then stage III melanomas spread to regional lymph nodes and serum lactate dehydrogenase (LDH) might be elevated[60 62]. Stage III melanoma patients are classified by the number of metastatic lymph nodes[60]. Stage IV metastasizes into other organs and potentially elevated LDH[60]. LDH is an enzyme that converts pyruvate into lactate, it is upregulated under anaerobic conditions, increasing effectiveness of glycolysis, allowing the tumor to grow under these conditions[63].

The site of metastasis (M-category) categorizes stage IV patients[60 61]. In the seventh edition of the AJCC guidelines, on which this work is based on, patients can be classified as M1a (with distant skin, subcutaneous, or nodal metastases), M1b (lung metastases) or M1c (with any other visceral metastases and/or elevated LDH serum level)[60]. In the revised version from 2017, LDH levels are considered at every M-category (indicated as 0 or 1 following the M-category) and separates the M1c group into two groups: M1c with distant metastasis in non-central nervous system (CNS) visceral sites and patients with metastasis in CNS sites are categorized in M1d[61]. In both versions of the classification systems shorter survival is associated with the advanced M-category and Stage[60 61 64]. While Stages 0-II were usually treatable and stage III melanomas have a heterogenous outcome, stage IV melanoma was basically untreatable until the advent of immune checkpoint blockade[61]. As described above in section 6.1.3.

6.2.2. Melanoma treatment

Until the 1990s chemotherapy was the most prominent treatment option[65]. In 1995 high dose IFN-α was the first immune modulating therapy that was approved by the FDA[66] and followed by IL-2 treatment only 3 years later in 1998[65]. In 2011 the first immune checkpoint blockade Ipilimumab, an antagonistic anti-CTLA-4-antibody was approved by the FDA, followed by antagonistic anti-PD-1 antibodies in 2014[65]. ICB has improved cancer treatment in several solid cancers, including melanoma[67 68 69] accomplishing survival rates of about 50%[58]. This remarkable success was rewarded with the Nobel Prize in 2018[70]. Almost simultaneously to ICB, targeted therapy using e.g. B-Raf or N-RAS kinase inhibitors, were approved by the FDA, for patients with mutations in these

genes[65]. ICB however, improved patient survival enormously[71]. A brief, not extensive overview of the historic evolution of melanoma therapy is given in Figure 1.

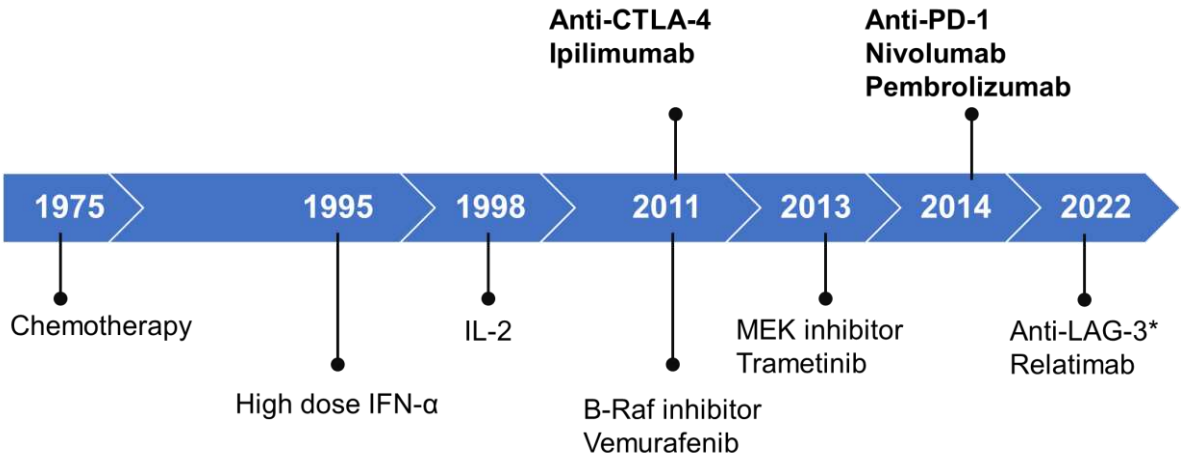

Figure 1: A brief, not extensive overview of the evolution of melanoma therapy. Adapted from Millet et al.[65] and further expanded. The star indicates FDA approval but not EMA approval[72].

Despite the great success and even though, mono or combination therapy of anti-PD-1- and/or anti-CTLA-4-antibodies is safe and prolongs patients' survival not all patients benefit from ICB and therefore, more ICB treatment options are investigated[73] [74]. With anti-CTLA-4 treatment alone (Ipilimumab) patients had 3-year survival rates of roughly 30%[69]. Under anti-PD-1 monotherapy (Nivolumab) 3-year survival rates were at 52% and with a combination of anti-CTLA-4 and anti-PD-1 antibodies survival rates were at 58%[75]. Treatment with both antibodies revealed higher response rates, but the severity of adverse events needs close supervision by experienced personnel[76]. Common adverse events are skin issues or gastrointestinal events, less frequent in patients under anti-PD-1 treatment than in patients under anti-CTLA-4 treatment[75]. Additionally, anti-LAG-3 antibodies for the treatment of melanoma patients were approved by the FDA in 2022[72]. LAG-3 binds to MHC-II molecules on the surface of

APC – dampening the CD4+ response. Furthermore, it crosslinks with CD3 and inhibits proliferation and TCR signaling on both CD4+ and CD8+ T cells.[72]

6.2.3. Biomarkers

Despite improvement of survival rates through ICB, predictive and/ or surrogate biomarkers to identify patients, that benefit from ICB are urgently sought. Ideally, biomarkers should be easy to access, and their measurement and interpretations should be fast and inexpensive[77]. Biomarkers can be tissue based for example *BRAF* or *NRAS* mutation status as well as H&E staining to investigate TIL infiltration or serum based like LDH or S100 calcium binding acidic cytoplasmic protein b (S100b)[77 78]. High levels of LDH or S100b are correlated with worse outcome for melanoma patients, under ICB and other therapies[43 77-79]. Other interesting candidates are routine blood counts such as high frequencies of myeloid cells[43], low numbers of eosinophils and lymphocytes[79] or a high neutrophil-to-lymphocyte ratio (NLR)[80 81] and have been correlated to a worse outcome. These serum-based markers are easy to obtain and measure. In comparison, tissue-based biomarkers require biopsy or surgery, with additional sample preparation for either sequencing (for determination of mutations) or for histopathological staining like H&E, Ki67 on tumor-infiltrating lymphocytes (TIL), or PD-L1 on tumor cells[77]. So far efforts have been made to identify and phenotype T cell and myeloid cell populations in peripheral blood that might predict response to ICB[43 82] as well as functional characterization of TAA-specific T cells[8]. Because of their pro-tumor functions, M-MDSC frequency have been discussed as a biomarker: higher frequencies of MDSC correlate with shorter overall survival in melanoma patients[43 83 84] So far, LDH serum levels are the only established biomarkers. Therefore, they are urgently needed, and further characterizations of the current candidates are inevitable.

7. Aim of the thesis

The treatment of stage IV melanoma is still limited, with 5-year survival rates of approximately 50% for patients treated with ICB[58]. Loss of MHC expression, poor T cell infiltration and the tumors expressing T cell inhibiting ligands (e.g. PD-L1) are only a fraction of the potential explanations for ICB failure[85]. Therefore, new treatments like cancer vaccines are currently gaining more attention[86] [87]. Vaccines enhancing recognition of TAA expressed by the tumor are an attractive option because they are not as personalized as vaccination strategies using neo-epitopes. So far, some TAAs have been used in such studies, NY-ESO-1 and tyrosinase amongst others. To have more patients benefit from such therapies, the identification of TAAs that are frequently recognized by T cells across patients that aid in tumor recognition and rejection are urgently sought. We performed immune monitoring in three overlapping cohorts in late-stage melanoma patients.

On one side, CD8+ and CD4+ T cells were investigated. We aimed to assess which epitopes are most frequently detected by CD8+ T cells using pMHC-multimers (here, so-called “dextramers” were used). These investigations shall help understand, how tumors are detected and to find potential association with survival in melanoma patients. Not only CD8+ T cells can recognize epitopes bound to MHC-complex, but also CD4+ T cells. In the ideal case, after antigen recognition in the TME, cytokines are released to eliminate the cancer cells and/or to attract further immune cells. Therefore, we aimed to investigate the functionality of T cells *in vitro*, against selected antigens. Thereby, we could understand which antigen-specific T cells could eliminate cancer cells when they potentially migrate into the tumor.

Additionally, peripheral immune cell profiles (from clinical routine blood counts and flow cytometry) and the phenotypes of T cells were investigated in the third study. As a

result, we could determine if some immune cell types, and/ or profiles (the combination of certain immune cells) are potential biomarker candidates that associate with melanoma patients' survival. Investigation of T cell phenotypes (e.g. expression of exhaustion markers) could also shed more light on the before mentioned associations of epitope and antigen-specific T cells and patients' survival and explain the observed mechanisms.

Investigation of the dynamics (of T cells and other biomarker candidates like M-MDSC) allows investigations of surrogate biomarkers early under therapy. The use of surrogate biomarkers could help in early therapy intervention if it seems that the patient will not profit from the therapy.

8. Summaries of included manuscripts

8.1. Summary 1: “Dynamics of melanoma-associated epitope-specific CD8+ T cells in the blood correlate with clinical outcome under PD-1 blockade”

T cells identifying cancer cells play an important role during cancer rejection. They recognize malignant cells through interaction of the TCR with a peptide-bound MHC-complex on the tumor cell surface. To overcome the limitations of ICB approaches like mRNA vaccines using shared antigens are currently being investigated. Recently, the CTA NY-ESO-1 (along with Tyrosinase, Melanoma antigen Gene (MAGE)-A3 and Transmembrane Phosphatase With Tensin Homology (TPTE)) was included in a study using a mRNA vaccine against melanoma[87]. However, knowledge about the frequency and dynamics of TAA recognition is still limited. To broaden the spectrum of antigens that can be utilized in such treatment options, to a point that most of the patients will benefit, new potential antigen targets are sought. These new potential antigens increase the insights into tumor rejection.

This project aimed to identify the dynamics of 167 melanoma-associated antigen (MAE)-specific CD8+ T cells, using peptide-loaded MHC (pMHC)-multimers in a unique cohort of 36 HLA-A*0201 patients under PD-1 ICB.

We investigated the dynamics of MAE-specific CD8+ T cells, in peripheral blood samples from before the start of ICB and in median of 42 days thereafter. The used panel comprised 167 MAEs and 117 MAE-specific T cells were detected across the entire cohort. Seventy-two MAE-specific CD8+ T cells were present at both time points, while 45 were present at only one of the two time points investigated.

A score ($T_{MAE}S$ B) to summarize the dynamics of the various MAE-specific T cells within a patient in one number was calculated. It reflects either an increase

($T_{MAE}S$ B>0) in the total number of MAE-specific CD8+ T cell populations or a decrease or balanced ($T_{MAE}S$ B≤0) number of total MAE-specific CD8+ T cell populations.

The first main finding of this study was that $T_{MAE}S$ B>0 correlated with significantly better overall- and progression-free survival compared to patients with $T_{MAE}S$ B≤0. Because previous studies suggested biomarker characteristics for M-MDSC and T cells[88 89] under ICB and upregulation of alternative checkpoints during *in vitro* ICB[90], phenotypes of myeloid and T cells including their expression profile of checkpoints were investigated in selected patients. We did not find significant differences at BL in either of the T cell or myeloid phenotypes investigated in these two groups nor significant changes of frequencies of CD8+ or CD4+ T cells, Tregs, CD25+ CD8+ T cells, or in the myeloid cells in either of the two groups $T_{MAE}S$ B>0 or $T_{MAE}S$ B≤0). However, we found a significant increase in frequencies of TIM-3+CD8+ T cells as well as LAG-3+CD4+ and LAG-3+Tregs in patients that experience an increase in the number of T cell populations ($T_{MAE}S$ B>0). Furthermore, patients with a decreasing/balanced number of MAE-specific CD8+ T cells experienced a significant decrease in TIM-3+CD4+ T cells. This highlighted the multifaced actions of ICB. However, TIM-3 and LAG-3 are not only markers of T cell activation but are also discussed to mark exhausted/dysfunctional T cells[34].

We then aimed to identify MAE-specific CD8+ T cell populations of particular interest using a machine learning-based elastic net regression approach and subsequent univariate Cox-regression. We identified 7 MAE-specific CD8+ T cell populations that were associated with OS. These were the overexpressed antigens, STEAP1 FLY, Tyrosinase CLL, and Telomerase RLF, as well as the CTA's MAGE-A10 SLL, TAG-1 SLG and TRAG-3 ILL and the differentiation antigen TRP-2 SVY. Multivariate Cox-regression using these seven MAE-specific T cell populations revealed the

second main result of this study: The dynamics of Telomerase RLF, TAG-1 SLG and TRP-2 SVY correlated significantly and independently with OS. A disappearance of at least one of those MAE-specific CD8+ T cell populations in peripheral blood correlated with significantly shorter OS.

Superficially, this result might contrast with the first result in this paper, that an increase is beneficial for OS as well as results from our previous study. There, a decrease of T cells reactive to Melan-A and/or NY-ESO-1 was correlated with beneficial OS (they probably migrate into the tumor, potentially induced through ICB). But it is important to note, that in this paper, we did not investigate the functionality of those MAE-specific CD8+ T cell populations- only the presence. We suggest, that these MAE-specific CD8+ T cell populations (recognizing TRP-2 SVY, Telomerase RLF, and TAG-1 SLG) might highlight a rather exhausted or dysfunctional T cell state, a well-described in late-stage cancer settings[91].

These results suggest, that the following factors might contribute (not exclusively) to the invigoration of T cells by ICB: i) T cell specificity[92], ii) the ability of the T cells to interact with epitopes, presented by the cancer cell[12] and iii) their functionality[10 93 94], as only functional T cells are able to eliminate cancer cells opposed to dysfunctional/exhausted T cells.

One limitation of the study is its restriction to HLA-A*0201. Ideally, such studies should be performed independent of HLA-A restriction, not only because these genes are highly polymorphic[1], but also because only half of the European descent population is HLA-A*0201+[95]. Furthermore, HLA-A genes can be hetero- or homozygous, apart from the fact, that people with a heterozygous HLA-type might be able to detect more different peptides, than those with a homozygous genotype[1]. However, the

consideration of these features is very difficult due to the limited availability of sample material.

Another limitation of the HLA-dependence is the prevention of a simultaneous investigation of MHC-II binding CD4+ T cells. The latter plays a crucial role in cancer rejection, and their specificity should ideally be assessed concurrently. However, the investigation of the presence of MAE-specific CD4+ T cells is so far challenging, because, among other reasons, the MHC-II production *in vitro* is more difficult[96], as MHC-II molecules bind longer peptides and are structurally highly diverse and bind epitopes with lower affinity than MHC-I molecules[97]. But new technologies are currently arising[97].

The experiments in this study were performed with bloodborne CD8+ T cells. Future experiments should include investigation of both, MAE-specific CD8+ and CD4+ T cells in peripheral blood and comparatively in tumor samples. Then obtained results from the TME should further be compared to the antigens, that are presented by the same tumor. Though research suggests that TIL can be detected in the blood[17] [18], functional investigation of both peripheral T cells and TIL might aid in a better understanding of immunosuppression through the tumor.

Taken together, this research gained important insights into the involvement of CD8+ T cells in cancer recognition and rejection and highlights that the dynamics of T cell populations in the blood underlie probably multiple mechanisms, that might be influenced by ICB. Furthermore, it lays the groundwork for additional investigations in blood and tumor.

8.2. Summary 2: "Early disappearance of peripheral multifunctional MAGE-A10- and TRP-2-reactive CD4+ T cells shortly after initiating anti-PD-1 checkpoint blockade is associated with improved survival of melanoma patients."

In the fight against cancer, the sole presence of certain MAE-specific CD8+ T cells in peripheral blood (discussed in paper one of this thesis (chapter 8.1)) is not all that is required, but much rather their functionality. Furthermore, it is known that multi-functional T cells (releasing more than two cytokines) are important to immediate effector function, whereas bi-functional (secreting two cytokines) T cells are important for maintaining a long-term memory function[98]. Furthermore, the magnitude of multifunctionality depends on the amount and the avidity of the expressed antigen[98]. Recent studies found a tumor-rejecting role of CD4+ T cells, not only by exhibiting helper functions but additionally through cytotoxic properties[3 99 100]. Moreover, it was shown, that CD4+ T cells elicit more T cell responses in cancer vaccination studies[101]. However, data on the dynamics of MAE- or TAA-recognizing and functionally active CD4+ T cells is still limited. The goal of this study was therefore to investigate the dynamics of multifunctional TAA-reactive CD4+ T cells in peripheral blood of melanoma patients, to search for potential associations with clinical outcome under PD-1 ICB. We aimed to gain a deeper understanding of tumor-antigen recognition and potential rejection by (multi-)functional CD4+ T cells and their occurrence in peripheral blood.

In this study PBMCs from 31 stage IV melanoma patients under anti-PD-1 therapy with or without additional anti-CTLA-4 therapy were investigated.

To test for functionality of MAGE-A10 and TRP-2 reactive T cells, they were analyzed after a 12-day *in vitro* culture. Simultaneous expression (multifunctionality) of TNF-α, IFN-γ, CD107a and CD40 after antigen stimulation was investigated.

The dynamics of multifunctional CD4+ T cells were investigated using a similar machine learning-based approach, as in paper one of this thesis (summarized in 8.1). However, with the changes of reactive T cells as an input. The disappearance of several multifunctional T cell populations was associated with significantly better overall survival. These populations displayed a functional phenotype of MAGE-A10 CD107a+CD154+IFN-γ+TNF-α+, TRP-2 CD107a+CD154+IFN-γ-TNF-α- and TRP-2 CD107a-CD154+IFN-γ-TNF-α+ and were identified to have an HR > 1.

The main finding of this study was, that a disappearance of certain multifunctional CD4+ T cells was associated with prolonged survival. One reason could be, that these multifunctional CD4+ T cells migrate to the tumor, where they exhibit tumor-killing function. This is in alignment with a previous study of our research group. In that previous study, the functionality of NY-ESO-1 and/or Melan-A reactive T cell populations was associated with prolonged survival in melanoma patients under ICB[10].

Simultaneous to MAE-reactivity, the presence of several immune cell subsets was investigated, namely: MDSC, monocytes, NK cells as well as Tregs, CD4+ and CD8+ T cell subsets and their expression of the checkpoints PD-1 and TIM-3, before and under therapy. Patients with a decrease in multifunctional T cells had before the start of therapy significantly more PD-1+ Tregs and PD-1+ CD8+ T cells. PD-1+ Tregs were mostly single positive, whereas PD-1+CD8+ T cells were mostly PD-1+TIM-3+. Under therapy, there was a significant increase in PD-1-TIM-3+ but not in PD-1+TIM-3+ expressing CD4 T cells. This feature might result from ICB-induced T cell activation, similar to the findings of paper one of this thesis (chapter 8.1). There was a significant

decrease in PD-1+ Tregs (mostly PD-1+TIM-3- Tregs) in patients with a decrease in multifunctional T cells. This is in accordance with previous studies, where a decrease in PD-1+ Tregs is associated with longer survival[102].

The results generated here could be used as the groundwork to identify new targets for vaccination approaches. Future experiments should simultaneously investigate the following three features: TCR specificity (e.g. through pMHC-multimers), functionality and markers of exhaustion, in both blood and tissue samples. This aids in the broader understanding of these three features in cancer rejection enabling a direct invigoration of the important T cell clones. Multifunctionality has been discussed to lead to a stronger response compared to single-cytokine-producing cells in antiviral responses[103] and this could potentially apply to the cancer context.

8.3. Summary 3: “Early decrease of blood myeloid-derived suppressor cells during checkpoint inhibition is a favorable biomarker in metastatic melanoma"

Myeloid-derived suppressor cells (MDSC) are a heterogeneous subset of incompletely differentiated myeloid cells. They are composed of mainly (but not limited to) two major subpopulations: monocytic (M-)MDSC and polymorphonuclear (PMN-)MDSC. Previously, M-MDSC have been suggested as a biomarker to predict the survival of melanoma patients by several research groups in various cohorts[83 89 104-106]. High baseline frequencies of M-MDSC have been associated with shorter survival in melanoma patients under chemotherapy or ICB[83 89 104-106]. These studies investigated stage IV melanoma patients in general – without the categorization via their site of metastasis (M-category). Even though it has been shown that patients' survival varied significantly, between the categories[64]. For this study, the 2009 AJCC classification was used, as it was the latest version at the time of sample collection and documentation of clinical data.

Thirty-three blood-borne biomarker candidates, that have been discussed before in the context of anti-PD-1 with or without simultaneous anti-CTLA-4 treatment were screened[107]. They either derived from routine blood counts or flow cytometric measurements. Among those were absolute monocyte and neutrophil counts, NLR, M-MDSC frequencies and Treg frequencies [89 104]. We collected PBMCs from EDTA blood from 141 M1c patients (visceral non-lung metastases). M1c patients have the worst survival[60], therefore they benefit the most from efficient therapies. Blood was drawn before the start of therapy and in a median of 44 days thereafter. A discovery cohort,

that consisted of 92 melanoma patients was investigated and potential biomarker candidates were validated /rejected in a second, independent cohort of 49 patients.

As expected, only “M-MDSC-high” patients (>18.1% of viable PBMCs) were associated with shorter survival in both cohorts. However, M-MDSC-high patients had significantly different immune profiles than M-MDSC-low (≤ 18.1% of viable PBMCs) patients. Patients in the former group had significantly more absolute and relative neutrophils, absolute (total and intermediate) monocytes, a higher NLR but fewer lymphocytes (absolute and relative) and a lower CD3+ T cell frequency before start of therapy.

Investigation of the two groups (M-MDSC-high vs M-MDSC-low) showed an increase in all LAG-3 and TIM-3 T cell subsets in M-MDSC-low patients. This is probably because after antigen recognition (possibly because of successful ICB) these (alternative checkpoint) molecules are upregulated[90 108 109]. A similar pattern was seen in papers one[110] and two of this thesis (chapters 8.1 and 8.2)). Furthermore, patients with high M-MDSC frequencies also at follow-up (FU) had a significantly shorter OS. However, patients with a decrease (from above to below the cut-off of 18.1%) in M-MDSC frequency experienced a significantly longer, similar to M-MDSC low patients. An increase of ≥ 50% change of the M-MDSC frequency was associated with significantly shorter OS, compared to a decreasing or stable frequency. Unfortunately, we could not assess further insights into the mechanisms of the regulation of M-MDSC dynamics early under PD-1 ICB, but we hypothesize that there is an influence of ICB on M-MDSC. It was found in mice that the activation of the PD-1/PD-L1 axis in myeloid progenitor cells probably contributes to M-MDSC accumulation[111]. However, the potential influences of PD-1 expression on myeloid progenitors on M-MDSC accumulation in humans remains unknown.

Not only cellular biomarker candidates were investigated, but also other biomarkers such as enzymes like LDH in the serum of patients. Until this day, the only established biomarker for melanoma is an elevated LDH serum level. A ratio > 1.5 x was associated with a significantly shorter OS as well as an increase of over 25% as previously described[78]. A multivariate Cox regression including the here investigated potential markers that were significantly associated with OS (elevated LDH at BL and changes under therapy, M-MDSC at BL, FU and changes under therapy) was performed. It showed, that only M-MDSC frequency at FU, > 50% change of M-MDSC frequency under therapy (independent of BL frequency) as well as a > 25% change of the LDH ratio correlated independently with significantly shorter overall survival. The combination of these factors into a model shows, that the “positive” biomarker status a patient had, the shorter was the patients’ overall survival. M-MDSC could be a biomarker, not only before the start of ICB but also early under ICB. However, the determination of peripheral M-MDSC levels is dependent on flow cytometry experiments and expert-guiding data evaluation. Therefore, M-MDSC frequencies are probably not easy to implement in clinical routines. The dynamic changes of M-MDSC under ICB could be used to define patients, that don’t respond to ICB and discuss different treatment options.

To the best of our knowledge, we described here for the first time that a fraction of M-MDSC high patients at BL (“poor prognosis” group), still experienced a benefit from PD-1 ICB. Furthermore, in this paper, the M-MDSC frequency cut-off is much higher than in other studies, where commonly a cut-off of already 10-13% M-MDSC of total viable PBMCs was associated with worse survival[83 84]. The observed difference might be simply caused by the use of divergent detection approaches - however, it might be more likely that ICB is now used as a first-line treatment[112] and thus patients with an

initially poorer prognosis (intermediate M-MDSC frequencies (10-18,1%) have now a better prognosis. Further experiments should work on the understanding of that mechanism – to identify patients that might benefit from M-MDSC targeted therapies potentially in combination with ICB[47].

9. Discussion

Tumor-specific T cells play a major role in cancer detection and rejection. Ideally, CD8+ and/or CD4+ T cells, activated in secondary lymphoid organs, migrate through the blood to the site of inflammation or to the cancer site where they accumulate and reject the tumor in an ideal case. The investigation of peripheral blood is an easy, minimally invasive method to investigate T cell frequencies, phenotypes and functionality. For this reason, peripheral blood of patients with unresectable melanoma (chapters 8.1-8.3) was investigated here. It was shown that tumor-reactive TCR repertoires were found in the blood[17]. For example, CD8+ "TIL precursor cells" were identified in the peripheral blood of lung cancer patients[113]. Oliveira et al. found that most CD8+ [114] and CD4+[115] T cells with tumor-epitope recognizing TCR in the periphery are not exhausted. Their findings furthermore suggest that the CD4+ TIL phenotype resembles CD4+ T cells outside of the TME[115]. Therefore, using PBMCs as a source for investigation presumably allows an estimation of T cell dynamics in the TME.

9.1. Unravelling associations between survival and dynamics of melanoma-associated antigen-specific CD8+ T cells

In paper number one of this thesis (summarized in chapter 8.1) dynamics of MAE-specific CD8+ T cells in melanoma patients under ICB were investigated. The first finding was an increase in the abundance of MAE-specific CD8+ T cells under ICB. This increase in variety was associated with longer survival in 17 patients. This phenomenon is called epitope-spreading[12 13]. Previous studies by others in melanoma patients and mouse models under ICB showed similar results: epitope-spreading correlated with prolonged OS[15 116]. We assume that epitope-spreading might be

induced through successful ICB. ICB directly impacts T cell functionality through interacting with checkpoints such as PD-1 or CTLA-4 on the T cell surface[32]. T cells destroy cancer cells, which release new antigens, that are taken up by APC and now a broader spectrum of epitopes is presented to T cells[12]. Here, the presence of predefined specific T cells in peripheral blood was measured using peptide-loaded MHC multimers[19]. This allows the investigation of only a fraction of predefined TCR specificities. Furthermore, due to the MHC dependency in this assay, solely HLA-A*0201+ patients were investigated.

The second finding of paper one of this thesis (chapter 8.1) was dynamics of 3 MAE-specific CD8+ T cell populations correlated negatively with OS in melanoma patients, identified using a machine learning-based elastic-net regression model. Here: A disappearance of at least one of those was associated with a significantly shorter OS. We hypothesize, that these disappearing populations could presumably be dysfunctional, or migration into the TME is inhibited by the tumor cells. The exact mechanism could not be investigated here due to the lack of precious patient material, no functional assays could be performed to either validate or reject the hypothesis. However, bulk immune phenotyping was performed, to find correlations with the dynamics of MAE-specific CD8+ T cells, which will be discussed later in section 9.3. To test this hypothesis, additional functionality or exhaustion markers (e.g. IL-2 or TIM-3, respectively) could be investigated to simultaneous pMHC-based detection techniques Thereby we could determine if the detected MAE-specific T cells are functionally active and are potentially inhibited in the TME or if they are exhausted. Alternatively, for functional investigation of pre-known MAE-specific T cells could be expanded with pMHC-multimers, with costimulatory molecules bound to the multimer backbone[117]. After expansion cells could be re-challenged and measured using flow

cytometry experiments, as described throughout this thesis. To test if T cell migration is inhibited, patient-matched tumor slides could be stained for PD-L1 or other immune suppressive cells to evaluate the suppressive capacity of the TME[118].

However, this contrasts our earlier studies where a disappearance of at least one functionally reactive TAA-reactive CD8+ and/or CD4+ T cell population was associated with longer survival[10]. We concluded in previous studies that these T cell populations migrate into the TME where they might contribute to rejecting cancer cells[10] and in the first paper of this thesis, it was concluded that T cells are either dysfunctional or the immune response is inhibited. This is in line with previous research by others, that has shown that tumor infiltration by lymphocytes was increased after PD-1 ICB [37 119].

9.2. Insights into melanoma-specific multifunctional CD4+ T cells and associations with patient survival

In paper two of this thesis (chapter 8.2), we investigated multi-functional CD4+ T cells, because CD4+ have been found not only to assist in CD8+ T cell activation but are able to eliminate tumor cells themselves[2 3]. After further analysis of the data from paper number one of this thesis and extensive literature research, we here studied the (multi-) functionality of MAGE-A10, TRP-2 reactive CD4+ T cells using protein-spanning overlapping peptide libraries. A disappearance of at least one of certain multifunctional CD4+ T cell populations was associated with longer OS. We hypothesized similar mechanisms as discussed before in 9.1 and in our previous studies, where T cells migrate into the tumor. In the Tumor, CD4+ T cells not only directly target tumor cells or activate CD8+ T cells but also are able to recruit other cell types like macrophages to the TME[4]. TAA- or MAE-specific CD4+ have been poorly investigated in the past but have gained more interest in recent years. Recent work by

others shows, that adoptively transferred CD4+ T cells eradicate tumor cells with MHC-loss in mice[5]. Recently, it was shown in mice, that CD4+ T cells are activated by MHC-II positive melanoma cells[120]. These studies underline the advantageous role of CD4+ in cancer rejection. Additionally, it was shown by others that CD4+ TIL might be more important in cancer rejection after ACT: TIL infusion products that consisted predominantly of CD4+ TIL induced better responses compared to those consisting predominantly of CD8+ TIL[100]. Some of the patients only had CD4+ responses – highlighting the important role of cancer rejection by CD4+ T cells. However, for similar reasons as for paper number one of this thesis, the underlying mechanism could not be investigated due to the lack of sample material.

One limitation of paper two (chapter 8.2) is, that we do not know the specific epitopes that were detected and induced CD4+ T cell responses. For example: Proteins of the MAGE-family are homolog and share epitopes across different family members in HLA-A*0201+ patients[121]. Thereby it could be, that T cells are not specific for MAGE-A10, but another member of the MAGE-family within a particular patient. These homologous epitopes are (at least for the HLA-A*0201 gene) only low-affinity binders, with little to no immunogenic capacity. Consequently, the probability is modest but still has to be considered.

The first two papers summarized in this thesis (chapters 8.1 and 8.2) broaden the knowledge of T cell recognition of melanoma antigens and their role in cancer rejection. However, the two papers only investigate one trait at a time – either TCR specificity or functionality. For a comprehensive understanding of common antigens and their detecting T cells in melanoma patients, both presence and functionality must be investigated in future experiments of both, CD8+ and CD4+ T cells. To investigate CD4+ T cell specificity, MHC-II multimers are needed. There are current developments

to broaden the spectrum of available, peptide-loadable MHC-II multimers[97 122]. Additionally, peptides that bind to MHC-II have more variable binding characteristics and therefore there are more potential binding motifs, which makes the prediction of suitable and subsequent investigation of the incidence of peptides more challenging. MHC-II alleles show a higher diversity than MHC-I alleles, resulting in a maximum expression in only 30% of any human population[96]. Investigation of CD4+ T cell specificity of multifunctional CD4+ T cells would aid in the definition of new vaccination strategies.

9.3. Associations of T cell phenotypes with dynamics of melanoma-associated antigen-specific CD8+ T cells and multifunctional CD4+ T cells

In the first two papers of this thesis (chapters 8.1 and 8.2), bulk T cell phenotypes were additionally investigated. The goals were to gain a broader understanding of T cell populations and investigate potential biomarker candidates and potential associations with the dynamics of MAE-specific CD8+ T cells and TAA-reactive CD4+ T cells. There was an increase in LAG-3+CD8+ and CD4+ T cells (in the first paper of the thesis) and TIM-3+ CD8+ and CD4+ T cells in both papers of this thesis (chapters 8.1 and 8.2). In the first paper of this thesis (chapter 8.1)[110], these increases were predominantly in the patient group with prolonged survival. It was shown in the past, by others that the upregulation of alternative checkpoints such as LAG-3 or TIM-3 might indicate past activation and thus be a sign of T cell exhaustion[109 123]. This upregulation potentially prevents overstimulation of the immune system and might be ICB-induced. These patients could further benefit from TIM-3 or LAG-3 ICB, experiencing even faster cancer rejection. Currently, ICB treatment strategies using antagonistic antibodies

against TIM-3 or LAG-3 are investigated in combination with anti-PD-1 treatment in several clinical trials[30 74 124]. Combinatorial treatment with anti-PD-1 and anti-LAG-3 antibodies resulted in prolonged progression-free survival compared to those treated with anti-PD-1 alone with slightly more adverse events[74] and was approved in 2022[72]. It was shown before that LAG-3 inhibition is effective, independent of LAG-3 expression on tumor cells[74]. This was also shown in *in vitro* co-culture experiments in a melanoma model: a decreased tumor cell number in the presence of TIL as well as anti-PD-1 antibodies alone or combined with anti-LAG-3 antibodies[125]. Likely, a combination of the effects of PD-1 antibodies on TIL and LAG-3 antibodies on TIL and potentially tumor cells[125]. In the second paper of this thesis (chapter 8.2) LAG-3 expression was not evaluated, because LAG-3+ populations in the blood are very small. In the second paper of this thesis (chapter 8.2), an increase of TIM-3+ increase was seen in both patient groups (long vs short survival). As mentioned before, TIM-3 is upregulated upon successful (ICB induced) T cell stimulation. However, here the increases in TIM-3 were also seen in the patient group with shorter survival. Therefore, we hypothesize, that multiple mechanisms are observed here as two different T cell populations were investigated in the two papers (chapters 8.1 and 8.2). We assume, that in paper one we see in concordance with the observed epitope-spreading, indications for successful ICB. In paper two, where the cohort was dichotomized after CD4+ functionality, we assume the effects of ICB in the upregulation of alternative checkpoints are not related to the same mechanism underlying in the disappearance of certain multifunctional CD4+ T cells. These and other mechanisms, such as the expression of ligands by the tumor, that prevent T cell stimulation and T cell exclusion from the tumor[118] could not be investigated here, as we didn't have corresponding tumor material available. Furthermore, in the second paper of this thesis (chapter 8.2), another staining protocol was used, enabling investigation of PD-1 expression under

PD-1 targeted ICB: There was a decrease in the number of PD-1+ Tregs in the group with shorter OS, as also seen in other studies[102]. At baseline, PD-1+ Treg frequency was higher in patients with prolonged survival. This might seem counterintuitive as Tregs are known to enhance resistance to PD-1 treatment[42]. Some research however has found that high levels of tumor infiltrating Tregs correlated to a better prognosis in colorectal cancer[44]. Lowther et al. found that PD-1high Treg in healthy show signs of exhaustion but expressed IFN-γ, but repressive activity was restored upon anti-PD-1 treatment[126]. Thereby we assume that in paper number two of this thesis patients with high PD-1+Tregs, PD-1+Tregs might release IFN-γ and are potentially eliminating the tumor. During anti-PD-1 ICB both Treg, CD8+ and CD4+ T cell effector functions are restored – in an equilibrium of inhibition through Tregs and tumor elimination through effector T cells. However, the mechanism behind the positive role of Tregs in cancer rejection remains largely unknown and it is yet to clarify whether (PD-1+) Tregs exhibit pro- or anti-tumor functions in different cancer settings. Additionally, patients with prolonged OS in the second paper of this thesis (chapter 8.2) had more PD-1+ CD8+ T cells at BL. High frequencies of PD-1+ CD8+ T cells have been associated with better clinical outcome[127]. We assume, that PD-1 antibodies can bind PD-1 on the CD8+ T cell surface and thereby invigorate the immune response, whereas in patients without PD-1 expression on T cells tumor rejection is prevented differently. Furthermore, it was shown that high frequencies of PD-1+ CD8+ T cells can balance the potential inhibitory effects of PD-1+Tregs in cancer rejection[128].

9.4. Highlighting the role of M-MDSC dynamics under immune checkpoint blockade

T cell functionality could be inhibited through M-MDSC. M-MDSC are beyond that a cellular biomarker candidate to predict the survival of melanoma patients under ICB. In the third paper (chapter 8.3) M-MDSC were the only out of 33 investigated cellular biomarker candidates that correlated with patients' survival. The two independent cohorts of the third paper of this thesis (chapter 8.3) consisted of a total of 149 melanoma patients. Only M-MDSC frequencies over 18.1% of viable PBMCs could be validated as a predictive biomarker for clinical outcomes after PD-1 ICB. Patients with a high M-MDSC frequency before the start of therapy had significantly shorter OS compared to patients with a lower M-MDSC frequency. Potentially because the tumor releases cytokines that promote M-MDSC accumulation[47 48]. M-MDSC have been discussed as a biomarker in several melanoma and other cancer types[83 104 106 129 130]. This can be detected in peripheral blood of patients as a potential indicator for T cell inhibition. Additionally, patients with high M-MDSC frequency at BL exhibited a lower number of absolute and relative lymphocytes and a higher number of absolute and relative neutrophils compared to patients with. Neutrophils not only promote tumor growth through the expression of various cytokines but are also able to inhibit the immune response in the TME[131 132]. But pro-tumor functions have been reported as well[131 132]. We thereby hypothesize that in our cohort of melanoma patients, neutrophils execute mostly anti-tumor functions. Of note, in clinical routine blood counts cells are determined by size and granularity. Therefore, we cannot rule out, that this population might contain PMN-MDSC, as PMN-MDSC and neutrophils have a similar size and granularity[132]. High absolute lymphocyte and low absolute neutrophil counts are also

discussed as predictive biomarker candidates in non-small cell lung cancer patients[130], therefore they could be discussed as cellular biomarker for several cancer types in the future.

The key finding of this paper was that a decrease of M-MDSC from over to under the 18.1% cut-off and a cut-off-independent decrease identified patients that also had a benefit from ICB, despite initially high M-MDSC frequencies. Studies in mouse models have shown that mice lacking PD-1 signaling in myeloid cells have lower MDSC frequencies, presumably because it affects MDSC differentiation[111]. Therefore, we assume that there could be two mechanisms involved in the decrease in M-MDSC frequency: (i) successful ICB causes shrinking of the tumor size[37 75] and therefore less M-MDSC accumulate during ICB due to tumor signals. (ii) Blocking of the PD-1-PD-L1 axis in myeloid cells additionally hinders M-MDSC accumulation[111].

It was not possible for us to investigate this hypothesis, due to limited data on tumor sizes and limited sample volume. Therefore, future studies should investigate the interaction of both MAE-specific CD8+ or CD4+ T cells or their functionality in *in vitro* co-culture experiments of T cells and M-MDSC[133-135]. This could explain interactions of M-MDSC and certain specific CD4+ or CD8+ T cell subsets and the role of certain detected antigens. For example, similar to experiments performed by OuYang et al., where MDSC controlled T cell proliferation *in vitro*[135]. They induced MDSC in by co-culturing CD33+ cells from patients' PBMC, with a colorectal cancer cell line. The induced MDSCs were then added to patients' T cells and a proliferation assay was performed. In this experiment, *in vitro* generated MDSC inhibited T cell proliferation[135]. Besides, the interactions of certain specific T cells or different T cell phenotypes and M-MDSC under PD-1 therapy could be performed in an *in vitro* model to confirm the results from paper three of this thesis (chapter 8.3). It furthermore underscores the

need for immunotherapies, targeting other immune cells besides T cells. Several (pre-)clinical studies investigate MDSC targeted therapy that augments ICB[134 136 137]. For example, MDSC inhibitors like phosphodiesterase-5 (PDE5) inhibitors which downregulate ARG-1 and iNOS expression[134]. Furthermore, MDSC differentiation could be induced through All-trans-retinoic acid (ATRA) via the Erk1/2 pathway into macrophages[134].

When comparing multiple studies on MDSC, some things must be considered. One is the definition of M-MDSC. In 2016 Bronte et al. suggested a minimal flow cytometry panel, to determine the different MDSC subsets, consisting of CD11b, CD33 CD14, CD15, HLA-DR as well as the linage markers exclude other cell types[51]. The third paper of this thesis (chapter 8.3) used all of the suggested markers except for CD15. CD15 is used to distinguish between M-MDSC and PMN-MDSC. Because PMN-MDSC are more sensitive to cryopreservation and die during the process[138], this discrimination was not necessary here. Most studies by others define M-MDSC as CD14+HLA-DRlow/-, mostly without the simultaneous determination of CD11b and CD33[83 104], because a machine learning-based study found CD11b and CD33 to be redundant[139]. This discrepancy (simultaneous detection and CD11b and CD33) is one potential reason for the diversity of defined cut-offs. Furthermore, manually gating of flow cytometry data by experts influences MDSC frequencies, because each person defines this population slightly differently[140] making comparisons between studies especially between different laboratories more difficult.

Future studies should consider using fresh samples to additionally determine the frequencies of PMN-MDSC and E-MDSC as well, as to investigate the associations of

all MDSC subsets with patients' survival as well as their therapy associated changes within the MDSC compartment. Because the different MDSC subsets hinder T cell activity in different actions, thereby requiring different therapeutic regimens in patients that fail to respond to ICB.

10. Conclusion

This thesis summarizes three immune phenotyping studies, assessing outcome-associated T cell subsets, or modulators of the latter in metastasized melanoma patients under PD-1 ICB.

Tumor-specific CD8+ and CD4+ T cells play a crucial role in cancer rejection, however even though the TCR repertoire in the TME resembles those in peripheral blood, future studies should include simultaneous investigation of CD8+ and CD4+ T cells in both, tumor and blood samples for a comprehensive understanding of TCR specificity and T cell functionality during cancer rejection under ICB and to determine whether or not T cells might migrate to the TME or are inhibited there. Additionally, investigation of antigens, expressed by the tumor e.g. via single-cell sequencing of tumor tissue and prediction of possible, presented antigens, could further aid in revealing the tumor-rejecting mechanism of CD4+ and CD8+ T cells. These findings may not only aid in the development of new therapeutic strategies but there is also the potential that certain specific T cells could be defined as biomarker candidates. If their implementation into clinical routines is feasible. One such biomarker candidate was confirmed in the third paper of this thesis (chapter 8.3) with additional newly reported results: changes in M-MDSC frequency early under PD-1 blockade. When early under treatment patients with a less favorable outcome could be identified, the therapeutic strategy could be adapted accordingly. For example, therapies that inhibit MDSC function[47 136] could potentially complement ICB[136 137].

All of the results described above could be used to generate new hypotheses on the ICB-driven dynamics of tumor-specific T cells in the blood and sequencing and can in addition be used to identify and eventually help patients that need different therapeutic regimens.

References

1. Havel JJ, Chowell D, Chan TA. The evolving landscape of biomarkers for checkpoint inhibitor immunotherapy. *Nat Rev Cancer* 2019;19(3):133-50. doi: 10.1038/s41568-019-0116-x [published Online First: 2019/02/14]
2. Borst J, Ahrends T, Babala N, et al. CD4(+) T cell help in cancer immunology and immunotherapy. *Nat Rev Immunol* 2018;18(10):635-47. doi: 10.1038/s41577-018-0044-0 [published Online First: 2018/07/31]
3. Ben Khelil M, Godet Y, Abdeljaoued S, et al. Harnessing Antitumor CD4(+) T Cells for Cancer Immunotherapy. *Cancers (Basel)* 2022;14(1) doi: 10.3390/cancers14010260 [published Online First: 2022/01/12]
4. Poncette L, Bluhm J, Blankenstein T. The role of CD4 T cells in rejection of solid tumors. *Curr Opin Immunol* 2022;74:18-24. doi: 10.1016/j.coi.2021.09.005 [published Online First: 2021/10/08]
5. Kruse B, Buzzai AC, Shridhar N, et al. CD4(+) T cell-induced inflammatory cell death controls immune-evasive tumours. *Nature* 2023;618(7967):1033-40. doi: 10.1038/s41586-023-06199-x [published Online First: 2023/06/15]
6. Kabelitz D. Gamma Delta T Cells (gammadelta T Cells) in Health and Disease: In Memory of Professor Wendy Havran. *Cells* 2020;9(12) doi: 10.3390/cells9122564 [published Online First: 2020/12/04]
7. Andersen RS, Thrue CA, Junker N, et al. Dissection of T-cell antigen specificity in human melanoma. *Cancer Res* 2012;72(7):1642-50. doi: 10.1158/0008-5472.CAN-11-2614
8. Weide B, Zelba H, Derhovanessian E, et al. Functional T cells targeting NY-ESO-1 or Melan-A are predictive for survival of patients with distant melanoma metastasis. *J Clin Oncol* 2012;30(15):1835-41. doi: 10.1200/JCO.2011.40.2271 [published Online First: 2012/04/25]
9. Raza A, Merhi M, Inchakalody VP, et al. Unleashing the immune response to NY-ESO-1 cancer testis antigen as a potential target for cancer immunotherapy. *J Transl Med* 2020;18(1):140. doi: 10.1186/s12967-020-02306-y [published Online First: 2020/03/30]
10. Bochem J, Zelba H, Spreuer J, et al. Early disappearance of tumor antigen-reactive T cells from peripheral blood correlates with superior clinical outcomes in melanoma under anti-PD-1 therapy. *J Immunother Cancer* 2021;9(12) doi: 10.1136/jitc-2021-003439 [published Online First: 2021/12/23]
11. Schumacher TN, Scheper W, Kvistborg P. Cancer Neoantigens. *Annu Rev Immunol* 2019;37:173-200. doi: 10.1146/annurev-immunol-042617-053402 [published Online First: 2018/12/15]
12. Brossart P. The Role of Antigen Spreading in the Efficacy of Immunotherapies. *Clin Cancer Res* 2020;26(17):4442-47. doi: 10.1158/1078-0432.CCR-20-0305
13. Hardwick N, Chain B. Epitope spreading contributes to effective immunotherapy in metastatic melanoma patients. *Immunotherapy* 2011;3(6):731-3. doi: 10.2217/imt.11.62 [published Online First: 2011/06/15]
14. Hu Z, Leet DE, Allesoe RL, et al. Personal neoantigen vaccines induce persistent memory T cell responses and epitope spreading in patients with melanoma. *Nat Med* 2021 doi: 10.1038/s41591-020-01206-4 [published Online First: 2021/01/23]
15. Memarnejadian A, Meilleur CE, Shaler CR, et al. PD-1 Blockade Promotes Epitope Spreading in Anticancer CD8(+) T Cell Responses by Preventing Fratricidal Death of Subdominant Clones To Relieve Immunodomination. *J Immunol* 2017;199(9):3348-59. doi: 10.4049/jimmunol.1700643 [published Online First: 2017/09/25]
16. Lo JA, Kawakubo M, Juneja VR, et al. Epitope spreading toward wild-type melanocyte-lineage antigens rescues suboptimal immune checkpoint blockade responses. *Sci Transl Med* 2021;13(581) doi: 10.1126/scitranslmed.abd8636 [published Online First: 2021/02/19]
17. Valpione S, Galvani E, Tweedy J, et al. Immune-awakening revealed by peripheral T cell dynamics after one cycle of immunotherapy. *Nat Cancer* 2020;1(2):210-21. doi: 10.1038/s43018-019-0022-x [published Online First: 2020/02/29]

18. Huang AC, Postow MA, Orlowski RJ, et al. T-cell invigoration to tumour burden ratio associated with anti-PD-1 response. *Nature* 2017;545(7652):60-65. doi: 10.1038/nature22079 [published Online First: 2017/04/12]
19. Bentzen AK, Marquard AM, Lyngaa R, et al. Large-scale detection of antigen-specific T cells using peptide-MHC-I multimers labeled with DNA barcodes. *Nat Biotechnol* 2016;34(10):1037-45. doi: 10.1038/nbt.3662 [published Online First: 2016/08/30]
20. Mahnke YD, Brodie TM, Sallusto F, et al. The who's who of T-cell differentiation: human memory T-cell subsets. *Eur J Immunol* 2013;43(11):2797-809. doi: 10.1002/eji.201343751 [published Online First: 2013/11/22]
21. Snook JP, Kim C, Williams MA. TCR signal strength controls the differentiation of CD4(+) effector and memory T cells. *Sci Immunol* 2018;3(25) doi: 10.1126/sciimmunol.aas9103 [published Online First: 2018/07/22]
22. Schroder K, Hertzog PJ, Ravasi T, et al. Interferon-gamma: an overview of signals, mechanisms and functions. *J Leukoc Biol* 2004;75(2):163-89. doi: 10.1189/jlb.0603252 [published Online First: 2003/10/04]
23. Balkwill F. TNF-alpha in promotion and progression of cancer. *Cancer Metastasis Rev* 2006;25(3):409-16. doi: 10.1007/s10555-006-9005-3 [published Online First: 2006/09/05]
24. Farhood B, Najafi M, Mortezaee K. CD8(+) cytotoxic T lymphocytes in cancer immunotherapy: A review. *J Cell Physiol* 2019;234(6):8509-21. doi: 10.1002/jcp.27782 [published Online First: 2018/12/07]
25. Aktas E, Kucuksezer UC, Bilgic S, et al. Relationship between CD107a expression and cytotoxic activity. *Cell Immunol* 2009;254(2):149-54. doi: 10.1016/j.cellimm.2008.08.007 [published Online First: 2008/10/07]
26. Hassan GS, Stagg J, Mourad W. Role of CD154 in cancer pathogenesis and immunotherapy. *Cancer Treat Rev* 2015;41(5):431-40. doi: 10.1016/j.ctrv.2015.03.007
27. Eskelinen EL. Roles of LAMP-1 and LAMP-2 in lysosome biogenesis and autophagy. *Mol Aspects Med* 2006;27(5-6):495-502. doi: 10.1016/j.mam.2006.08.005 [published Online First: 2006/09/16]
28. Agarwal AK, Srinivasan N, Godbole R, et al. Role of tumor cell surface lysosome-associated membrane protein-1 (LAMP1) and its associated carbohydrates in lung metastasis. *J Cancer Res Clin Oncol* 2015;141(9):1563-74. doi: 10.1007/s00432-015-1917-2 [published Online First: 2015/01/24]
29. Bachsais M, Salti S, Zaoui K, et al. CD154 inhibits death of T cells via a Cis interaction with the alpha5beta1 integrin. *PLoS One* 2020;15(8):e0235753. doi: 10.1371/journal.pone.0235753
30. Cai L, Li Y, Tan J, et al. Targeting LAG-3, TIM-3, and TIGIT for cancer immunotherapy. *J Hematol Oncol* 2023;16(1):101. doi: 10.1186/s13045-023-01499-1 [published Online First: 2023/09/06]
31. Wei SC, Levine JH, Cogdill AP, et al. Distinct Cellular Mechanisms Underlie Anti-CTLA-4 and Anti-PD-1 Checkpoint Blockade. *Cell* 2017;170(6):1120-33 e17. doi: 10.1016/j.cell.2017.07.024 [published Online First: 2017/08/15]
32. Buchbinder EI, Desai A. CTLA-4 and PD-1 Pathways: Similarities, Differences, and Implications of Their Inhibition. *Am J Clin Oncol* 2016;39(1):98-106. doi: 10.1097/COC.0000000000000239 [published Online First: 2015/11/13]
33. Wei SC, Duffy CR, Allison JP. Fundamental Mechanisms of Immune Checkpoint Blockade Therapy. *Cancer Discov* 2018;8(9):1069-86. doi: 10.1158/2159-8290.CD-18-0367 [published Online First: 2018/08/18]
34. Anderson AC, Joller N, Kuchroo VK. Lag-3, Tim-3, and TIGIT: Co-inhibitory Receptors with Specialized Functions in Immune Regulation. *Immunity* 2016;44(5):989-1004. doi: 10.1016/j.immuni.2016.05.001 [published Online First: 2016/05/19]
35. Sucker A, Zhao F, Pieper N, et al. Acquired IFNgamma resistance impairs anti-tumor immunity and gives rise to T-cell-resistant melanoma lesions. *Nat Commun* 2017;8:15440. doi: 10.1038/ncomms15440 [published Online First: 2017/06/01]

36. Kamphorst AO, Pillai RN, Yang S, et al. Proliferation of PD-1+ CD8 T cells in peripheral blood after PD-1-targeted therapy in lung cancer patients. *Proc Natl Acad Sci U S A* 2017;114(19):4993-98. doi: 10.1073/pnas.1705327114 [published Online First: 2017/04/28]
37. Huang AC, Orlowski RJ, Xu X, et al. A single dose of neoadjuvant PD-1 blockade predicts clinical outcomes in resectable melanoma. *Nat Med* 2019;25(3):454-61. doi: 10.1038/s41591-019-0357-y [published Online First: 2019/02/26]
38. Vignali DA, Collison LW, Workman CJ. How regulatory T cells work. *Nat Rev Immunol* 2008;8(7):523-32. doi: 10.1038/nri2343 [published Online First: 2008/06/21]
39. Owen DL, Sjaastad LE, Farrar MA. Regulatory T Cell Development in the Thymus. *J Immunol* 2019;203(8):2031-41. doi: 10.4049/jimmunol.1900662 [published Online First: 2019/10/09]
40. Sun CM, Hall JA, Blank RB, et al. Small intestine lamina propria dendritic cells promote de novo generation of Foxp3 T reg cells via retinoic acid. *J Exp Med* 2007;204(8):1775-85. doi: 10.1084/jem.20070602 [published Online First: 2007/07/11]
41. Santegoets SJ, Dijkgraaf EM, Battaglia A, et al. Monitoring regulatory T cells in clinical samples: consensus on an essential marker set and gating strategy for regulatory T cell analysis by flow cytometry. *Cancer Immunol Immunother* 2015;64(10):1271-86. doi: 10.1007/s00262-015-1729-x [published Online First: 2015/07/01]
42. Sakaguchi S, Mikami N, Wing JB, et al. Regulatory T Cells and Human Disease. *Annu Rev Immunol* 2020;38:541-66. doi: 10.1146/annurev-immunol-042718-041717 [published Online First: 2020/02/06]
43. Martens A, Wistuba-Hamprecht K, Geukes Foppen M, et al. Baseline Peripheral Blood Biomarkers Associated with Clinical Outcome of Advanced Melanoma Patients Treated with Ipilimumab. *Clin Cancer Res* 2016;22(12):2908-18. doi: 10.1158/1078-0432.CCR-15-2412 [published Online First: 2016/01/21]
44. Salama P, Phillips M, Grieu F, et al. Tumor-infiltrating FOXP3+ T regulatory cells show strong prognostic significance in colorectal cancer. *J Clin Oncol* 2009;27(2):186-92. doi: 10.1200/JCO.2008.18.7229 [published Online First: 2008/12/10]
45. Gabrilovich DI, Nagaraj S. Myeloid-derived suppressor cells as regulators of the immune system. *Nat Rev Immunol* 2009;9(3):162-74. doi: 10.1038/nri2506 [published Online First: 2009/02/07]
46. Cassetta L, Baekkevold ES, Brandau S, et al. Deciphering myeloid-derived suppressor cells: isolation and markers in humans, mice and non-human primates. *Cancer Immunol Immunother* 2019;68(4):687-97. doi: 10.1007/s00262-019-02302-2
47. Fleming V, Hu X, Weber R, et al. Targeting Myeloid-Derived Suppressor Cells to Bypass Tumor-Induced Immunosuppression. *Front Immunol* 2018;9:398. doi: 10.3389/fimmu.2018.00398 [published Online First: 2018/03/20]
48. Groth C, Hu X, Weber R, et al. Immunosuppression mediated by myeloid-derived suppressor cells (MDSCs) during tumour progression. *Br J Cancer* 2019;120(1):16-25. doi: 10.1038/s41416-018-0333-1 [published Online First: 2018/11/11]
49. Veglia F, Sanseviero E, Gabrilovich DI. Myeloid-derived suppressor cells in the era of increasing myeloid cell diversity. *Nat Rev Immunol* 2021;21(8):485-98. doi: 10.1038/s41577-020-00490-y [published Online First: 2021/02/03]
50. Bayik D, Tross D, Klinman DM. Factors Influencing the Differentiation of Human Monocytic Myeloid-Derived Suppressor Cells Into Inflammatory Macrophages. *Front Immunol* 2018;9:608. doi: 10.3389/fimmu.2018.00608 [published Online First: 2018/04/11]
51. Bronte V, Brandau S, Chen SH, et al. Recommendations for myeloid-derived suppressor cell nomenclature and characterization standards. *Nat Commun* 2016;7:12150. doi: 10.1038/ncomms12150 [published Online First: 2016/07/07]
52. Ostrand-Rosenberg S, Fenselau C. Myeloid-Derived Suppressor Cells: Immune-Suppressive Cells That Impair Antitumor Immunity and Are Sculpted by Their Environment. *J Immunol* 2018;200(2):422-31. doi: 10.4049/jimmunol.1701019 [published Online First: 2018/01/10]

53. Khan ANH, Emmons TR, Wong JT, et al. Quantification of Early-Stage Myeloid-Derived Suppressor Cells in Cancer Requires Excluding Basophils. *Cancer Immunol Res* 2020;8(6):819-28. doi: 10.1158/2326-6066.CIR-19-0556 [published Online First: 2020/04/03]
54. Jimenez-Cortegana C, Galassi C, Klapp V, et al. Myeloid-Derived Suppressor Cells and Radiotherapy. *Cancer Immunol Res* 2022:OF1-OF13. doi: 10.1158/2326-6066.CIR-21-1105 [published Online First: 2022/04/16]
55. Wang S, Tan Q, Hou Y, et al. Emerging Roles of Myeloid-Derived Suppressor Cells in Diabetes. *Front Pharmacol* 2021;12:798320. doi: 10.3389/fphar.2021.798320 [published Online First: 2022/01/04]
56. Erdmann F, Spix C, Katalinic A, et al. Krebs in Deutschland

für 2017/2018. In: institut RK, ed., 2021.
57. Saginala K, Barsouk A, Aluru JS, et al. Epidemiology of Melanoma. *Med Sci (Basel)* 2021;9(4) doi: 10.3390/medsci9040063 [published Online First: 2021/10/27]
58. Jenkins RW, Fisher DE. Treatment of Advanced Melanoma in 2020 and Beyond. *J Invest Dermatol* 2021;141(1):23-31. doi: 10.1016/j.jid.2020.03.943 [published Online First: 2020/04/09]
59. Alexandrov LB, Nik-Zainal S, Wedge DC, et al. Signatures of mutational processes in human cancer. *Nature* 2013;500(7463):415-21. doi: 10.1038/nature12477 [published Online First: 2013/08/16]
60. Balch CM, Gershenwald JE, Soong SJ, et al. Final version of 2009 AJCC melanoma staging and classification. *J Clin Oncol* 2009;27(36):6199-206. doi: 10.1200/JCO.2009.23.4799 [published Online First: 2009/11/18]
61. Keung EZ, Gershenwald JE. The eighth edition American Joint Committee on Cancer (AJCC) melanoma staging system: implications for melanoma treatment and care. *Expert Rev Anticancer Ther* 2018;18(8):775-84. doi: 10.1080/14737140.2018.1489246 [published Online First: 2018/06/21]
62. Kumar AB, Aguilera JV, Velazquez A, et al. The role of serum lactate dehydrogenase level as a prognostic indicator in resected, high risk melanoma. *Dermatol Ther* 2019;32(2):e12813. doi: 10.1111/dth.12813 [published Online First: 2019/01/09]
63. Miao P, Sheng S, Sun X, et al. Lactate dehydrogenase A in cancer: a promising target for diagnosis and therapy. *IUBMB Life* 2013;65(11):904-10. doi: 10.1002/iub.1216 [published Online First: 2013/11/23]
64. Forschner A, Eichner F, Amaral T, et al. Improvement of overall survival in stage IV melanoma patients during 2011-2014: analysis of real-world data in 441 patients of the German Central Malignant Melanoma Registry (CMMR). *J Cancer Res Clin Oncol* 2017;143(3):533-40. doi: 10.1007/s00432-016-2309-y [published Online First: 2016/11/24]
65. Millet A, Martin AR, Ronco C, et al. Metastatic Melanoma: Insights Into the Evolution of the Treatments and Future Challenges. *Med Res Rev* 2017;37(1):98-148. doi: 10.1002/med.21404 [published Online First: 2016/08/30]
66. Achkar T, Tarhini AA. The use of immunotherapy in the treatment of melanoma. *J Hematol Oncol* 2017;10(1):88. doi: 10.1186/s13045-017-0458-3 [published Online First: 2017/04/25]
67. Gong J, Chehrazi-Raffle A, Reddi S, et al. Development of PD-1 and PD-L1 inhibitors as a form of cancer immunotherapy: a comprehensive review of registration trials and future considerations. *J Immunother Cancer* 2018;6(1):8. doi: 10.1186/s40425-018-0316-z [published Online First: 2018/01/24]
68. Pilard C, Ancion M, Delvenne P, et al. Cancer immunotherapy: it's time to better predict patients' response. *Br J Cancer* 2021;125(7):927-38. doi: 10.1038/s41416-021-01413-x [published Online First: 2021/06/12]
69. Hodi FS, O'Day SJ, McDermott DF, et al. Improved survival with ipilimumab in patients with metastatic melanoma. *N Engl J Med* 2010;363(8):711-23. doi: 10.1056/NEJMoa1003466 [published Online First: 2010/06/08]
70. . https://www.nobelprize.org/prizes/medicine/2018/press-release/: Nobel Prize, 2018.

71. Michielin O, Atkins MB, Koon HB, et al. Evolving impact of long-term survival results on metastatic melanoma treatment. *J Immunother Cancer* 2020;8(2) doi: 10.1136/jitc-2020-000948 [published Online First: 2020/10/11]
72. Kreidieh FY, Tawbi HA. The introduction of LAG-3 checkpoint blockade in melanoma: immunotherapy landscape beyond PD-1 and CTLA-4 inhibition. *Ther Adv Med Oncol* 2023;15:17588359231186027. doi: 10.1177/17588359231186027 [published Online First: 2023/07/24]
73. Atkinson V, Khattak A, Haydon A, et al. Eftilagimod alpha, a soluble lymphocyte activation gene-3 (LAG-3) protein plus pembrolizumab in patients with metastatic melanoma. *J Immunother Cancer* 2020;8(2) doi: 10.1136/jitc-2020-001681 [published Online First: 2020/11/22]
74. Tawbi HA, Schadendorf D, Lipson EJ, et al. Relatlimab and Nivolumab versus Nivolumab in Untreated Advanced Melanoma. *N Engl J Med* 2022;386(1):24-34. doi: 10.1056/NEJMoa2109970 [published Online First: 2022/01/06]
75. Wolchok JD, Chiarion-Sileni V, Gonzalez R, et al. Overall Survival with Combined Nivolumab and Ipilimumab in Advanced Melanoma. *N Engl J Med* 2017;377(14):1345-56. doi: 10.1056/NEJMoa1709684
76. Garbe C, Amaral T, Peris K, et al. European consensus-based interdisciplinary guideline for melanoma. Part 1: Diagnostics: Update 2022. *Eur J Cancer* 2022;170:236-55. doi: 10.1016/j.ejca.2022.03.008 [published Online First: 2022/05/16]
77. Rizk EM, Seffens AM, Trager MH, et al. Biomarkers Predictive of Survival and Response to Immune Checkpoint Inhibitors in Melanoma. *Am J Clin Dermatol* 2020;21(1):1-11. doi: 10.1007/s40257-019-00475-1 [published Online First: 2019/10/12]
78. Wagner NB, Forschner A, Leiter U, et al. S100B and LDH as early prognostic markers for response and overall survival in melanoma patients treated with anti-PD-1 or combined anti-PD-1 plus anti-CTLA-4 antibodies. *Br J Cancer* 2018;119(3):339-46. doi: 10.1038/s41416-018-0167-x [published Online First: 2018/06/29]
79. Weide B, Martens A, Hassel JC, et al. Baseline Biomarkers for Outcome of Melanoma Patients Treated with Pembrolizumab. *Clin Cancer Res* 2016;22(22):5487-96. doi: 10.1158/1078-0432.CCR-16-0127 [published Online First: 2016/11/01]
80. Capone M, Giannarelli D, Mallardo D, et al. Baseline neutrophil-to-lymphocyte ratio (NLR) and derived NLR could predict overall survival in patients with advanced melanoma treated with nivolumab. *J Immunother Cancer* 2018;6(1):74. doi: 10.1186/s40425-018-0383-1 [published Online First: 2018/07/18]
81. Valero C, Lee M, Hoen D, et al. Pretreatment neutrophil-to-lymphocyte ratio and mutational burden as biomarkers of tumor response to immune checkpoint inhibitors. *Nat Commun* 2021;12(1):729. doi: 10.1038/s41467-021-20935-9 [published Online First: 2021/02/03]
82. Krieg C, Nowicka M, Guglietta S, et al. High-dimensional single-cell analysis predicts response to anti-PD-1 immunotherapy. *Nat Med* 2018;24(2):144-53. doi: 10.1038/nm.4466
83. Pico de Coana Y, Wolodarski M, van der Haar Avila I, et al. PD-1 checkpoint blockade in advanced melanoma patients: NK cells, monocytic subsets and host PD-L1 expression as predictive biomarker candidates. *Oncoimmunology* 2020;9(1):1786888. doi: 10.1080/2162402X.2020.1786888 [published Online First: 2020/09/18]
84. Weber J, Gibney G, Kudchadkar R, et al. Phase I/II Study of Metastatic Melanoma Patients Treated with Nivolumab Who Had Progressed after Ipilimumab. *Cancer Immunol Res* 2016;4(4):345-53. doi: 10.1158/2326-6066.CIR-15-0193 [published Online First: 2016/02/14]
85. Zhou X, Ni Y, Liang X, et al. Mechanisms of tumor resistance to immune checkpoint blockade and combination strategies to overcome resistance. *Front Immunol* 2022;13:915094. doi: 10.3389/fimmu.2022.915094 [published Online First: 2022/10/04]
86. Li L, Goedegebuure SP, Gillanders W. Cancer vaccines: shared tumor antigens return to the spotlight. *Signal Transduct Target Ther* 2020;5(1):251. doi: 10.1038/s41392-020-00364-8 [published Online First: 2020/11/01]

87. Sahin U, Oehm P, Derhovanessian E, et al. An RNA vaccine drives immunity in checkpoint-inhibitor-treated melanoma. *Nature* 2020;585(7823):107-12. doi: 10.1038/s41586-020-2537-9 [published Online First: 2020/07/31]
88. Krebs FK, Trzeciak ER, Zimmer S, et al. Immune signature as predictive marker for response to checkpoint inhibitor immunotherapy and overall survival in melanoma. *Cancer Med* 2021;10(5):1562-75. doi: 10.1002/cam4.3710 [published Online First: 2021/01/16]
89. Baltussen JC, Welters MJP, Verdegaal EME, et al. Predictive Biomarkers for Outcomes of Immune Checkpoint Inhibitors (ICIs) in Melanoma: A Systematic Review. *Cancers (Basel)* 2021;13(24) doi: 10.3390/cancers13246366 [published Online First: 2021/12/25]
90. Zelba H, Bedke J, Hennenlotter J, et al. PD-1 and LAG-3 Dominate Checkpoint Receptor-Mediated T-cell Inhibition in Renal Cell Carcinoma. *Cancer Immunol Res* 2019;7(11):1891-99. doi: 10.1158/2326-6066.CIR-19-0146 [published Online First: 2019/09/06]
91. Thommen DS, Schumacher TN. T Cell Dysfunction in Cancer. *Cancer Cell* 2018;33(4):547-62. doi: 10.1016/j.ccell.2018.03.012
92. Gangaev A, Rozeman EA, Rohaan MW, et al. Differential effects of PD-1 and CTLA-4 blockade on the melanoma-reactive CD8 T cell response. *Proc Natl Acad Sci U S A* 2021;118(43) doi: 10.1073/pnas.2102849118
93. Weide B, Zelba H, Derhovanessian E, et al. Functional T Cells Targeting NY-ESO-1 or Melan-A Are Predictive for Survival of Patients With Distant Melanoma Metastasis. *Journal of Clinical Oncology* 2012;30(15):1835-41. doi: 10.1200/jco.2011.40.2271
94. Zelba H, Weide B, Martens A, et al. Circulating CD4+ T cells that produce IL4 or IL17 when stimulated by melan-A but not by NY-ESO-1 have negative impacts on survival of patients with stage IV melanoma. *Clin Cancer Res* 2014;20(16):4390-9. doi: 10.1158/1078-0432.CCR-14-1015
95. [Available from: https://cellero.com/blog/ask-scientist-half-caucasian-population/.
96. Hadrup SR, Newell EW. Determining T-cell specificity to understand and treat disease. *Nat Biomed Eng* 2017;1(10):784-95. doi: 10.1038/s41551-017-0143-4 [published Online First: 2017/10/01]
97. Vyasamneni R, Kohler V, Karki B, et al. A universal MHCII technology platform to characterize antigen-specific CD4(+) T cells. *Cell Rep Methods* 2023;3(1):100388. doi: 10.1016/j.crmeth.2022.100388 [published Online First: 2023/02/24]
98. Seder RA, Darrah PA, Roederer M. T-cell quality in memory and protection: implications for vaccine design. *Nat Rev Immunol* 2008;8(4):247-58. doi: 10.1038/nri2274 [published Online First: 2008/03/08]
99. Tay RE, Richardson EK, Toh HC. Revisiting the role of CD4(+) T cells in cancer immunotherapy-new insights into old paradigms. *Cancer Gene Ther* 2021;28(1-2):5-17. doi: 10.1038/s41417-020-0183-x [published Online First: 2020/05/28]
100. Hall MS, Teer JK, Yu X, et al. Neoantigen-specific CD4(+) tumor-infiltrating lymphocytes are potent effectors identified within adoptive cell therapy products for metastatic melanoma patients. *J Immunother Cancer* 2023;11(10) doi: 10.1136/jitc-2023-007288 [published Online First: 2023/10/08]
101. Ott PA, Hu Z, Keskin DB, et al. An immunogenic personal neoantigen vaccine for patients with melanoma. *Nature* 2017;547(7662):217-21. doi: 10.1038/nature22991 [published Online First: 2017/07/06]
102. Gambichler T, Schroter U, Hoxtermann S, et al. Decline of programmed death-1-positive circulating T regulatory cells predicts more favourable clinical outcome of patients with melanoma under immune checkpoint blockade. *Br J Dermatol* 2020;182(5):1214-20. doi: 10.1111/bjd.18379 [published Online First: 2019/07/31]
103. Kannanganat S, Ibegbu C, Chennareddi L, et al. Multiple-cytokine-producing antiviral CD4 T cells are functionally superior to single-cytokine-producing cells. *J Virol* 2007;81(16):8468-76. doi: 10.1128/JVI.00228-07 [published Online First: 2007/06/08]
104. Martens A, Wistuba-Hamprecht K, Foppen MG, et al. Baseline Peripheral Blood Biomarkers Associated with Clinical Outcome of Advanced Melanoma Patients Treated with Ipilimumab. *Clinical Cancer Research* 2016;22(12):2908-18. doi: 10.1158/1078-0432.ccr-15-2412

105. Weide B, Martens A, Zelba H, et al. Myeloid-derived suppressor cells predict survival of patients with advanced melanoma: comparison with regulatory T cells and NY-ESO-1- or melan-A-specific T cells. *Clin Cancer Res* 2014;20(6):1601-9. doi: 10.1158/1078-0432.CCR-13-2508
106. Pico de Coana Y, Masucci G, Hansson J, et al. Myeloid-derived suppressor cells and their role in CTLA-4 blockade therapy. *Cancer Immunol Immunother* 2014;63(9):977-83. doi: 10.1007/s00262-014-1570-7
107. Gaissler A, Bochem J, Spreuer J, et al. Early decrease of blood myeloid-derived suppressor cells during checkpoint inhibition is a favorable biomarker in metastatic melanoma. *J Immunother Cancer* 2023;11(6) doi: 10.1136/jitc-2023-006802 [published Online First: 2023/06/08]
108. Gorman JV, Colgan JD. Regulation of T cell responses by the receptor molecule Tim-3. *Immunol Res* 2014;59(1-3):56-65. doi: 10.1007/s12026-014-8524-1 [published Online First: 2014/05/16]
109. Maruhashi T, Sugiura D, Okazaki IM, et al. LAG-3: from molecular functions to clinical applications. *J Immunother Cancer* 2020;8(2) doi: 10.1136/jitc-2020-001014 [published Online First: 2020/09/16]
110. Gaißler A, Meldgaard TS, Heeke C, et al. Dynamics of Melanoma-Associated Epitope-Specific CD8+ T Cells in the Blood Correlate With Clinical Outcome Under PD-1 Blockade. *Frontiers in Immunology* 2022;13 doi: 10.3389/fimmu.2022.906352
111. Strauss L, Mahmoud MAA, Weaver JD, et al. Targeted deletion of PD-1 in myeloid cells induces antitumor immunity. *Sci Immunol* 2020;5(43) doi: 10.1126/sciimmunol.aay1863 [published Online First: 2020/01/05]
112. Huang AC, Zappasodi R. A decade of checkpoint blockade immunotherapy in melanoma: understanding the molecular basis for immune sensitivity and resistance. *Nat Immunol* 2022;23(5):660-70. doi: 10.1038/s41590-022-01141-1 [published Online First: 2022/03/05]
113. Gueguen P, Metoikidou C, Dupic T, et al. Contribution of resident and circulating precursors to tumor-infiltrating CD8(+) T cell populations in lung cancer. *Sci Immunol* 2021;6(55) doi: 10.1126/sciimmunol.abd5778 [published Online First: 2021/01/31]
114. Oliveira G, Stromhaug K, Klaeger S, et al. Phenotype, specificity and avidity of antitumour CD8(+) T cells in melanoma. *Nature* 2021;596(7870):119-25. doi: 10.1038/s41586-021-03704-y [published Online First: 2021/07/23]
115. Oliveira G, Stromhaug K, Cieri N, et al. Landscape of helper and regulatory antitumour CD4(+) T cells in melanoma. *Nature* 2022 doi: 10.1038/s41586-022-04682-5 [published Online First: 2022/05/05]
116. Menares E, Galvez-Cancino F, Caceres-Morgado P, et al. Tissue-resident memory CD8(+) T cells amplify anti-tumor immunity by triggering antigen spreading through dendritic cells. *Nat Commun* 2019;10(1):4401. doi: 10.1038/s41467-019-12319-x
117. Tvingsholm SA, Frej MS, Rafa VM, et al. TCR-engaging scaffolds selectively expand antigen-specific T-cells with a favorable phenotype for adoptive cell therapy. *J Immunother Cancer* 2023;11(8) doi: 10.1136/jitc-2023-006847 [published Online First: 2023/08/17]
118. van der Woude LL, Gorris MAJ, Halilovic A, et al. Migrating into the Tumor: a Roadmap for T Cells. *Trends Cancer* 2017;3(11):797-808. doi: 10.1016/j.trecan.2017.09.006 [published Online First: 2017/11/10]
119. Ribas A, Shin DS, Zaretsky J, et al. PD-1 Blockade Expands Intratumoral Memory T Cells. *Cancer Immunol Res* 2016;4(3):194-203. doi: 10.1158/2326-6066.CIR-15-0210 [published Online First: 2016/01/21]
120. Bawden EG, Wagner T, Schroder J, et al. CD4(+) T cell immunity against cutaneous melanoma encompasses multifaceted MHC II-dependent responses. *Sci Immunol* 2024;9(91):eadi9517. doi: 10.1126/sciimmunol.adi9517 [published Online First: 2024/01/19]
121. Graff-Dubois S, Faure O, Gross DA, et al. Generation of CTL recognizing an HLA-A*0201-restricted epitope shared by MAGE-A1, -A2, -A3, -A4, -A6, -A10, and -A12 tumor antigens: implication in a broad-spectrum tumor immunotherapy. *J Immunol* 2002;169(1):575-80. doi: 10.4049/jimmunol.169.1.575

122. Bentzen AK, Hadrup SR. Evolution of MHC-based technologies used for detection of antigen-responsive T cells. *Cancer Immunol Immunother* 2017;66(5):657-66. doi: 10.1007/s00262-017-1971-5 [published Online First: 2017/03/21]
123. Das M, Zhu C, Kuchroo VK. Tim-3 and its role in regulating anti-tumor immunity. *Immunol Rev* 2017;276(1):97-111. doi: 10.1111/imr.12520 [published Online First: 2017/03/05]
124. Acharya N, Sabatos-Peyton C, Anderson AC. Tim-3 finds its place in the cancer immunotherapy landscape. *J Immunother Cancer* 2020;8(1) doi: 10.1136/jitc-2020-000911 [published Online First: 2020/07/01]
125. Gestermann N, Saugy D, Martignier C, et al. LAG-3 and PD-1+LAG-3 inhibition promote anti-tumor immune responses in human autologous melanoma/T cell co-cultures. *Oncoimmunology* 2020;9(1):1736792. doi: 10.1080/2162402X.2020.1736792 [published Online First: 2020/08/28]
126. Lowther DE, Goods BA, Lucca LE, et al. PD-1 marks dysfunctional regulatory T cells in malignant gliomas. *JCI Insight* 2016;1(5) doi: 10.1172/jci.insight.85935 [published Online First: 2016/05/18]
127. Liu Y, Lu P, Ma Y, et al. Peripheral Polyfunctional PD1(+) CD8(+) T cells demonstrated strong immune protection in non-small cell lung cancer. *Eur J Immunol* 2022 doi: 10.1002/eji.202149570 [published Online First: 2022/06/12]
128. Kumagai S, Togashi Y, Kamada T, et al. The PD-1 expression balance between effector and regulatory T cells predicts the clinical efficacy of PD-1 blockade therapies. *Nat Immunol* 2020;21(11):1346-58. doi: 10.1038/s41590-020-0769-3 [published Online First: 2020/09/02]
129. de Coana YP, Wolodarski M, Poschke I, et al. Ipilimumab treatment decreases monocytic MDSCs and increases CD8 effector memory T cells in long-term survivors with advanced melanoma. *Oncotarget* 2017;8(13):21539-53. doi: 10.18632/oncotarget.15368 [published Online First: 2017/04/21]
130. Marcos Rubio A, Everaert C, Van Damme E, et al. Circulating immune cell dynamics as outcome predictors for immunotherapy in non-small cell lung cancer. *J Immunother Cancer* 2023;11(8) doi: 10.1136/jitc-2023-007023 [published Online First: 2023/08/04]
131. Hedrick CC, Malanchi I. Neutrophils in cancer: heterogeneous and multifaceted. *Nat Rev Immunol* 2022;22(3):173-87. doi: 10.1038/s41577-021-00571-6 [published Online First: 2021/07/08]
132. Zhou J, Nefedova Y, Lei A, et al. Neutrophils and PMN-MDSC: Their biological role and interaction with stromal cells. *Semin Immunol* 2018;35:19-28. doi: 10.1016/j.smim.2017.12.004 [published Online First: 2017/12/20]
133. Adeshakin AO, Adeshakin FO, Yan D, et al. Regulating Histone Deacetylase Signaling Pathways of Myeloid-Derived Suppressor Cells Enhanced T Cell-Based Immunotherapy. *Front Immunol* 2022;13:781660. doi: 10.3389/fimmu.2022.781660 [published Online First: 2022/02/11]
134. Shi H, Li K, Ni Y, et al. Myeloid-Derived Suppressor Cells: Implications in the Resistance of Malignant Tumors to T Cell-Based Immunotherapy. *Front Cell Dev Biol* 2021;9:707198. doi: 10.3389/fcell.2021.707198 [published Online First: 2021/08/03]
135. OuYang LY, Wu XJ, Ye SB, et al. Tumor-induced myeloid-derived suppressor cells promote tumor progression through oxidative metabolism in human colorectal cancer. *J Transl Med* 2015;13:47. doi: 10.1186/s12967-015-0410-7 [published Online First: 2015/02/02]
136. Li X, Zhong J, Deng X, et al. Targeting Myeloid-Derived Suppressor Cells to Enhance the Antitumor Efficacy of Immune Checkpoint Blockade Therapy. *Front Immunol* 2021;12:754196. doi: 10.3389/fimmu.2021.754196 [published Online First: 2022/01/11]
137. Hubert P, Roncarati P, Demoulin S, et al. Extracellular HMGB1 blockade inhibits tumor growth through profoundly remodeling immune microenvironment and enhances checkpoint inhibitor-based immunotherapy. *J Immunother Cancer* 2021;9(3) doi: 10.1136/jitc-2020-001966 [published Online First: 2021/03/14]
138. Kotsakis A, Harasymczuk M, Schilling B, et al. Myeloid-derived suppressor cell measurements in fresh and cryopreserved blood samples. *J Immunol Methods* 2012;381(1-2):14-22. doi: 10.1016/j.jim.2012.04.004 [published Online First: 2012/04/24]

139. Huber V, Di Guardo L, Lalli L, et al. Back to simplicity: a four-marker blood cell score to quantify prognostically relevant myeloid cells in melanoma patients. *J Immunother Cancer* 2021;9(2) doi: 10.1136/jitc-2020-001167 [published Online First: 2021/02/17]
140. Mandruzzato S, Brandau S, Britten CM, et al. Toward harmonized phenotyping of human myeloid-derived suppressor cells by flow cytometry: results from an interim study. *Cancer Immunol Immunother* 2016;65(2):161-9. doi: 10.1007/s00262-015-1782-5 [published Online First: 2016/01/06]

Appendix

1. Gaißler A, Meldgaard TS, Heeke C, Babaei S, Tvingsholm SA, Bochem J, Spreuer J, Amaral T, Wagner NB, Klein R, Meier F, Garbe C, Eigentler TK, Pawelec G, Claassen M, Weide B, Hadrup SR and Wistuba-Hamprecht K. Dynamics of Melanoma-Associated Epitope-Specific CD8+ T Cells in the Blood Correlate With Clinical Outcome Under PD-1 Blockade. Front. Immunol. 13:906352 (2022); doi: 10.3389/fimmu.2022.906352

2. Gaißler A, Babaei S, Bochem J, Spreuer J, Amaral T, Wagner N B, Claassen M, Weide B, Pawelec G, Eigentler K and Wistuba-Hamprecht K. Early disappearance of blood derived, multifunctional MAGE-A10 and TRP-2-reactive CD4+ T cells in melanoma under anti-PD-1 checkpoint blockade associate with improved survival. (Unsubmitted Manuscript)

3. Gaißler A*, Bochem J*, Spreuer J, Ottman S, Martens A, Amaral T, Wagner N B, Claassen M, Meier F, Terheyden P, Garbe C, Eigentler T, Weide B, Pawelec G and Wistuba-Hamprecht K. Early decrease of blood myeloid-derived suppressor cells during checkpoint inhibition is a favorable biomarker in metastatic melanoma. Journal for ImmunoTherapy of Cancer; 11:e006802 2023. doi:10.1136/jitc-2023-006802. * shared authorship

frontiers | Frontiers in Immunology

ORIGINAL RESEARCH
published: 07 July 2022
doi: 10.3389/fimmu.2022.906352

Dynamics of Melanoma-Associated Epitope-Specific CD8+ T Cells in the Blood Correlate With Clinical Outcome Under PD-1 Blockade

Andrea Gaißler[1,2], Trine Sundebo Meldgaard[3], Christina Heeke[3], Sepideh Babaei[2], Siri Amanda Tvingsholm[3], Jonas Bochem[1,2], Janine Spreuer[1,2], Teresa Amaral[1,4], Nikolaus Benjamin Wagner[1,5], Reinhild Klein[6], Friedegund Meier[7,8], Claus Garbe[1], Thomas K. Eigentler[9], Graham Pawelec[10,11], Manfred Claassen[2,12], Benjamin Weide[1], Sine Reker Hadrup[3†] and Kilian Wistuba-Hamprecht[1,2,10†]*

[1] Department of Dermatology, University Hospital Tübingen, Eberhard Karls University of Tübingen, Tübingen, Germany, [2] Internal Medicine I, University Hospital Tübingen, Eberhard Karls University of Tübingen, Tübingen, Germany, [3] Department of Health Technology, Danmarks Tekniske Universitet (DTU) HEALTH TECH, Copenhagen, Denmark, [4] Excellence Cluster (EXC) 2180, "Image Guided and Functionally Instructed Tumor Therapies" (iFIT), Tübingen, Germany, [5] Department of Dermatology, Venereology and Allergology, Kantonsspital St. Gallen, St. Gallen, Switzerland, [6] Internal Medicine II, University Hospital Tübingen, Eberhard Karls University of Tübingen, Tübingen, Germany, [7] Skin Cancer Center at the University Cancer Centre and National Center for Tumor Diseases Dresden, Dresden, Germany, [8] Department of Dermatology, Faculty of Medicine and University Hospital Carl Gustav Carus, Technische Universität Dresden, Dresden, Germany, [9] Department of Dermatology, Venereology and Allergology, Charité – Universitätsmedizin Berlin, corporate member of Freie Universität Berlin and Humboldt-Universität zu Berlin, Berlin, Germany, [10] Department of Immunology, Interfaculty Institute for Cell Biology, Eberhard Karls University Tübingen, Tübingen, Germany, [11] Health Sciences North Research Institute, Sudbury, ON, Canada, [12] Department of Computer Science, Eberhard Karls University of Tübingen, Tübingen, Germany

Immune checkpoint blockade (ICB) is standard-of-care for patients with metastatic melanoma. It may re-invigorate T cells recognizing tumors, and several tumor antigens have been identified as potential targets. However, little is known about the dynamics of tumor antigen-specific T cells in the circulation, which might provide valuable information on ICB responses in a minimally invasive manner. Here, we investigated individual signatures composed of up to 167 different melanoma-associated epitope (MAE)-specific CD8+ T cells in the blood of stage IV melanoma patients before and during anti-PD-1 treatment, using a peptide-loaded multimer-based high-throughput approach. Additionally, checkpoint receptor expression patterns on T cell subsets and frequencies of myeloid-derived suppressor cells and regulatory T cells were quantified by flow cytometry. Regression analysis using the MAE-specific CD8+ T cell populations was applied to identify those that correlated with overall survival (OS). The abundance of MAE-specific CD8+ T cell populations, as well as their dynamics under therapy, varied between patients. Those with a dominant increase of these T cell populations during PD-1 ICB had a longer OS and progression-free survival than those with decreasing or balanced signatures. Patients with a dominantly increased MAE-specific CD8+ T cell signature also exhibited an increase in TIM-3+ and LAG-3+ T cells. From these results, we created a model predicting improved/reduced OS by combining data on dynamics of the three most

OPEN ACCESS

Edited by:
William L. Redmond, Earle A. Chiles Research Institute, United States

Reviewed by:
Peter Steinberger, Medical University of Vienna, Austria
Carsten Krieg, Medical University of South Carolina, United States

***Correspondence:**
Kilian Wistuba-Hamprecht kilian.wistuba-hamprecht@uni-tuebingen.de

†These authors share last authorship

Specialty section:
This article was submitted to Cancer Immunity and Immunotherapy, a section of the journal Frontiers in Immunology

Received: *28 March 2022*
Accepted: *17 May 2022*
Published: *07 July 2022*

Citation:
Gaißler A, Meldgaard TS, Heeke C, Babaei S, Tvingsholm SA, Bochem J, Spreuer J, Amaral T, Wagner NB, Klein R, Meier F, Garbe C, Eigentler TK, Pawelec G, Claassen M, Weide B, Hadrup SR and Wistuba-Hamprecht K (2022) Dynamics of Melanoma-Associated Epitope-Specific CD8+ T Cells in the Blood Correlate With Clinical Outcome Under PD-1 Blockade. Front. Immunol. 13:906352. doi: 10.3389/fimmu.2022.906352

informative MAE-specific CD8+ T cell populations. Our results provide insights into the dynamics of circulating MAE-specific CD8+ T cell populations during ICB, and should contribute to a better understanding of biomarkers of response and anti-cancer mechanisms.

Keywords: T cells, checkpoint blockade, melanoma, melanoma-associated antigen, regression analysis, dextramer

INTRODUCTION

Immune checkpoint blockade (ICB) (1, 2) has revolutionized the treatment of metastatic melanoma and of an increasing number of other solid cancers (3, 4). Monotherapy with antagonistic antibodies targeting programmed cell death receptor 1 (PD-1, CD279) on the surface of T cells or combination therapy with antagonistic antibodies against cytotoxic T-lymphocyte-associated protein-4 (CTLA-4, CD152) are now standard-of-care treatments for patients with advanced melanoma with 5-year survival rates of approximately 50% (5). Thus, unfortunately, not all patients experience durable clinical benefit (6). Hence, a better understanding of the modes of action of ICB, and biomarkers predicting clinical outcome, are urgently required. Candidate markers such as frequencies of myeloid-derived suppressor cells (MDSCs), or T cell populations with certain phenotypes possess promising biomarker characteristics (7–12). However, defining tumor-specificity of T cells based on their phenotype is challenging, and the described cellular populations often lack proven specificity for the tumor. The high mutational burden of melanoma (13, 14) results in a potentially large number of T cell neo-epitopes derived specifically from the cancer mutagenome and is thus thought to be a key driver of successful ICB (15, 16). T cells recognizing such neo-epitopes may play an important role in anti-tumor immunity by recognizing cancer mutations unique to the tumor and eliminating the cells carrying them (17, 18). Antigens derived from non-mutated genes which are abnormally expressed, or expressed only at low levels by normal tissues [i.e. shared tumor-associated antigens (TAA)], may also contribute to tumor elimination through T cell recognition (19). Consequently, the identification of the products of such abnormally expressed genes that are also immunogenic is a promising approach for the development of new immunotherapy concepts. Unfortunately, due to inter- and intratumor heterogeneity, especially in a metastatic setting, this is only possible in a fragmented manner. An elegant alternative to study such tumor antigens expressed by primary tumors or metastases is to investigate tumor-specific T cells in the peripheral blood, which is the compartment allowing for cellular exchange between different tissues as well as metastases.

Using tests of T cell function, in metastatic melanoma patients not receiving anti-PD-1 treatment we have previously shown that the presence of circulating NY-ESO-1 and Melan-A-reactive T-cells was associated with prolonged overall survival (OS) (7, 20, 21). Also, earlier studies by others revealed that these TAAs might be promising targets for active interventions (22–24). Recently, we reported that the dynamics of NY-ESO-1- and Melan-A-reactive T cells under PD-1 ICB are associated with clinical outcome (25). However, data on the impact of ICB on the presence of circulating TAA-specific T cells (beyond established epitopes like those from NY-ESO-1 or Melan-A) and conclusively the presence of their antigens in the tumors is still limited. However, this is urgently required to supplement the range of T cell targets potentially recognized as a result of ICB induced/modulated TAA expression patterns in the tumor. This could lead to a significantly better understanding of ICB-associated changes/accessibility of TAAs in the tumors of patients who have been successfully treated, and thereby provide opportunities for the development of new immunotherapeutic treatments. Thus, the aim of the present study was to characterize a broad spectrum of a large number of different melanoma-associated epitope (MAE)-specific CD8+ T cell populations and their dynamics in the peripheral blood of anti-PD-1-treated patients to screen for further TAAs with potential clinical relevance. Therefore, we used a defined panel of 167 major histocompatibility complex (MHC) MAE dextramers in an *ex vivo*, high-throughput analytical approach, that also allows the detection of low affinity as well as high affinity T cell receptors (TCR) (26).

MATERIAL AND METHODS

Patient Material

Venous blood samples were obtained from HLA-A*0201+ stage IV melanoma patients (n=36) before [baseline (BL)] and during therapy [follow-up (FU)], at a median of 42 days after the first anti-PD-1 antibody dose (**Figure 1A**). Samples were collected between February 2016 and February 2019 at centers in Tübingen and Dresden. Within 24h of donation, peripheral blood mononuclear cells (PBMCs) were isolated using Ficoll-Hypaque density gradient centrifugation and were immediately cryopreserved until use. Patients' HLA-types were determined using LUMINEX-based high resolution HLA-typing following validated clinical routines (27). Patient characteristics are summarized in **Table 1**. All patients gave their written informed consent for biobanking and use of biomaterials as well as clinical data for scientific evaluation. The Ethics Committee of Tübingen University Hospital approved the study (490/2014BO1, 616/2018BO2).

Determination of MAE-Specific CD8+ T Cells

A library of HLA-A*0201-restricted peptide-loaded MHC (pMHC) multimers ("dextramers") representing a selection of

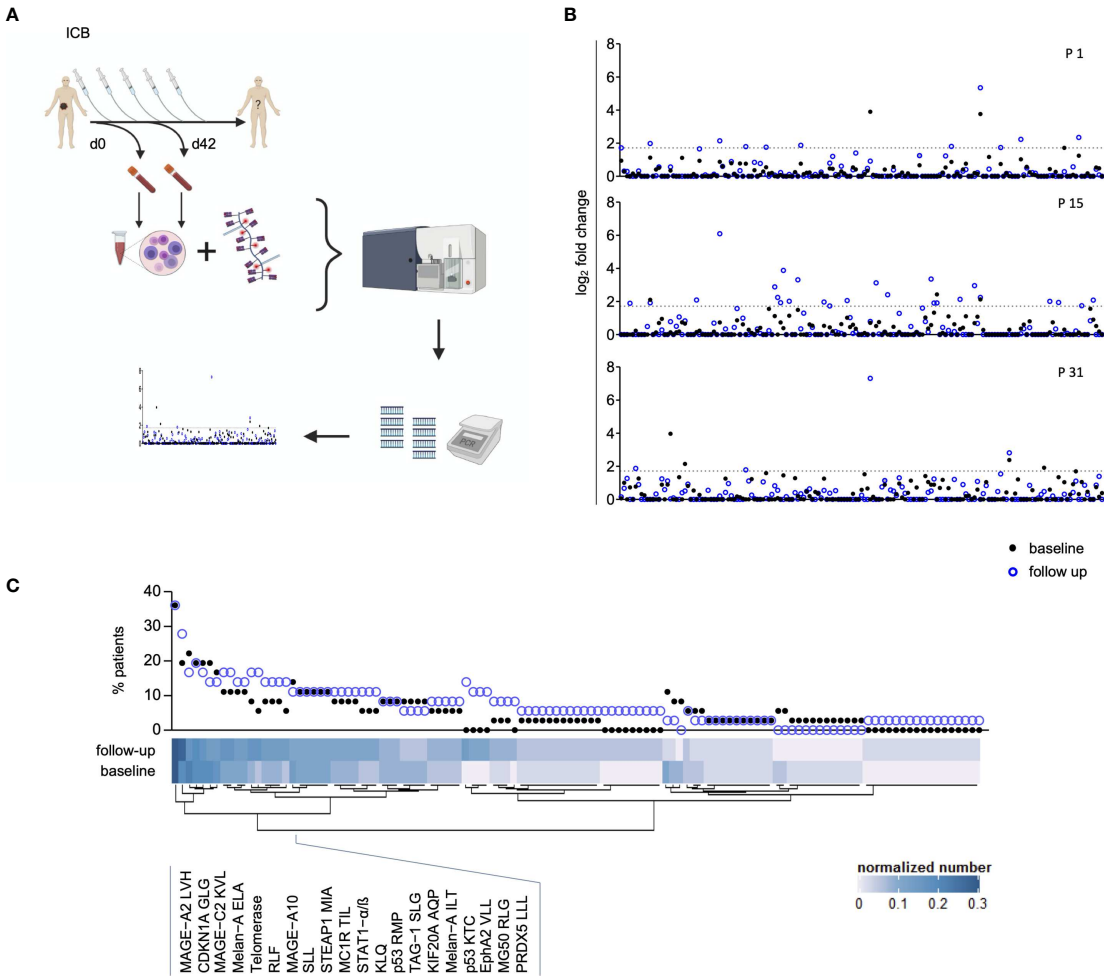

FIGURE 1 | Assessment of peripheral blood Melanoma-Associated Epitope (MAE)-specific CD8+ T cell signatures. The study design is depicted in **(A)** and was created with BioRender.com. Peripheral blood T cell screening profiles of three representative patients using 167 melanoma-associated epitopes. Data on the y-axis present the detected log fold-change of the individual T cell population (x-axis) relative to the input sample. The dotted lines represent the selected threshold level log_2FC **(B)**. The relative abundance of all detected 117 MAE-specific CD8+ T cells at baseline and follow-up within the investigated cohort is depicted in the scatter plot. The normalized numbers of each specific T cell population are illustrated in the heat map **(C)**.

167 MAE (**Figure 1B** and **Supplementary Table 1**) was used to screen cryopreserved PBMC samples for the presence of MAE-specific CD8+ T cells. A dextramer consists of a phycoerythrin-labeled dextran backbone to which multiple pMHC complexes are bound. Each dextramer has two 25-mer DNA barcodes, unique for the respective pMHC complex [for technical details see reference (26)]. The nomenclature used here for the MAE-specific CD8+ T cell populations combines the respective protein name and the first 3 letters of the peptide amino acid sequence (e.g., MAGE-A1 KVL represents the MAGE-A1 peptide with the amino acid sequence KVLEYVIKV).

The samples were treated as follows: PBMCs were thawed in batches and a median number of 5 x 10^6 cells per sample was incubated with the dextramer library. Dead cells were labeled and monoclonal antibodies against CD8 and lineage markers (CD4, CD14, CD16, CD19, CD40) were used to identify CD8+ T cells (**Supplementary Table 2**), followed by overnight fixation using 1% PFA in PBS. The next day, multimer-binding CD8+ T cells were isolated by fluorescence-activated cell sorting (FACS; Melody or Aria fusion, both BD; for gating strategy see **Supplementary Figure 1**). Next, the samples were centrifuged at 5000xg (to break up the cells), supernatant was discarded and the samples were stored as pellets in PBS at -20°C until amplification of the DNA barcodes *via* PCR was carried out. Additionally, an "input" sample (total dextramer library as triplicate) per batch was used to calculate barcode enrichment in individual samples as well as an internal quality control for the amplification of the barcode sequences in each individual sample *via* PCR. The primers employed contained unique DNA sequences (in-house generated "DNA keys") per patient sample to label the resulting DNA libraries for multiplexed sequencing of pooled samples. The PCR-products were

TABLE 1 | Cohort characteristics.

Factor	Category	n	%
Sex	male	24	66.7
	female	12	33.3
Clinical site	Tübingen	34	94.4
	Dresden	2	5.6
Therapy	anti-PD-1	17	47.2
	anti-PD-1 & -CTLA-4	19	52.8
Age	median	68	–
	≥60	22	61.1
	<60	14	38.9
M-category	M1a	2	5.6
(AJCC v7)	M1b	7	19.4
	M1c	24	66.7
	n.a.	3	8.3
HLA-A zygosity	heterozygous	33	91.7
	homozygous	3	8.3
Prior systemic therapies	immunotherapy	6	16.7
	targeted therapy	5	13.9
	chemotherapy	1	2.8
	none	24	66.7
LDH BL	elevated	11	30.6
	normal	25	69.4
LDH FU	elevated	15	41.7
	normal	20	55.6
	unknown	1	2.7

HLA, human leukocyte antigen; LDH, lactate dehydrogenase.

purified (QIAquick PCR purification kit, Qiagen) following the manufacturer´s instructions. The purified samples were then sequenced using the Ion Torrent approach (Thermo Fisher).

Sequencing data were processed by the software package Barracoda, available online at (https://services.healthtech.dtu.dk/service.php?Barracoda-1.8). The tool identifies the DNA barcodes annotated for a given experiment, assigns a sample ID and pMHC specificity to each DNA barcode, and counts the total number of reads and clonally reduced reads for each peptide-MHC-associated DNA barcode. Log_2FC in read counts mapped to a given sample relative to the mean read counts mapped to triplicate baseline samples are estimated using normalization factors determined by the trimmed mean of M-values method. A minimum read count fraction of 0.1% for a given DNA barcode of the total DNA barcode number in that given sample was set as threshold to avoid false-positive detection of T cell responses due to low number of reads in the baseline samples. DNA barcodes with $p<0.01$, estimated using the Benjamini–Hochberg method and $log_2FC>1,5$ over the input values for the total pMHC library were considered as T cell responses. Barracoda outputs were further processed and annotated using an R-based script. Frequency of a pMHC-specific CD8+ T cell population was estimated based on the % read count of the associated barcode relative to the total % multimer-positive CD8+ T cell population. Sum of the estimated frequency represents the pooled frequencies of all T cell populations in a given sample.

Visualization of MAE-Specific CD8+ T Cell Signatures and Their Dynamics

The pre-processed sequencing data (as described above) were used to identify and visualize the presence of individual MAE-specific CD8+ T cell populations per sample (output of the Barracoda package). The abundance of the populations within the cohort and the normalized number of detected MAE-specific CD8+ T cell populations provides an overview of all identified T cell clones. It was calculated as the sum of the absolute numbers of each population divided by the number of patients (n=36) for BL and FU samples separately.

Comparing BL and FU samples of each individual patient illustrates the dynamics within the MAE-specific CD8+ T cell signatures under therapy. These dynamics were visualized by the sum of the absolute numbers of detected MAE-specific CD8+ T cell populations per patient in subgroups where either they appeared (i.e. they were not present at BL, but detected at FU), remained stable (present at both time points) or disappeared (present at BL, but no longer detected at FU). The resulting patient-specific vectors (e.g. patient 15 had 24 appearing and 0 disappearing MAE-specific T cell populations under therapy while 3 populations were present at both time points) were designated "melanoma-associated epitope-specific T cell Score A" ($T_{MAE}S$ A). The latter was the basis for the calculation of the "melanoma-associated epitope-specific T cell Score B" ($T_{MAE}S$ B), which provides a single variable to visualize total changes in MAE-specific CD8+ T cell profiles per patient. $T_{MAE}S$ B was calculated by subtracting the sum of disappearing from the sum of appearing MAE-specific CD8+ T cell populations, resulting in a positive value (dominantly "increased" signature), a negative value (dominantly "decreased" signature) or "0" (balance between appearances and disappearances or the lack of MAE-specific CD8+ T cell populations at either timepoint; "balanced" signature). The heatmap was created by Complexheatmaps (28), Circlize (29) and RColorBrewer using R Studio (v1.2.1335).

Phenotyping of PBMCs

T cell and myeloid compartments were phenotyped for patients with additional cryopreserved PBMC samples available using flow cytometry (n=24 with a T cell antibody panel and n=22 with a myeloid antibody panel). In brief, samples were thawed, dead cells were stained with ethidium monoazide bromide (EMA, Biotinum) and Fcγ receptors were simultaneously blocked using human immunoglobulins (Gamunex, Grifols). For the T cell antibody panel, two aliquots per sample were stained simultaneously with antibodies against the extracellular markers or with the respective isotype-controls. Next, the cells were fixed and permeabilized (eBioscience FoxP3 Transcription Factor Staining Buffer Set, Thermo Fisher Scientific) and stained for FoxP3 expression (**Supplementary Table 3**). For the myeloid cell panel, the samples were stained for cell surface markers (**Supplementary Table 4**).

Samples from both panels were acquired immediately after staining on an LSR II cytometer (BD). Data analysis was performed with FlowJo (v10.7.1, BD), using established gating strategies (**Supplementary Figures 2**, **3**). In brief, single viable lymphocytes were gated for CD3+ T cells. Tregs (CD4+CD25+ CD127lowFoxP3+), CD4+ (all CD4+ non-Tregs) and CD8+ T cells were selected for the analysis of checkpoint receptor (TIM-3, LAG-3 and PD-1) and CD25 expression. PD-1 expression was only quantified in BL-samples, as commercially

available diagnostic antibody clones cannot reliably stain all PD-1 molecules in patients treated with therapeutic anti-PD-1 antibodies. Myeloid cells were gated as single, viable, lineage-negative (CD3-CD19-CD56-) cells expressing CD11b and CD33. MDSCs were defined as CD14+HLA-DRlow/-, classical monocytes as CD14+CD16-HLA-DR+, intermediate monocytes were defined as CD14+CD16+HLA-DR+ and non-classical monocytes as CD14dimCD16+HLA-DR+.

Statistical Analyses

OS was defined as the time from the first administration of ICB until death or the end of follow-up. Progression-free survival (PFS) was defined from the start of ICB to the last follow-up or disease progression using RECIST 1.1 criteria (30). Disease-specific survival probabilities (OS and PFS) were analyzed using the Kaplan-Meier method and the respective arms compared using log-rank testing (Prism v5, GraphPad). To test for unintended confounding factors, correlations between clinical parameters and OS were calculated by the confounding function using the swamp R package (31). Changes of the individual immune cell phenotypes under ICB were investigated using the Wilcoxon matched-pairs signed rank test. Group comparisons of immune cell phenotypes between BL and FU were statistically evaluated using the Mann-Whitney U test (Prism v5, GraphPad). Non-parametric Spearman correlations were computed to test for correlations between continuous variables (Prism v5, GraphPad). $P<0.05$ was considered statistically significant.

To identify dynamic changes of particular MAE-specific CD8+ T cell populations that correlated with patients' OS, we trained an elastic net regression model (32) on the changes in numbers of MAE-specific T cell populations under therapy (FU sample – BL sample). We computed the elastic net regularization for the Cox models using the glmnet R package (33). To select the elastic net model hyperparameter α ($0\leq\alpha\leq1$), the patient cohort was divided into a training and a test set (80% and 20% of the samples, respectively). Here, $\alpha=1$ is equivalent to a lasso regression, whereas the model reduces to ridge regression with $\alpha=0$. The best α in [0.1, 1] was selected when we achieved the highest prediction accuracy on the test set. The regularization parameter λ that penalized the least absolute shrinkage (lasso) was selected from 10-fold cross-validation on the training set. The identified MAE-specific CD8+ T cell populations were further investigated for correlations with patients' OS using uni- and multivariate Cox regressions. Only those T cell populations that revealed robust statistical correlations with patients' OS in univariate Cox regressions were considered for the calculation of a multivariate Cox proportional hazard model (34). The Cox model was fitted to the data using the survival R package (35).

RESULTS

Patients

In this study, the dynamics of 167 MAE-specific CD8+ T cell populations in the peripheral blood of 36 HLA-A*0201+ stage IV melanoma patients under anti-PD-1 ICB were investigated. Blood was drawn before starting therapy and at a median of 42 days thereafter (**Figure 1A**). Median patient age was 68 years (range: 28-88), 66.7% were male and 33.3% were female (n=24 and 12, respectively); 47.2% (n=17) were treated with anti-PD-1 antibody monotherapy, while the remaining 52.8% received a combination of anti-PD-1 and anti-CTLA-4 antibodies (n=19). The one-year OS was 76.1% and the median PFS was 9 months. Cohort characteristics are summarized in **Table 1**.

Melanoma-Associated Epitope-Specific CD8+ T Cell Signatures

T cells carrying receptors specific for 117 of the 167 MAE-specific dextramers tested were present in at least one sample. We identified T cells specific for a variety of cancer-testis antigens (CTAs), overexpressed antigens and differentiation-specific antigens (36) in 33 of 36 patients. Seventy-two MAE-specific CD8+ T cell populations were present both at baseline (BL) and follow-up (FU) whereas 31 that had not been present at BL appeared at FU; there were also 14 present at BL that were no longer detectable at FU. A qualitative assessment of these 117 shared MAE-specific CD8+ T cell populations revealed a high degree of inter-individual variability suggesting a relatively "private" composition of these T cell signatures, while the observed intra-individual variability reflects ICB-induced effects (**Figure 1B**).

The most prevalent MAE-specific CD8+ T cell population carried receptors for the MAGE-A2 LVH peptide (36.1% of patients at BL and FU), followed by CDKN1A GLG (19.4% at BL and 27.8% at FU) and MAGE-C2 KVL peptide (22.2% at BL and 16.7% at FU). **Figure 1C** depicts the prevalence and the normalized absolute numbers of the 117 detected MAE-specific CD8+ T cell populations at BL and FU. The patterns of MAE-specific CD8+ T cell populations are highly heterogeneous and suggest a patient-unique T cell profile. Similar patterns were also identified for the impact of PD-1 ICB on the estimated frequencies of the individual MAE-specific CD8+ T cell populations (**Supplementary Figure 4** and **Supplementary Table 5**).

Dynamics of the MAE-Specific CD8+ T Cell Signature Under ICB Correlate With Clinical Outcome

Dynamics of the investigated MAE-specific CD8+ T cell signatures were investigated in patients receiving PD-1 ICB alone or in combination with CTLA-4 antibodies (**Figure 2A**). To assign ICB-driven dynamics to the individual patient, we defined an MAE-specific CD8+ T cell score A ($T_{MAE}S$ A) that summarizes the individual numbers of i) appearing, ii) disappearing or iii) stable MAE-specific CD8+ T cell populations in the blood under ICB (**Figure 2A**). We identified patients with dominantly increasing, dominantly decreasing, or with little or no change in the total MAE-specific CD8+ T cell $T_{MAE}S$ A. These three parameters were then used to define the score $T_{MAE}S$ B reflecting the dominance of either an increasing or not-increased (decreased or balanced) MAE-specific CD8+ T cell signature (**Figure 2A**).

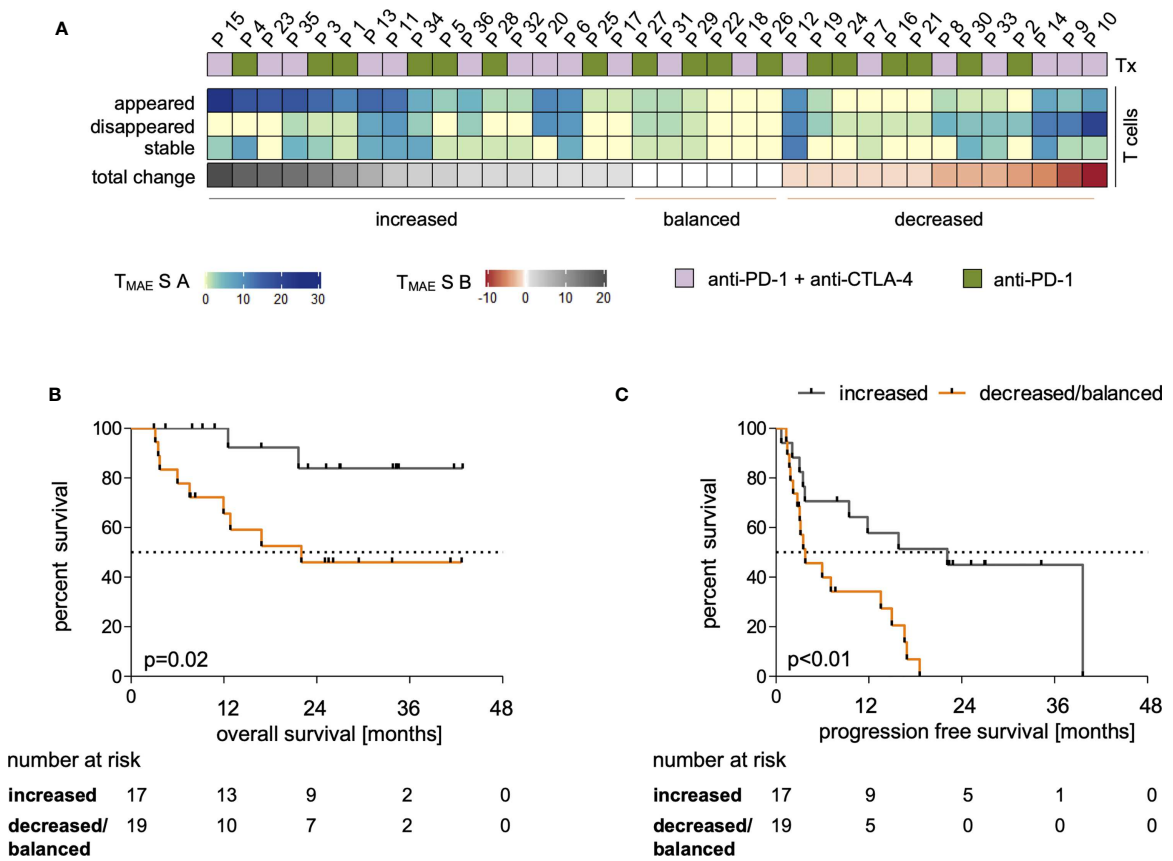

FIGURE 2 | Dynamics within the MAE-specific CD8+ T cell signature correlate with clinical outcome. The applied therapy (Tx) is displayed for each patient in (**A**, top row) and changes within the individual MAE-specific CD8+ T cell signatures under PD-1 ICB are indicated in the absolute number of appearing, disappearing and stable MAE-specific T cell populations summarized as "T_{MAE}S A" – a 3 digit score - on a per patient basis (**A**, middle 3 rows). Dominant changes as a single digit value of the MAE-specific CD8+ T cell signature of each patient are displayed in ("T_{MAE}S B") (A, lower row). The cohort was dichotomized for Kaplan-Meier analysis after T_{MAE}S B >0 (dominant increased) versus ≤0 (balanced or decreased) T cell signature) and correlated with patients' OS **(B)** and PFS **(C)**.

Dichotomizing the cohort according to T_{MAE}S B as defined above allowed a correlation to be made with clinical outcome. We found that a T_{MAE}S B >0 (dominantly increased CD8+ MAE-specific T cell signature) was associated with both prolonged OS (p=0.02, HR:0.24, **Figure 2B**) and PFS (p<0.01, HR:0.3, **Figure 2C**). Not only the qualitative, but also a semi-quantitative analysis identified a significant increase of the estimated frequencies of the CD8+ MAE-specific T cell populations in patients with a T_{MAE}S B >0 (p=0.04), but not in those with a T_{MAE}S B ≤0 (p=0.39) (**Supplementary Figure 5**). The swimmer plot in **Supplementary Figure 6** summarizes further clinical follow-up data for each individual patient.

Major demographic and clinical factors (age, sex, type of therapy, elevated LDH and previous systemic therapies), that might confound the identified associations of MAE-specific CD8+ T cell signatures and dynamics under ICB with clinical outcome were correlated with each other. The confounding function matrix revealed no concerning correlations with OS and PFS (**Supplementary Figure 7**). By univariate analyses, there were also no statistically significant differences in OS or PFS between patients receiving anti-PD-1 antibodies alone or in combination with anti-CTLA-4 antibodies (**Supplementary Figure 8A**); there were also no correlations with age (**Supplementary Figure 8B**). Furthermore, there was no significant correlation between age and T_{MAE}S B (**Supplementary Figure 8C**). Thus, the identified dominantly increasing MAE-specific CD8+ T cell signatures under ICB (T_{MAE}S B >0) in patients with prolonged OS and PFS can be considered as not confounded by typical clinical and demographic variables.

Alterations in Cellular Phenotypes Correlate With the Dynamics of MAE-Specific CD8+ T Cell Signatures Under ICB

To study the associations of the expression profiles of checkpoint molecules on T cells and the abundance of immune regulatory cells in the context of the above-described beneficial increase of the individual MAE-specific CD8+ T cell signatures (T_{MAE}S B >0), we assessed phenotypic profiles of myeloid cells and T cells. These phenotypes were comparatively evaluated in patients with increased (T_{MAE}S B >0) or decreased/balanced (T_{MAE}S B ≤0) MAE-specific CD8+ T cell signatures, as defined above. We found

no differences between the two patient groups at BL for any of the observed immune cell phenotypes (**Figures 3A–F**), including frequencies of PD-1+ cells within CD8+ T cells, CD4+ T cells and Tregs (**Figure 3B**). There were also no differences regarding changes of total CD8+ T cells, CD4+ T cells or Treg frequencies (**Figure 3A**). However, patients with an increasing MAE-specific CD8+T cell signature under ICB had increasing frequencies of TIM-3+CD8+ T cells (p=0.04, **Figure 3C**), whereas no differences were found in the CD25+CD8+ T cell population (**Figure 3D**). Furthermore, we observed that a LAG-3+ subset of the CD4+ and Treg populations increased significantly in patients with an increasing MAE-specific CD8+ T cell signature (p=0.04 and p=0.01, respectively, **Figure 3E**) but not in the reciprocal group. Vice versa, patients with a decreased/balanced MAE-specific CD8+ T cell signature exhibited a decrease in the frequency of TIM-3+CD4+ T cells (p=0.02, **Figure 3C**).

The frequencies of MDSCs, intermediate, classical- and non-classical monocytes revealed no statistically significant changes under ICB either in patients with increasing or with decreasing/balanced MAE-specific CD8+ T cell signatures (**Figure 3F**). The medians and interquartile ranges (IQR) of all these populations are shown in **Table 2**.

Regression-Based Identification of MAE-Specific CD8+ T Cell Populations Correlating With OS

Next, we aimed to identify the most relevant dynamics of certain MAE-specific CD8+ T cell populations through correlations with patients' OS. We first noticed that similar to the previously studied NY-ESO-1 TAA (25), the disappearance of NY-ESO-1 QLS and SLL-specific T cells from the periphery tended to correlate with a prolonged OS under ICB (p=0.14; data not

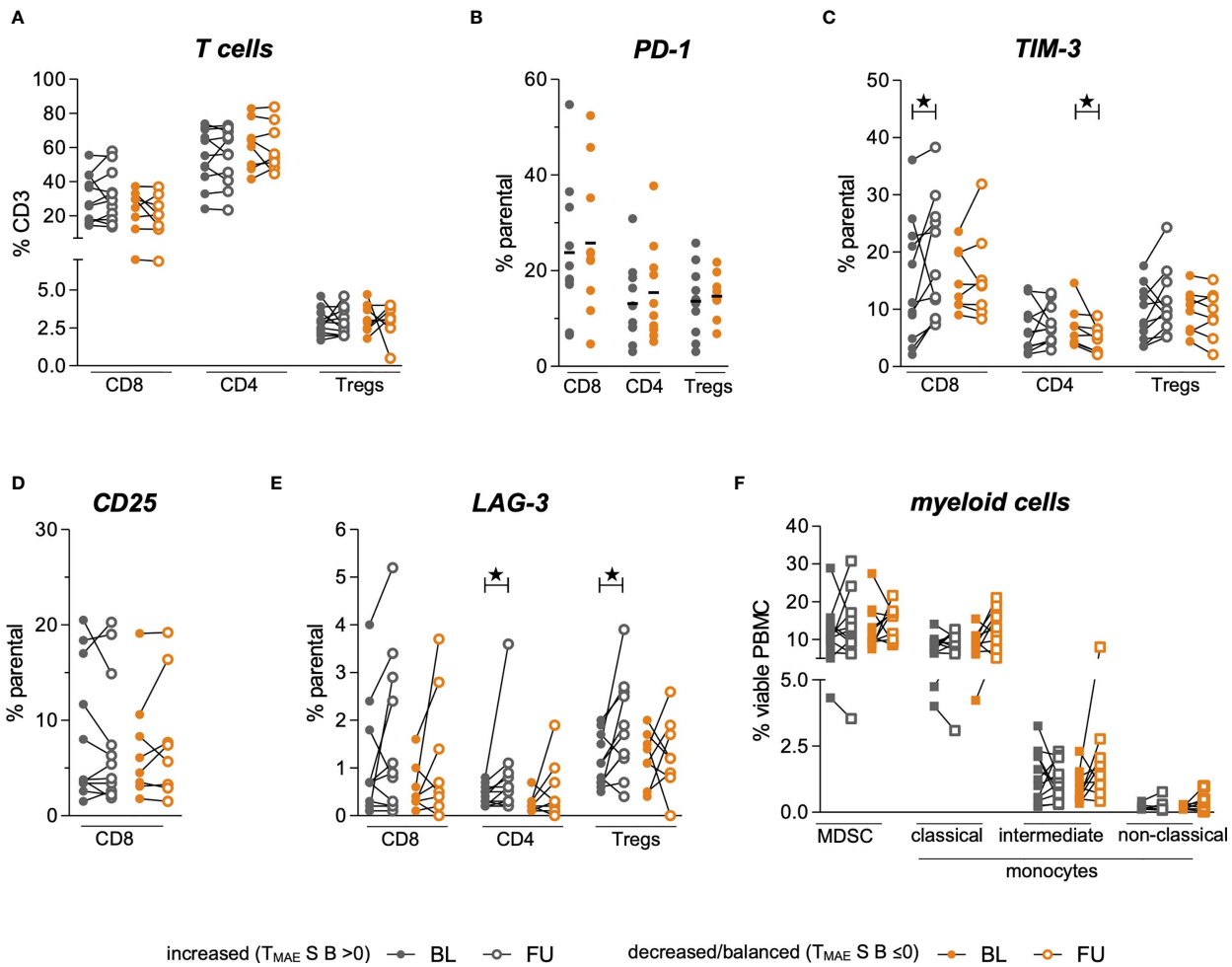

FIGURE 3 | Comparison of myeloid and T cell phenotypes in a group of patients dichotomized by $T_{MAE}S$ (B) Baseline (BL, full symbol) and follow-up samples (FU, empty symbols) of each individual patient are connected by a line. Frequencies of patients with an increased MAE-specific CD8+ T cell $T_{MAE}S$ B are displayed in grey, those with a decreased/balanced in orange. Frequencies of Tregs, CD8+ and CD4+ T cells among all CD3+ T cells **(A)**. Frequency of PD-1-expressing subsets at baseline **(B)**. Alterations of frequencies of TIM-3-expressing **(C)**, CD25-expressing **(D)** and LAG-3-expressing **(E)** T cell subsets. Changes of frequencies of MDSC and monocytic phenotypes are shown in **(F)** ★ indicate p-values <0.05.

TABLE 2 | Median and IQRs of the determined immune phenotypes, dichotomized by $T_{MAE}S$ B (>0: increased vs ≤0: decreased/balanced).

Cell subset	Time point	Increased		Decreased/balanced	
		Median	IQR	Median	IQR
CD8+	BL	26.6	26.1	27.3	18.0
	FU	29.2	27.5	20.7	18.1
CD4+	BL	55.3	27.6	62.4	27.0
	FU	56.1	28.7	55.3	25.5
Tregs	BL	2.9	1.3	3.0	1.5
	FU	2.6	1.7	3.2	1.3
PD1+CD8+	BL	19.7	19.5	23.0	23.0
PD1+CD4+	BL	11.0.	11.6	11.9	14.4
PD1+Tregs	BL	13.6	13.1	14.4	4.6
TIM-3+CD8+	BL	11.2	17.9	13.3	9.3
	FU	16.0	17.8	14.2	10.1
TIM-3+CD4+	BL	5.8	5.6	6.2	4.5
	FU	6.6	5.8	5.2	4.0
TIM-3+Tregs	BL	7.7	8.3	10.3	6.1
	FU	9.8	7.8	9.3	6.6
CD25+ CD8+	BL	3.8	13.6	5.3	6.8
	FU	5.4	12.3	6.6	11.2
LAG-3+CD8+	BL	0.7	1.6	0.4	0.6
	FU	0.9	2.7	0.6	2.2
LAG-3+CD4+	BL	0.4	0.4	0.2	0.2
	FU	0.6	0.6	0.3	0.8
LAG-3+Tregs	BL	0.7	1.6	0.4	0.6
	FU	0.9	2.7	0.6	2.2
MDSC	BL	10.8	6.7	11.6	8.1
	FU	11.3	9.5	16.5	7.3
Classical monocytes	BL	7.8	3.0	9.2	4.3
	FU	9.0	4.9	12.1	10.0
Intermediate monocytes	BL	1.1	1.7	0.8	0.9
	FU	1.1	1.4	1.6	1.3
Non-classical monocytes	BL	0.2	0.2	0.2	0.2
	FU	0.2	0.3	0.4	0.4

BL, baseline; FU, follow-up; IQR, interquartile range; MDSC, myeloid derived suppressor cells.

shown). Next, we performed several regression analyses in parallel and/or in sequence (**Figure 4A**) to identify those MAE-specific T cell populations with the greatest relevance for therapy outcome in an unbiased approach. First, an elastic net model was trained to identify associations of the dynamics of MAE-specific CD8+ T cell populations with patients' OS. The resulting model achieved the highest prediction accuracy as well as a smaller set of features at an α of 0.7 (**Supplementary Table 6**). Dynamics of 9 of the 117 detected MAE-specific CD8+ T cell populations (the CTAs MAGE-A10 SLL, TAG-1 SLG, TRAG-3 ILL, the differentiation antigen TRP-2 SVY and the overexpressed antigens STEAP1 FLY, P-cadherin FII, Telomerase RLF, Telomerase ILA and Tyrosinase CLL) were identified as most informative for predicting clinical outcome by regression analysis. Univariate Cox regression analysis using Wald and log-rank testing identified the dynamics of two of these 9 MAE-specific CD8+ T cell populations as potentially unreliable and they were excluded from further modelling (P-cadherin FII and Telomerase ILA; see **Supplementary Table 7**). Multivariate Cox regression analysis of the remaining 7 MAE-specific CD8+ T cell populations revealed independent correlations of the dynamics of CD8+ T cells specific for TAG-1 SLG, Telomerase RFL and TRP-2 SVY ($p<0.01$, HR:0.01, $p=0.03$, HR:0.01; and $p=0.02$, HR:0.03, respectively; **Figure 4B**). A combinatorial model, comprising the dynamics of these 3 MAE-specific CD8+ T cell populations suggested that patients exhibiting a disappearance from the peripheral blood of at least one of these MAE-specific CD8+ T cell populations under therapy had a significantly shorter OS compared to those patients with appearing or stable T cell populations ($p<0.01$, HR:40.96, **Figure 4C**). Importantly, the disappearance of these selected MAE-specific CD8+ T cells, did not correlate with any observed dynamics of all other investigated MAE-specific CD8+ T cell populations ($T_{MAE}S$ A or B) at the individual patient level (P35, P34, P29, P12, P16, P9).

Furthermore, patients in the appearing/stable group also experienced an increase in the sum of estimated frequencies of these three T cell populations specific for TAG-1 SLG, Telomerase RFL and TRP-2 SVY (**Supplementary Figure 9A**; $p=0.03$). Interestingly, the sum of the estimated frequencies of these three MAE-specific CD8+ T cell populations was higher at BL in patients with a disappearance of at least one of them under therapy compared to the reciprocal group (**Supplementary Figure 9A**; $p<0.01$). No significant differences were found in this subset-analysis applying the sum of estimated frequencies of all detected MAE-specific CD8+ T cell populations (**Supplementary Figure 9B**).

Taken together, these results underscore the importance of the composition, the frequency and the dynamics of the individual peripheral anti-melanoma T cell repertoire early under ICB.

DISCUSSION

Here, we applied a high-throughput approach to investigate the *ex vivo* dynamics of peripheral blood melanoma-associated epitope-specific CD8+ T cell signatures in HLA-A*0201+ stage IV melanoma patients under ICB. To this end, using multiple pMHC dextramers, we investigated 167 MAE-specific CD8+ T cell populations of which 117 were found to be present in one or more patients at one or more time points. We observed T cell recognition most prevalent towards an epitope (LVH) derived from the differentiation antigen MAGE-A2, which was detected in over one-third of the cohort. Also, other previously-identified MAE-specific CD8+ T cell populations such as Melan-A ELA were detected in about 20% of pre-treatment baseline as well as follow-up samples. Other tumor-associated epitopes such as Telomerase RLF or p53 RMP were less frequently recognized. In agreement with expectations, the distribution of the abundance of the different MAE-specific CD8+ T cell populations varied greatly between BL and FU, and the identified individual signatures were heterogeneous and often private (37). On a per-patient level, the dynamics of MAE-specific CD8+ T cell populations were of particular interest. On the basis of these dynamics, we defined two scores. One of these, $T_{MAE}S$ A consisted of 3 variables reflecting the number of appearing, disappearing and stable MAE-specific CD8+ T cell populations. Secondly, based on $T_{MAE}S$ A we defined $T_{MAE}S$ B as

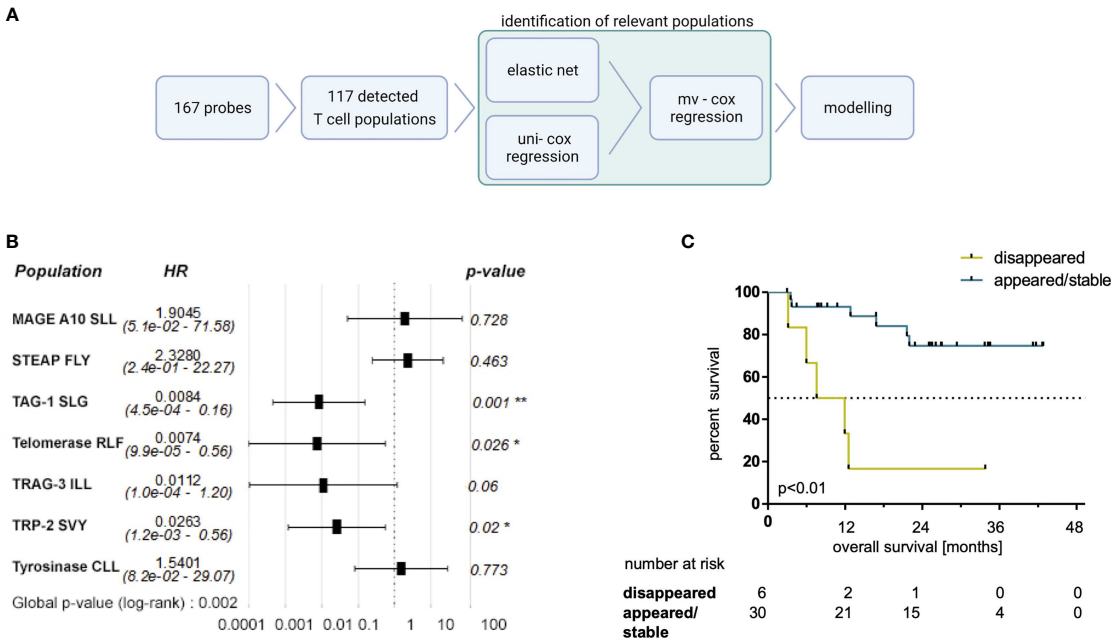

FIGURE 4 | Selected MAE-specific CD8+ T cell populations identified by a regression approach correlate with clinical outcome. The applied workflow to identify relevant MAE-specific T cell populations **(A)** (created with BioRender.com) and the resulting hazard ratios (HR) (including the 95% confidence intervals) of the identified MAE-specific T cell populations are shown in a forest plot **(B)**. Those CD8+ T cell populations, specific for TAG-1 SLG, Telomerase RLF and TRP2 SVY, independently correlating with OS, were combined in a comprehensive model. Patients with a disappearance of at least one of those populations had a shorter OS **(C)** compared to the reciprocal group. * indicate p-values <0.05 and ** indicate p-values <0.01.

a single variable reflecting a dominant increasing or not-increasing (decreasing or balanced) T cell signature. As expected, we found ICB-associated dynamics of MAE-specific CD8+ T cell signatures in the majority of the observed patients, regardless of whether they received PD-1 monotherapy or a combination of PD-1 and CTLA-4 antibodies, similar to reports on the dynamics of selected TAA- or virus-specific T cells under PD-1 ICB (11, 12, 38) or neo-epitope specific T cells under PD-L1 ICB (39). However, our findings contrast with those of a recent study from Gangaev et al. who reported a broadening of MAE-specific CD8+ T cells mostly in patients treated with anti-CTLA-4 antibodies (but only rarely under PD-1 monotherapy) (37). Despite highly overlapping pMHC-multimer panels in both studies, the discrepancy may be explained by the different multimer approaches employed. Thus, we detected 117 MAE-specific CD8+ T cell populations using 167 dextramers while Gangaev et al. found 7 MAE-specific CD8+ T cell populations in anti-PD-1 and 6 in anti-CTLA-4 treated patients using 71 tetramers. Admittedly, both studies enrolled a modest number of patients (36 in the current study-vs-9 in the anti-CTLA-4- and 24 in the anti-PD-1-treated cohorts in the work of Gangaev et al.). Thus, future investigations of MAE-specific CD8+ T cells under ICB are warranted.

The main finding of the present study was that dominantly increasing MAE-specific CD8+ T cell signatures summarized in $T_{MAE}S$ B correlated with prolonged OS and PFS. This complements published data that associates epitope spreading (40) or induction of TCR repertoire divergence (41) under ICB with beneficial clinical outcomes. ICB-induced epitope spreading and disease control requires the patient´s possession of an appropriate T cell receptor repertoire and retention of T cell functionality. Additionally, the presence of regulatory immune cells such as MDSCs, or Tregs that might dampen anti-cancer T cell responses can play a critical role in cancer immunotherapy (42, 43). To evaluate the impact of the abundance of such immune regulatory cells in the context of the above-described beneficial increase of the individual MAE-specific CD8+ T cell score B ($T_{MAE}S$ B), we assessed phenotypic MDSC and Treg data, and also checkpoint receptor expression on T cell subsets in our cohort. Our findings revealed no differences between patients with dominantly decreasing/balanced ($T_{MAE}S$ B ≤0) or increasing ($T_{MAE}S$ B >0) MAE-specific CD8+ T cell signatures before the start of ICB (BL) in any of the observed cellular phenotypes including frequencies of PD-1+, LAG-3+ and TIM-3+ cells within Tregs, CD8+ and CD4+ T cell populations. Perhaps this is not surprising, despite reports that PD-1+ peripheral blood T cell subsets harbor tumor-specific T cell populations (44), because the expression of PD-1, LAG-3 and TIM-3 alone has not been identified as a predictive biomarker candidate for successful ICB. Nonetheless, recent reports suggest that combinatorial analyses of several such checkpoint receptor-expressing T cell subsets may reveal an association with clinical outcome. For example, the PD-1+CD8+/PD-1+Treg ratio in tumor-resident cells was reported to predict the clinical efficacy of PD-1 ICB (45), and a combinatorial analysis of LAG-3 expression on several peripheral blood cell subsets (prominently

on CD8+ T cells) before the start of PD-1 ICB correlated with poorer clinical outcome (46). Also the utility of examining relationships between phenotypes and clinical features under ICB, such as a validated negative association with OS of the expression of Ki67 on circulating PD-1+ CD8+ T cells and tumor burden has been reported (12).

However, comparative analyses of alterations in the observed T cell phenotypes under PD-1 ICB identified significant differences in our cohort that were dichotomized according to their $T_{MAE}S$ B. We observed an increase of TIM-3+CD8+ T cells in patients with ($T_{MAE}S$ B >0) but not in those without ($T_{MAE}S$ B ≤0) an increasing MAE-specific CD8+ T cell signature, which might reflect a PD-1 blockade-driven evasion of co-inhibitory signaling through the TCR complex for negative regulatory checkpoint receptors other than TIM-3. The latter mechanism has been described in a mouse model of lung adenocarcinoma, where adaptive resistance to anti-PD-1 treatment was associated with an upregulation of TIM-3 on PD-1+ T cells in the tumor (47). Whether such an increase in the TIM-3+CD8+ T cell population in our study correlates with exhaustion of CD8+ T cells (48) or rather marks competent/reactive CD8+ T cells could not be functionally assessed here. The dynamics of changes of CD8+ T cells expressing the activation marker CD25 did not allow further conclusions either. Increases in LAG-3+CD4+ T cells and LAG-3+ Tregs in patients with increasing MAE-specific CD8+ T cell signatures, but also a decrease of TIM-3+CD4+ T cells in patients with decreasing/balanced MAE-specific CD8+ T cell signatures, might additionally illustrate the multifaceted modulatory effects of ICB on the CD4+ as well as the CD8+ T cell population, which could not be examined in detail here. In particular, the increases of LAG-3+CD4+ T cell and LAG-3+Treg frequencies in patients with an increasing MAE-specific CD8+ T cell signature underscores our hypothesis that these patients have retained a competent T cell compartment and therefore have a better chance of obtaining clinical benefit through ICB. This hypothesis is consistent with data from a study by Zelba et al. who reported an increase of LAG-3+ and TIM-3+ CD4+ and CD8+ T cells in an *in-vitro* PD-1 ICB assay in renal cell carcinoma TILs (49). Unexpectedly, we did not see differences in monocytic and MDSC subsets between the two patient groups, suggesting no direct associations between dynamics of MAE-specific CD8+ T cell populations and the peripheral frequencies of these cells that were previously reported as biomarker candidates in melanoma under ICB (8, 9).

We exploited our dataset further by applying a regression-based approach to identify those MAE-specific CD8+ T cell populations that were most informative for OS – the most robust endpoint of our study. We found that a loss of CD8+ T cells specific for the differentiation antigen TRP-2 SVY, the CTA TAG-1 SLG and the overexpressed antigen Telomerase RLF was associated significantly and independently with shorter OS. The resulting combinatorial model defined a subgroup of patients with a significantly reduced OS, characterized by a loss of at least one of the three MAE-specific CD8+ T cell populations. Reasons for the disappearance of TAA-specific T cells – and thus also the loss of these mostly apparently clinically-beneficial MAE-specific CD8+ T cells - from the periphery might be diverse. This might be of particular relevance as we recently reported the early disappearance of functional Melan-A- or NY-ESO-1-reactive CD4+ and/or CD8+ T cells from the peripheral blood in some melanoma patients with superior OS and PFS under PD-1 ICB resulting from a hypothetical migration to the metastases (25). A similar pattern for the dynamics of NY-ESO-1-specific CD8+ T cells was also found in the present study. However, the (opposite) correlation of the loss of T cells specific for the TRP-2 SVY-, TAG-1 SLG- and Telomerase RLF-peptide-MHC complexes with OS noted here might be explained by these cells being dysfunctional or exhausted already before the start of ICB, as commonly reported in advanced stages of cancer (50). Taken together, we hypothesize that T cell specificity (37), kinetics of (ICB triggered) epitope accessibility (40) and essentially also functionality (20–22, 24, 25) at the single cell level might be considered as major features to classify T cell populations that actively contribute to cancer immunosurveillance as opposed to those from dysfunctional and/or anergic subsets that cannot be reinvigorated by ICB. Thus, such future evaluations of TAG-1-, Telomerase- and TRP-2-reactive T cells (including also CD4+ T cells) is warranted to discriminate between functionally competent and dysfunctional specific T cell clones, similar to our previous studies on MAGE-A3, Survivin-, Melan-A- and NY-ESO-1-reactive T cell populations (7, 20, 21).

Taken together, our pilot study shows a high degree of individuality in the MAE-specific CD8+ T cell profiles in these melanoma patients. Nevertheless, we were able to identify some epitopes that might contribute to the search for targets for novel TAA-based cancer vaccines, which are currently regaining attention (19, 51, 52). However, this requires further in-depth studies of these epitopes and in addition to the qualitative investigations described in this pilot study, must also include functional studies. Furthermore, our results provide important insights into the dynamics of circulating MAE-specific CD8+ T cells under ICB and should contribute to a better understanding of the role of these cells in cancer rejection.

DATA AVAILABILITY STATEMENT

The raw data supporting the conclusions of this article will be made available by the authors, without undue reservation.

ETHICS STATEMENT

The studies involving human participants were reviewed and approved by Ethics Committee of Tübingen University Hospital. The patients/participants provided their written informed consent to participate in this study.

AUTHOR CONTRIBUTIONS

KW-H, BW, and SH contributed to conceptualization. AG, SB, SH, and KW-H contributed to the methodology. AG, SH, and KW-H were administering this project. AG, TM, CH, ST, JB, JS, SH, and

KW-H were involved in investigation. AG, TM, CH, ST, SH, and KW-H contributed to data curation, formal analysis and investigation. AG, SB, TM, SH, and KW-H were involved in formal analysis and visualization. TA, NW, RK, FM, CG, and TE were providing resources and funding was acquired by CG, BW, KW-H, and SH. This project was supervised by TE, GP, MC, KW-H, and SH. AG, GP, and KW-H wrote the first draft of the manuscript. SB and SH wrote sections of the manuscript. All authors contributed to manuscript revision, read and approved the submitted version.

FUNDING

This work was partially funded by the Medical Faculty of the University of Tübingen (2509-0-0), Bristol-Myers Squibb (CA209-9P4) and the Klaus Tschira Foundation (00.316.2017) (to KW-H). Additionally, it was in part supported by the European Research Council, StG 677268 NextDART, the Lundbeck Foundation Fellowship R190–2014–4178 and the Carlsberg foundation (to SH).

ACKNOWLEDGMENTS

We thank Shannon Ottmann and Anne Mohrholz for their support in sample preparation, staining and acquisition and Daniel Soffel for the support in the assessment of clinical data in this project.

SUPPLEMENTARY MATERIAL

The Supplementary Material for this article can be found online at: https://www.frontiersin.org/articles/10.3389/fimmu.2022.906352/full#supplementary-material

REFERENCES

1. Hodi FS, O'Day SJ, McDermott DF, Weber RW, Sosman JA, Haanen JB, et al. Improved Survival With Ipilimumab in Patients With Metastatic Melanoma. *N Engl J Med* (2010) 363(8):711–23. doi: 10.1056/NEJMoa1003466
2. Wolchok JD, Chiarion-Sileni V, Gonzalez R, Rutkowski P, Grob JJ, Cowey CL, et al. Overall Survival With Combined Nivolumab and Ipilimumab in Advanced Melanoma. *N Engl J Med* (2017) 377(14):1345–56. doi: 10.1056/NEJMoa1709684
3. Pilard C, Ancion M, Delvenne P, Jerusalem G, Hubert P, Herfs M. Cancer Immunotherapy: It's Time to Better Predict Patients' Response. *Br J Cancer* (2021) 125(7):927–938. doi: 10.1038/s41416-021-01413-x
4. Gong J, Chehrazi-Raffle A, Reddi S, Salgia R. Development of Pd-1 and Pd-L1 Inhibitors as a Form of Cancer Immunotherapy: A Comprehensive Review of Registration Trials and Future Considerations. *J Immunother Cancer* (2018) 6 (1):8. doi: 10.1186/s40425-018-0316-z
5. Jenkins RW, Fisher DE. Treatment of Advanced Melanoma in 2020 and Beyond. *J Invest Dermatol* (2021) 141(1):23–31. doi: 10.1016/j.jid.2020.03.943
6. Ribas A, Wolchok JD. Cancer Immunotherapy Using Checkpoint Blockade. *Science* (2018) 359(6382):1350–5. doi: 10.1126/science.aar4060
7. Weide B, Martens A, Zelba H, Stutz C, Derhovanessian E, Di Giacomo AM, et al. Myeloid-Derived Suppressor Cells Predict Survival of Patients With Advanced Melanoma: Comparison With Regulatory T Cells and Ny-Eso-1- or Melan-A-Specific T Cells. *Clin Cancer Res an Off J Am Assoc Cancer Res* (2014) 20(6):1601–9. doi: 10.1158/1078-0432.CCR-13-2508
8. Martens A, Wistuba-Hamprecht K, Foppen MG, Yuan J, Postow MA, Wong P, et al. Baseline Peripheral Blood Biomarkers Associated With Clinical Outcome of Advanced Melanoma Patients Treated With Ipilimumab. *Clin Cancer Res* (2016) 22(12):2908–18. doi: 10.1158/1078-0432.ccr-15-2412
9. Krieg C, Nowicka M, Guglietta S, Schindler S, Hartmann FJ, Weber LM, et al. High-Dimensional Single-Cell Analysis Predicts Response to Anti-Pd-1 Immunotherapy. *Nat Med* (2018) 24(2):144–53. doi: 10.1038/nm.4466
10. Araujo B, Hansen M, Spanggaard I, Rohrberg K, Reker Hadrup S, Lassen U, et al. Immune Cell Profiling of Peripheral Blood as Signature for Response During Checkpoint Inhibition Across Cancer Types. *Front Oncol* (2021) 11:558248. doi: 10.3389/fonc.2021.558248
11. Kamphorst AO, Pillai RN, Yang S, Nasti TH, Akondy RS, Wieland A, et al. Proliferation of Pd-1+ Cd8 T Cells in Peripheral Blood After Pd-1-Targeted Therapy in Lung Cancer Patients. *Proc Natl Acad Sci USA* (2017) 114 (19):4993–8. doi: 10.1073/pnas.1705327114
12. Huang AC, Postow MA, Orlowski RJ, Mick R, Bengsch B, Manne S, et al. T-Cell Invigoration to Tumour Burden Ratio Associated With Anti-Pd-1 Response. *Nature* (2017) 545(7652):60–5. doi: 10.1038/nature22079
13. Alexandrov LB, Nik-Zainal S, Wedge DC, Aparicio SA, Behjati S, Biankin AV, et al. Signatures of Mutational Processes in Human Cancer. *Nature* (2013) 500 (7463):415–21. doi: 10.1038/nature12477
14. Yarchoan M, Hopkins A, Jaffee EM. Tumor Mutational Burden and Response Rate to Pd-1 Inhibition. *N Engl J Med* (2017) 377(25):2500–1. doi: 10.1056/NEJMc1713444
15. Yi M, Qin S, Zhao W, Yu S, Chu Q, Wu K. The Role of Neoantigen in Immune Checkpoint Blockade Therapy. *Exp Hematol Oncol* (2018) 7:28. doi: 10.1186/s40164-018-0120-y
16. McGranahan N, Furness AJ, Rosenthal R, Ramskov S, Lyngaa R, Saini SK, et al. Clonal Neoantigens Elicit T Cell Immunoreactivity and Sensitivity to Immune Checkpoint Blockade. *Science* (2016) 351(6280):1463–9. doi: 10.1126/science.aaf1490
17. Hu Z, Leet DE, Allesoe RL, Oliveira G, Li S, Luoma AM, et al. Personal Neoantigen Vaccines Induce Persistent Memory T Cell Responses and Epitope Spreading in Patients With Melanoma. *Nat Med* (2021) 27(3):515–525. doi: 10.1038/s41591-020-01206-4
18. Schumacher TN, Scheper W, Kvistborg P. Cancer Neoantigens. *Annu Rev Immunol* (2019) 37:173–200. doi: 10.1146/annurev-immunol-042617-053402
19. Li L, Goedegebuure SP, Gillanders W. Cancer Vaccines: Shared Tumor Antigens Return to the Spotlight. *Signal Transduct Target Ther* (2020) 5 (1):251. doi: 10.1038/s41392-020-00364-8
20. Weide B, Zelba H, Derhovanessian E, Pflugfelder A, Eigentler TK, Giacomo AMD, et al. Functional T Cells Targeting Ny-Eso-1 or Melan-A Are Predictive for Survival of Patients With Distant Melanoma Metastasis. *J Clin Oncol* (2012) 30(15):1835–41. doi: 10.1200/jco.2011.40.2271
21. Zelba H, Weide B, Martens A, Derhovanessian E, Bailur JK, Kyzirakos C, et al. Circulating Cd4+ T Cells That Produce Il4 or Il17 When Stimulated by Melan-A But Not by Ny-Eso-1 Have Negative Impacts on Survival of Patients With Stage Iv Melanoma. *Clin Cancer Res an Off J Am Assoc Cancer Res* (2014) 20(16):4390–9. doi: 10.1158/1078-0432.CCR-14-1015
22. Raza A, Merhi M, Inchakalody VP, Krishnankutty R, Relecom A, Uddin S, et al. Unleashing the Immune Response to Ny-Eso-1 Cancer Testis Antigen as a Potential Target for Cancer Immunotherapy. *J Trans Med* (2020) 18(1):140. doi: 10.1186/s12967-020-02306-y
23. Thomas R, Al-Khadairi G, Roelands J, Hendrickx W, Dermime S, Bedognetti D, et al. Ny-Eso-1 Based Immunotherapy of Cancer: Current Perspectives. *Front Immunol* (2018) 9:947. doi: 10.3389/fimmu.2018.00947
24. Pittet MJ, Zippelius A, Valmori D, Speiser DE, Cerottini JC, Romero P. Melan-A/Mart-1-Specific Cd8 T Cells: From Thymus to Tumor. *Trends Immunol* (2002) 23(7):325–8. doi: 10.1016/s1471-4906(02)02244-5

25. Bochem J, Zelba H, Spreuer J, Amaral T, Gaissler A, Pop OT, et al. Early Disappearance of Tumor Antigen-Reactive T Cells From Peripheral Blood Correlates With Superior Clinical Outcomes in Melanoma Under Anti-Pd-1 Therapy. *J Immunother Cancer* (2021) 9(12). doi: 10.1136/jitc-2021-003439
26. Bentzen AK, Marquard AM, Lyngaa R, Saini SK, Ramskov S, Donia M, et al. Large-Scale Detection of Antigen-Specific T Cells Using Peptide-Mhc-I Multimers Labeled With DNA Barcodes. *Nat Biotechnol* (2016) 34 (10):1037–45. doi: 10.1038/nbt.3662
27. Testi M, Andreani M. Luminex-Based Methods in High-Resolution Hla Typing. *Methods Mol Biol* (2015) 1310:231–45. doi: 10.1007/978-1-4939-2690-9_19
28. Gu Z, Eils R, Schlesner M. Complex Heatmaps Reveal Patterns and Correlations in Multidimensional Genomic Data. *Bioinformatics* (2016) 32(18):2847–9. doi: 10.1093/bioinformatics/btw313
29. Gu Z, Gu L, Eils R, Schlesner M, Brors B. Circlize Implements and Enhances Circular Visualization in R. *Bioinformatics* (2014) 30(19):2811–2. doi: 10.1093/bioinformatics/btu393
30. Eisenhauer EA, Therasse P, Bogaerts J, Schwartz LH, Sargent D, Ford R, et al. New Response Evaluation Criteria in Solid Tumours: Revised Recist Guideline (Version 1.1). *Eur J Cancer* (2009) 45(2):228–47. doi: 10.1016/j.ejca.2008.10.026
31. Lauss M, Visne I, Kriegner A, Ringner M, Jonsson G, Hoglund M. Monitoring of Technical Variation in Quantitative High-Throughput Datasets. *Cancer Inform* (2013) 12:193–201. doi: 10.4137/CIN.S12862
32. Hui Zou TH. Regularization and Variable Selection *Via* the Elastic Net. *J R Stat Soc* (2005) 67(2):310–20. doi: 10.1111/j.1467-9868.2005.00503.x
33. Friedman J, Hastie T, Tibshirani R. Regularization Paths for Generalized Linear Models *Via* Coordinate Descent. *J Stat Software* (2010) 33(1):1–22. doi: 10.18637/jss.v033.i01
34. Lin DY, Wei LJ. The Robust Inference for the Cox Proportional Hazards Model. *J Am Stat Assoc* (1989) 84(408):1074–8. doi: 10.1080/01621459.1989.10478874
35. Therneau T. Package 'Survival'. *R Top Doc* (2015) 128(10):28–33.
36. Andersen RS, Thrue CA, Junker N, Lyngaa R, Donia M, Ellebaek E, et al. Dissection of T-Cell Antigen Specificity in Human Melanoma. *Cancer Res* (2012) 72(7):1642–50. doi: 10.1158/0008-5472.CAN-11-2614
37. Gangaev A, Rozeman EA, Rohaan MW, Isaeva OI, Philips D, Patiwael S, et al. Differential Effects of Pd-1 and Ctla-4 Blockade on the Melanoma-Reactive Cd8 T Cell Response. *Proc Natl Acad Sci USA* (2021) 118(43). doi: 10.1073/pnas.2102849118
38. Huang AC, Orlowski RJ, Xu X, Mick R, George SM, Yan PK, et al. A Single Dose of Neoadjuvant Pd-1 Blockade Predicts Clinical Outcomes in Resectable Melanoma. *Nat Med* (2019) 25(3):454–61. doi: 10.1038/s41591-019-0357-y
39. Holm JS, Funt SA, Borch A, Munk KK, Bjerregaard AM, Reading JL, et al. Neoantigen-Specific Cd8 T Cell Responses in the Peripheral Blood Following Pd-L1 Blockade Might Predict Therapy Outcome in Metastatic Urothelial Carcinoma. *Nat Commun* (2022) 13(1):1935. doi: 10.1038/s41467-022-29342-0
40. Brossart P. The Role of Antigen Spreading in the Efficacy of Immunotherapies. *Clin Cancer Res an Off J Am Assoc Cancer Res* (2020) 26 (17):4442–7. doi: 10.1158/1078-0432.CCR-20-0305
41. Valpione S, Galvani E, Tweedy J, Mundra PA, Banyard A, Middlehurst P, et al. Immune-Awakening Revealed by Peripheral T Cell Dynamics After One Cycle of Immunotherapy. *Nat Cancer* (2020) 1(2):210–21. doi: 10.1038/s43018-019-0022-x
42. Ostrand-Rosenberg S, Fenselau C. Myeloid-Derived Suppressor Cells: Immune-Suppressive Cells That Impair Antitumor Immunity and Are Sculpted by Their Environment. *J Immunol* (2018) 200(2):422–31. doi: 10.4049/jimmunol.1701019
43. Tanaka A, Sakaguchi S. Regulatory T Cells in Cancer Immunotherapy. *Cell Res* (2017) 27(1):109–18. doi: 10.1038/cr.2016.151
44. Gros A, Parkhurst MR, Tran E, Pasetto A, Robbins PF, Ilyas S, et al. Prospective Identification of Neoantigen-Specific Lymphocytes in the Peripheral Blood of Melanoma Patients. *Nat Med* (2016) 22(4):433–8. doi: 10.1038/nm.4051
45. Kumagai S, Togashi Y, Kamada T, Sugiyama E, Nishinakamura H, Takeuchi Y, et al. The Pd-1 Expression Balance Between Effector and Regulatory T Cells Predicts the Clinical Efficacy of Pd-1 Blockade Therapies. *Nat Immunol* (2020) 21(11):1346–58. doi: 10.1038/s41590-020-0769-3
46. Shen R, Postow MA, Adamow M, Arora A, Hannum M, Maher C, et al. Lag-3 Expression on Peripheral Blood Cells Identifies Patients With Poorer Outcomes After Immune Checkpoint Blockade. *Sci Trans Med* (2021) 13 (608). doi: 10.1126/scitranslmed.abf5107
47. Koyama S, Akbay EA, Li YY, Herter-Sprie GS, Buczkowski KA, Richards WG, et al. Adaptive Resistance to Therapeutic Pd-1 Blockade Is Associated With Upregulation of Alternative Immune Checkpoints. *Nat Commun* (2016) 7:10501. doi: 10.1038/ncomms10501
48. Wolf Y, Anderson AC, Kuchroo VK. Tim3 Comes of Age as an Inhibitory Receptor. *Nat Rev Immunol* (2020) 20(3):173–85. doi: 10.1038/s41577-019-0224-6
49. Zelba H, Bedke J, Hennenlotter J, Mostbock S, Zettl M, Zichner T, et al. Pd-1 and Lag-3 Dominate Checkpoint Receptor-Mediated T-Cell Inhibition in Renal Cell Carcinoma. *Cancer Immunol Res* (2019) 7(11):1891–9. doi: 10.1158/2326-6066.CIR-19-0146
50. Thommen DS, Schumacher TN. T Cell Dysfunction in Cancer. *Cancer Cell* (2018) 33(4):547–62. doi: 10.1016/j.ccell.2018.03.012
51. Romero P, Banchereau J, Bhardwaj N, Cockett M, Disis ML, Dranoff G, et al. The Human Vaccines Project: A Roadmap for Cancer Vaccine Development. *Sci Transl Med* (2016) 8(334):334ps9. doi: 10.1126/scitranslmed.aaf0685
52. Sebastian M, Schroder A, Scheel B, Hong HS, Muth A, von Boehmer L, et al. A Phase I/Iia Study of the Mrna-Based Cancer Immunotherapy Cv9201 in Patients With Stage Iiib/Iv Non-Small Cell Lung Cancer. *Cancer Immunol Immunother* (2019) 68(5):799–812. doi: 10.1007/s00262-019-02315-x

Conflict of Interest: CG reports receiving commercial research grants from Bristol-Myers Squibb, Novartis, and Roche, and is a consultant/advisory board member for Amgen, Bristol-Myers Squibb, Merck Sharp & Dohme, Novartis, and Roche. BW reports receiving commercial research grants from, is a consultant/advisory board member for, and reports receiving travel reimbursement from Bristol-Myers Squibb and Merck Sharp & Dohme. FM reports receiving commercial research grants from Novartis and Roche, and has received travel support or/and speaker´s fees or/and advisor´s honoraria by Novartis, Roche, Bristol-Myers Squibb, Merck Sharp & Dohme, and Pierre Fabre. NW reports an advisory role for Pierre-Fabre and Sanofi, consultant's honoraria from Novartis, and has received travel support from AbbVie and Amgen outside the submitted work. GP has received speaker´s honoraria from Novartis, Roche, Pfizer, GlaxoSmithKline and Astellas. KW-H received commercial research grants from the CatalYm GmbH and travel support from SITC (Society for Immunotherapy of Cancer). SH is the cofounder of Immumap, Tetramer-shop and PokeAcell and is the co-inventor of the patents WO2015185067 and WO2015188839 for the barcoded MHC technology which is licensed to Immudex. The data presented in this study is not directly involved in these activities. TE has received travel support or/and speaker´s fees or/and advisor´s honoraria by Sanofi, Novartis, Bristol-Myers Squibb, Merck Sharp & Dohme, Almiral Hermal, and Pierre Fabre. TA reports institutional grants from SkylineDx, institutional grants and personal fees from Novartis, institutional grants from NeraCare, personal fees from BMS, institutional grants from Sanofi, personal fees from CeCaVa, personal fees from Pierre Fabre, outside the submitted work.

The remaining authors declare that the research was conducted in the absence of any commercial or financial relationships that could be construed as a potential conflict of interest.

Publisher's Note: All claims expressed in this article are solely those of the authors and do not necessarily represent those of their affiliated organizations, or those of the publisher, the editors and the reviewers. Any product that may be evaluated in this article, or claim that may be made by its manufacturer, is not guaranteed or endorsed by the publisher.

Dynamics of melanoma-associated epitope-specific CD8+ T cells in the blood correlate with clinical outcome under PD-1 blockade

Andrea Gaißler, Trine Sundebo Meldgaard, Christina Heeke, Sepideh Babaei, Siri Amanda Tvingsholm, Jonas Bochem, Janine Spreuer, Teresa Amaral, Nikolaus Benjamin Wagner, Reinhild Klein, Friedegund Meier, Claus Garbe, Thomas Eigentler, Graham Pawelec, Manfred Claassen, Benjamin Weide, Sine Reker Hadrup*, Kilian Wistuba-Hamprecht*

* shared last authorship

supplementary material

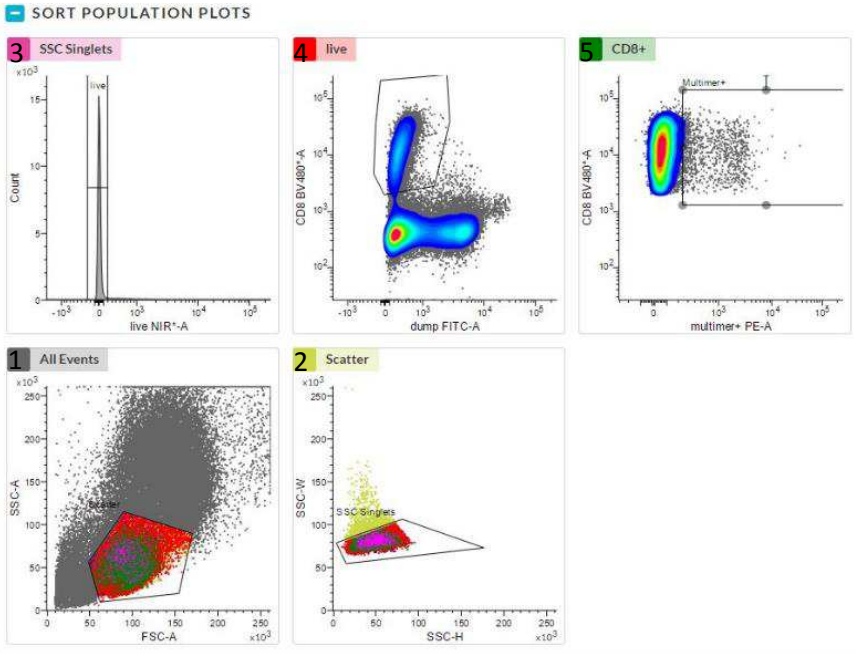

Supplementary Figure 1: Gating strategy for fluorescence activated cell sorting of MAE-specific CD8+ T cells.

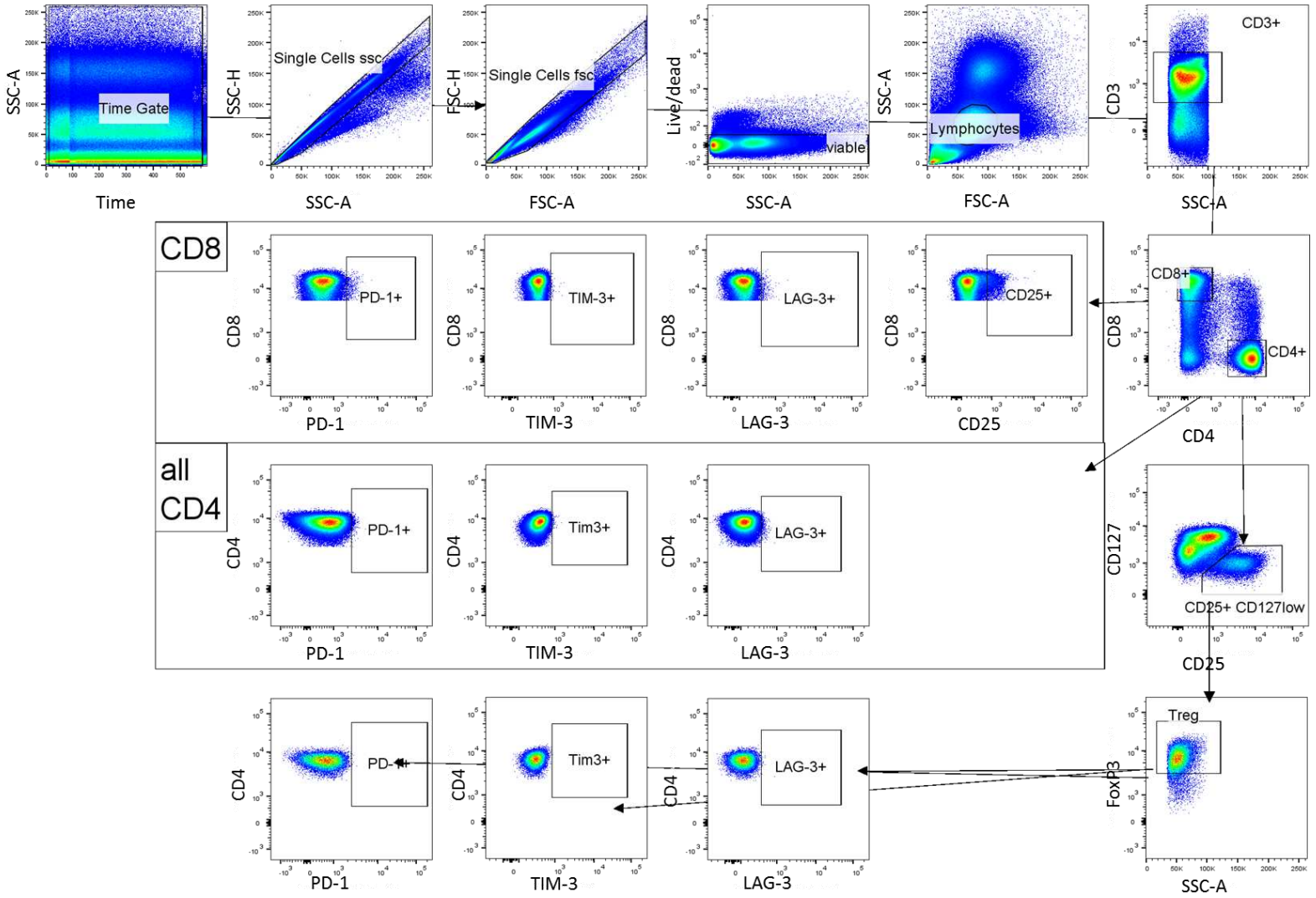

Supplementary Figure 2: Gating strategy for phenotypic assessment of peripheral blood T cells. Gating for checkpoint molecules (PD-1, LAG-3 and TIM-3) was established on the basis of isotype controls on each sample**.**

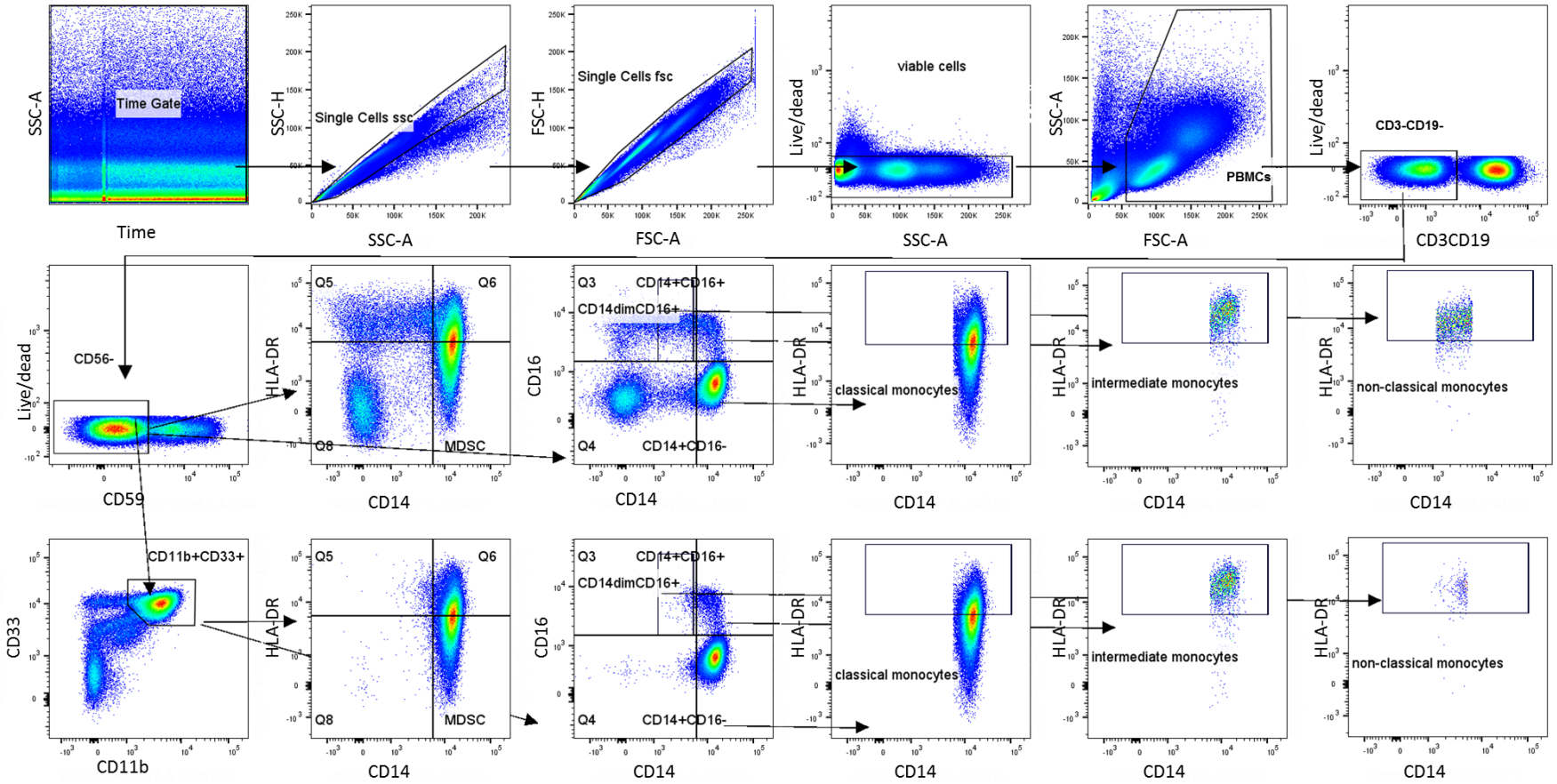

Supplementary Figure 3: Gating strategy for phenotypic assessment of myeloid cells. Gates of MDSC, classical- intermediate- and non-classical monocytes were set on CD3-CD19-CD56- cells (middle panel) and then copied on the CD11b+CD33+ population (lower panel).

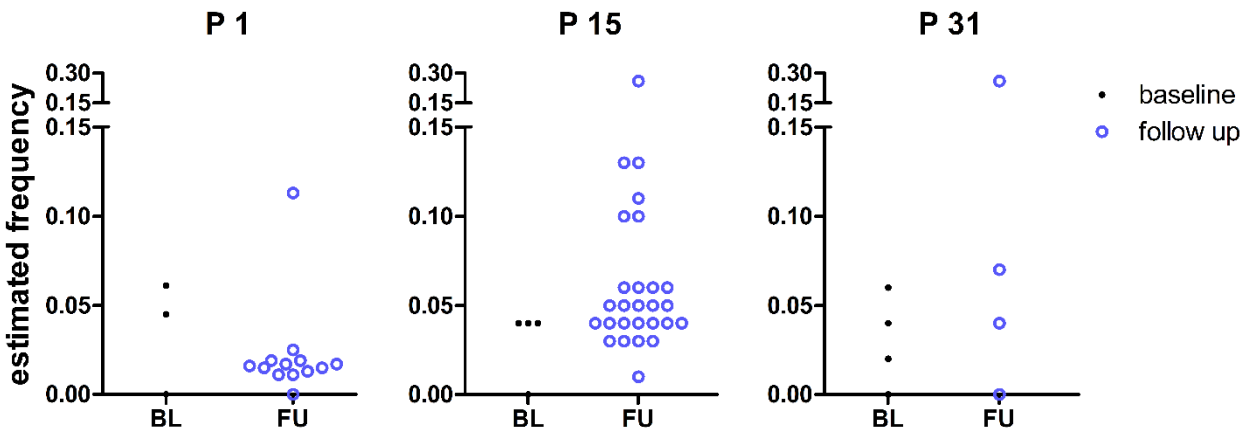

Supplementary Figure 4: Estimated frequency of MAE-specific CD8+ T cell populations in representative patients at BL and FU.

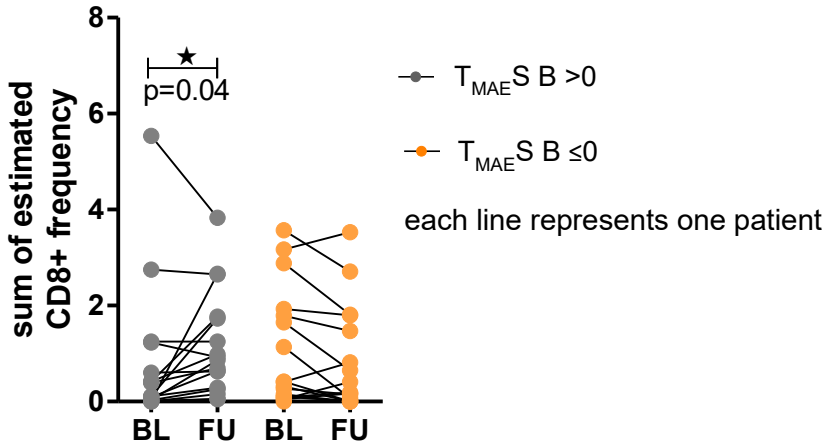

Supplementary Figure 5: Sum of estimated frequencies of all MAE-specific CD8+ T cell populations relative to all CD8+ T cells. Each line, that connects two dots represents one patient. Patients with an T_{MAE}S B >0 (dominantly increasing signature) are displayed with grey symbols, while those with an T_{MAE}S B ≤0 (balanced or dominantly decreasing signature) are illustrated using orange symbols.

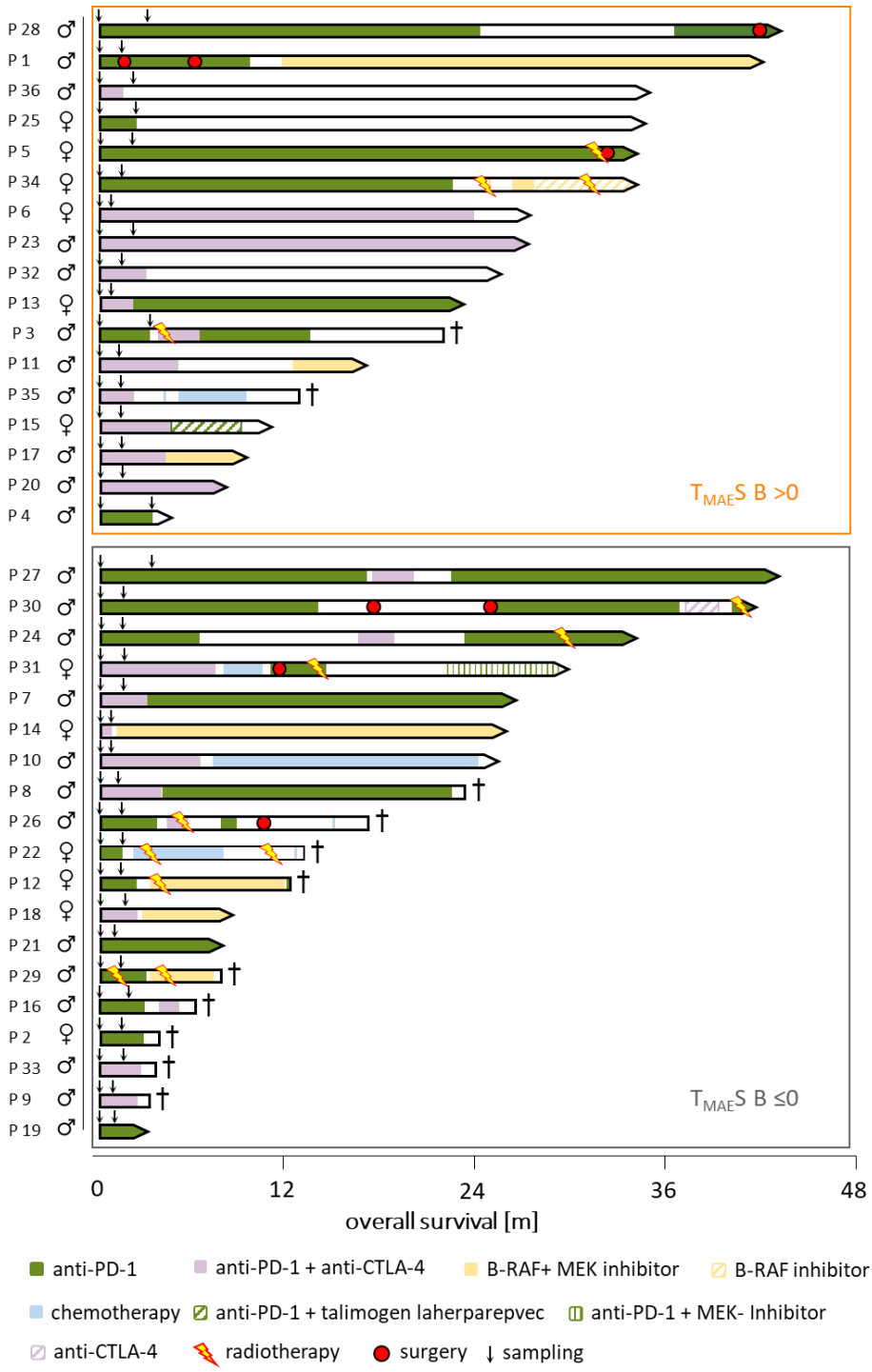

Supplementary Figure 6: Overview of the clinical follow up of the individual patients in this study. The swimmer plot illustrates sampling, therapies and clinical follow up until last contact or death of each individuum. The cohort is dichotomized by dynamics of the melanoma-associated epitope (MAE)-specific CD8+ T cell populations, defined by $T_{MAE}S$ B. This score reflects either a dominantly increasing ($T_{MAE}S$ B >0) or a dominantly decreasing or stable ($T_{MAE}S$ B ≤0) T cell signature under therapy.

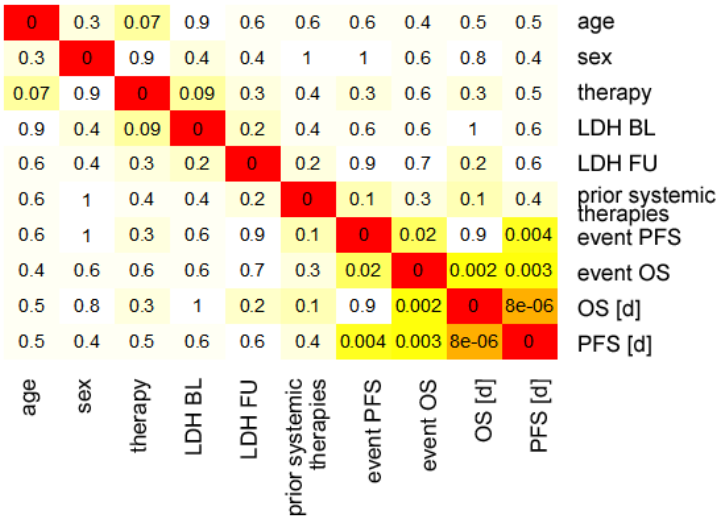

Supplementary Figure 7: ‘Confounding matrix’ displaying p-values of the individual correlations of potentially confounding demographic and clinical data. Heatmap colors represent the p-value of the chi-square test. Data description: LDH: lactate dehydrogenase levels in patients’ serum, divided by diagnostic cut-off; prior systemic therapies: yes/no and included prior immunotherapy, kinase inhibition, and chemotherapy; event PFS/OS: whether the patient had a progress or deceased; OS [d]: overall survival in days; PFS [d]: progression free survival in days

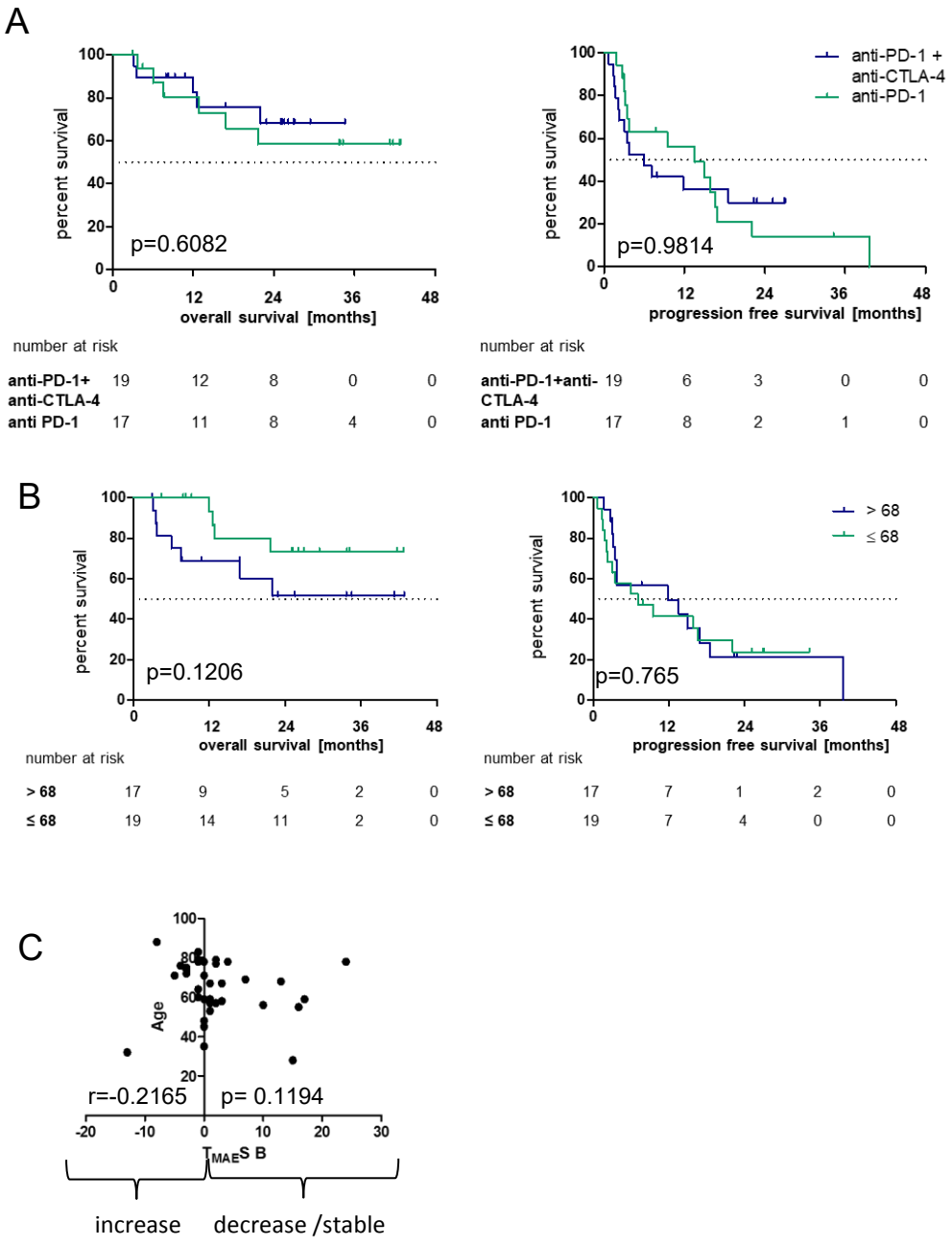

Supplementary Figure 8: Investigation of a potential impact of the applied therapies (A) or age (dichotomization after the median) (B) on patients' OS (left panel) and PFS (right panel). Analysis of a potential correlation between age and $T_{MAE}S$ B using non-parametric Spearman correlation statistics (C).

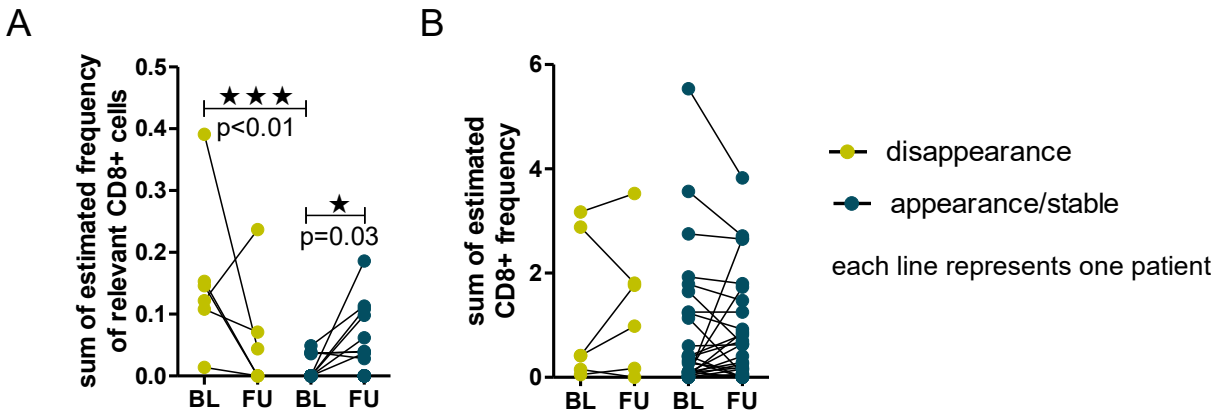

Supplementary Figure 9: Visualization of the sum of estimated frequencies of MAE-specific T cell populations relative to all CD8+ T cells per patient on the basis of the model described in Figure 4 C. Patients were grouped in those with a disappearance (yellow) or those with an appearance/stable T cell population (blue) of at least one of the three most relevant T cell epitopes (TAG-1 SLG, Telomerase RLF and TRP2 SVY MAE)(A).Sum of estimated frequencies of all detected MAE-specific T cell populations (B).

Supplementary Table 1: Overview of the abundance of the MAE-specific CD8+ T cells in samples before and under PD-1 ICB.

Display Name	Antigen Name	Epitope sequence	BL	FU	appearance	disappearance	stable
707-AP RVA	707-AP	RVAALARDAP	2	3	3	2	0
alpha-actinin-4 FIA	alpha-actinin-4	FIASNGVKLV	1	0	0	1	0
ATIC RLD	ATIC (AICRT)	RLDFNLIRV	0	1	1	0	0
BA46 GLQ	BA46(MFGE8)	GLQHWVPEL	1	0	0	1	0
BAP31 KLD	BAP31	KLDVGNAEV	0	1	1	0	0
Bcl-2 WLS	Bcl-2	WLSLKTLLSL	2	3	2	1	1
Bcl-xL YLN	Bcl-xL	YLNDHLEPWI	0	2	2	0	0
B-RAF LATE	B-RAF	LATEKSRWS	1	2	1	0	1
P-cadherin FII	P-cadherin	FIIENLKAA	4	1	0	3	1
CDCA1/NUF2 KLA	CDCA1/NUF2	KLATAQFKI	1	1	1	1	0
CDK4 ACD	CDK4	ACDPHSGHFV	0	4	4	0	0
CDKN1A FAW	CDKN1A	FAWERVRGL	0	1	1	0	0
CDKN1A GLG	CDKN1A	GLGLPKLYL	7	10	7	4	3
CDKN1A LMA	CDKN1A	LMAGCIQEA	0	2	2	0	0
CLP NLV	CLP (coactosin-like protein)	NLVRDDGSAV	1	2	2	1	0
CLP RLF	CLP (coactosin-like protein)	RLFAFVRFT	2	3	3	2	0
c-MET YVD	c-MET	YVDPVITSI	0	1	1	0	0
CML28 ALV	CML28 (EXOSC5)	ALVDAGVPM	1	0	0	1	0
COA-1 RLL	COA-1 (UBXN11)	RLLASLQDL	1	2	2	1	0
CPSF KVH	CPSF	KVHPVIWSL	0	1	1	0	0
Cyclin B1 AKY	cyclin B1	AKYLMELTM	1	1	1	1	0
Cyclin B1 ILI	cyclin B1	ILIDWLVQV	1	3	2	0	1
Cyclin D1 LLG	cyclin D1	LLGATCMFV	1	2	2	1	0
Cyclophilin B KLK	cyclophilin B (Cyp-B)	KLKHYGPGWV	0	1	1	0	0
DAM-6 FLW	DAM-6, -10	FLWGPRAYA	0	2	2	0	0
EphA2 IMN	EphA2	IMNDMPIYM	0	2	2	0	0
EphA2 VLL	EphA2	VLLLVLAGV	3	5	3	1	2
EZH2 FMV	EZH2	FMVEDETVL	0	1	1	0	0
GnTV VLPV	GnTV	VLPDVFIRCV	3	2	2	3	0
gp100 AML	gp100 / Pmel17	AMLGTHTMEV	0	1	1	0	0
gp100 ITD	gp100 / Pmel17	ITDQVPFSV	1	2	1	0	1
gp100 KTW	gp100 / Pmel17	KTWGQYWQV	1	2	1	0	1
gp100 LLD	gp100 / Pmel17	LLDGTATLRL	4	4	2	2	2
gp100 MLG	gp100 / Pmel17	MLGTHTMEV	0	1	1	0	0
gp100 RLM	gp100 / Pmel17	RLMKQDFSV	0	1	1	0	0
gp100 RLP	gp100 / Pmel17	RLPRIFCSC	1	2	2	1	0
gp100 SLA	gp100 / Pmel17	SLADTNSLAV	0	1	1	0	0
gp100 YLE	gp100 / Pmel17	YLEPGPVTA	2	1	1	2	0
HERV-K-MEL MLA	HERV-K-MEL	MLAVISCAV	1	2	1	0	1
hsp70 LLD	hsp70	LLDVAPLSL	0	1	1	0	0
hsp70 LLL	hsp70	LLLLDVAPL	0	1	1	0	0
IDO1 ALL	IDO1	ALLEIASCL	0	2	2	0	0
IMP-3 NLS	IMP-3	NLSSAEVVV	1	0	0	1	0
KIF20A AQP	KIF20A	AQPDTAPLPV	3	6	3	0	3
KIF20A LLS	KIF20A	LLSDDDVVV	1	3	2	0	1
LAGE-1 MLM	LAGE-1	MLMAQEALAFL	3	4	3	2	1
Livin RLA	Livin (ML-IAP)	RLASFYDWLP	3	3	2	2	1
Livin SLG	Livin (ML-IAP)	SLGSPVLGL	3	4	3	2	1
M2BP RID	M2BP	RIDITLSSV	1	1	1	1	0
MAGE-A1 KVL	MAGE-A1	KVLEYVIKV	4	4	3	3	1
MAGE-A1 YLE	MAGE-A1	YLEYRQVPV	4	4	3	3	1
MAGE-A10 GLY	MAGE-A10	GLYDGMEHL	1	1	1	1	0
MAGE-A10 SLL	MAGE-A10	SLLKFLAKV	7	5	1	3	4
MAGE-A12 FLW	MAGE-A12	FLWGPRALV	1	2	2	1	0
MAGE-A2 KMV	MAGE-A2	KMVELVHFL	2	4	4	2	0

MAGE-A2 LVH	MAGE-A2	LVHFLLLKY	13	13	1	1	12
MAGE-A2 LVQ	MAGE-A2	LVQENYLEY	1	1	1	1	0
MAGE-A2 YLQ	MAGE-A2	YLQLVFGIEV	4	4	3	3	1
MAGE-A3 KVA	MAGE-A3	KVAELVHFL	0	5	5	0	0
MAGE-A4 GVY	MAGE-A4	GVYDGREHTV	1	2	1	0	1
MAGE-A8 KVA	MAGE-A8	KVAELVRFL	2	0	0	2	0
MAGE-A9 ALS	MAGE-A9	ALSVMGVYV	0	2	2	0	0
MAGE-C2 ALK	MAGE-C2	ALKDVEERV	1	2	2	1	0
MAGE-C2 KVL	MAGE-C2	KVLEFLAKL	8	6	3	5	3
MAGE-C2 LLF	MAGE-C2	LLFGLALIEV	4	4	1	1	3
MAGE-C2 TLD	MAGE-C2	TLDEKVAELV	1	1	1	1	0
MAGE-C2 VIW	MAGE-C2	VIWEVLNAV	0	1	1	0	0
MC1R TIL	MC1R	TILLGIFFL	4	6	3	1	3
Melan-A AAG	Melan-A / MART-1	AAGIGILTV	1	1	0	0	1
Melan-A EAA	Melan-A / MART-1	EAAGIGILTV	3	4	2	1	2
Melan-A ELA	Melan-A / MART-1	ELAGIGILTV	7	7	2	2	5
Melan-A ILT	Melan-A / MART-1	ILTVILGVL	2	6	5	1	1
Meloe-1 TLN	Meloe-1	TLNDECWPA	1	0	0	1	0
Meloe-2 RLP	Meloe-2	RLPPKPPLA	1	1	1	1	0
MG50 CMH	MG50	CMHLLLEAV	1	3	3	1	0
MG50 LLL	MG50	LLLEAVPAV	0	1	1	0	0
MG50 RLG	MG50	RLGPTLMCL	3	5	3	1	2
MG50 TLK	MG50	TLKCDCEIL	3	4	3	2	1
NY-ESO-1 QLS	NY-ESO-1 / LAGE-2	QLSLLMWIT	3	2	2	3	0
NY-ESO-1 SLL	NY-ESO-1 / LAGE-2	SLLMWITQC	3	2	0	1	2
P Polypeptide IML	P Polypeptide	IMLCLIAAV	1	1	1	1	0
p53 KLC	p53	KLCPVQLWV	0	2	2	0	0
p53 KTC	p53	KTCPVQLWV	3	5	3	1	2
p53 LLG	p53	LLGRNSFEV	2	0	0	2	0
p53 RMP	p53	RMPEAAPPV	4	5	5	4	0
p53 SMP	p53	SMPPPGTRV	2	3	3	2	0
p53 VVP	p53	VVPCEPPEV	1	1	1	1	0
p53 YLG	p53	YLGSYGFRL	1	2	2	1	0
PGK1 IIG	PGK1	IIGGGMAFT	1	0	0	1	0
PRDX5 LLL	PRDX5	LLLDDLLVSI	2	5	4	1	1
RAB38 VLH	RAB38 / NY-MEL-1	VLHWDPETV	0	2	2	0	0
RAGE-1 LKL	RAGE-1	LKLSGVVRL	0	4	4	0	0
RAGE-1 PLP	RAGE-1	PLPPARNGGL	0	1	1	0	0
SART-3 RLA	SART-3	RLAEYQAYI	3	3	1	1	2
Secernin 1 KMD	secernin 1	KMDAEHPEL	3	2	2	3	0
SSX-2 KAS	SSX-2	KASEKIFYV	2	2	0	0	2
SSX-2 RLQ	SSX-2	RLQGISPKI	3	0	0	3	0
STAT1-alpha/ß KLQ	STAT1-alpha/ß	KLQELNYNL	4	6	3	1	3
STEAP1 FLY	STEAP1	FLYTLLREV	2	4	4	2	0
STEAP1 LLL	STEAP1	LLLGTIHAL	1	0	0	1	0
STEAP1 MIA	STEAP1	MIAVFLPIV	6	5	3	4	2
Survivin LML	Survivin	LMLGEFLKL	0	3	3	0	0
Survivin QMF	Survivin	QMFFCFKEL	1	0	0	1	0
TAG-1 SLG	TAG-1	SLGWLFLLL	4	5	3	2	2
Telomerase ILA	Telomerase	ILAKFLHWL	0	4	4	0	0
Telomerase RLFF	Telomerase	RLFFYRKSV	7	6	2	3	4
Topoisomerase II FLY	Topoisomerase II	FLYDDNQRV	1	0	0	1	0
TRAG-3 ILL	TRAG-3	ILLRDAGLV	2	4	3	1	1
TRP-2 FVW	TRP-2	FVWLHYYSV	5	4	2	3	2
TRP-2 SVY	TRP-2	SVYDFFVWL	3	3	2	2	1
TRP-2 TLD	TRP-2	TLDSQVMSL	0	1	1	0	0
TRP-2 VYD	TRP-2	VYDFFVWLHY	2	1	0	1	1
TRP2-6b ATT	TRP2-6b	ATTNILEHY	1	0	0	1	0
Tyrosinase CLL	tyrosinase	CLLWSFQTSA	3	1	1	3	0
Tyrosinase MLL	tyrosinase	MLLAVLYCL	2	3	3	2	0

Tyrosinase YMD	tyrosinase	YMDGTMSQV	0	2	2	0	0
XBP-1 LLS	XBP-1	LLSGQPASA	1	0	0	1	0
adipophilin SVA	adipophilin	SVASTITGV	-	-	-	-	-
ATIC (AICRT) MVY	ATIC (AICRT)	MVYDLYKTL	-	-	-	-	-
BA46 (MFGE8) NLF	BA46 (MFGE8)	NLFETPVEA	-	-	-	-	-
Bcl-2 PLF	Bcl-2	PLFDFSWLSL	-	-	-	-	-
BING-4 CQW	BING-4	CQWGRLWQL	-	-	-	-	-
B-RAF LAT	B-RAF	LATEKSRWSG	-	-	-	-	-
P-cadherin FIL	Cadherin 3/P-cadherin	FILPVLGAV	-	-	-	-	-
CDCA1 YMM	CDCA1/NUF2	YMMPVNSEV	-	-	-	-	-
CLP VVQ	CLP (coactosin-like protein)	VVQNFAKEFV	-	-	-	-	-
COA-1FMT	COA-1 (UBXN11)	FMTRKLWDL	-	-	-	-	-
CPSF LML	CPSF	LMLQNALTTM	-	-	-	-	-
Cyclin I LL	Cyclin I	LLDRFLATV	-	-	-	-	-
cyclin B1 AGY	cyclin B1	AGYLMELCC	-	-	-	-	-
cyclophilin B VLE	cyclophilin B (Cyp-B)	VLEGMEVV	-	-	-	-	-
CYP1B1 WLQ	CYP1B1	WLQYFPNPV	-	-	-	-	-
EphA2 TLA	EphA2	TLADFDPRV	-	-	-	-	-
EphA2 VLA	EphA2	VLAGVGFFI	-	-	-	-	-
EZH2 FIN	EZH2	FINDEIFVEL	-	-	-	-	-
GnTV VLP	GnTV	VLPDVFIRC	-	-	-	-	-
gp100 IMD	gp100 / Pmel17	IMDQVPFSV	-	-	-	-	-
gp100 VLY	gp100 / Pmel17	VLYRYGSFSV	-	-	-	-	-
IMP-3 RLL	IMP-3	RLLVPTQFV	-	-	-	-	-
KIF20A CIA	KIF20A	CIAEQYHTV	-	-	-	-	-
Livin QLC	Livin (ML-IAP)	QLCPICRAPV	-	-	-	-	-
MAGE-A3 LVF	MAGE-A3	LVFGIELMEV	-	-	-	-	-
MAGE-A8 GLM	MAGE-A8	GLMDVQIPT	-	-	-	-	-
MAGE-C2 FLA	MAGE-C2	FLAKLNNTV	-	-	-	-	-
Meloe-2 RCP	Meloe-2	RCPPKPPLA	-	-	-	-	-
MG50 VLS	MG50	VLSVNVPDV	-	-	-	-	-
MG50 WLP	MG50	WLPKILGEV	-	-	-	-	-
NY-ESO-1 SLA	NY-ESO-1 / LAGE-2	SLLMWITQA	-	-	-	-	-
NY-ESO-1 SLL	NY-ESO-1 / LAGE-2	SLLMWITQCFL	-	-	-	-	-
p53 GLA	p53	GLAPPQHLIRV	-	-	-	-	-
p53 LLP	p53	LLPENNVLSPV	-	-	-	-	-
p53 VVP	p53	VVPCEPPEV	-	-	-	-	-
PRAME ALY	PRAME	ALYVDSLFFL	-	-	-	-	-
PRAME SLL	PRAME	SLLQHLIGL	-	-	-	-	-
PRAME SLY	PRAME	SLYSFPEPEA	-	-	-	-	-
PRAME VLD	PRAME	VLDGLDVLL	-	-	-	-	-
PRDX5 AMA	PRDX5	AMAPIKVRL	-	-	-	-	-
Rep. protein A YLM	Replication protein A	YLMDTSGKV	-	-	-	-	-
SART-3 LLQ	SART-3	LLQAEAPRL	-	-	-	-	-
SOX10 AWI	SOX10	AWISKPPGV	-	-	-	-	-
SOX10 SAW	SOX10	SAWISKPPGV	-	-	-	-	-
Survivin ELT	Survivin	ELTLGEFLKL	-	-	-	-	-
Survivin TLP	Survivin	TLPPAWQPFL	-	-	-	-	-
Telomerase RLV	Telomerase	RLVDDFLLV	-	-	-	-	-
Telomerase LLT	Telomerase	LLTSRLRFI	-	-	-	-	-
TRP-2 SLD	TRP-2	SLDDYNHLV	-	-	-	-	-
TYMS LMA	TYMS	LMALPPCHAL	-	-	-	-	-

Supplementary Table 2: Antibody panels that were used to stain multimer+ CD8+ T cells.

marker	*fluorophore*	*clone*	*vendor*	*cat*
CD8	BV480	RPA-T8	BD	566121
CD8	BV510	RPA-T8	BD	563256
CD4	FITC	SK3	BD	345768
CD14	FITC	MΦP9	BD	345784
CD16	FITC	NKP15	BD	335035
CD19	FITC	4G7	BD	345776
CD40	FITC	LOB7/6	BioRad	MCA1590F

Supplementary Table 3: Antibody panels that were used to stain CD8+, CD4+ T cells, Tregs and checkpoint molecules.

marker	*fluorophore*	*clone*	*vendor*	*cat*
CD25	PE	M-A251	BD	555432
CD127	BV510	AO19D5	Biolegend	351322
CD8	APC-fire	SK1	Biolegend	344746
CD8	APC-Cy7	SK1	Biolegend	344714
CD3	A700	UCHT1	Biolegend	300424
CD4	PerCP	SK3	BD	345770
Lag-3	BV421	11C3C65	Biolegend	369314
PD-1	BV711	EH12.2H7	Biolegend	329928
TIM3	BB515	7D3	BD	565569
FoxP3	A647	259DC7	BD	560045
Isotype	BV421	MOPC-21	Biolegend	400158
Isotype	BV711	MOPC-22	Biolegend	400168
Isotype	BB515	X40	BD	564416

Supplementary Table 4: Antibody panels that were used to identify MDSC and classical monocytes.

marker	*fluorophore*	*clone*	*vendor*	*cat*
CD3	BV605	OKT3	Biolegend	317322
CD19	BV605	HIB19	Biolegend	302244
CD16	PacificBlue	3G8	Biolegend	302032
CD11b	APC-fire	ICRF44	Biolegend	301352
CD14	PE-Cy7	M5E2	Biolegend	301814
CD33	FITC	P67.6	Biolegend	366620
HLA-DR	PerCP-Cy5.5	L243	BD	339216
CD56	BV711	HCD56	Biolegend	318336
CD56	BV605	HCD56	Biolegend	318334

Supplementary Table 5: Estimated frequencies of the detected MAE-specific CD8+ T cell populations in each patient at BL and FU.

Patient	Name	baseline	follow-up
1	MAGE-A10 SLL	0,061%	0,113%
	MAGE-A1 YLE	0.000%	0.025%
	Melan-A ILT	0.000%	0.019%
	CDK4 ACD	0.000%	0.019%
	MAGE-A1 KVL	0.000%	0.017%
	CDKN1A GLG	0.000%	0.017%
	KIF20A AQP	0.000%	0.016%
	p53 KLC	0.000%	0.015%
	DAM-6 FLW	0.000%	0.015%
	p53 SMP	0.000%	0.013%
	gp100 RLP	0.000%	0.011%
	MG50 TLK	0.000%	0.011%
	MAGE-A2 LVH	0.045%	0.000%
2	MAGE-A10 SLL	0.282%	0.000%
	MAGE-A1 YLE	0.059%	0.000%
	CDKN1A GLG	0.045%	0.000%
	MG50 TLK	0.029%	0.000%
3	Bcl-2 WLS	0.000%	0.346%
	MAGE-A2 LVH	0.009%	0.062%
	MAGE-A10 GLY	0.000%	0.057%
	MAGE-A10 SLL	0.020%	0.053%
	RAB38 VLH	0.000%	0.021%
	COA-1 RLL	0.000%	0.012%
	MAGE-A1 YLE	0.000%	0.012%
	EphA2 VLL	0.018%	0.010%
	Bcl-xL YLN	0.000%	0.010%
	CDK4 ACD	0.000%	0.008%
	CDKN1A GLG	0.000%	0.008%
	MAGE-A1 KVL	0.000%	0.008%
	RAGE-1 LKL	0.000%	0.007%
	KIF20A AQP	0.000%	0.007%
	p53 SMP	0.000%	0.006%
	MG50 TLK	0.000%	0.006%
	gp100 SLA	0.000%	0.005%
	Cyclin D1 LLG	0.042%	0.000%
5	gp100 KTW	0.043%	0.554%
	Melan-A ELA	0.000%	0.116%
	ATIC RLD	0.000%	0.098%
	MG50 CMH	0.000%	0.097%
7	MAGE-A2 LVH	1.054%	0.068%
	NY-ESO-1 QLS	0.088%	0.000%
8	gp100 LLD	0.000%	0.564%
	HERV-K-MEL MLA	0.000%	0.086%
	MAGE-A2 YLQ	0.499%	0.000%
	Melan-A ELA	0.349%	0.000%
	CDKN1A GLG	0.310%	0.000%
	p53 YLG	0.298%	0.000%
	MAGE-C2 KVL	0.192%	0.000%

Patient	Name	baseline	follow-up
4	MAGE-A10 SLL	0.119%	0.224%
	MAGE-A2 LVH	0.141%	0.118%
	MAGE-A1 YLE	0.025%	0.040%
	CDK4 ACD	0.000%	0.027%
	CDKN1A GLG	0.019%	0.026%
	KIF20A AQP	0.018%	0.026%
	Melan-A ILT	0.000%	0.023%
	MAGE-A1 KVL	0.019%	0.023%
	DAM-6 FLW	0.000%	0.021%
	p53 KLC	0.000%	0.020%
	p53 SMP	0.000%	0.018%
	MG50 TLK	0.012%	0.017%
	CDKN1A LMA	0.000%	0.015%
	M2BP RID	0.000%	0.014%
	gp100 RLP	0.000%	0.013%
	MAGE-A4 GVY	0.000%	0.010%
	PRDX5 LLL	0.000%	0.010%
	gp100 RLM	0.000%	0.009%
	TRP-2 VYD	0.033%	0.008%
	MG50 LLL	0.000%	0.008%
	c-MET YVD	0.000%	0.008%
	EphA2 IMN	0.000%	0.007%
	MAGE-A2 LVQ	0.000%	0.006%
	Cyclin B1 ILI	0.000%	0.006%
6	STEAP1 MIA	0.055%	0.253%
	Livin RLA	0.000%	0.165%
	CLP RLF	0.000%	0.144%
	SSX-2 KAS	0.040%	0.113%
	Melan-A ELA	0.000%	0.084%
	P Polypeptide IML	0.000%	0.067%
	TRAG-3 ILL	0.000%	0.060%
	MAGE-C2 KVL	0.066%	0.059%
	KIF20A AQP	0.000%	0.050%
	gp100 KTW	0.000%	0.048%
	EphA2 IMN	0.000%	0.045%
	707-AP RVA	0.000%	0.043%
	STAT1-alpha/ß KLQ	0.000%	0.041%
	TRP-2 FVW	0.053%	0.039%
	PRDX5 LLL	0.000%	0.024%
	CDKN1A GLG	0.000%	0.022%
	gp100 LLD	0.353%	0.000%
	MAGE-A1 KVL	0.143%	0.000%
	MAGE-A2 YLQ	0.100%	0.000%
	MAGE-A1 YLE	0.096%	0.000%
	NY-ESO-1 QLS	0.081%	0.000%
	PRDX5 LLL	0.064%	0.000%
	P-cadherin FII	0.062%	0.000%
	GnTV VLPV	0.041%	0.000%
	STAT1-alpha/ß KLQ	0.034%	0.000%
	p53 RMP	0.034%	0.000%
	SART-3 RLA	0.028%	0.000%

9	gp100 AML	0.000%	1.295%	10	NY-ESO-1 QLS	0.000%	0.247%
	Melan-A ELA	0.577%	0.197%		Survivin LML	0.000%	0.217%
	STAT1-alpha/ß KLQ	0.000%	0.113%		MAGE-C2 ALK	0.000%	0.144%
	Livin SLG	0.267%	0.109%		Melan-A ELA	0.136%	0.137%
	Tyrosinase MLL	0.000%	0.072%		CLP NLV	0.000%	0.134%
	CDKN1A GLG	0.000%	0.029%		MG50 CMH	0.000%	0.125%
	MAGE-A2 KMV	0.337%	0.000%		Telomerase ILA	0.000%	0.123%
	p53 RMP	0.280%	0.000%		STEAP1 FLY	0.000%	0.114%
	MAGE-A10 SLL	0.273%	0.000%		Telomerase RLF	0.049%	0.113%
	STEAP1 MIA	0.196%	0.000%		MAGE-C2 VIW	0.000%	0.113%
	MAGE-C2 KVL	0.195%	0.000%		MAGE-A1 YLE	0.291%	0.000%
	MAGE-A1 KVL	0.171%	0.000%		Livin RLA	0.180%	0.000%
	gp100 YLE	0.128%	0.000%		TRP-2 VYD	0.112%	0.000%
	Tyrosinase CLL	0.127%	0.000%		Cyclin D1 LLG	0.109%	0.000%
	Melan-A EAA	0.098%	0.000%		MG50 RLG	0.108%	0.000%
	TAG-1 SLG	0.077%	0.000%		LAGE-1 MLM	0.102%	0.000%
	Telomerase RLF	0.076%	0.000%		MAGE-A2 KMV	0.080%	0.000%
	gp100 LLD	0.075%	0.000%		STAT1-alpha/ß KLQ	0.070%	0.000%
11	Melan-A ELA	0.000%	1.095%		MAGE-A10 GLY	0.065%	0.000%
	MAGE-A12 FLW	0.000%	0.960%		MAGE-A2 YLQ	0.065%	0.000%
	MG50 RLG	0.000%	0.593%		MAGE-C2 KVL	0.064%	0.000%
	LAGE-1 MLM	0.000%	0.318%		Livin SLG	0.060%	0.000%
	MAGE-C2 LLF	0.049%	0.288%		Meloe-1 TLN	0.059%	0.000%
	Melan-A EAA	0.185%	0.149%		TRP-2 FVW	0.048%	0.000%
	KIF20A AQP	0.021%	0.087%		707-AP RVA	0.041%	0.000%
	SSX-2 KAS	0.141%	0.069%		STEAP1 MIA	0.041%	0.000%
	MAGE-A3 KVA	0.000%	0.038%		P-cadherin FII	0.035%	0.000%
	NY-ESO-1 QLS	0.000%	0.037%		CLP RLF	0.027%	0.000%
	MAGE-A2 KMV	0.000%	0.034%		p53 KTC	0.023%	0.000%
	MAGE-A2 YLQ	0.000%	0.028%		SSX-2 RLQ	0.013%	0.000%
	TAG-1 SLG	0.000%	0.023%		CDKN1A GLG	0.011%	0.000%
	Tyrosinase YMD	0.000%	0.022%	21	gp100 YLE	0.101%	0.000%
	Tyrosinase MLL	0.000%	0.020%	22	-	-	-
	gp100 LLD	3.334%	0.017%	23	Livin SLG	0.000%	0.746%
	Telomerase RLFF	0.000%	0.016%		p53 RMP	0.000%	0.363%
	TRP-2 FVW	0.000%	0.016%		707-AP RVA	0.000%	0.348%
	GnTV VLPV	0.000%	0.014%		MAGE-C2 KVL	0.000%	0.253%
	PRDX5 LLL	0.000%	0.010%		TAG-1 SLG	0.000%	0.186%
	Melan-A ELA	1.516%	0.000%		Livin RLA	0.000%	0.183%
	p53 RMP	0.094%	0.000%		STEAP1 MIA	0.000%	0.129%
	Tyrosinase CLL	0.038%	0.000%		MAGE-A2 YLQ	0.000%	0.119%
	Telomerase RLF	0.037%	0.000%		MAGE-A3 KVA	0.000%	0.059%
	STEAP1 MIA	0.026%	0.000%		MAGE-A1 YLE	0.000%	0.052%
	CLP NLV	0.026%	0.000%		p53 KTC	0.000%	0.045%
	MAGE-C2 KVL	0.021%	0.000%		CDKN1A GLG	0.000%	0.044%
	Livin RLA	0.018%	0.000%		B-RAF LATE	0.000%	0.043%
	Secernin 1 KMD	0.018%	0.000%		Meloe-2 RLP	0.000%	0.041%
	PGK1 IIG	0.016%	0.000%		CDKN1A FAW	0.000%	0.033%
	XBP-1 LLS	0.004%	0.000%		CLP NLV	0.000%	0.022%

12	gp100 LLD	0.052%	2.242%	13	MAGE-A1 KVL	0.042%	0.933%
	MAGE-C2 KVL	0.098%	0.436%		p53 KTC	0.000%	0.265%
	KIF20A LLS	0.000%	0.086%		TRP-2 FVW	0.085%	0.224%
	P-cadherin FII	0.256%	0.073%		Secernin 1 KMD	0.000%	0.202%
	TAG-1 SLG	0.079%	0.071%		LAGE-1 MLM	0.282%	0.194%
	MAGE-A2 YLQ	0.000%	0.064%		p53 RMP	0.000%	0.098%
	MAGE-A3 KVA	0.000%	0.060%		MAGE-C2 KVL	0.220%	0.092%
	p53 RMP	0.000%	0.056%		Tyrosinase MLL	0.000%	0.073%
	MAGE-A1 KVL	0.000%	0.053%		STAT1-alpha/ß KLQ	0.000%	0.064%
	LAGE-1 MLM	0.000%	0.048%		MAGE-A2 KMV	0.000%	0.062%
	p53 KTC	0.026%	0.043%		STEAP1 MIA	0.000%	0.060%
	707-AP RVA	0.000%	0.041%		BAP31 KLD	0.000%	0.055%
	gp100 MLG	0.000%	0.038%		MG50 TLK	0.000%	0.054%
	Cyclin D1 LLG	0.000%	0.034%		Livin SLG	0.000%	0.053%
	Livin RLA	0.072%	0.033%		Telomerase ILA	0.000%	0.052%
	STEAP1 MIA	0.128%	0.032%		SART-3 RLA	0.032%	0.044%
	MAGE-A2 KMV	0.000%	0.028%		Telomerase RLF	0.036%	0.040%
	Melan-A EAA	0.000%	0.022%		Tyrosinase CLL	0.000%	0.035%
	MG50 RLG	0.023%	0.020%		MG50 RLG	0.000%	0.031%
	SART-3 RLA	0.106%	0.019%		TRAG-3 ILL	0.024%	0.023%
	STAT1-alpha/ß KLQ	0.020%	0.017%		707-AP RVA	0.949%	0.000%
	CDKN1A GLG	0.072%	0.013%		p53 VVP	0.817%	0.000%
	MAGE-A10 SLL	0.955%	0.000%		GnTV VLPV	0.092%	0.000%
	Cyclin D1 LLG	0.577%	0.000%		MAGE-C2 ALK	0.073%	0.000%
	TRP-2 FVW	0.207%	0.000%		p53 SMP	0.055%	0.000%
	Secernin 1 KMD	0.110%	0.000%		MAGE-A8 KVA	0.039%	0.002%
	Livin SLG	0.085%	0.000%	15	CDKN1A GLG	0.000%	0.257%
	MAGE-A2 LVQ	0.068%	0.000%		MAGE-C2 KVL	0.000%	0.127%
	Tyrosinase MLL	0.061%	0.000%		p53 KTC	0.000%	0.127%
	P Polypeptide IML	0.053%	0.000%		Livin SLG	0.000%	0.110%
	KIF20A LLS	0.049%	0.000%		CLP RLF	0.000%	0.102%
	Telomerase RLF	0.029%	0.000%		STEAP1 MIA	0.000%	0.096%
	Tyrosinase CLL	0.026%	0.000%		LAGE-1 MLM	0.000%	0.063%
	SSX-2 RLQ	0.015%	0.000%		MAGE-A3 KVA	0.000%	0.063%
20	EZH2 FMV	0.000%	0.180%		MAGE-C2 ALK	0.000%	0.057%
	MAGE-C2 KVL	0.000%	0.108%		p53 VVP	0.000%	0.057%
	Cyclophilin B KLK	0.000%	0.102%		p53 YLG	0.000%	0.053%
	Telomerase RLF	0.000%	0.098%		Secernin 1 KMD	0.000%	0.051%
	p53 YLG	0.000%	0.085%		MAGE-A2 KMV	0.000%	0.050%
	hsp70 LLD	0.000%	0.078%		Cyclin D1 LLG	0.000%	0.048%
	CDKN1A LMA	0.000%	0.066%		MAGE-A10 SLL	0.037%	0.047%
	gp100 YLE	0.000%	0.059%		STAT1-alpha/ß KLQ	0.000%	0.043%
	Survivin LML	0.000%	0.054%		Tyrosinase YMD	0.000%	0.042%
	CDK4 ACD	0.000%	0.050%		MAGE-A12 FLW	0.000%	0.041%
	CDCA1/NUF2 KLA	0.000%	0.042%		GnTV VLPV	0.000%	0.040%
	MG50 TLK	0.316%	0.000%		p53 RMP	0.000%	0.038%
	TRP2-6b ATT	0.205%	0.000%		KIF20A AQP	0.037%	0.037%
	p53 SMP	0.140%	0.000%		Telomerase RLF	0.000%	0.037%
	p53 RMP	0.110%	0.000%		Telomerase ILA	0.000%	0.035%
	STEAP1 LLL	0.101%	0.000%		KIF20A LLS	0.000%	0.031%
	MAGE-A12 FLW	0.086%	0.000%		MG50 RLG	0.038%	0.031%
	MAGE-C2 TLD	0.082%	0.000%		SART-3 RLA	0.000%	0.027%
	alpha-actinin-4 FIA	0.073%	0.000%		PRDX5 LLL	0.000%	0.015%
	IMP-3 NLS	0.072%	0.000%				
	CLP RLF	0.051%	0.000%				

14	MAGE-A3 KVA	0.000%	1.515%
	gp100 LLD	0.000%	0.673%
	Melan-A ELA	0.080%	0.100%
	Meloe-2 RLP	0.092%	0.097%
	IDO1 ALL	0.000%	0.046%
	MAGE-A2 YLQ	0.099%	0.045%
	MG50 RLG	0.000%	0.036%
	MAGE-C2 LLF	0.053%	0.031%
	HERV-K-MEL MLA	0.078%	0.031%
	MAGE-A4 GVY	0.035%	0.029%
	Telomerase RLF	0.039%	0.028%
	STAT1-alpha/ß KLQ	0.862%	0.018%
	KIF20A LLS	0.000%	0.018%
	Melan-A EAA	0.000%	0.017%
	p53 KTC	0.027%	0.017%
	CDKN1A GLG	0.009%	0.012%
	MAGE-C2 KVL	1.071%	0.000%
	Survivin QMF	0.495%	0.000%
	Secernin 1 KMD	0.213%	0.000%
	Tyrosinase MLL	0.123%	0.000%
	NY-ESO-1 QLS	0.067%	0.000%
	M2BP RID	0.063%	0.000%
	LAGE-1 MLM	0.063%	0.000%
	STEAP1 MIA	0.037%	0.000%
	TRP-2 FVW	0.037%	0.000%
	MAGE-A8 KVA	0.020%	0.000%
	PRDX5 LLL	0.010%	0.000%
16	TAG-1 SLG	0.146%	0.000%
17	Survivin LML	0.000%	0.165%
18	-	-	-
19	TRP-2 TLD	0.000%	0.113%
	CLP RLF	0.000%	0.041%
	GnTV VLPV	0.108%	0.000%
	BA46 GLQ	0.094%	0.000%
	CDCA1/NUF2 KLA	0.071%	0.000%
24	MG50 CMH	0.316%	0.000%
25	CPSF KVH	0.000%	0.048%
26	-	-	-
27	EphA2 VLL	0.000%	0.146%
	MAGE-A2 LVH	0.021%	0.051%
	TRAG-3 ILL	0.000%	0.046%
	SSX-2 RLQ	0.064%	0.000%
	MC1R TIL	0.040%	0.000%
28	MAGE-A2 LVH	0.030%	0.217%
	Melan-A ILT	0.000%	0.124%
	MC1R TIL	0.000%	0.039%
29	MAGE-A2 LVH	0.044%	0.188%
	MC1R TIL	0.000%	0.090%
	TRP-2 SVY	0.016%	0.000%
30	Melan-A ELA	0.358%	0.955%
	Melan-A EAA	0.261%	0.656%
	Melan-A AAG	0.109%	0.256%
	MC1R TIL	0.129%	0.206%
	TRP-2 SVY	0.000%	0.135%
	MAGE-A2 LVH	0.381%	0.051%
	STEAP1 FLY	0.429%	0.000%
	Melan-A ILT	0.128%	0.000%
	CML28 ALV	0.061%	0.000%
	Topoisomerase II FLY	0.030%	0.000%
31	MAGE-A2 LVH	0.000%	0.260%
	MC1R TIL	0.022%	0.073%
	MAGE-A9 ALS	0.000%	0.044%
	Melan-A ELA	0.063%	0.000%
	P-cadherin FII	0.037%	0.000%
32	MAGE-A2 LVH	0.016%	0.060%
	MC1R TIL	0.000%	0.041%
	Melan-A ILT	0.000%	0.015%
33	MC1R TIL	0.049%	0.656%
	MAGE-A2 LVH	0.028%	0.613%
	Melan-A ILT	0.067%	0.250%
	STEAP1 FLY	0.000%	0.223%
	EphA2 VLL	0.823%	0.000%
	TRAG-3 ILL	0.250%	0.000%
	COA-1 RLL	0.091%	0.000%
	Bcl-2 WLS	0.042%	0.000%

34	Cyclin B1 ILI	0.014%	0.499%	35	Bcl-2 WLS	0.000%	0.207%
	TAG-1 SLG	0.000%	0.237%		EphA2 VLL	0.000%	0.166%
	RAGE-1 LKL	0.000%	0.190%		NY-ESO-1 SLL	0.017%	0.106%
	STEAP1 FLY	0.000%	0.158%		MAGE-A2 LVH	0.002%	0.060%
	NY-ESO-1 SLL	0.043%	0.108%		CDKN1A GLG	0.000%	0.054%
	Bcl-2 WLS	0.055%	0.098%		TRAG-3 ILL	0.000%	0.052%
	EphA2 VLL	0.017%	0.091%		Cyclin B1 ILI	0.000%	0.050%
	gp100 ITD	0.000%	0.086%		RAGE-1 LKL	0.000%	0.040%
	PRDX5 LLL	0.000%	0.084%		MG50 CMH	0.000%	0.030%
	MAGE-A9 ALS	0.000%	0.077%		RAGE-1 PLP	0.000%	0.029%
	B-RAF LATE	0.026%	0.069%		TAG-1 SLG	0.032%	0.027%
	MAGE-C2 LLF	0.056%	0.046%		Cyclin B1 AKY	0.000%	0.026%
	MAGE-A2 LVH	0.022%	0.026%		COA-1 RLL	0.000%	0.024%
	TRP-2 SVY	0.122%	0.000%		TRP-2 SVY	0.347%	0.016%
	Cyclin B1 AKY	0.035%	0.000%		RAB38 VLH	0.000%	0.016%
	CDKN1A GLG	0.028%	0.000%		STEAP1 FLY	0.000%	0.016%
36	hsp70 LLL	0.000%	0.281%		MAGE-C2 LLF	0.000%	0.015%
	TRP-2 FVW	0.000%	0.146%		Bcl-xL YLN	0.000%	0.014%
	RAGE-1 LKL	0.000%	0.077%		Melan-A ILT	0.000%	0.013%
	TRP-2 SVY	0.000%	0.062%		gp100 ITD	0.009%	0.012%
	EphA2 VLL	0.000%	0.043%		p53 RMP	0.000%	0.007%
	MAGE-A2 LVH	0.024%	0.022%		MAGE-A10 SLL	0.000%	0.001%
	STEAP1 FLY	0.289%	0.000%		Telomerase RLF	0.012%	0.000%
	MAGE-C2 LLF	0.154%	0.000%		gp100 RLP	0.003%	0.000%
	NY-ESO-1 SLL	0.134%	0.000%				

Supplementary Table 6: Identified correlations of MAE-specific CD8+ T cell populations with OS using a trained elastic net approach.

alpha	accuracy training set	accuracy test set	Identified MAE-specific CD8+ T cell populations
1	0.66	0.85	
0.9	0.72	0.85	TAG-1 SLG
0.8	0.65	0.85	
0.7	***0.89***	***0.85***	***P-cadherin FII; MAGE-A10 SLL; STEAP1 FLY; TAG-1 SLG; Telomerase ILA; Telomerase RLFF; TRAG-3 ILL; TRP-2 SVY; Tyrosinase CLL***
0.6	0.79	0.85	TAG-1 SLG; Telomerase RLF; Tyrosinase CLL
0.5	0.96	0.85	Bcl-xL YLN; P-cadherin FII; Cyclin B1 AKY; EphA2 VLL; gp100 RLP; LAGE-1 MLM; MAGE-A10 GLY; MAGE-A10 SLL; MAGE-A9 ALS; Melan-A EAA; Melan-A ELA; MG50 TLK; NY-ESO-1 QLS; RAB38 VLH; STAT1-alpha/β KLQ; STEAP1 FLY; TAG-1 SLG; Telomerase ILA; Telomerase RLF; TRAG-3 ILL; TRP-2 SVY; Tyrosinase CLL
0.4	0.93	0.85	Bcl-xL YLN; P-cadherin FII; EphA2 VLL; LAGE-1 MLM; MAGE-A10 SLL; RAB38 VLH; STEAP1 FLY; TAG-1 SLG; Telomerase ILA; Telomerase RLF; TRAG-3 ILL; TRP-2 SVY; Tyrosinase CLL
0.3	0.96	0.71	ATIC RLD; Bcl-xL YLN; P-cadherin FII; CLP NLV; Cyclin B1 AKY; EphA2 VLL; gp100 AML; gp100 RLP; gp100 YLE; LAGE-1 MLM; MAGE-A10 GLY; MAGE-A10 SLL; MAGE-A9 ALS; MAGE-C2 KVL; MAGE-C2 LLF; Melan-A EAA; Melan-A ELA; MG50 TLK; NY-ESO-1 QLS; RAB38 VLH; SSX-2 RLQ; STAT1-alpha/β KLQ; STEAP1 FLY; Survivin LML; TAG-1 SLG; Telomerase ILA; Telomerase RLF; TRAG-3 ILL; TRP-2 SVY; Tyrosinase CLL; Tyrosinase MLL
0.2	0.65	0.85	
0.1	0.93	0.42	707-AP RVA; ATIC RLD; Bcl-xL YLN; P-cadherin FII; CLP NLV; CML28 ALV; Cyclin B1 AKY; Cyclin B1 ILI; Cyclin D1 LLG; DAM-6 FLW; EphA2 VLL; GnTV VLPV; gp100 AML gp100 ITD; gp100 LLD; gp100 RLP; gp100 SLA; gp100 YLE; HERV-K-MEL MLA; IDO1 ALL; KIF20A LLS; LAGE-1 MLM; Livin SLG; M2BP RID; MAGE-A1 YLE; MAGE-A10 GLY; MAGE-A10 SLL; MAGE-A2 KMV; MAGE-A2 YLQ; MAGE-A3 KVA; MAGE-A8 KVA; MAGE-A9 ALS; MAGE-C2 KVL; MAGE-C2 LLF; MAGE-C2 VIW; MC1R TIL; Melan-A ILT; Melan-A EAA: Melan-A ELA; Meloe-1 TLN; MG50 TLK; NY-ESO-1 QLS; P Polypeptide IML; p53 KLC; p53 RMP; p53 SMP; p53 YLG; RAB38 VLH; RAGE-1 PLP; Secernin 1 KMD; SSX-2 RLQ; STAT1-alpha/β KLQ; STEAP1 FLY; STEAP1 MIA; Survivin LML; Survivin QMF; TAG-1 SLG; Telomerase ILA; Telomerase RLF; Topoisomerase II FLY; TRAG-3 ILL; TRP-2 SVY; TRP-2 VYD; Tyrosinase CLL; Tyrosinase MLL

Supplementary Table 7: Result of the univariate cox regression of the MAE-specific CD8+ T cell populations. that were identified as associated with OS a in trained elastic net approach.

	LRT	HR	Wald	log rank
TAG-1 SLG	0.002	0.039	0.001	0.006
Telomerase RLF	0.006	0.096	0.002	0.001
MAGE-A10 SLL	0.025	0.107	0.010	0.009
Tyrosinase CLL	0.063	0.197	0.034	0.045
TRAG-3 ILL	0.235	0.215	0.283	0.303
STEAP1 FLY	0.243	2.180	0.229	0.235
TRP-2 SVY	0.288	0.424	0.272	0.287
Telomerase ILA	0.074	4.43E-09	0.999	0.190
P-cadherin FII	0.092	81728653.8	0.998	0.217

LRT: likelihood ratio test. HR: hazard ratio

Early disappearance of peripheral multifunctional MAGE-A10- and TRP-2-reactive CD4+ T cells shortly after initiating anti-PD-1 checkpoint blockade is associated with improved survival of melanoma patients.

Andrea Gaißler[1,2], Sepideh Babei[2,3], Jonas Bochem[1,2], Janine Spreuer[1,2], Teresa Amaral[1,4,5], Nikolaus Benjamin Wagner[1,6], Claus Garbe[1], Manfred Claassen[2,3,7], Benjamin Weide[1], Graham Pawelec[8,9], Thomas Eigentler[10], Kilian Wistuba-Hamprecht[1,2,8,11,12,13]

1 Department of Dermatology, University Hospital Tübingen, Eberhard Karls University of Tübingen, Tübingen, Germany.
2 Internal Medicine I, University Hospital Tübingen, Eberhard Karls University of Tübingen, Tübingen, Germany
3 The M3 Research Center, Eberhard-Karls Universität Tübingen, Germany;
4 Skin Cancer Clinical Trials Center, University Hospital Tübingen, Eberhard Karls University of Tübingen, Tübingen, Germany
5 Cluster of Excellence iFIT (EXC 2180) "Image Guided and Functionally Instructed Tumor Therapies", Tübingen, Germany
6 Department of Dermatology, Venereology and Allergology, Kantonsspital St. Gallen, St. Gallen, Switzerland
7 Department of Computer Science, Eberhard Karls University of Tübingen, Tübingen, Germany
8 Department of Immunology, Interfaculty Institute for Cell Biology, Eberhard Karls University Tübingen, Tübingen, Germany
9 Health Sciences North Research Institute, Sudbury, ON, Canada
10 Charité – Universitätsmedizin Berlin, corporate member of Freie Universität Berlin and Humboldt-Universität zu Berlin, Department of Dermatology, Venereology and Allergology, Berlin, Germany
11Skin Cancer Unit, German Cancer Research Center (DKFZ), Heidelberg, Germany
12 Department of Dermatology, Venereology and Allergology, University Medical Center Mannheim, Ruprecht-Karl University of Heidelberg, Mannheim, Germany
13 DKFZ Hector Cancer Institute at the University Medical Center Mannheim, Mannheim, Germany

Corresponding author
Kilian Wistuba-Hamprecht
Internal Medicine I, University Hospital Tübingen,
Ottfried-Müller-Straße 37
72076 Tübingen, Germany
Mail: kilian.wistuba-hamprecht@uni-tuebingen.de
Phone: +49 7071 29 89639

Short title: Decrease in multifunctional CD4+ T cells

Keywords: melanoma, multifunctional T cells, checkpoint blockade,

Total number of figures / tables: 5/2

Funding
This work was partially funded by the Medical Faculty of the University of Tübingen (2509-0-0), Bristol-Myers Squibb (CA209-9P4) and the Klaus Tschira Foundation (00.316.2017).

Disclosure of Potential Conflicts of Interest

T. Amaral reports institutional grants and travel grants from SkylineDx, institutional grants and personal fees from Novartis, institutional grants and personal fees from NeraCare, personal fees from BMS, institutional grants from Sanofi, personal fees from CeCaVa, personal fees from Pierre Fabre, personal fees from Delcath, outside the submitted work. **G. Pawelec** has received travel support or/and speaker´s fees or/and advisor´s honoraria from Novartis, Roche, Sanofi, Pfizer, GlaxoSmithKline, Seqirus and Astellas. **T. Eigentler** has received travel support or/and speaker´s fees or/and advisor´s honoraria by Sanofi, Novartis, Bristol-Myers Squibb, Merck Sharp & Dohme, Pierre Fabre, Anaveon, CureVec and Merck Darmstadt. **B. Weide** reports receiving commercial research grants

from Bristol-Myers Squibb and Merck Sharp & Dohme. **K. Wistuba-Hamprecht** received commercial research grants from the CatalYm GmbH and travel support from SITC (Society for Immunotherapy of Cancer).
No potential conflicts of interest were disclosed by the other authors

Abstract

Immune checkpoint blockade (ICB) is currently the standard of care for patients with melanoma. It is believed that a major mechanism of action of ICB is the reinvigoration of CD8+ T cells. However, little is known about the role and function of multifunctional tumor-reactive CD4+ T cells in this context. Here, we investigate the dynamics of functionally reactive CD4+ T cells in the blood of melanoma patients early after the initiation of anti-PD-1 therapy. To this end, we identified two candidate tumor-associated proteins, MAGE-A10 and TRP-2, based on published data and in silico epitope prediction scores. T cell clones specific for epitopes derived from these molecules were expanded from peripheral blood by stimulation with protein-spanning overlapping peptides from these two candidates for 12 days, followed by rechallenge with the respective peptides to investigate multifunctional profiles in a cohort of 31 stage IV patients. The resulting signatures and their dynamics over time were correlated with patients' survival to assess clinical relevance. Additionally, these dynamics were also correlated with phenotypes of myeloid cells and immune checkpoint molecule expression on Tregs, CD4+ and CD8+ T cells before starting and during ICB. Using a machine learning approach, we found that the disappearance from the blood of certain multifunctional CD4+ T cell populations correlated with longer overall survival. Patients exhibiting this early loss phenotype possessed a distinct peripheral immune cell signature (more PD-1+ Tregs and PD-1+CD8+ T cells). The data from this pilot study suggest that the initial presence but early disappearance from the blood of multifunctional tumor antigen-reactive CD4+ T cell populations is a potential biomarker for response to ICB in advanced melanoma.

Introduction

Immune checkpoint blockade (ICB) targeting programmed death receptor 1 (PD-1) on the surface of T cells either alone or in combination with cytotoxic T-lymphocyte-associated protein-4 (CTLA-4) is currently standard of care for the treatment of advanced melanoma and other solid cancers[1 2]. However, long-term clinical benefit is still limited to a fraction of patients (roughly 50%)[3 4]. Therapeutic efficacy has been, for the most part, ascribed to a reinvigoration/induction of tumor antigen-reactive CD8+ T cells, but there is increasing awareness of essential roles of CD4+ T cells, including direct tumor cell lysis, induction of senescence in tumor cells, or execution of a wide range of T_{helper} functions[5]. Not only multifunctional tumor-specific CD8+ T cells but also CD4+ T cells are found in the tumor microenvironment (TME) of melanomas[6,7] and their presence in the tumor has been linked to a better clinical outcome[8-10]. In the mRNA-vaccination setting, post-vaccination CD4+ T cell responses were more prominent than those of CD8+ T cells in melanoma[11 12], despite the vaccines used in these studies being designed to include both MHC-I and MHC-II epitopes[11 12]. Along these lines, in the pre-checkpoint era, we previously reported that the presence of peripheral CD4+ and CD8+ T cell responses against the tumor-associated antigens (TAA) NY-ESO-1 or Melan-A was associated with prolonged overall survival (OS) of stage IV melanoma patients[13]. Moreover, in later studies of patients treated with anti-PD-1 ICB, the disappearance from the blood of these TAA-reactive T cells approximately 2 months after treatment initiation boded well for patient survival[14].

However, knowledge about TAA-reactive CD4+ T cells in advanced melanoma under ICB is still sparse. Thus, the aim of the current study was to investigate the presence before and dynamics of multifunctional CD4+ TAA-reactive T cells and their potential associations with patients' survival, to further elucidate biomarkers for and potential

mechanisms of CD4+ T cell-mediated anti-cancer responses. The TAAs MAGE-A10 and TRP-2 were identified as most promising targets through intensive screening of published data, and a second analysis of existing data of previous studies[15] and in silico MHC class I epitope prediction scores.

Materials and Methods

Patients

Venous blood from 31 stage IV melanoma patients before starting ICB and a median of 48 days thereafter was collected. PBMC were isolated using ficoll-gradient centrifugation and cryopreserved until further use in Roswell Park Memorial Institute (RPMI) 1640 medium containing 10% DMSO and 20% FCS and stored in liquid N_2. The samples were collected between March 2016 and July 2020. The cohort is partially overlapping with previous studies[14-16]. This study was approved by the Ethics Committee of Tübingen University Hospital (490/2014BO1, 616/2018BO2). All patients gave their written informed consent for use of biomaterials, biobanking, and their anonymized clinical data for scientific evaluation.

T cell epitope in silico prediction

netMHCpan 4.1 (available at https://services.healthtech.dtu.dk/service.php?NetMHCpan-4.1 as of 26.10.22 6.20 p.m.) for MHC-I binding and netMHCIIpan 4.0 (available at https://services.healthtech.dtu.dk/service.php?NetMHCIIpan-4.0 as of 26.10.22 6.20 p.m.) for MHC-II binding, were used to estimate potential MHC-binders in the protein sequences of MAGE-A10 and TRP-2. The HLA-types investigated in this

analysis (Supplementary Table 2) are published reference sets that cover most of world's population[17 18].

Assessment of multifunctional T cells

To determine the (multi-)functionality of the T cells, 2 x 10^6 PBMC were expanded for 12 days in the presence of protein-spanning overlapping peptides of either MAGE-A10, TRP-2 or FLU as a control (1 µg/mL; PepMix; JPT Peptide Technologies, BerlinMAGE-A10 batch. No.: 37625FWe-01; TRP-2 batch. No.:100815SASS-1, FLU (Influenza A, MP1(H3N2)) batch No.: 38389Gro-01). After 4 days IL-2 was added (40 U/ml) and after 12 days each sample was divided into two aliquots to be either restimulated or not. All samples from the same donor were adjusted to the same number of cells across proteins investigated.

The PepMixes used contained different numbers of peptides because the selected proteins varied in length. To stimulate all samples with an equal number of peptides, the concentration employed was normalized to the TAA PepMix with the lowest number of different peptides (MAGE-A10). Hence, MAGE-A10 and the control FLU expanded samples were restimulated with 5 µg/ml and TRP-2 with 3.5 µg/ml of the respective PepMix in the presence of transport-inhibitors (Golgi-Plug (1:1000; BD) and Golgi-Stop (1:1500; BD), as well as anti-CD107a-antibodies. After 12 hours dead cells were labelled with live/dead fixable red (Thermofisher Scientific), then Fc-γ receptors were blocked with Gamunex (Grifols). Next, samples were stained for cell surface markers and after fixation and permeabilization using the BD Cytofix/Cytoperm kit the samples were stained for intracellular activation markers and cytokines (Supplementary Table 1). Samples were afterwards acquired immediately on an LSR II cytometer (BD).

Flow cytometry data were analyzed using FlowJo (v10.7.1, BD). The gating strategy (Supplementary Figure 1) for T cells and their cytokine expression was adjusted on the

non-restimulated control and then copied to the respective re-stimulated sample. For the investigation of multifunctional T cells, Boolean combination gates were calculated by FlowJo, using the manual gates of each individual functional marker relative to their parental population (CD4+ or CD8+ T cells). TAA-reactive T cells were defined as present when the percentage of any functional marker in the re-stimulated sample was at least two-fold higher than in the respective non-restimulated control.

Dichotomization of the investigated patient cohorts according to multifunctional T cell populations

Patients with at least one disappearance of multifunctional CD4+ T cell populations under ICB were assigned to the “disappearance” group, whereas patients with an appearance of at least one as well those with a stable present or absent detection were assigned to the “appearance/stable” group. OS of the two groups was compared.

Phenotyping

To investigate phenotype and frequencies of NK cells, T cells, monocytic myeloid derived suppressor cells (M-MDSCs) and monocytes, we analyzed cryopreserved PBMC using flow cytometry. To stain cells of the myeloid compartment, samples were thawed, Fc-γ receptors blocked (Gamunex, Grifols) and dead cells stained with ethidium monoazide bromide (EMA, Biotinum). The samples were then stained for surface markers (Supplementary Tables 2). To investigate the T cell compartment, samples were thawed and separated into two aliquots; dead cells were labelled with live/dead fixable red (Thermofisher Scientific). Next, all PD-1 binding sites were saturated using anti-PD-1 antibody nivolumab, which was then labelled with a PE-

conjugated anti-IgG4-antibody. The samples were then stained for surface markers or with their respective isotype control (Supplementary Table 3). Afterwards, both aliquots were fixed and permeabilized (eBioscience FoxP3 Transcription Factor staining buffer set by Thermo Fisher Scientific) to stain for FoxP3 expression. Samples from both panels were acquired immediately after staining (LSR II cytometer (BD)) and were analyzed with FlowJo (v10.7.1, BD). Myeloid cells, NK cells and T cell subsets were gated as previously described[15 16] and the gating strategy is depicted in Supplementary Figures 2 and 3.

Statistics

Overall survival (OS) was determined from start of therapy (day of sampling) until death or last contact. The Kaplan-Meier method was applied to estimate the melanoma-specific survival probability of two patient groups dichotomized according to the identified immunological features. Log-rank testing was performed to evaluate potential differences of the survival of the investigated patient groups with a minimum group size of 5 (Prism, v5, GraphPad). The immune phenotypes of two patient groups were compared using Man-Whitney U testing and changes between baseline (BL) and follow-up (FU) with Wilcoxon matched pairs signed rank test (both Prism, v5, GraphPad). A p-value <0.05 was considered as significant.

Changes in the presence of TAA-reactive T cells that were associated with OS were investigated by training an elastic net regression model as described before, separately for MAGE-A10 and TRP-2 reactive T cells[15 19] Inputs were “appearance”, “disappearance” and “stable” (whereby not-detected populations where categorized as stable). Briefly, the cohort was divided into a test and a training set to select the best elastic net model hyper parameter α (75% and 25% of the samples, respectively). The

best alpha [0.1;1] was selected for the highest prediction accuracy from 10 randomly selected data partitions. The associations between selected TAA-reactive T cells and OS were investigated using multivariate Cox-regression[20], and multifunctional T cells with an HR >1 that were independently associated with survival were considered in the resulting model. We did not consider multifunctional CD4+ T cell populations with an HR >1, because there were not enough patients with an appearance in at least one of the multifunctional T cell populations (n=3)(Supplementary figure 5).

Visualizations

Heatmaps were created in R (version 4.2.0) using the packages complexheatmap[21], RColorBrewer and circlize[22]. Frequencies of the identified Immune cell subsets were Z-score normalized (mean of zero and standard deviation of one) for visualization. The cohort was dichotomized after the categorization of TAA-reactive CD4+ T cell dynamics. Clusters and dendrograms were calculated using the default settings of complexheatmap (distance: complete; method: euclidean).

Results and Discussion

Patients

Patients received either anti-PD-1 monotherapy or in combination with anti-CTLA-4 antibody (22.6% and 77.4% of patients, respectively). This unequal distribution between therapy groups was the result of the long-time span over which samples were collected – patients included at a later timepoint were mostly treated with the combination of antibodies. Most patients were male (67.7%), and the median age was 63 years. Patients were mostly categorized as M1c (80.6% M1c, 16.1% M1b and 3.2% M1a – according to AJCC 2009[23]). Just over half (51.6%) of the cohort was previously treated with systemic therapy (Table 1). Median survival was 28 months, and 2-year OS rate was 57.6%.

Table 1: Patient characteristics.

factor	category	n	%
age	median	63	-
therapy	anti-PD-1	7	22.6
	anti-PD-1+anti-CTLA-4	24	77.4
sex	female	10	32.3
	male	21	67.7
M-category	M1a	1	3.2
	M1b	5	16.1
	M1c	25	80.6
previous systemic therapies	immunotherapy	14	45.2
	targeted therapy	4	12.9
	chemotherapy	5	16.1
	other	2	6.5
	none	15	48.4
LDH-serum level	elevated	9	29.0
	normal	21	67.7
	unknown	1	3.2

LDH: Lactate dehydrogenase

In silico prediction of potential MHC-binders

We predicted the number of potential MHC-I and -II binders of peptides derived from MAGE-A10 and TRP-2 using netMHCpan and netMHCIIpan.

Table 2: Number of strong and weak MHC-I and MHC-II binders determined with netMHCpan and netMHCIIpan, respectively. The number of binders is summed over all HLA-classes investigated.

		MHC-I		MHC-II	
Protein	amount Peptides in PepMix	strong binder	weak binder	strong binder	weak binder
MAGE-A10	90	0	8	21	66
TRP-2	128	3	5	21	81

Table 2 summarizes results showing that more MHC-II than MHC-I binders were predicted for both proteins. Accordingly, we detected a strong dominance of CD4+ over CD8+ T cell responses (Supplementary Figure 4). Figure 1 A summarizes the study design.

Disappearance of multifunctional TAA-reactive CD4+ T cells from the blood is associated with prolonged OS

To investigate the association between OS and the dynamics of multifunctional CD4+ T cells early under ICB we performed an elastic net regression for MAGE-A10- or TRP-2-reactive cells. Combinatorial Boolean gates with a change in the presence of the effector molecules (CD154, IFN-γ, TNF-α and CD107a) during therapy were used as an input for the elastic net regression. Dynamics of all observed TAA-reactive CD4+ T cell populations are depicted in Figure 1 B, each column represents a patient. Six MAGE-A10-reactive CD4+ T cell populations correlated significantly with OS in a multivariate Cox-regression and 3 revealed an independent predictive capacity. Nine TRP-2-reactive CD4+ T cell populations were identified via elastic net regression as correlating with OS of which four presented an independent predictive feature for patients' OS in a multivariate Cox-regression (p=0.001). The results of the Cox-regression are shown in Figure 2 A and B and the independently predictive T cell populations are highlighted with asterisks after the p-value.

The three independently predictive multifunctional CD4+ T cell populations (with 2 or more functional markers expressed): MAGE-A10 CD107+CD154+IFN-γ+TNF-α+, TRP-2 CD107a+CD154+IFN-γ-TNF-α- and TRP-2 CD107a-CD154+IFN-γ-TNF-α+- with an HR >1 (Figure 2 C) were combined in a comprehensive model illustrating the superior survival of patients with an early disappearance of at least one of the identified

populations compared to those with appearing/stable cell populations (Figure 2 D, p=0.038).

These findings are in line with one of our previous studies in which we found that a disappearance of Melan-A- and/or NY-ESO-1-reactive T cells in peripheral blood of melanoma patients was associated with prolonged survival[14].

Patients with a disappearance of multifunctional CD4+ T cells express more PD-1 on CD8+ T cells and Tregs before ICB

Multifunctional T cells are often less exhausted or senescent than single functional T cells. High expression patterns of PD-1 and Tim-3 are associated with a more exhausted state of T cells[24]. To investigate potential correlations of the dynamics of multifunctional T cells under ICB with the peripheral T cell and myeloid cell signature before the start of therapy, we compared the latter in patients belonging to either the "disappearance" or "appearance/stable" group (Table 4).

278 **Table 3:** Median immune cell frequencies in peripheral blood of the "disappearance" and
279 "appearance/stable" groups and the Mann-Whitney U test p-value between these two groups. Due to
280 sample availability, there were 25 patients with phenotypical data at BL. Bolded populations are
281 significantly different in the two groups at p <0.05.

		disappearance		appearance/stable		
		median	**IQR**	**median**	**IQR**	**p**
T cell panel	CD3+ [Lymphocytes]	69.6	22.1	73	13.3	0.602
	Tregs [CD3]	4.6	1.7	5	2.1	0.750
	Tim-3	1.9	1.8	1.1	2.7	0.954
	PD1	**28.4**	**9.1**	**18.6**	**13.5**	**0.016**
	PD-1-Tim3+	0.6	0.6	0.7	1.7	0.601
	PD1+Tim-3-	**27.3**	**11.4**	**17.2**	**14.4**	**0.024**
	PD-1+ Tim3+	1	1.4	0.7	1.0	0.283
	CD8+[CD3]	25.4	21.8	31.1	20.2	0.401
	CD25	7.8	6.1	11.7	10.7	0.524
	Tim-3	4.3	4.4	2.4	3.5	0.192
	PD1	**32.7**	**24.7**	**19.5**	**12.4**	**0.043**
	PD-1-Tim3+	2.7	1.8	1.8	2.9	0.523
	PD1+Tim-3-	31	22.8	18	12.2	0.064
	PD1+Tim3+	**1.1**	**1.4**	**0.6**	**0.8**	**0.037**
	CD4 [CD3]	60.5	18.7	56.8	26.2	0.817
	Tim-3	1.2	1.6	1	1.0	0.415
	PD1	22.6	17.9	23	17.9	0.977
	PD-1-Tim3+	0.8	0.8	0.7	1.1	0.884
	PD1+Tim-3-	22.1	18.2	22	17.5	0.908
	PD-1+ Tim3+	24.3	19.1	24.6	18.1	0.931
myeloid cell panel	MDSC [viable PBMC]	11.1	3.5	11.9	12.7	0.417
	classical monocytes [viable PBMC]	9.6	3.8	9.5	6.2	0.643
	intermediate monocytes [viable PBMC]	0.7	0.9	0.4	0.5	0.320
	non-classical monocytes [viable PBMC]	0.2	0.2	0.2	0.2	0.891
	functional NK cells [viable PBMC]	8.8	11.3	6.8	4.4	0.325
	CD57+	63.3	20.3	62.7	21.0	0.750
	intermediate NK cells [viable PBMC]	0.2	0.2	0.1	0.3	0.752
	CD57+	3.1	2.6	2.1	2.9	0.212
	regulatory NK cells [viable PBMC]	0.3	0.2	0.2	0.2	0.975
	CD57	0.5	0.4	0.3	0.8	0.244

282

We found no significant difference in the frequencies of CD3+ T cells, Tregs, CD4+ or CD8+ T cells, but patients in the “disappearance” group had more PD-1+ CD8+ T cells, PD-1+ TIM-3+ CD8+ T cells (p=0.043 and p=0.037, respectively) and tended to have more PD-1+ TIM-3- CD8+ T cells (p=0.064) (Supplementary Figure 6). Patients with a disappearance of at least one of the multifunctional T cells in the model had significantly more PD-1+ Tregs (p=0.016) and more PD-1+TIM-3- (p=0.024), but not PD-1+TIM-3+ Tregs (p=0.283). The role of peripheral Treg subsets in solid cancers is still a matter of debate. There are reports that high PD-1+ (effector) Treg frequencies associate with shorter survival in NSCLC patients[25]. Populations significantly different in the two groups “disappearance” and “appearance/stable” also formed a cluster in a heatmap visualization of the Z-transformed frequencies (Figure 3). The observed differences in this study in the CD8+ T cell signature might be independent of the dynamics of multifunctional CD4+ T cells but are nonetheless associated with longer survival[26], similar to patients in the “disappearance” group. However, these differences could be a result of CD4+ T cell helper function, but potential exhaustion of these cells could not be investigated here, as cell numbers were too low, and CD4+ T cells also show hallmarks of exhaustion different from those of CD8+ T cells[27 28].

There were no significant differences between patients in the appearance/stable or disappearance groups with respect to the frequency of M-MDSC (Supplementary Figure 6 and Table 4), monocytes or NK-cells, even though these have been reported to be useful biomarkers in other studies[26 29 30]. Because in this study only 31 patients were investigated, further evaluation of these results future studies should be performed.

ICB driven changes in checkpoint expression are mostly seen in PD-1-TIM-3+ T cells

We next investigated changes of the T cell subsets under therapy, in the two groups "disappearance" and "appearance/stable". The goal here was to investigate potential synergies of changes of CD4+ multifunctional T cells and the phenotype of several T cell populations. We found that while there was no significant change in the number of CD8+ and CD4+ T cells or Tregs (Figure 4A and Supplementary Figure 7A), there was a significant decrease in PD-1+ Tregs in patients that manifested a decrease in multifunctional CD4+ T cells (Figure 4B). This is in line with previous work from others that associated such a decrease of PD-1+Tregs under ICB with favorable clinical outcome in melanoma[31].

Similar to the results in our earlier study[15] and other studies[32 33], we saw what was presumably an ICB-driven increase in TIM-3+ CD4+ T cells and Tregs in both groups (Figure 4C). PD-1 and TIM-3 phenotyping showed that mostly PD-1-Tim-3+ but not PD-1+Tim-3+ CD4+ T cells and Tregs were responsible for the ICB-induced increases in nearly all investigated T cell subsets, except for the CD4+ T cells of patients in the disappearance group (Figure 4D, E). Here, we propose an ICB-driven effect, potentially unrelated to changes in multifunctional CD4+ T cells. PD-1+TIM-3- T cells decreased significantly in Tregs in the disappearance group (Figure 4F). There was no change in the CD25 or PD-1 expression in CD8+ T cells under checkpoint blockade (Supplementary Figure 7B, C) but we detected an increase in Tim-3 expression in CD8+ T cells under therapy in all patients (Supplementary Figure 7D). This increase was not only driven by PD-1-Tim-3+ T cells, but also by PD-1+Tim-3+ T cells (Supplementary Figure 7 E, F). There were no changes in PD-1+Tim-3- T cells (Supplementary Figure 7G). These are commonly driven by ICB itself. Additionally,

there were no significant changes under ICB in myeloid cells (Supplementary Figure 7H), even though a decrease in the M-MDSC frequency has been described as beneficial[16].

We conclude that changes of the dynamics of TAA-reactive multifunctional CD4+ T cells and certain phenotypes were not visible here because TAA-reactive multifunctional CD4+ T cells are rare in the blood. Therefore, immune phenotyping cannot be used to assess the dynamics of CD4+ T cells in melanoma patients.

Conclusions

This pilot study shows that the dynamics of certain TAA-reactive multifunctional CD4+ T cells is associated with longer OS in patients with stage IV melanoma treated with ICB. We previously hypothesized[15] that important features of successful T cell re-invigoration by ICB are ICB-modulated kinetics of epitope accessibility[34] and existing or ICB-induced T cell specificity[35] and functionality[13 14 36 37]. This study adds that also the dynamics of multifunctionality of CD4+ T cells could be predictive of a beneficial outcome of ICB. To the best of our knowledge, very few studies thus far describe the multifunctionality of CD4+ T cells in melanoma or other cancers. Associations with certain dynamics of effector T cell populations early during ICB may suggest a potential CD4+ cytotoxic functionality but also putative helper functions in facilitating T cell melanoma rejection.

References:

1. Pilard C, Ancion M, Delvenne P, et al. Cancer immunotherapy: it's time to better predict patients' response. *Br J Cancer* 2021;125(7):927-38. doi: 10.1038/s41416-021-01413-x [published Online First: 2021/06/12]
2. Gong J, Chehrazi-Raffle A, Reddi S, et al. Development of PD-1 and PD-L1 inhibitors as a form of cancer immunotherapy: a comprehensive review of registration trials and future considerations. *J Immunother Cancer* 2018;6(1):8. doi: 10.1186/s40425-018-0316-z [published Online First: 2018/01/24]
3. Hodi FS, Chiarion-Sileni V, Gonzalez R, et al. Nivolumab plus ipilimumab or nivolumab alone versus ipilimumab alone in advanced melanoma (CheckMate 067): 4-year outcomes of a multicentre, randomised, phase 3 trial. *Lancet Oncol* 2018;19(11):1480-92. doi: 10.1016/S1470-2045(18)30700-9 [published Online First: 2018/10/27]
4. Hodi FS, -Sileni VC, Lewis KD, et al. Long-term survival in advanced melanoma for patients treated with nivolumab plus ipilimumab in CheckMate 067. *Journal of Clinical Oncology* 2022;40(16_suppl):9522-22. doi: 10.1200/JCO.2022.40.16_suppl.9522
5. Borst J, Ahrends T, Babala N, et al. CD4(+) T cell help in cancer immunology and immunotherapy. *Nat Rev Immunol* 2018;18(10):635-47. doi: 10.1038/s41577-018-0044-0 [published Online First: 2018/07/31]
6. Donia M, Hansen M, Sendrup SL, et al. Methods to improve adoptive T-cell therapy for melanoma: IFN-gamma enhances anticancer responses of cell products for infusion. *J Invest Dermatol* 2013;133(2):545-52. doi: 10.1038/jid.2012.336 [published Online First: 2012/09/28]
7. Oliveira G, Stromhaug K, Cieri N, et al. Landscape of helper and regulatory antitumour CD4(+) T cells in melanoma. *Nature* 2022 doi: 10.1038/s41586-022-04682-5 [published Online First: 2022/05/05]
8. Donia M, Kjeldsen JW, Andersen R, et al. PD-1(+) Polyfunctional T Cells Dominate the Periphery after Tumor-Infiltrating Lymphocyte Therapy for Cancer. *Clin Cancer Res* 2017;23(19):5779-88. doi: 10.1158/1078-0432.CCR-16-1692 [published Online First: 2017/07/07]
9. Liu Y, Lu P, Ma Y, et al. Peripheral Polyfunctional PD1(+) CD8(+) T cells demonstrated strong immune protection in non-small cell lung cancer. *Eur J Immunol* 2022 doi: 10.1002/eji.202149570 [published Online First: 2022/06/12]
10. Imai N, Tawara I, Yamane M, et al. CD4(+) T cells support polyfunctionality of cytotoxic CD8(+) T cells with memory potential in immunological control of tumor. *Cancer Sci* 2020;111(6):1958-68. doi: 10.1111/cas.14420 [published Online First: 2020/04/19]
11. Ott PA, Hu Z, Keskin DB, et al. An immunogenic personal neoantigen vaccine for patients with melanoma. *Nature* 2017;547(7662):217-21. doi: 10.1038/nature22991 [published Online First: 2017/07/06]
12. Sahin U, Oehm P, Derhovanessian E, et al. An RNA vaccine drives immunity in checkpoint-inhibitor-treated melanoma. *Nature* 2020;585(7823):107-12. doi: 10.1038/s41586-020-2537-9 [published Online First: 2020/07/31]
13. Weide B, Zelba H, Derhovanessian E, et al. Functional T cells targeting NY-ESO-1 or Melan-A are predictive for survival of patients with distant melanoma metastasis. *J Clin Oncol* 2012;30(15):1835-41. doi: 10.1200/JCO.2011.40.2271 [published Online First: 2012/04/25]
14. Bochem J, Zelba H, Spreuer J, et al. Early disappearance of tumor antigen-reactive T cells from peripheral blood correlates with superior clinical outcomes in melanoma under anti-PD-1 therapy. *J Immunother Cancer* 2021;9(12) doi: 10.1136/jitc-2021-003439 [published Online First: 2021/12/23]
15. Gaißler A, Meldgaard TS, Heeke C, et al. Dynamics of Melanoma-Associated Epitope-Specific CD8+ T Cells in the Blood Correlate With Clinical Outcome Under PD-1 Blockade. *Frontiers in Immunology* 2022;13 doi: 10.3389/fimmu.2022.906352

16. Gaissler A, Bochem J, Spreuer J, et al. Early decrease of blood myeloid-derived suppressor cells during checkpoint inhibition is a favorable biomarker in metastatic melanoma. *J Immunother Cancer* 2023;11(6) doi: 10.1136/jitc-2023-006802 [published Online First: 2023/06/08]
17. Greenbaum J, Sidney J, Chung J, et al. Functional classification of class II human leukocyte antigen (HLA) molecules reveals seven different supertypes and a surprising degree of repertoire sharing across supertypes. *Immunogenetics* 2011;63(6):325-35. doi: 10.1007/s00251-011-0513-0 [published Online First: 2011/02/10]
18. Weiskopf D, Angelo MA, de Azeredo EL, et al. Comprehensive analysis of dengue virus-specific responses supports an HLA-linked protective role for CD8+ T cells. *Proc Natl Acad Sci U S A* 2013;110(22):E2046-53. doi: 10.1073/pnas.1305227110 [published Online First: 2013/04/13]
19. Hui Zou TH. Regularization and variable selection via the elastic net. *Journal of the royal statistical society* 2005;67(2):310-20.
20. Lin DY, Wei LJ. The Robust Inference for the Cox Proportional Hazards Model. *Journal of the American Statistical Association* 1989;84(408):1074-78. doi: 10.1080/01621459.1989.10478874
21. Gu Z, Eils R, Schlesner M. Complex heatmaps reveal patterns and correlations in multidimensional genomic data. *Bioinformatics* 2016;32(18):2847-9. doi: 10.1093/bioinformatics/btw313
22. Gu Z, Gu L, Eils R, et al. circlize Implements and enhances circular visualization in R. *Bioinformatics* 2014;30(19):2811-2. doi: 10.1093/bioinformatics/btu393
23. Balch CM, Gershenwald JE, Soong SJ, et al. Final version of 2009 AJCC melanoma staging and classification. *J Clin Oncol* 2009;27(36):6199-206. doi: 10.1200/JCO.2009.23.4799 [published Online First: 2009/11/18]
24. Blank CU, Haining WN, Held W, et al. Defining 'T cell exhaustion'. *Nat Rev Immunol* 2019;19(11):665-74. doi: 10.1038/s41577-019-0221-9 [published Online First: 2019/10/02]
25. Kumagai S, Togashi Y, Kamada T, et al. The PD-1 expression balance between effector and regulatory T cells predicts the clinical efficacy of PD-1 blockade therapies. *Nature immunology* 2020;21(11):1346-58. doi: 10.1038/s41590-020-0769-3 [published Online First: 2020/09/02]
26. Krieg C, Nowicka M, Guglietta S, et al. High-dimensional single-cell analysis predicts response to anti-PD-1 immunotherapy. *Nat Med* 2018;24(2):144-53. doi: 10.1038/nm.4466
27. Balanca CC, Salvioni A, Scarlata CM, et al. PD-1 blockade restores helper activity of tumor-infiltrating, exhausted PD-1hiCD39+ CD4 T cells. *JCI Insight* 2021;6(2) doi: 10.1172/jci.insight.142513 [published Online First: 2020/12/18]
28. Miggelbrink AM, Jackson JD, Lorrey SJ, et al. CD4 T-Cell Exhaustion: Does It Exist and What Are Its Roles in Cancer? *Clin Cancer Res* 2021;27(21):5742-52. doi: 10.1158/1078-0432.CCR-21-0206 [published Online First: 2021/06/16]
29. Martens A, Wistuba-Hamprecht K, Foppen MG, et al. Baseline Peripheral Blood Biomarkers Associated with Clinical Outcome of Advanced Melanoma Patients Treated with Ipilimumab. *Clinical Cancer Research* 2016;22(12):2908-18. doi: 10.1158/1078-0432.ccr-15-2412
30. Baltussen JC, Welters MJP, Verdegaal EME, et al. Predictive Biomarkers for Outcomes of Immune Checkpoint Inhibitors (ICIs) in Melanoma: A Systematic Review. *Cancers (Basel)* 2021;13(24) doi: 10.3390/cancers13246366 [published Online First: 2021/12/25]
31. Gambichler T, Schroter U, Hoxtermann S, et al. Decline of programmed death-1-positive circulating T regulatory cells predicts more favourable clinical outcome of patients with melanoma under immune checkpoint blockade. *Br J Dermatol* 2020;182(5):1214-20. doi: 10.1111/bjd.18379 [published Online First: 2019/07/31]
32. Zelba H, Bedke J, Hennenlotter J, et al. PD-1 and LAG-3 Dominate Checkpoint Receptor-Mediated T-cell Inhibition in Renal Cell Carcinoma. *Cancer Immunol Res* 2019;7(11):1891-99. doi: 10.1158/2326-6066.CIR-19-0146 [published Online First: 2019/09/06]
33. Koyama S, Akbay EA, Li YY, et al. Adaptive resistance to therapeutic PD-1 blockade is associated with upregulation of alternative immune checkpoints. *Nat Commun* 2016;7:10501. doi: 10.1038/ncomms10501

34. Brossart P. The Role of Antigen Spreading in the Efficacy of Immunotherapies. *Clin Cancer Res* 2020;26(17):4442-47. doi: 10.1158/1078-0432.CCR-20-0305
35. Gangaev A, Rozeman EA, Rohaan MW, et al. Differential effects of PD-1 and CTLA-4 blockade on the melanoma-reactive CD8 T cell response. *Proc Natl Acad Sci U S A* 2021;118(43) doi: 10.1073/pnas.2102849118
36. Zelba H, Weide B, Martens A, et al. Circulating CD4+ T cells that produce IL4 or IL17 when stimulated by melan-A but not by NY-ESO-1 have negative impacts on survival of patients with stage IV melanoma. *Clin Cancer Res* 2014;20(16):4390-9. doi: 10.1158/1078-0432.CCR-14-1015
37. Pittet MJ, Zippelius A, Valmori D, et al. Melan-A/MART-1-specific CD8 T cells: from thymus to tumor. *Trends Immunol* 2002;23(7):325-8. doi: 10.1016/s1471-4906(02)02244-5 [published Online First: 2002/07/10]

Figure Legends

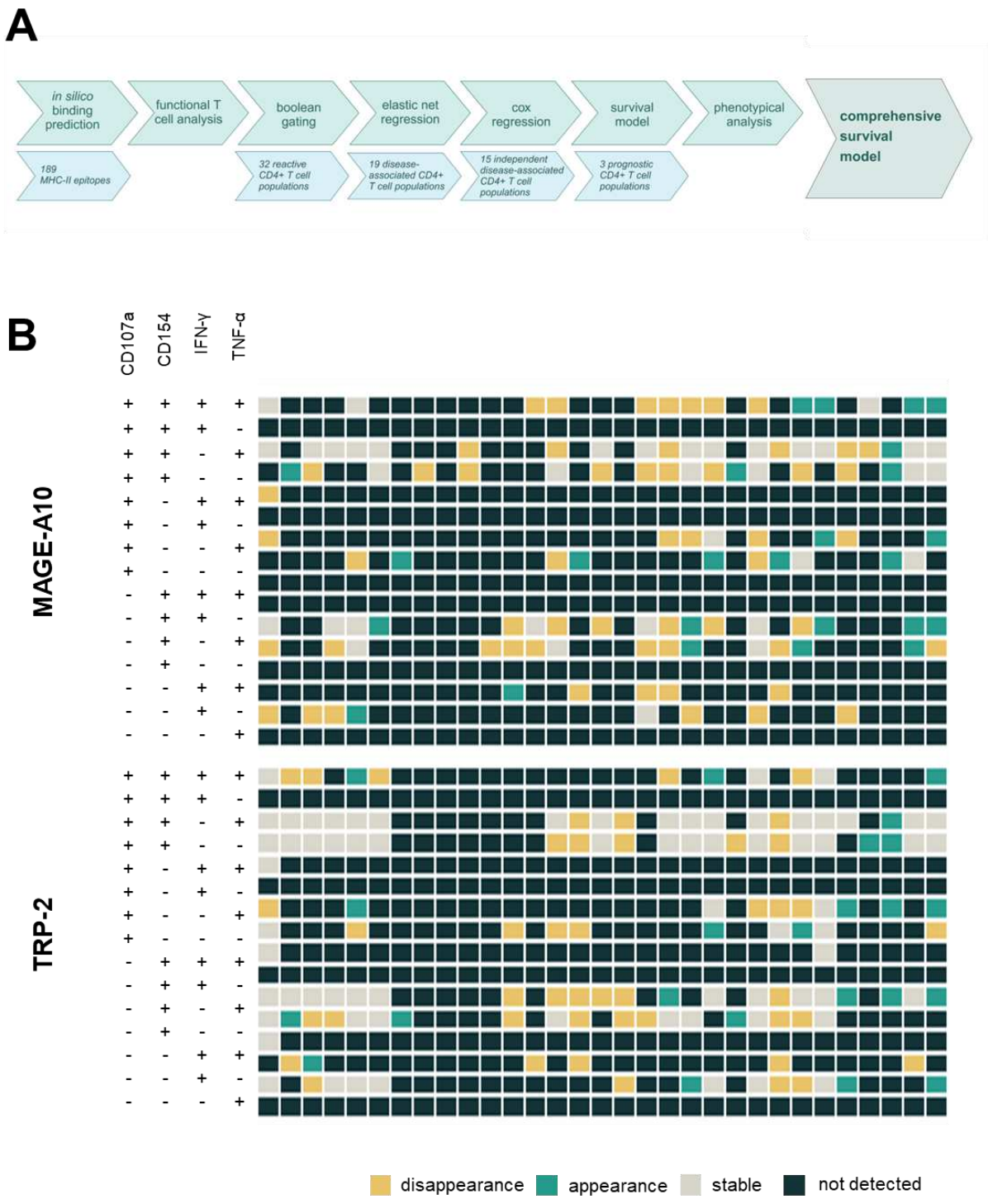

Figure 1: Flow chart overview of this study (A) and overview of the dynamics MAGE-A10 and TRP-2 multifunctional CD4+ T cells each column represents a patient (B). (A was created with BioRender.com)

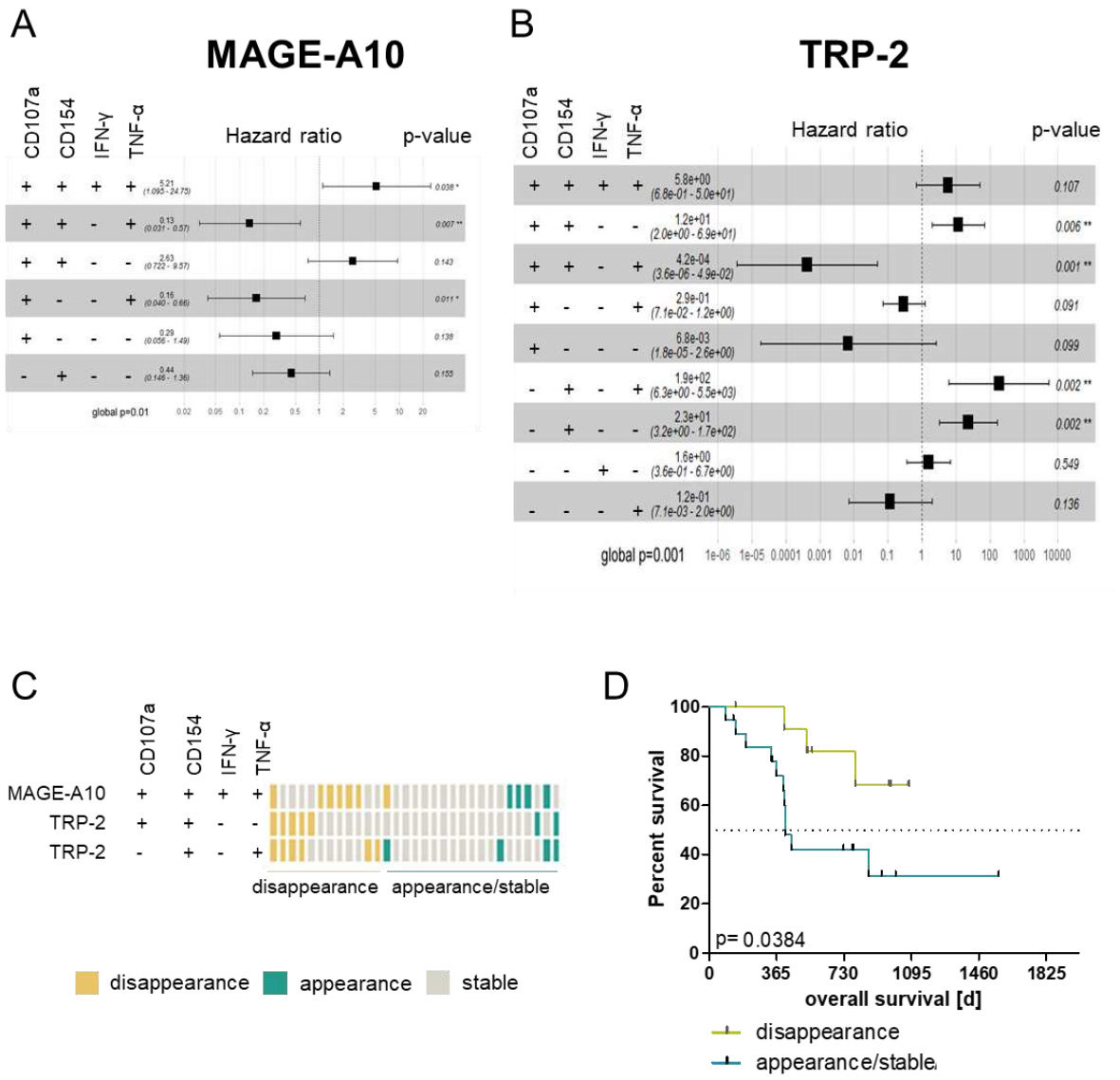

Figure 2: Forest plot of the functional CD4+ T cells reactive against MAGE-A10 PepMixes (A) and TRP-2 PepMixes (B), that were highlighted in an elastic net regression. Overview of the dynamics of the multifunctional T cells early under anti-PD-1 immune checkpoint therapy with HR >1. each column represents a patient (C). Kaplan-Meier plot of a combinatorial model dichotomizing the cohort after dynamics of multifunctional CD4+ T cells under therapy (D).

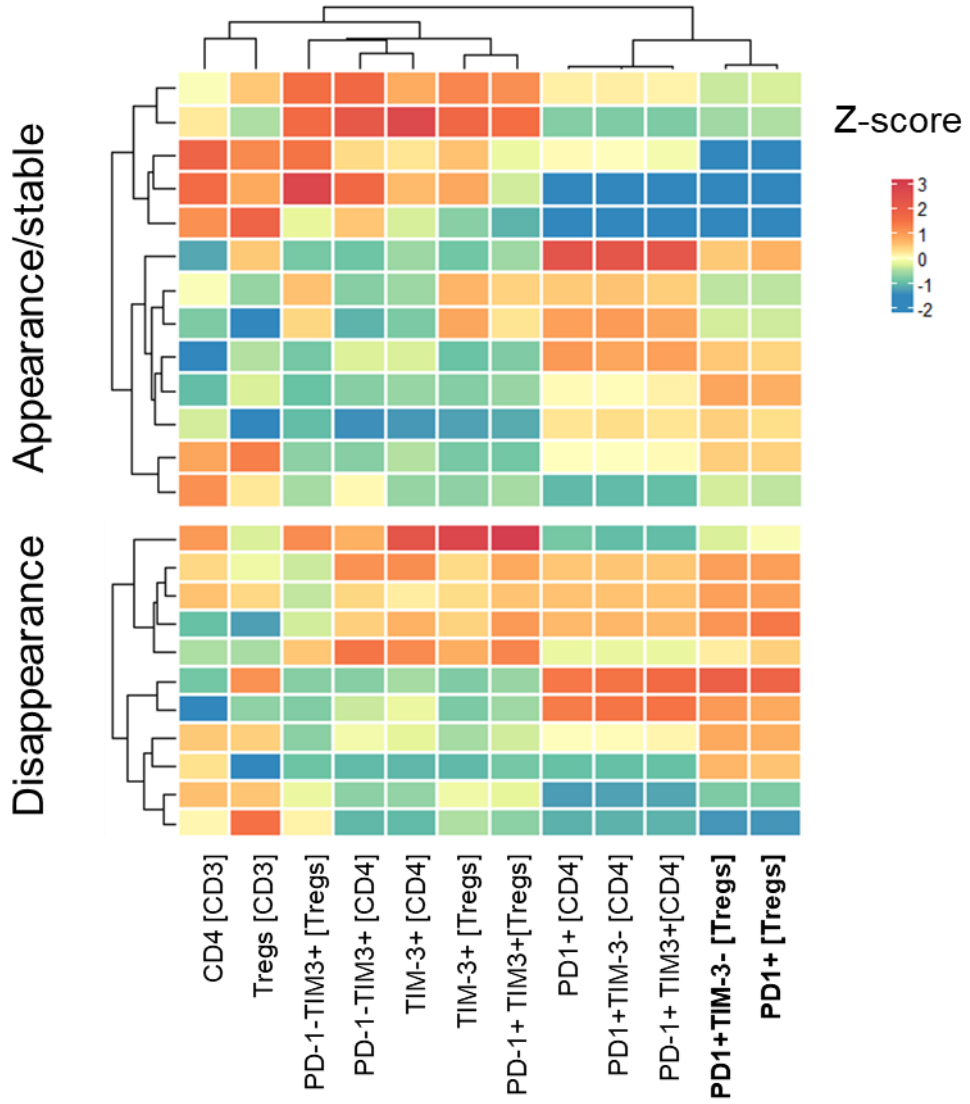

Figure 3: Visualization of frequencies of peripheral CD4+ T cell and Treg populations and their checkpoint molecule expression in a heatmap (columns), normalized to a mean of zero and a standard deviation of one in 24 melanoma patients (rows) prior to start of PD-1 ICB. The cohort is dichotomized after the categorization of TAA-reactive CD4+ T cell dynamics under PD-1 immune checkpoint therapy. Significant differences (Mann-Whitney U test) in frequencies of the individual populations are highlighted in bold. Clusters and dendrograms were calculated using the default settings of complexheatmap (distance: complete; method: euclidean).

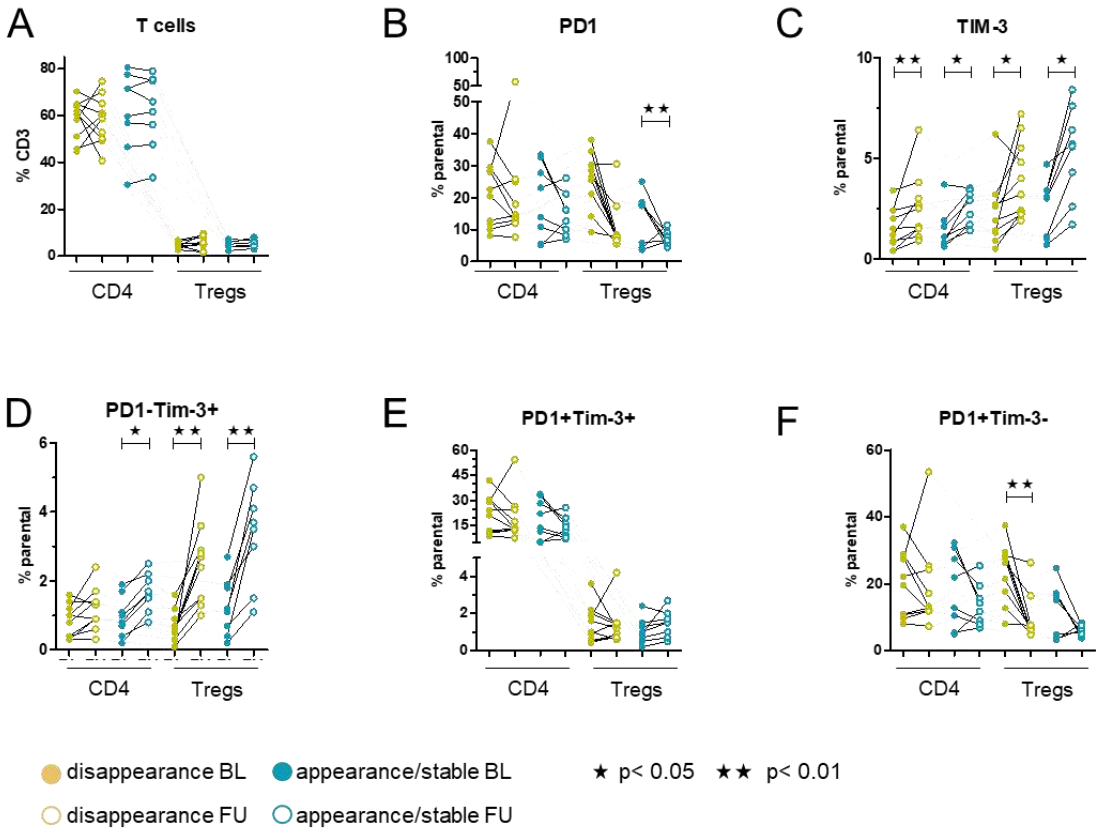

492

493 **Figure 4:** Changes of CD4+ T cell subset frequencies (A) and their respective PD-1
494 (B), TIM-3(C) subpopulations, as well as their subpopulations, defined by their
495 combinatorial expression PD-1-TIM-3+ (D), PD-1+TIM-3+ (E) and PD-1+TIM-3-(F).

496

Supplementary Information

Supplementary Table 1: Antibodies used for the detection of TAA-reactive T cells, as well as myeloid cells and T cell subsets and their checkpoint molecule expression.

Panel	Target	Fluorophore	Clone	company	cat
functional T cells	CD3	BV510	UCHT1	BioLegend	300448
	CD8	APC-fire	SK1	BioLegend	344746
	CD4	Alexa647	RPA-T4	BioLegend	300520
	IFN-g	PE-Cy7	B27	BD Pharmingen	557643
	TNF-a	Alexa700	Mab11	BioLegend	502928
	CD154	BV711	24-31	BioLegend	310383
	CD107a	Pacific Blue	H4A3	BioLegend	328624
myeloid cells	CD3	BV605	Okt 03	Biolegend	317322
	CD19	BV605	HIB19	Biolegend	302244
	CD16	PacificBlue	3G8	Biolegend	302032
	CD11b	APC-fire	ICRF44	Biolegend	301352
	CD14	PE-Cy7	M5E2	Biolegend	301814
	CD33	FITC	P67.6	Biolegend	366620
	HLA-DR	PerCP-Cy5.5	L243	BD	339216
	CD57	APC	HCD57	Biolegend	322214
	CD56	BV711	HCD56	Biolegend	318336
	CD45	BV510	H130	Biolegend	304036
checkpoint molecule expression on T cells	CD3	A700	OKT3	Biolegend	300424
	CD4	PerCP	SK3	Biolegend	344624
	CD8	APC-fire	SK1	Biolegend	960179
	CD25	BV421	M-A251	Biolegend	356114
	CD127	BV510	AO19D5	Biolegend	351322
	CD45	PE-Cy7	H130	Biolegend	304016
	Lag-3	BV711	11C3C65	Biolegend	369320
	TIM3	BB515	7D3	BD	565569
	Isotype control	PE	MOPC-21	Biolegend	400114
	Isotype control	BV711	MOPC-21	Biolegend	400168
	Isotype control	BB515	X40	BD	564416
	FoxP3	A647	20	BD	560045
	PD-1	-	Nivolumab		
	Anti Human IgG4	PE	HP6025	southern biotech	9200-09

Supplementary Table 2: Input MHC-I and MHC-II alleles in netMHCpan and netMHCIIpan analysis.

MHC-I	MHC-II
HLA-A*0101	HLA-DRB1*0101
HLA-A*0201	HLA-DRB1*0301
HLA-A*0203	HLA-DRB1*0401
HLA-A*0206	HLA-DRB1*0405
HLA-A*0301	HLA-DRB1*0701
HLA-A*1101	HLA-DRB1*0802
HLA-A*2301	HLA-DRB1*0901
HLA-A*2402	HLA-DRB1*1101
HLA-A*2601	HLA-DRB1*1201
HLA-A*3001	HLA-DRB1*1302
HLA-A*3002	HLA-DRB1*1501
HLA-A*3101	HLA-DRB3*0101
HLA-A*3201	HLA-DRB3*0202
HLA-A*3301	HLA-DRB4*0101
HLA-A*6801	HLA-DRB5*0101
HLA-A*6802	HLA-DQA1*0501/DQB1*0201
HLA-B*0702	HLA-DQA1*0501/DQB1*0301
HLA-B*0801	HLA-DQA1*0301/DQB1*0302
HLA-B*1501	HLA-DQA1*0401/DQB1*0402
HLA-B*3501	HLA-DQA1*0101/DQB1*0501
HLA-B*4001	HLA-DQA1*0102/DQB1*0602
HLA-B*4402	HLA-DPA1*0201/DPB1*0101
HLA-B*4403	HLA-DPA1*0103/DPB1*0201
HLA-B*5101	HLA-DPA1*0103/DPB1*0401
HLA-B*5301	HLA-DPA1*0301/DPB1*0402
HLA-B*5701	HLA-DPA1*0201/DPB1*0501
HLA-B*5801	HLA-DPA1*0201/DPB1*1401

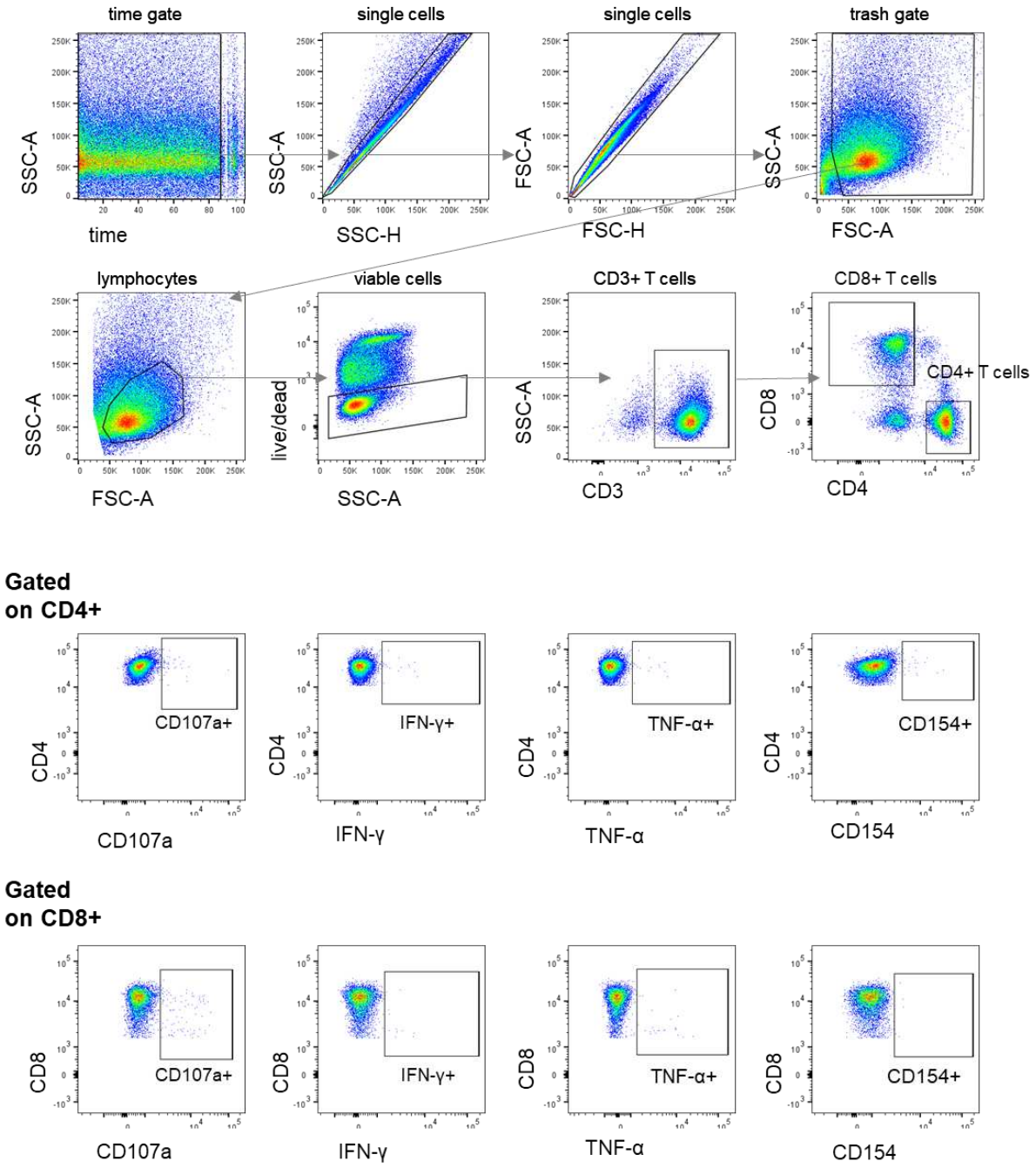

509

510 **Supplementary Figure 1**: Gating strategy to determine functionally TAA-reactive CD4+ and CD8+ cells
511 from PBMC.

512

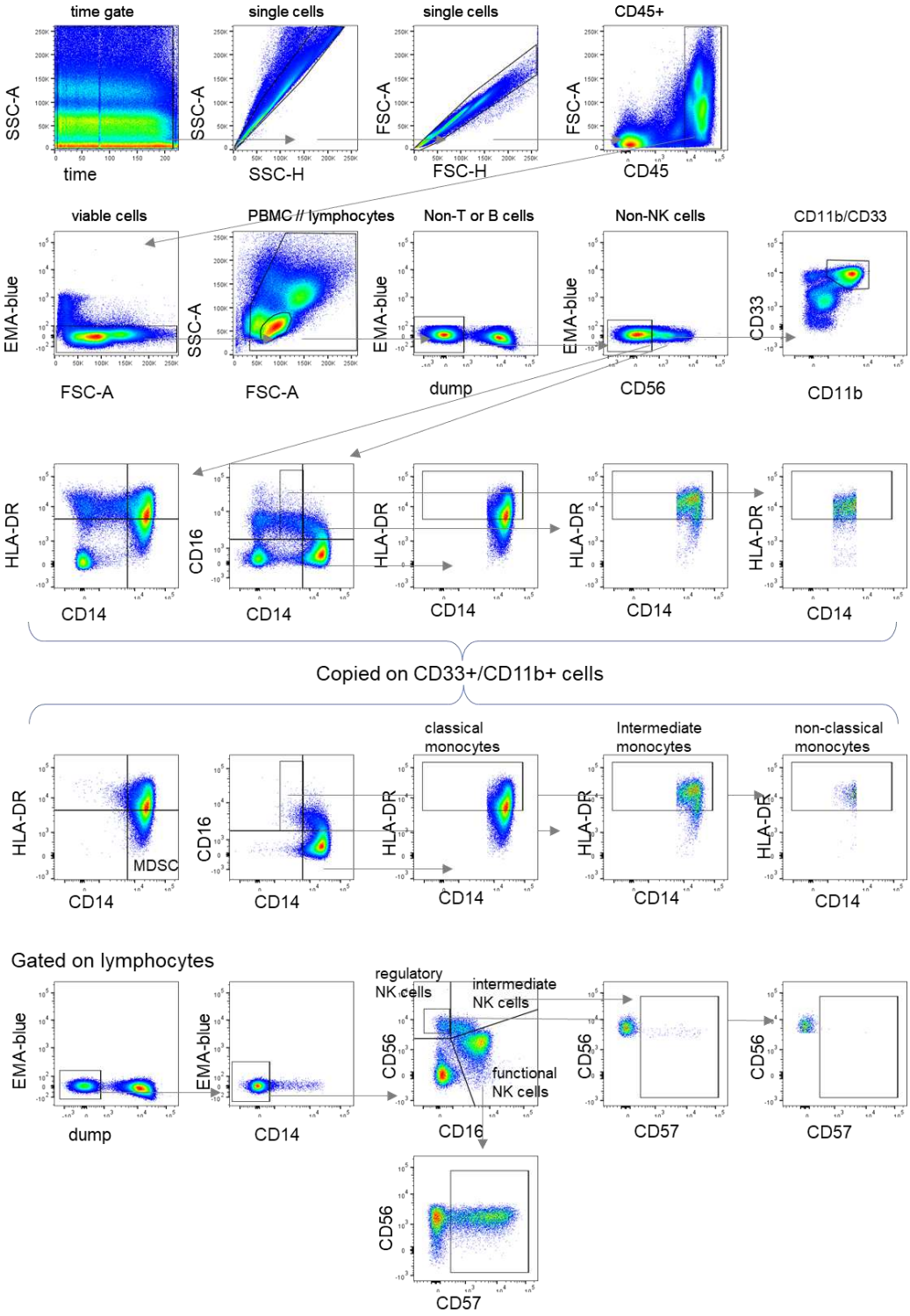

513

514 **Supplementary Figure 2**: Gating strategy for classical, intermediate and non-classical monocytes as
515 well as MDSC in PBMCs. Functional, intermediate and regulatory NK-cells were determined on
516 lymphocytes.

517

518

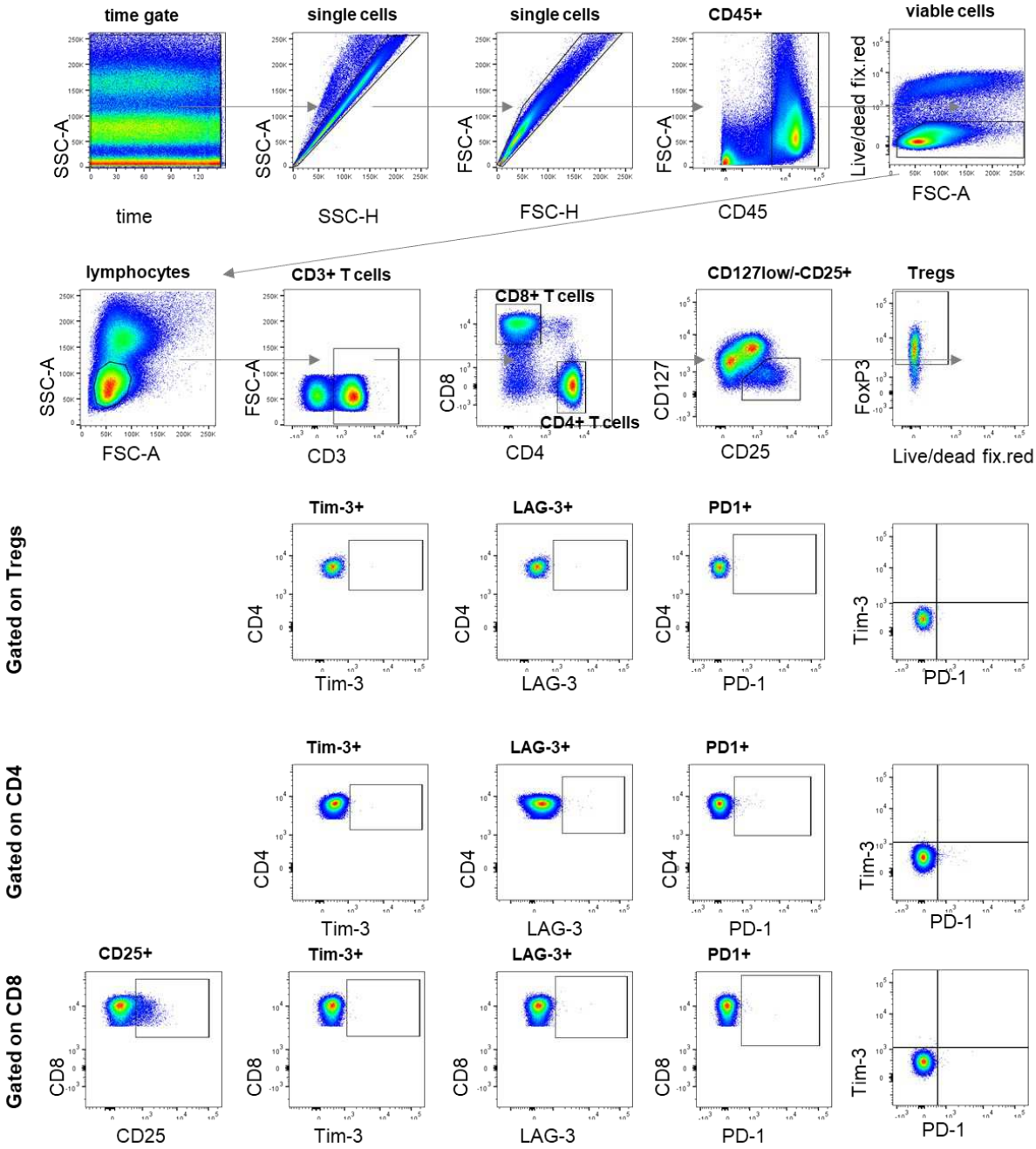

519

520

521 **Supplementary Figure 3**: Gating strategy to determine CD4+ T cells, CD8+ T cells and regulatory T
522 cells as well as their checkpoint molecule expression.

523

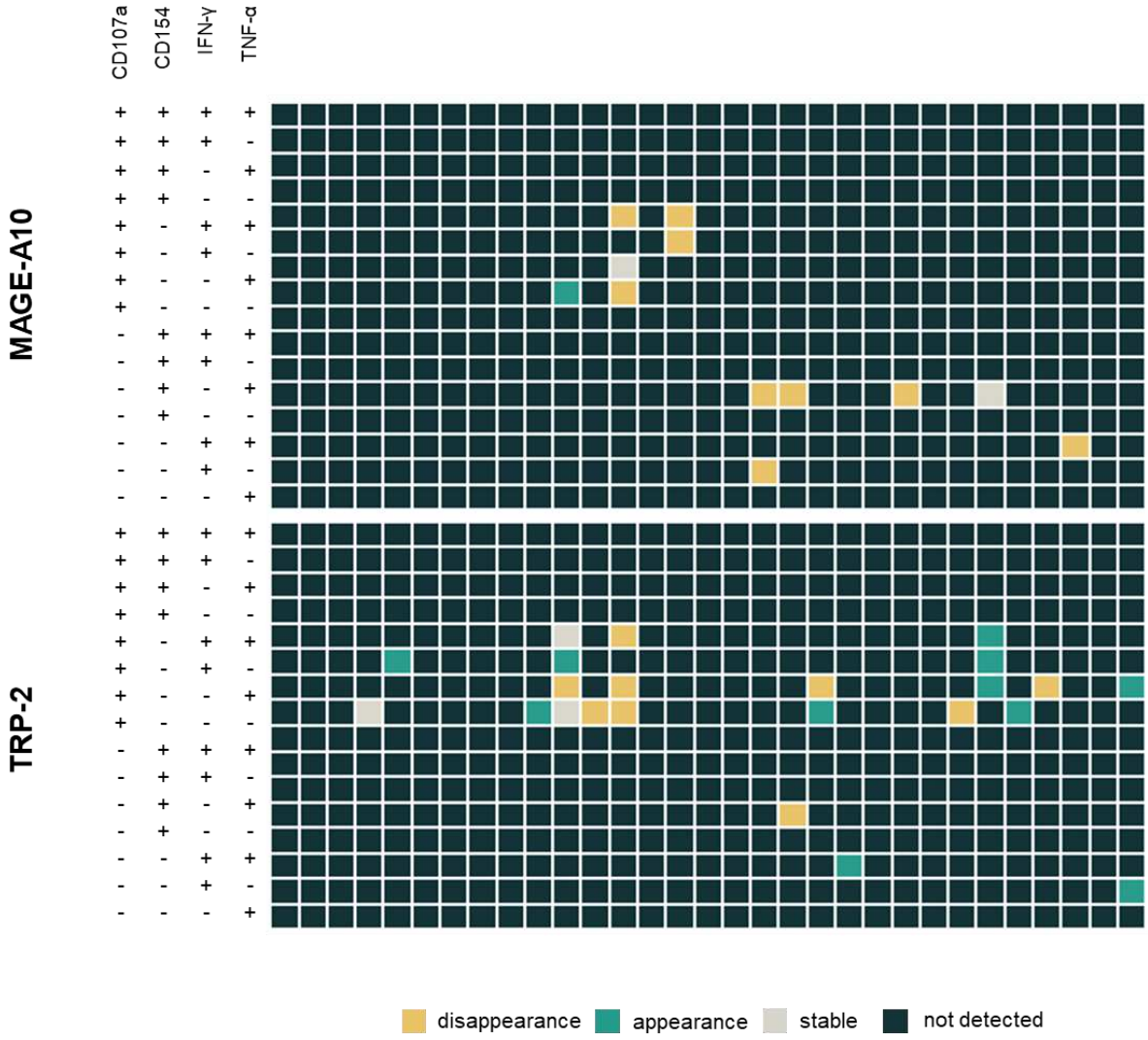

Supplementary Figure 4: Overview of the dynamics MAGE-A10 and TRP-2 multifunctional CD8+ T cells. Each column represents one patient.

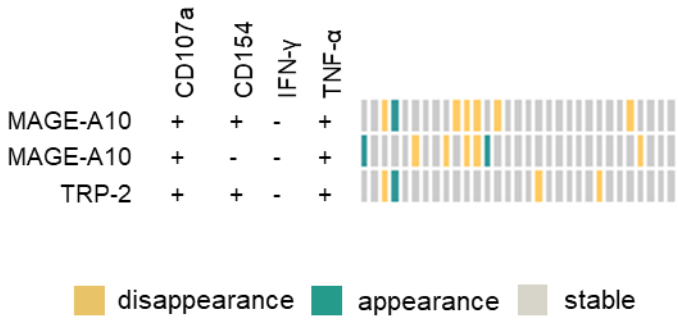

Supplementary Figure 5: Overview of multifunctional T cell populations, that correlated independently with overall survival and had an HR < 1. Each Column represents one patient.

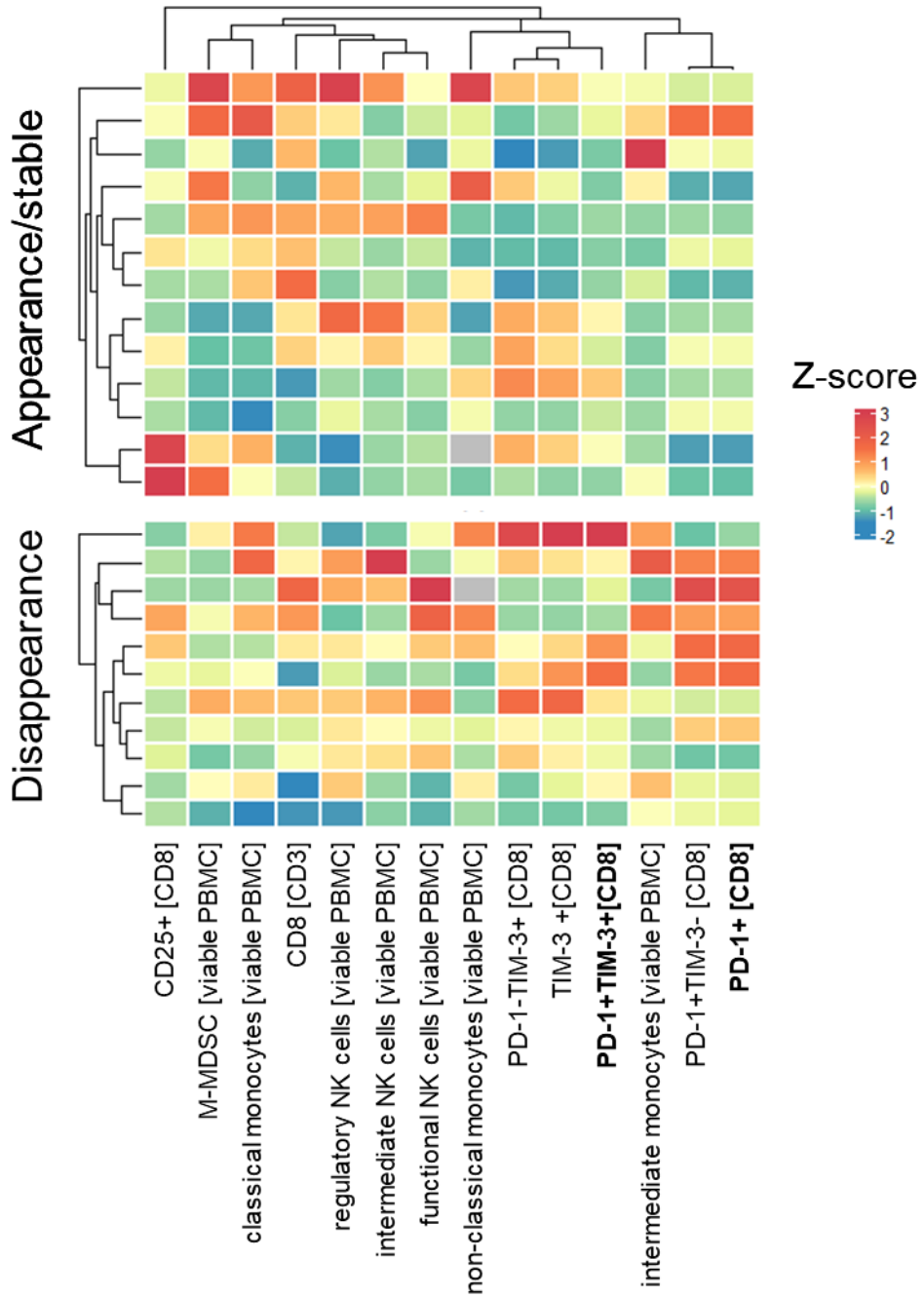

Supplementary Figure 6: Heatmap-cluster analysis of the Z-transformed frequencies of myeloid cells, NK cells CD8+ T cells and their checkpoint molecule expression in a heatmap (columns), normalized to a mean of zero and a standard deviation of one in 24 melanoma patients (rows) prior to start of PD-1 ICB. Significant populations from Mann-Whitney U testing are highlighted in bold.

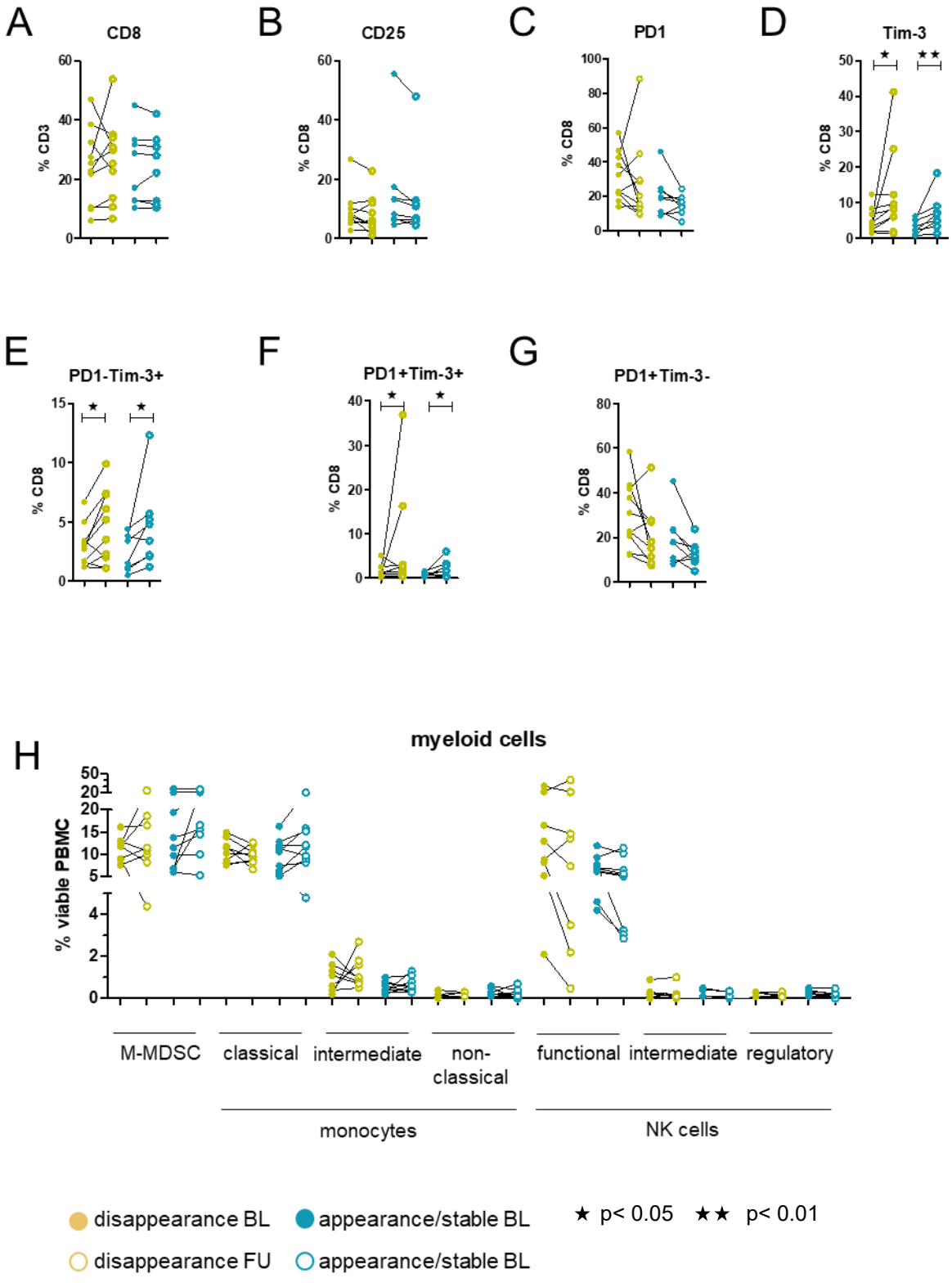

Supplementary Figure 7: Changes of CD8+ T cell subsets (A) and their CD25(B), PD-1 (C), TIM-3(D) expression separately, as well as their combined expression patterns of PD-1-TIM-3+ (E). PD-1+TIM-3+ (F) and PD-1+TIM-3- T cells (G). Changes of myeloid cells were also investigated (H). We had samples 17 patients with myeloid cell data at FU available and from 18 patients with phenotypic T cell data.

Journal for ImmunoTherapy of Cancer

Early decrease of blood myeloid-derived suppressor cells during checkpoint inhibition is a favorable biomarker in metastatic melanoma

Andrea Gaißler,[1,2] Jonas Bochem,[1,2] Janine Spreuer,[1,2] Shannon Ottmann,[1] Alexander Martens,[1] Teresa Amaral,[1,3] Nikolaus Benjamin Wagner,[1,4] Manfred Claassen,[2,5] Friedegund Meier ,[6] Patrick Terheyden ,[7] Claus Garbe,[1] Thomas Eigentler,[8] Benjamin Weide,[1] Graham Pawelec ,[9,10] Kilian Wistuba-Hamprecht [1,2,9]

To cite: Gaißler A, Bochem J, Spreuer J, *et al*. Early decrease of blood myeloid-derived suppressor cells during checkpoint inhibition is a favorable biomarker in metastatic melanoma. *Journal for ImmunoTherapy of Cancer* 2023;**11**:e006802. doi:10.1136/jitc-2023-006802

► Additional supplemental material is published online only. To view, please visit the journal online (http://dx.doi.org/10.1136/jitc-2023-006802).

AG and JB are joint first authors.

Accepted 28 April 2023

For numbered affiliations see end of article.

Correspondence to
Dr Kilian Wistuba-Hamprecht; kilian.wistuba-hamprecht@uni-tuebingen.de

ABSTRACT

Background The need for reliable clinical biomarkers to predict which patients with melanoma will benefit from immune checkpoint blockade (ICB) remains unmet. Several different parameters have been considered in the past, including routine differential blood counts, T cell subset distribution patterns and quantification of peripheral myeloid-derived suppressor cells (MDSC), but none has yet achieved sufficient accuracy for clinical utility.

Methods Here, we investigated potential cellular biomarkers from clinical routine blood counts as well as several myeloid and T cell subsets, using flow cytometry, in two independent cohorts of a total of 141 patients with stage IV M1c melanoma before and during ICB.

Results Elevated baseline frequencies of monocytic MDSCs (M-MDSC) in the blood were confirmed to predict shorter overall survival (OS) (HR 2.086, p=0.030) and progression-free survival (HR 2.425, p=0.001) in the whole patient cohort. However, we identified a subgroup of patients with highly elevated baseline M-MDSC frequencies that fell below a defined cut-off during therapy and found that these patients had a longer OS that was similar to that of patients with low baseline M-MDSC frequencies. Importantly, patients with high M-MDSC frequencies exhibited a skewed baseline distribution of certain other immune cells but these did not influence patient survival, illustrating the paramount utility of MDSC assessment.

Conclusion We confirmed that in general, highly elevated frequencies of peripheral M-MDSC are associated with poorer outcomes of ICB in metastatic melanoma. However, one reason for an imperfect correlation between high baseline MDSCs and outcome for individual patients may be the subgroup of patients identified here, with rapidly decreasing M-MDSCs on therapy, in whom the negative effect of high M-MDSC frequencies was lost. These findings might contribute to developing more reliable predictors of late-stage melanoma response to ICB at the individual patient level. A multifactorial model seeking such markers yielded only MDSC behavior and serum lactate dehydrogenase as predictors of treatment outcome.

WHAT IS KNOWN ON THIS TOPIC

⇒ So far, serum lactate dehydrogenase (LDH) levels are the only established, clinically used biomarkers for predicting the prognosis of metastatic melanoma.

⇒ However, high peripheral blood baseline monocytic myeloid-derived suppressor cell (M-MDSC) frequencies prior to immunotherapy are consistently statistically significantly associated with worse clinical outcome in many studies.

WHAT THIS STUDY ADDS

⇒ We confirm that elevated M-MDSC frequencies are associated with shorter survival on average, and describe a subset of patients whose high baseline M-MDSC frequencies decrease early during immunotherapy.

⇒ These patients have an overall survival (OS) similar to those initially with low MDSC frequencies.

⇒ Furthermore, we establish a multifactor model associated with OS which includes serum LDH levels and MDSC behavior.

HOW THIS STUDY MIGHT AFFECT RESEARCH, PRACTICE OR POLICY:

⇒ This study shows that monitoring of peripheral blood M-MDSC frequency during therapy provides a method for the early identification of patients responding to immunotherapy versus those who might benefit more from other therapies.

BACKGROUND

Over the last decade, there have been great improvements in the survival of patients with advanced melanoma due to the use of immune checkpoint inhibitors targeting the cytotoxic T-lymphocyte antigen-4 (CTLA-4) and programmed cell death protein 1 (PD-1) on the surface of activated T cells.[1 2] However, although many patients experience at least temporary clinical benefits, a subset does

not respond or develops resistance to such immune-checkpoint blockade (ICB).[3] Thus, the identification of specific biomarkers predicting response, ideally derived non-invasively from peripheral blood, remains an important clinical need. The serum lactate dehydrogenase (LDH) level is the only established biomarker in melanoma so far.[4 5] However, other parameters like routine blood counts,[6–8] circulating tumor DNA,[9] frequency of activated monocytes,[10] defined T cell subsets or myeloid-derived suppressor cells (MDSCs) have been suggested as promising candidates.[6 11–15] While molecular mechanisms of therapy response or resistance to ICB are not yet fully understood, the inhibition or acceleration of the activity of certain T cell subsets in the periphery and tumor microenvironment seems to be of great importance for clinical outcome.[16–18] Suppression of T cells by MDSCs contributes to profound immune dysfunction[19 20] and cancer immune evasion strategies,[21] mediated mostly, but not exclusively by monocytic MDSCs (M-MDSC) which are the largest subset. High peripheral blood frequencies of M-MDSCs are more prevalent in patients with melanoma than in healthy donors,[22] and correlate with clinical cancer stages,[23] and are associated with tumor development and progression.[24]

Here, we screened defined myeloid and T cell subsets in the blood of patients with late-stage melanoma before initiating and early during ICB to investigate potential associations with clinical outcome. We confirm the well-known general finding of ourselves and others that highly elevated frequencies of peripheral M-MDSCs associate significantly but not very closely with poorer outcomes of ICB in metastatic melanoma at the population level.[6 13 23–25] However, we find that in a subgroup of patients with rapidly decreasing M-MDSCs early during therapy, the poor prognosis associated with high baseline (BL) M-MDSC frequencies is lost, increasing the possibility of using levels of these cells as dynamic biomarkers of clinical outcome at the individual patient level.

METHODS

Patients

Only patients with stage IV melanoma classified by the site of metastasis and their LDH level as M1c according to American Joint Committee on Cancer (AJCC) 2009[5] were included in this study to investigate peripheral blood immune correlates with clinical outcome at a very late stage of disease. For the discovery cohort, we used cryopreserved peripheral blood mononuclear cells (PBMCs) from venous EDTA blood drawn before start of immunotherapy (baseline, BL) and a median of 44 days thereafter (follow-up (FU)) from 92 patients with melanoma treated between May 2015 and March 2017 at clinical centers in Dresden, Lübeck and Tübingen. For the validation cohort, samples from 49 patients were obtained from our biobank and derived also from the centers in Dresden and Tübingen from April 2017 to October 2019 following our established protocols. Clinical routine hemograms determined before or on the day of sampling (IQR 0–3 days) of the respective time point were used for analyses in this study. The cohorts investigated here overlap partially with cohorts from earlier published studies.[26 27] Detailed patient characteristics are given in table 1.

Flow cytometry

Patient samples were thawed in batches and stained with monoclonal antibody panels to characterize myeloid and T cells as described previously.[27] In brief, in the myeloid cell panel, dead cells were excluded using ethidium monoazide bromide (EMA, Biotinum) with simultaneous blockade of free Fcγ-receptors (Gamunex, Grifols) and stained for extracellular cell surface markers (online supplemental table 1). M-MDSC were defined as viable lineage-negative (CD3-CD19-CD56–) cells expressing CD11b, CD33 and CD14 but little or no HLA-DR. Monocytes were defined as viable lineage-negative CD11b+CD33+HLA-DR+ cells and are further subcategorized by their different CD14 and CD16 expression. Classical monocytes were defined as CD14+CD16–, intermediate monocytes as CD14+CD16+ and non-classical monocytes as CD14dimCD16+ cells (online supplemental figure 1). To investigate T cells and their checkpoint expression, two aliquots of the same PBMC samples that were used for the myeloid cell panel were concurrently stained. After staining of dead cells (EMA, Biotinum) and blockade of free Fcγ-receptors (Gamunex, Grifols), samples were incubated with antibodies against cell surface markers. Both aliquots were stained with antibodies against CD3, CD4, CD8, CD25 and CD127. For investigation of checkpoint expression, cells were either stained with antibodies against PD-1, lymphocyte activation gene 3 (LAG-3) and T cell immunoglobulin and mucin-domain containing-3 (TIM-3) or with their respective isotype controls. To identify regulatory T cells (Tregs), the samples were fixed and permeabilized using the FoxP3 Transcription Factor staining buffer set (Thermo Fisher Scientific) and then incubated with FoxP3 antibodies (online supplemental table 1). T cells were defined as CD3+ viable lymphocytes and further subdivided with antibodies against CD4 and CD8 to detect the major T cell subsets in addition to Tregs identified as CD25+CD127low/-FoxP3+CD4+ T cells. Checkpoint expression was defined as the fraction of positive cells within the parental T cell subset.

The samples were acquired immediately after staining on an LSR II cytometer (BD) and data analyzed using FlowJo (V.10.7.1, BD) using established gating strategies (online supplemental figures 1 and 2).

Statistical analyses

Overall survival (OS) was defined as the time from the start of therapy until death or last patient contact. Other causes of death were regarded as censored events. Progression-free survival (PFS) was defined as the time between the start of therapy and disease progression or last FU. Response was evaluated using RECIST V.1.1 criteria.[28] OS and PFS probabilities were calculated and analyzed using the Kaplan-Meier approach and log-rank testing (Prism, V.5.0e; GraphPad Software). Neutrophil-to-lymphocyte ratios (NLR) were

Table 1 Patients' characteristics

Factor	Category	Discovery		Validation	
		N	%	N	%
Age	Median	67		64	
	IQR	21.5		22	
Sex	Female	34	37.0	18	36.7
	Male	58	63.0	31	63.3
Center	Tübingen	67	72.8	42	85.7
	Dresden	17	18.5	7	14.3
	Lübeck	8	8.7	0	0.0
Therapy	**Anti-PD-1**	**51**	**55.4**	**14**	**28.6**
	2 mg/kg once every 3 weeks Pembro	42	45.7	8	16.3
	3 mg/kg once every 3 weeks Pembro	3	3.3	0	0.0
	4 mg/kg once every 6 weeks Pembro	1	1.1	0	0.0
	400 mg once every 6 weeks Pembro	0	0.0	1	2,0
	3 mg/kg once every 2 weeks Nivo	5	5.4	0	0.0
	240 mg once every 2 weeks Nivo	0	0.0	1	2.0
	480 mg once every 4 weeks Nivo	0	0.0	4	8.2
	Anti-PD-1+anti-CTLA-4	**41**	**44.6**	**35**	**71.4**
	1 mg/kg Ipi+3 mg/kg Nivo once every 3 weeks	4	4.3	3	6.1
	3 mg/kg Ipi+1 mg/kg Nivo once every 3 weeks	37	40.2	32	65.3
Previous systemic therapies	Immunotherapy	20	21.7	15	30.6
	Targeted therapy	22	23.9	10	20.4
	Chemotherapy	4	4.3	4	8.2
	None	56	60.9	26	53.1
LDH serum level BL	Normal	42	45.7	20	40.8
	Elevated	50	54.3	27	55.1
	Unknown	0	0.0	2	4.1

BL, baseline; CTLA-4, cytotoxic T-lymphocyte-associated protein 4; Ipi, ipilimumab; LDH, lactate dehydrogenase; n.a., not available; Nivo, nivolumab; PD-1, programmed cell death protein 1; Pembro, pembrolizumab.

calculated by the absolute numbers of neutrophils relative to lymphocytes in fresh blood counts, and the LDH ratio was calculated by the LDH serum level relative to the upper limit of normal (ULN).

To investigate potential associations between cellular parameters and OS before the start of therapy, we used a minimized cut-off screening approach, similar to that published earlier.[6 13 29] In brief, the cellular features at BL of the first cohort were divided into three equal subsets (<33 percentile, 33–66 percentile and >66 percentile) to identify two cut-off points for the dichotomization of the BL samples to consider extreme values in addition to the median values. Features and cut-off points that correlated with patients' OS in the discovery cohort were then validated or rejected in an analysis of the second cohort. The resulting p values were corrected for multiple testing using the Bonferroni method, and throughout this study $p<0.05$ was considered statistically significant.

BL and FU samples were compared using Wilcoxon matched-pairs signed rank testing, and groups by the Mann-Whitney U test (Prism V.5.0e; GraphPad Software). To visualize cell populations, violin plots were created using the packages ggplot2 and introdataviz in R studio (R V.4.2.0 in R studio V.1.1.463). For the statistical evaluation of more than two groups, one-way analysis of variance (Kruskal-Wallis test) with Dunn's post hoc testing was performed. Correlations of features were evaluated using the Spearman's R test.

The Cox proportional hazards regression model and the resulting forest plots were calculated using the survminer and the survival package[30] using R studio (R V.4.2.0 in R studio V.1.1.463). For multivariate Cox proportional hazards regression modeling, patients with missing data in the variables were excluded from the multivariate analysis.

RESULTS

Patients

In total, 141 patients with stage IV melanoma were recruited in daily clinical practice at the centers in Tübingen, Dresden and Lübeck, to investigate peripheral

blood-derived cellular biomarker candidates informative for clinical outcome. Ninety-two patients were included in the discovery cohort, and 49 in the validation cohort (median age: 67 (IQR 55–76) years and 64 (IQR 53–75) years, respectively). In both cohorts, there were more male than female patients (discovery 63% vs 37% and validation 63.3% vs 36.7%, respectively). Patients received either anti-PD-1 antibodies alone or in combination with anti-CTLA-4 antibodies. Because of the real-world study setting, although the number of patients in the discovery cohort receiving either therapy was similar (55.4% vs 44.6%, respectively), the validation cohort collected at a later time point included significantly more patients treated with the antibody combination (71.4% vs 28.5%, p=0.003, Fisher's exact test). Nonetheless, there was no significant difference in the OS of patients between the two treatments, age or sex in both cohorts (online supplemental figure 3A,B). In the discovery and validation cohorts, 60.9% and 53.1% of patients had not received any previous systemic therapy. Detailed patient characteristics are provided in table 1 and the treatment and sampling scheme is summarized in online supplemental figure 4. The 2-year OS of the discovery cohort was 37.5% and of the validation cohort 58.9%, and 2-year PFS was 14.1% and 22.8%, respectively.

Highly elevated baseline M-MDSC frequencies correlate with poor survival

Thirty-three cellular features were determined from routine blood counts and in-depth immunophenotyping investigations, including frequencies of cells with M-MDSC, monocyte, CD4+, CD8+ and Treg cell phenotypes in blood samples drawn before the start of therapy (BL) from patients of the discovery cohort. To identify potential correlations of these with patients' OS, we stratified the discovery cohort according to the median value and two additional cutoffs (<33 and >66 percentile) per cellular feature, similar to approaches that have been published before.[6 13 29] Of all investigated cellular variables, only the upper cut-off values of absolute basophil counts (0.07×1000 cells/µL) and M-MDSC frequencies of total mononuclear leucocytes (>18.1%) were selected as predictive candidate features for patients' OS. Only the latter could be validated in an independent analysis of the second cohort (online supplemental tables 2–4). Thus, patients with a BL M-MDSC frequency >18.1% ('M-MDSC-high') had on average a significantly shorter OS than those with a frequency ≤18.1% ('M-MDSC-low') in both the discovery and validation cohorts (HR 2.086, p=0.030; HR 7.652, p<0.001, figure 1A,B, respectively). These findings were independent of the PD-1 therapy received (online supplemental figure 5). M-MDSC-high patients also experienced significantly shorter PFS in the discovery and in the validation cohort (HR 2.425, p=0.001 and HR 3.344, p=0.007, respectively, figure 1C,D). Potential confounding factors such as type of therapy (monotherapy vs combination therapy) (online supplemental figure 6), previous therapies (online supplemental figure 7), age, LDH, S100 serum levels (online supplemental figure 8) or centers (online supplemental figure 9) did not associate significantly with the determined M-MDSC frequencies. Moreover, the predictive biomarker characteristics of the M-MDSC frequencies before the start of therapy for the clinical outcome under therapy correlated independently of the only biomarker established in the clinic, the LDH levels, with patients' OS in a multivariate Cox regression analysis (online supplemental figure 10).

M-MDSC-high patients display a skewed peripheral immune cell signature

Combined analyses of both cohorts revealed that the peripheral immune cell signature of M-MDSC-high patients, although not informative for survival in univariate analyses, had a skewed composition at BL. Thus, M-MDSC-high patients had significantly lower lymphocytes (blood counts and flow cytometry investigations), CD3+ T cells and eosinophils (relative and absolute number), but higher absolute monocytes (presumably caused by the highly elevated M-MDSC frequencies), higher relative and absolute neutrophil counts, intermediate monocytes, PD-1+Tregs and a higher NLR compared with M-MDSC-low patients (figure 2 and online supplemental table 5).

Significant signature composition changes early under therapy were seen in M-MDSC-high and M-MDSC-low patients as follows: increased absolute and relative eosinophils (figure 3A), and LAG-3+CD4+, TIM-3+CD4+ and LAG-3+CD8+ T cells (figure 3B). In contrast, increased CD4+ T cells (figure 3C), LAG-3+ and TIM-3+Tregs, TIM-3+CD4+ and LAG-3+CD8+ T cells (figure 3B) and absolute leukocyte and relative lymphocyte counts (online supplemental figure 11A) were only present in the M-MDSC-low patients. Interestingly, there were no significant changes of the frequency of total lymphocytes, CD3+ and CD8+ T cells, Tregs and monocyte subsets in either group (online supplemental figure 11CB+) but some of the patients in the M-MDSC-high group had a significant decrease in their M-MDSC frequency under ICB (p=0.010, figure 4A). Despite these differences in the frequencies of the investigated immune cells, except for the MDSCs, there were no associations of these features with OS, as described in the previous section.

A fraction of M-MDSC-high patients does benefit from anti-PD-1 ICB

Based on the identified changes of M-MDSC frequencies early under therapy, we developed a model to investigate the potential impact of these changes on the identified biomarker cut-off value of 18.1% in a combined analysis of both cohorts. Because no differences were found between patients receiving PD-1 monotherapy or a combination with anti-CTLA-4 antibodies, patients who received either PD-1 antibodies alone or in combination with CTLA-4 antibodies were examined here, as before. As expected, patients with M-MDSC frequencies ≤18.1% before and under therapy had in general a superior OS

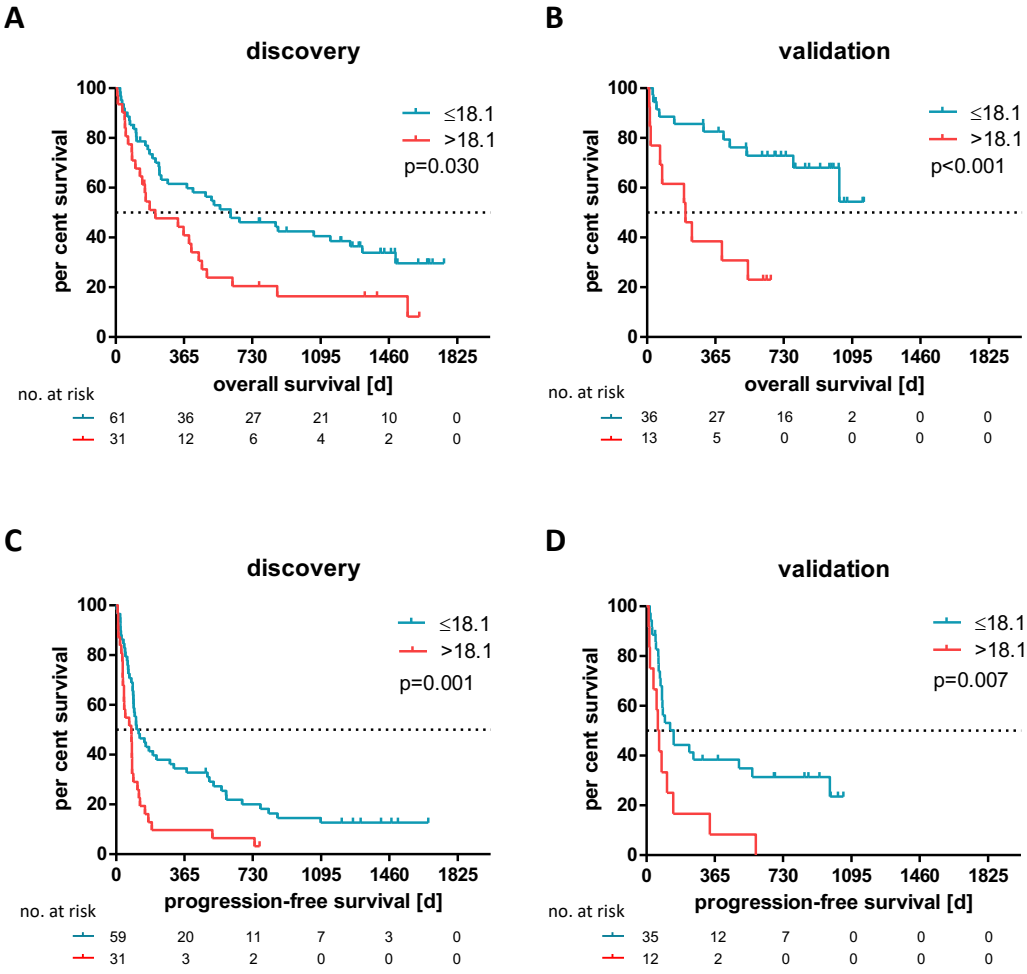

Figure 1 High monocytic myeloid-derived suppressor cell frequencies before start of immune checkpoint blockade correlate significantly with shorter overall and progression-free survival in the discovery (A: p=0.030 and C: p=0.001) and validation cohort (B: p<0.001 and D: p=0.007).

compared with those with frequencies >18.1% at both time points (HR 0.004, p<0.001, figure 4B). However, those M-MDSC-high patients whose M-MDSC frequency declined to below 18.1% under ICB had a prolonged OS relative to those whose M-MDSC frequency remained high early during treatment (HR 4.133, p=0.030, figure 4B). No significant difference in OS was found for patients with M-MDSC frequencies exceeding the cut-off of 18.1% at FU, compared with those with values >18.1% at both time points (HR 0.331, p=0.078). The 2-year survival rate for patients whose M-MDSC frequency did not decline to under 18.1% was 0%, and for patients with increasing M-MDSC frequencies (low to high) it was 33.3%. In contrast, for patients with M-MDSC frequencies falling to below the cut-off (high to low), it was 55.6% and for patients with a BL M-MDSC frequency below the cut-off and for low-MDSC patients remaining low it was 71.4%.

Determination of a risk factor model

To evaluate the identified biomarker properties of highly elevated M-MDSC, we tested their dependency on the only established biomarker, the LDH serum level, as these two parameters were the only ones to show significant associations with OS. Univariate analysis of the combined cohorts revealed a negative correlation of highly elevated M-MDSC frequencies with patients' OS at BL (HR 2.86, p<0.001, online supplemental figure 12A). A 1.5-fold elevated BL LDH ratio, which was described previously as clinically meaningful,[31] correlated with shorter survival (HR 1.98, p=0.014, online supplemental figure 12B). In addition, a general increase of >25% of the LDH ratio determined at BL was indicative of patients with shorter OS (HR 4.00, p=0.004, online supplemental figure 12C). Patients with M-MDSC frequencies >18.1% at FU, or those with a marked increase of >50% (>1.5-fold) also had significantly shorter OS (HR 6.97, p<0.001 and HR 3.08, p=0.026, respectively, online supplemental figure 5D,E). To investigate dependencies of those features that correlated in univariate analyses significantly with patients' OS, we performed multivariate Cox regression analysis including in addition to the BL features serum LDH ratio (>1.5×ULN) and M-MDSC frequencies (>18.1%). We identified highly elevated M-MDSC

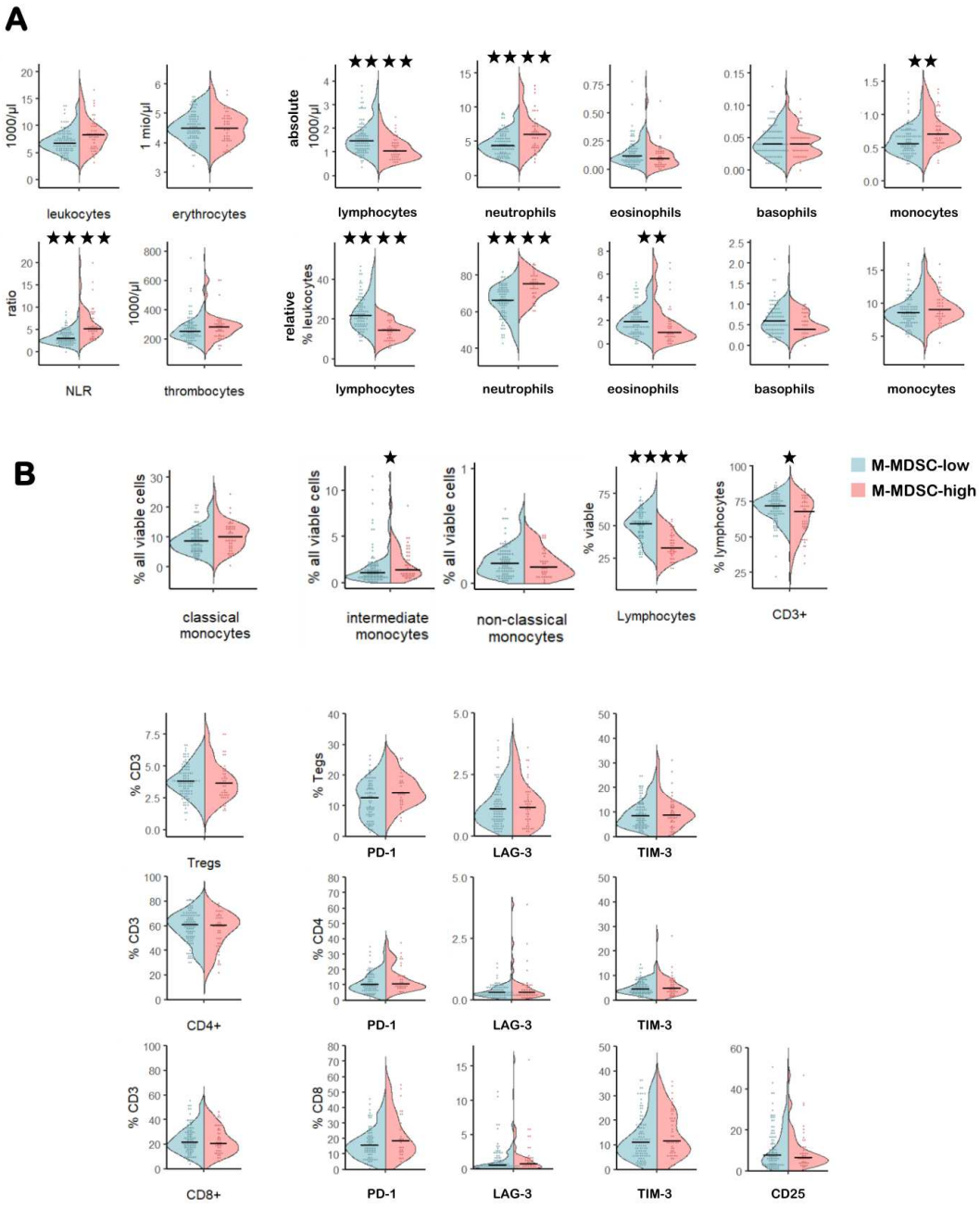

Figure 2 Comparison of the peripheral immune signature in M-MDSC-high versus M-MDSC-low patients. Violin plots depicting blood counts from the hemogram (A) and flow cytometry-derived frequencies of myeloid cells, T cells and their checkpoint receptor expression (B). *P<0.05, **p<0.01, ***p<0.005, ****p<0.0001. LAG-3, lymphocyte activation gene 3; M-MDSC, monocytic myeloid-derived suppressor cell; NLR, neutrophil-to-lymphocyte ratio; PD-1, programmed cell death protein 1; TIM-3, T cell immunoglobulin and mucin-domain containing-3; Treg, regulatory T cell.

FU frequencies (HR 3.581, p=0.002), a general increase of M-MDSCs (HR 3.060, p=0.019) and LDH levels (HR 1.441, p=0.009) as independent significant markers for poor OS with a global p<0.001 (figure 5A). A combinatorial model of these three independent markers was constructed, where patients were stratified according to the sum of risk factors (figure 5B). The more risk factors a patient accumulated, the shorter was the OS. The 2-year survival rate for patients with zero risk factors was 72%, for patients with at least one risk factor was 48% and for those with two to three risk factors was 0%.

DISCUSSION

Here, employing a validated multicentric study, we sought more informative biomarker candidates derived from routine blood counts and peripheral T cell and myeloid cell subset phenotyping in patients with advanced stage IV

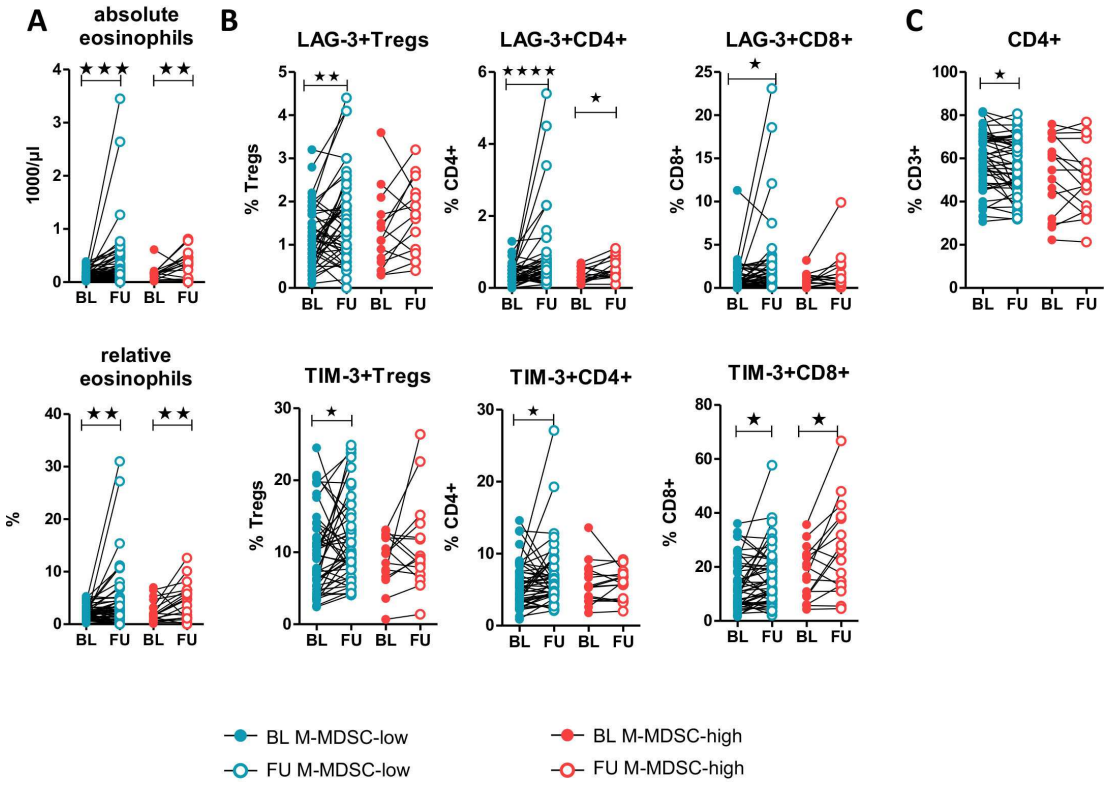

Figure 3 Comparison of significant changes in the abundance of immune cell subsets under immune checkpoint blockade in M-MDSC-high versus M-MDSC-low patients: eosinophils (A), checkpoint receptor expression on T cells (B) and total CD4+ T cell frequencies (C). *P<0.05, **p<0.01, ***p<0.005, ****p<0.0001. BL, baseline; FU, follow-up; LAG-3, lymphocyte activation gene 3; M-MDSC, monocytic myeloid-derived suppressor cell; TIM-3, T cell immunoglobulin and mucin-domain containing-3.

melanoma. We found that of all parameters analyzed, only extremely elevated frequencies of >18.1% of circulating CD33+CD11b+CD14+HLA-DRlow/− M-MDSC before and under anti-PD-1±anti-CTLA-4 ICB were significantly associated with shorter OS. Elevated M-MDSC frequencies are a well-known cellular biomarker candidate that has been repeatedly reported to correlate negatively with OS in patients treated with anti-PD-1 monotherapy[32–34]

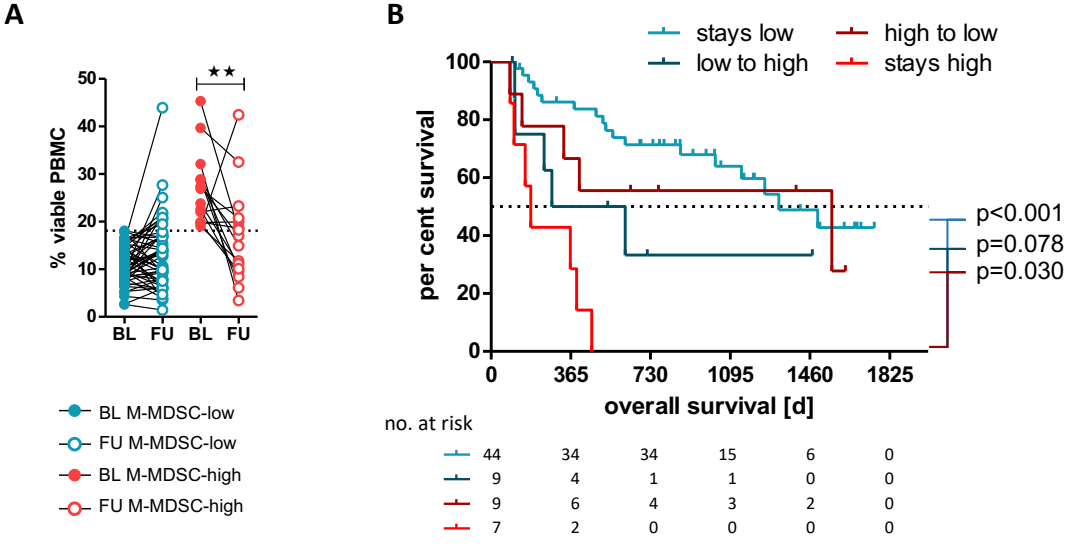

Figure 4 Comparison of changes in the M-MDSC frequencies in M-MDSC-low versus M-MDSC-high patients under immune checkpoint blockade. Patients in the M-MDSC-high group had a significant decrease in their M-MDSC frequencies (A, p=0.010). Those patients whose M-MDSC frequency stayed high had a significantly shorter overall survival compared with those with a decrease or an M-MDSC frequency that stayed low (B). **P<0.01. BL, baseline; FU, follow-up; M-MDSC, monocytic myeloid-derived suppressor cell; PBMC, peripheral blood mononuclear cell.

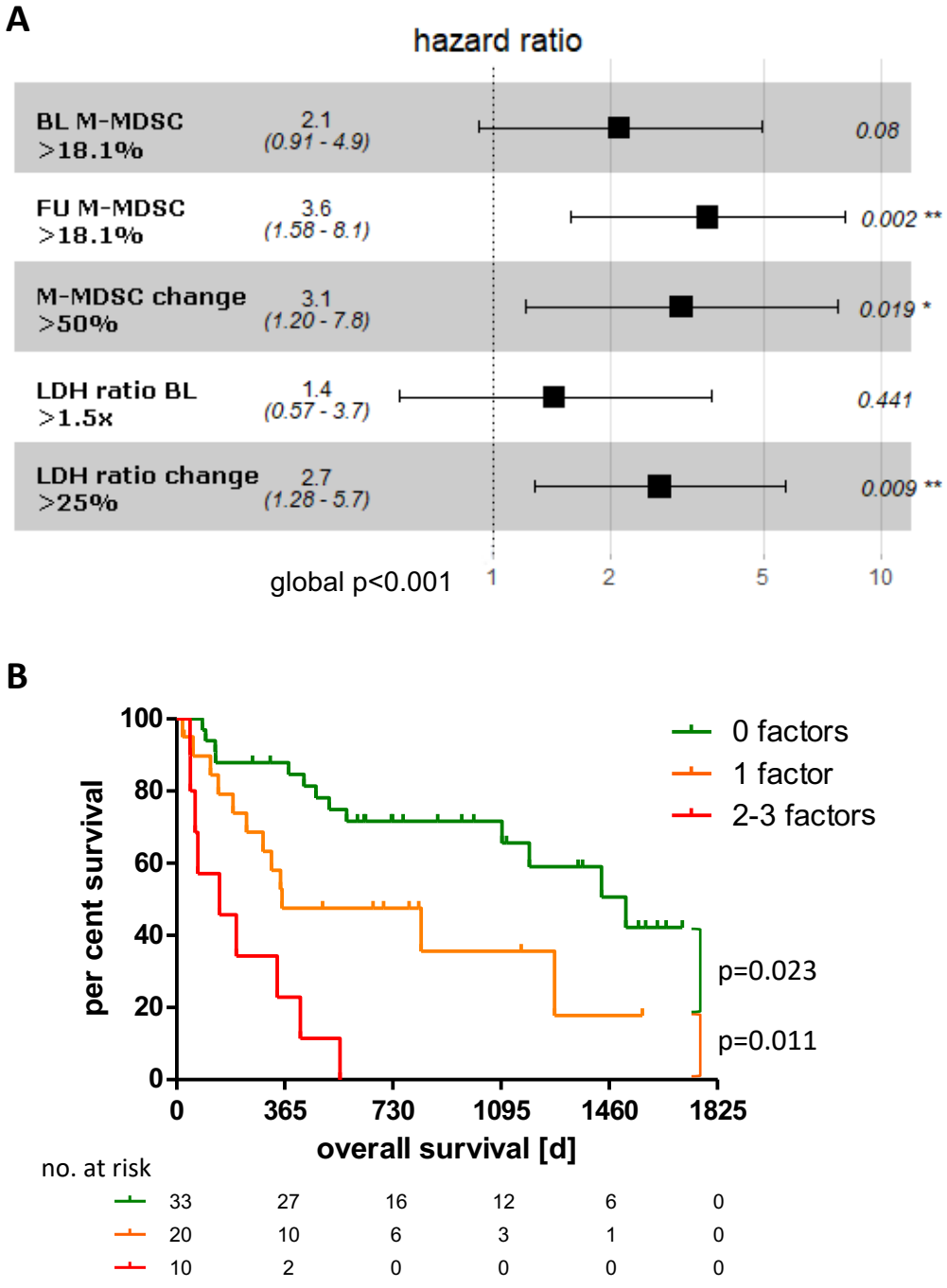

Figure 5 Multivariate modeling of biomarker candidates that correlate significantly with overall survival in univariate analysis. Results of multivariate Cox regression (A). The significantly independent features of the multivariate Cox regression have been used to compute a combinatorial predictive biomarker model (B). *P<0.05, **p<0.01. BL, baseline; FU, follow up; LDH, lactate dehydrogenase; M-MDSC, monocytic myeloid-derived suppressor cell.

or anti-CTLA-4 monotherapy.[6 35] However, somewhat in contrast to previous studies with M-MDSC cut-off values of ~10%–13%,[33 34] in the present study we identified this negative association only in patients with very highly elevated M-MDSC frequencies (>18.1%). Similar to our findings, a recent study using a machine learning-based myeloid index score in patients with melanoma with mixed treatments found that only the very high-frequency percentiles of 85% of M-MDSC were informative for higher risk of progression and shorter OS.[36] These findings may be due to the evolving clinical routine (first-line) treatment using ICB, implying that patients with intermediate MDSC frequencies may now also be benefiting from this therapy. Although quantification of M-MDSCs is non-standardized and very likely dependent on technical factors in different centers, the clinical relevance of the cutoffs in this and other current studies[36] compared with previous studies[6 33–35] is consistent.

Despite the fact that many immune cell subsets examined do not correlate with patients' OS in univariate analyses, examination of the composition of the peripheral immune signature of M-MDSC-low and M-MDSC-high patients revealed differences between them. We found that the latter had a skewed immune cell signature including cellular features already associated with impaired cancer immunosurveillance in some studies, such as fewer lymphocytes, CD3+ T cells and eosinophils and a higher NLR. The latter, for example, is used as a measure of an impaired immune system and has been associated with worse clinical outcomes across several cancer types, including melanoma.[37 38] Several effects of ICB observed here are consistent with published studies, such as an increase in absolute and relative eosinophils, which has already been reported for patients with melanoma treated with anti-CTLA-4 antibodies.[39] Even though we did not find correlations of T cells with survival, we observed increases in frequencies of LAG-3-positive and TIM-3-positive cells within CD4+ and CD8+ T cell populations in M-MDSC-low patients. These increases might be the result of an ICB-induced activation of alternative regulatory pathways. They could thus be a sign of T cell response to therapy and presumably not of an increase of T cell inactivity.[40 41]

Along those lines, M-MDSC-high patients with poor clinical outcome revealed only an increase of checkpoint receptor-positive populations in a few T cell subsets, supporting the hypothesis of an immune-compromised status of these patients. However, the majority of these patients had a significant decrease in M-MDSC frequencies under ICB, suggesting a therapy-associated modulatory effect. Of particular interest was the finding that those M-MDSC-high patients that experienced an early decrease of M-MDSC frequencies down to below the cut-off of 18.1% had a superior clinical benefit from ICB, similar to those with an initially low M-MDSC frequency. To the best of our knowledge, published studies have so far only revealed negative associations of MDSC frequencies under CTLA-4[6 42] and PD-1[34] therapies with patients' OS, but there have been no reports on changes of MDSC frequencies under therapy of patients who were initially assigned to a poor prognosis group. These patients are characterized by a significant reduction of M-MDSC frequencies early under therapy. However, not only the categorical dichotomization of M-MDSC frequencies according to the identified 18.1% cut-off but also a strong increase of their frequencies early under ICB (independent of the BL value) correlated negatively with patients' OS. This was independent of the established biomarker LDH (risk factor model) and thus complements earlier published findings. For example, similar associations of clinical benefit with a decrease of MDSCs 3 weeks[42] and 6 weeks[43] after starting anti-CTLA-4 therapy were previously described using univariate analysis in patients with melanoma. Also, in non-small cell lung cancer and urothelial carcinoma under anti-PD-1 ICB, decreased M-MDSC frequencies were associated with better clinical responses.[44 45] The involvement of PD-1 blockade in differentiation and development of M-MDSCs in humans is still unknown. However, mice deficient for PD-1 have fewer M-MDSCs suggesting that PD-1 contributes presumably to the differentiation of M-MDSCs.[46 47] If PD-1 contributes to MDSC differentiation, then PD-1 blockade might be responsible for the decrease of M-MDSC observed in our study. Future studies of matched samples of peripheral blood and tumor tissue will be required to (i) determine possible kinetics under therapy and to (ii) provide further insights into the role of MDSCs in ICB, because available data suggest that the circulating levels of MDSCs mirror those within the tumor microenvironment.[48]

There are limitations to this study that need to be considered, particularly the combined analysis of patients receiving anti-PD-1 antibodies alone or in combination with anti-CTLA-4. There is a body of data describing different mechanisms and consequently different immune cell phenotypes as being relevant for one or the other treatment strategy.[14 49 50] Unfortunately, our cohort size did not allow a comparative analysis, but the M-MDSC data and the associated changes in the immune cell signature under ICB are so clear that it is unlikely that the results are relevant only to one treatment strategy.

In conclusion, our data suggest that contrary to the general consensus, possessing pre-existing highly elevated frequencies of peripheral M-MDSC before ICB does not accurately identify all patients who fail to benefit from treatment. Rather, the dynamic change under therapy serves as a better predictor of clinical benefit in patients with metastatic melanoma. Understanding the mechanisms responsible for these changes in some but not other patients with high BL MDSC levels should facilitate rational interventions to increase the proportion of clinically responsive patients.

Author affiliations
[1]Department of Dermatology, University Hospital Tübingen, Eberhard Karls University of Tübingen, Tübingen, Germany
[2]Internal Medicine I, University Hospital Tübingen, Eberhard Karls University of Tübingen, Tübingen, Germany
[3]Cluster of Excellence iFIT (EXC 2180) "Image Guided and Functionally Instructed Tumor Therapies", Tübingen, Germany
[4]Department of Dermatology, Venereology and Allergology, Kantonsspital St Gallen, Sankt Gallen, Switzerland
[5]Department of Computer Science, Eberhard Karls University of Tübingen, Tübingen, Germany
[6]Skin Cancer Center at the University Cancer Centre and National Center for Tumor Diseases Dresden; Department of Dermatology, Faculty of Medicine and University Hospital Carl Gustav Carus, Technische Universität Dresden, Dresden, Germany
[7]Department of Dermatology, University of Lübeck, Lübeck, Germany
[8]Charité – Universitätsmedizin Berlin, corporate member of Freie Universität Berlin and Humboldt-Universität zu Berlin, Department of Dermatology, Venereology and Allergology, Berlin, Germany
[9]Department of Immunology, Interfaculty Institute for Cell Biology, Eberhard Karls University Tübingen, Tübingen, Germany
[10]Health Sciences North Research Institute, Sudbury, Ontario, Canada

Correction notice This article has been corrected since it was first published online. The licence was updated to CC-BY in September 2023. The funding statement has been updated to include the following "we acknowledge support from the Open Access Publishing Fund of the University of Tübingen".

Twitter Teresa Amaral @TeresaSAmaral

Acknowledgements We thank Anne Mohrholz for her support during sample collection and preparation. Furthermore, we thank Daniel Soffel, Stanley Krickmann and Marc Sauer for their help in documentation of the clinical data of the patients. We also thank the patients for participating in this study.

Contributors Conceptualization: BW, KW-H, GP. Formal analysis: AG, JB, KW-H. Funding acquisition: BW, KW-H. Investigation: AG, JB, JS, SO, AM. Methodology: AG, JB, KW-H. Project administration: KW-H. Resources (provision of study materials, reagents, materials, patients, instrumentation, computing resources): TA, NBW, FM, PT, CG, TE, BW, KW-H. Supervision: KW-H. Visualization: AG, JB. Writing—original draft: AG, JB, GP, KW-H. Writing—reviewing and editing: AG, JB, JS, SO, AM, TA, NBW, MC, FM, PT, CG, GP, TE, BW, KW-H.

Funding This work was partially funded by the Medical Faculty of the University of Tübingen (2509-0-0), Bristol-Myers Squibb (CA209-9P4), Merck Sharp & Dohme (52518) and the Klaus Tschira Foundation (00.316.2017). In addition, we acknowledge support from the Open Access Publishing Fund of the University of Tübingen.

Competing interests TA reports institutional grants from SkylineDx, institutional grants and personal fees from Novartis, institutional grants from NeraCare, personal fees from BMS, institutional grants from Sanofi, personal fees from CeCaVa, personal fees from Pierre Fabre, outside the submitted work. NW reports an advisory role for Pierre Fabre and Sanofi, consultant's honoraria from Novartis, and has received travel support from AbbVie and Amgen outside the submitted work. FM reports receiving commercial research grants from Novartis and Roche; and has received travel support and/or speaker's fees and/or advisor's honoraria by Novartis, Roche, Bristol-Myers Squibb, Merck Sharp & Dohme and Pierre Fabre. PT has received travel support and/or speaker's fees and/or advisor's honoraria by Almirall, Biofrontera, Bristol-Myers Squibb, Curevac, Kyowa Kirin, Merck, Merck Sharp & Dohme, Novartis, Pierre Fabre, Roche, Sanofi and 4SC. CG reports receiving commercial research grants from Bristol-Myers Squibb, Novartis and Roche; and is a consultant/advisory board member for Amgen, Bristol-Myers Squibb, Merck Sharp & Dohme, Novartis and Roche. GP has received speaker's honoraria from Novartis, Roche, Pfizer, GlaxoSmithKline and Astellas. TE has received travel support and/or speaker's fees and/or advisor's honoraria by Sanofi, Novartis, Bristol-Myers Squibb, Merck Sharp & Dohme, Almiral Hermal and Pierre Fabre. BW reports receiving commercial research grants from, is a consultant/advisory board member for and reports receiving travel reimbursement from Bristol-Myers Squibb and Merck Sharp & Dohme. KW-H received commercial research grants from CatalYm GmbH and travel support from Society for Immunotherapy of Cancer. No potential conflicts of interest were disclosed by the other authors.

Patient consent for publication Consent obtained directly from patient(s).

Ethics approval The Ethics Committee of Tübingen University Hospital approved this study (490/2014BO1, 616/2018BO2) and all patients gave their written informed consent for use of biomaterials, biobanking and their anonymized clinical data for scientific evaluation.

Provenance and peer review Not commissioned; externally peer reviewed.

Data availability statement Data are available on reasonable request.

ORCID iDs
Friedegund Meier http://orcid.org/0000-0003-4340-9706
Patrick Terheyden http://orcid.org/0000-0002-5894-1677
Graham Pawelec http://orcid.org/0000-0002-3600-0163
Kilian Wistuba-Hamprecht http://orcid.org/0000-0002-3104-8512

REFERENCES

1 Hodi FS, Chiarion-Sileni V, Gonzalez R, *et al*. Nivolumab plus Ipilimumab or Nivolumab alone versus Ipilimumab alone in advanced Melanoma (Checkmate 067): 4-year outcomes of a Multicentre, randomised, phase 3 trial. *Lancet Oncol* 2018;19:1480–92.
2 Wolchok JD, Chiarion-Sileni V, Gonzalez R, *et al*. Overall survival with combined Nivolumab and Ipilimumab in advanced Melanoma. *N Engl J Med* 2017;377:1345–56.
3 Ribas A, Wolchok JD. Cancer Immunotherapy using Checkpoint blockade. *Science* 2018;359:1350–5.
4 Eton O, Legha SS, Moon TE, *et al*. Prognostic factors for survival of patients treated Systemically for disseminated Melanoma. *J Clin Oncol* 1998;16:1103–11.
5 Balch CM, Gershenwald JE, Soong S-J, *et al*. Final version of 2009 AJCC Melanoma staging and classification. *J Clin Oncol* 2009;27:6199–206.
6 Martens A, Wistuba-Hamprecht K, Foppen MG, *et al*. Baseline peripheral blood biomarkers associated with clinical outcome of advanced Melanoma patients treated with Ipilimumab. *Clin Cancer Res* 2016;22:2908–18.
7 Weide B, Martens A, Hassel JC, *et al*. Baseline biomarkers for outcome of Melanoma patients treated with Pembrolizumab. *Clin Cancer Res* 2016;22:5487–96.
8 Baltussen JC, Welters MJP, Verdegaal EME, *et al*. Predictive biomarkers for outcomes of immune Checkpoint inhibitors (Icis) in Melanoma: A systematic review. *Cancers (Basel)* 2021;13:6366.
9 Gracie L, Pan Y, Atenafu EG, *et al*. Circulating tumour DNA (ctDNA) in metastatic Melanoma, a systematic review and meta-analysis. *Eur J Cancer* 2021;158:191–207.
10 Krieg C, Nowicka M, Guglietta S, *et al*. High-dimensional single-cell analysis predicts response to anti-PD-1 Immunotherapy. *Nat Med* 2018;24:144–53.
11 Verma V, Shrimali RK, Ahmad S, *et al*. PD-1 blockade in Subprimed Cd8 cells induces dysfunctional PD-1(+)Cd38(Hi) cells and anti-PD-1 resistance. *Nat Immunol* 2019;20:1231–43.
12 Capone M, Fratangelo F, Giannarelli D, *et al*. Frequency of circulating Cd8+Cd73+T cells is associated with survival in Nivolumab-treated Melanoma patients. *J Transl Med* 2020;18:121.
13 Kitano S, Postow MA, Ziegler CGK, *et al*. Computational algorithm-driven evaluation of Monocytic myeloid-derived Suppressor cell frequency for prediction of clinical outcomes. *Cancer Immunol Res* 2014;2:812–21.
14 Gide TN, Quek C, Menzies AM, *et al*. Distinct immune cell populations define response to anti-PD-1 monotherapy and anti-PD-1/anti-CTLA-4 combined therapy. *Cancer Cell* 2019;35:238–55.
15 Huang AC, Postow MA, Orlowski RJ, *et al*. T-cell invigoration to tumour burden ratio associated with anti-PD-1 response. *Nature* 2017;545:60–5.
16 Tumeh PC, Harview CL, Yearley JH, *et al*. PD-1 blockade induces responses by inhibiting adaptive immune resistance. *Nature* 2014;515:568–71.
17 Thomas NE, Busam KJ, From L, *et al*. Tumor-infiltrating lymphocyte grade in primary Melanomas is independently associated with Melanoma-specific survival in the population-based genes, environment and Melanoma study. *J Clin Oncol* 2013;31:4252–9.
18 Anagnostou V, Smith KN, Forde PM, *et al*. Evolution of Neoantigen landscape during immune Checkpoint blockade in non-small cell lung cancer. *Cancer Discov* 2017;7:264–76.
19 Veglia F, Sanseviero E, Gabrilovich DI. Myeloid-derived Suppressor cells in the era of increasing myeloid cell diversity. *Nat Rev Immunol* 2021;21:485–98.
20 Groth C, Hu X, Weber R, *et al*. Immunosuppression mediated by myeloid-derived Suppressor cells (Mdscs) during tumour progression. *Br J Cancer* 2019;120:16–25.
21 De Cicco P, Ercolano G, Ianaro A. The new era of cancer Immunotherapy: targeting myeloid-derived Suppressor cells to overcome immune evasion. *Front Immunol* 2020;11:1680.
22 Rudolph BM, Loquai C, Gerwe A, *et al*. Increased frequencies of Cd11B(+) Cd33(+) Cd14(+) HLA-DR(Low) myeloid-derived Suppressor cells are an early event in Melanoma patients. *Exp Dermatol* 2014;23:202–4.
23 Diaz-Montero CM, Salem ML, Nishimura MI, *et al*. Increased circulating myeloid-derived Suppressor cells correlate with clinical cancer stage, metastatic tumor burden, and doxorubicin-cyclophosphamide chemotherapy. *Cancer Immunol Immunother* 2009;58:49–59.
24 Umansky V, Blattner C, Gebhardt C, *et al*. The role of myeloid-derived Suppressor cells (MDSC) in cancer progression. *Vaccines (Basel)* 2016;4:36.
25 Weide B, Martens A, Zelba H, *et al*. Myeloid-derived Suppressor cells predict survival of patients with advanced Melanoma: comparison

with regulatory T cells and NY-ESO-1- or Melan-A-specific T cells. *Clin Cancer Res* 2014;20:1601–9.
26 Bochem J, Zelba H, Spreuer J, *et al*. Early disappearance of tumor antigen-reactive T cells from peripheral blood correlates with superior clinical outcomes in Melanoma under anti-PD-1 therapy. *J Immunother Cancer* 2021;9:e003439.
27 Gaißler A, Meldgaard TS, Heeke C, *et al*. Dynamics of Melanoma-associated EPITOPE-specific Cd8+ T cells in the blood correlate with clinical outcome under PD-1 blockade. *Front Immunol* 2022;13.
28 Eisenhauer EA, Therasse P, Bogaerts J, *et al*. New response evaluation criteria in solid tumours: revised RECIST guideline (version 1.1). *European Journal of Cancer* 2009;45:228–47.
29 Camp RL, Dolled-Filhart M, Rimm DL. X-tile: a new bio-Informatics tool for biomarker assessment and outcome-based cut-point optimization. *Clin Cancer Res* 2004;10:7252–9.
30 Therneau T. Package 'survival'. 2015.
31 Wagner NB, Forschner A, Leiter U, *et al*. S100B and LDH as early Prognostic markers for response and overall survival in Melanoma patients treated with anti-PD-1 or combined anti-PD-1 plus anti-CTLA-4 antibodies. *Br J Cancer* 2018;119:339–46.
32 Mengos AE, Gastineau DA, Gustafson MP. The Cd14(+)HLA-DR(Lo/Neg) monocyte: an immunosuppressive phenotype that restrains responses to cancer Immunotherapy. *Front Immunol* 2019;10:1147.
33 Weber J, Gibney G, Kudchadkar R, *et al*. Phase I/II study of metastatic Melanoma patients treated with Nivolumab who had progressed after Ipilimumab. *Cancer Immunol Res* 2016;4:345–53.
34 Pico de Coaña Y, Wolodarski M, van der Haar Àvila I, *et al*. PD-1 Checkpoint blockade in advanced Melanoma patients: NK cells, Monocytic Subsets and host PD-L1 expression as predictive biomarker candidates. *OncoImmunology* 2020;9:1786888.
35 Pico de Coaña Y, Masucci G, Hansson J, *et al*. Myeloid-derived Suppressor cells and their role in CTLA-4 blockade therapy. *Cancer Immunol Immunother* 2014;63:977–83.
36 Huber V, Di Guardo L, Lalli L, *et al*. Back to simplicity: a four-marker blood cell score to quantify Prognostically relevant myeloid cells in Melanoma patients. *J Immunother Cancer* 2021;9:e001167.
37 Zhang Y, Liu B, Kotenko S, *et al*. Prognostic value of neutrophil-lymphocyte ratio and lactate dehydrogenase in Melanoma patients treated with immune Checkpoint inhibitors: A systematic review and meta-analysis. *Medicine (Baltimore)* 2022;101:e29536.
38 Capone M, Giannarelli D, Mallardo D, *et al*. Baseline neutrophil-to-lymphocyte ratio (NLR) and derived NLR could predict overall survival in patients with advanced Melanoma treated with Nivolumab. *J Immunother Cancer* 2018;6:74.
39 Martens A, Wistuba-Hamprecht K, Yuan J, *et al*. Increases in absolute lymphocytes and circulating Cd4+ and Cd8+ T cells are associated with positive clinical outcome of Melanoma patients treated with Ipilimumab. *Clin Cancer Res* 2016;22:4848–58.
40 Maruhashi T, Sugiura D, Okazaki I-M, *et al*. LAG-3: from molecular functions to clinical applications. *J Immunother Cancer* 2020;8:e001014.
41 Gorman JV, Colgan JD. Regulation of T cell responses by the receptor molecule Tim-3. *Immunol Res* 2014;59:56–65.
42 de Coaña YP, Wolodarski M, Poschke I, *et al*. Ipilimumab treatment decreases Monocytic Mdscs and increases Cd8 Effector memory T cells in long-term survivors with advanced Melanoma. *Oncotarget* 2017;8:21539–53.
43 Tarhini AA, Edington H, Butterfield LH, *et al*. Immune monitoring of the circulation and the tumor Microenvironment in patients with regionally advanced Melanoma receiving Neoadjuvant Ipilimumab. *PLoS One* 2014;9:e87705.
44 Feng J, Chen S, Li S, *et al*. The association between Monocytic myeloid-derived Suppressor cells levels and the anti-tumor efficacy of anti-PD-1 therapy in NSCLC patients. *Transl Oncol* 2020;13:100865.
45 Teshima T, Kobayashi Y, Kawai T, *et al*. Principal component analysis of early immune cell Dynamics during Pembrolizumab treatment of advanced urothelial carcinoma. *Oncol Lett* 2022;24:265.
46 Wu W-C, Sun H-W, Chen H-T, *et al*. Circulating hematopoietic stem and progenitor cells are myeloid-Biased in cancer patients. *Proc Natl Acad Sci U S A* 2014;111:4221–6.
47 Strauss L, Mahmoud MAA, Weaver JD, *et al*. Targeted deletion of PD-1 in myeloid cells induces antitumor immunity. *Sci Immunol* 2020;5:eaay1863.
48 Najjar YG, Rayman P, Jia X, *et al*. Myeloid-derived Suppressor cell subset accumulation in renal cell carcinoma parenchyma is associated with Intratumoral expression of Il1Beta, Il8. *Clin Cancer Res* 2017;23:2346–55.
49 Subrahmanyam PB, Dong Z, Gusenleitner D, *et al*. Distinct predictive biomarker candidates for response to anti-CTLA-4 and anti-PD-1 Immunotherapy in Melanoma patients. *J Immunother Cancer* 2018;6:18.
50 Wei SC, Anang N-AAS, Sharma R, *et al*. Combination anti-CTLA-4 plus anti-PD-1 Checkpoint blockade utilizes cellular mechanisms partially distinct from Monotherapies. *Proc Natl Acad Sci U S A* 2019;116:22699–709.

Early decrease of blood myeloid-derived suppressor cells during checkpoint inhibition is a favourable biomarker in metastatic melanoma

Andrea Gaißler*[1,2], Jonas Bochem*[1,2], Janine Spreuer[1,2], Shannon Ottmann[1], Alexander Martens[1], Teresa Amaral[1,3], Nikolaus Benjamin Wagner[1,4], Manfred Claassen[2,5], Friedegund Meier[6], Patrick Terheyden[7], Claus Garbe[1], Thomas Eigentler[8], Benjamin Weide[1], Graham Pawelec[9,10], Kilian Wistuba-Hamprecht[1,2,9]

*Shared first authorship

Supplementary Information

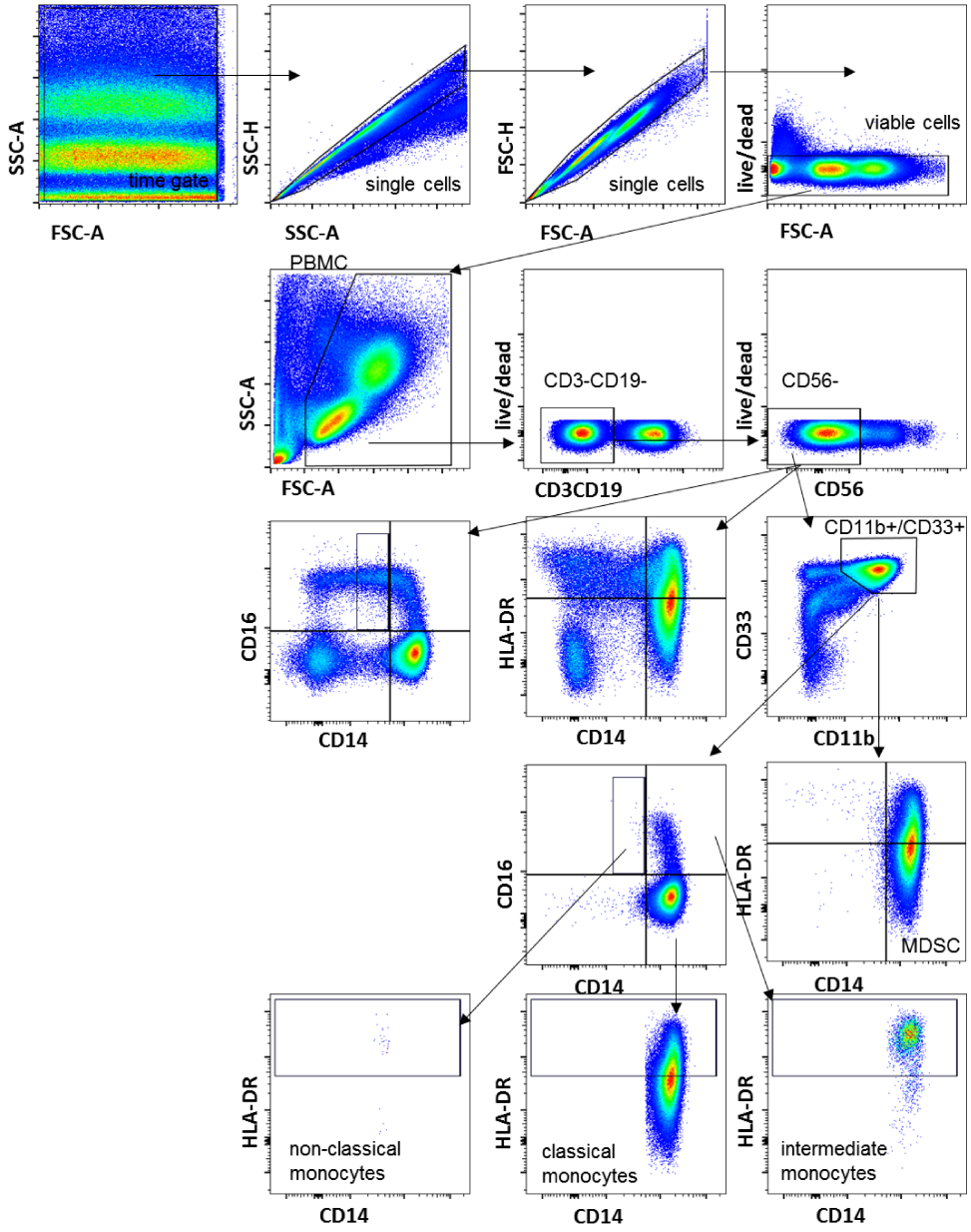

Supplementary Figure 1: Gating strategy of the myeloid cell panel. Adjustment of the gates for MDSCs and CD14+CD16-, CD14+CD16+ and CD14dimCD16+ cells were performed on the CD56- population and then copied to the CD11b+CD33+ population. M-MDSC frequencies were calculated to all assessed leukocytes within the PBMC gate.

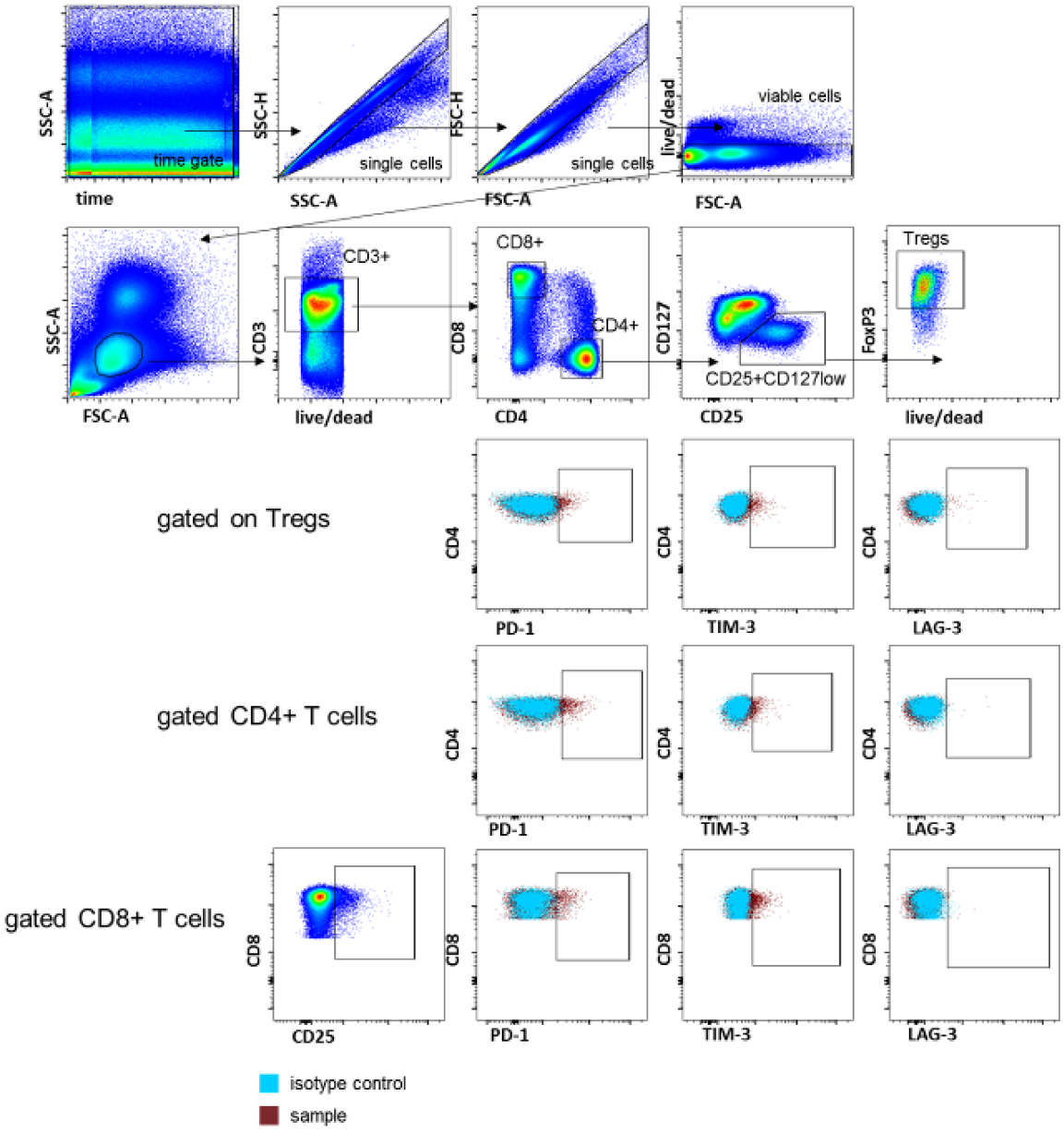

Supplementary Figure 2: Gating strategy of the T cell-panel. Gates for the checkpoint molecules were set on the isotype control (blue) and then copied to the sample (red).

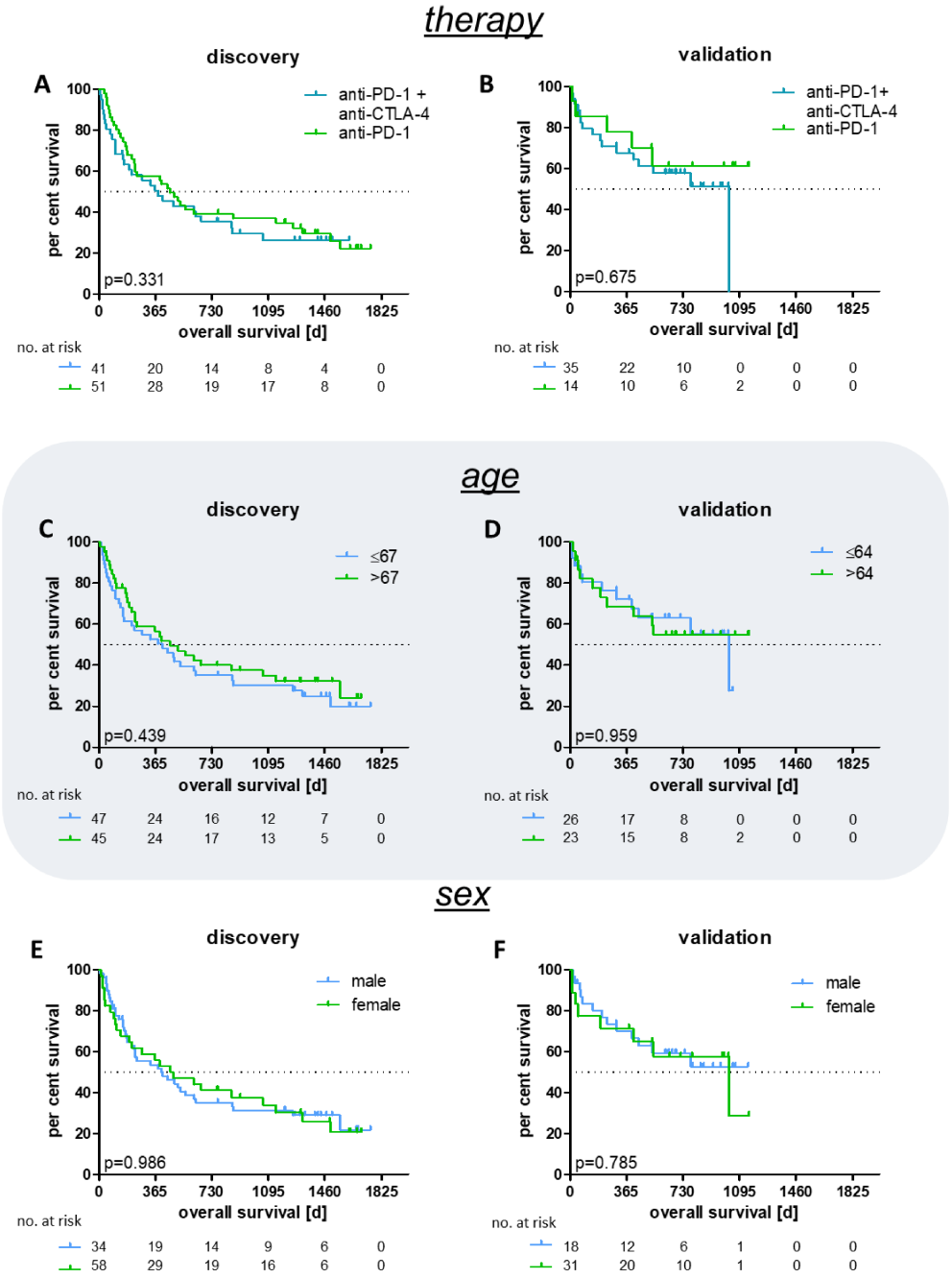

Supplementary Figure 3: Investigation of potential correlations of therapy (A: p=0.331 and B. p=0.650), age (C: p=0.439 and D: p=0.959) and sex (E: p=0.986 and F: p=0.785) with overall survival in the discovery and validation cohort using log-rank testing.

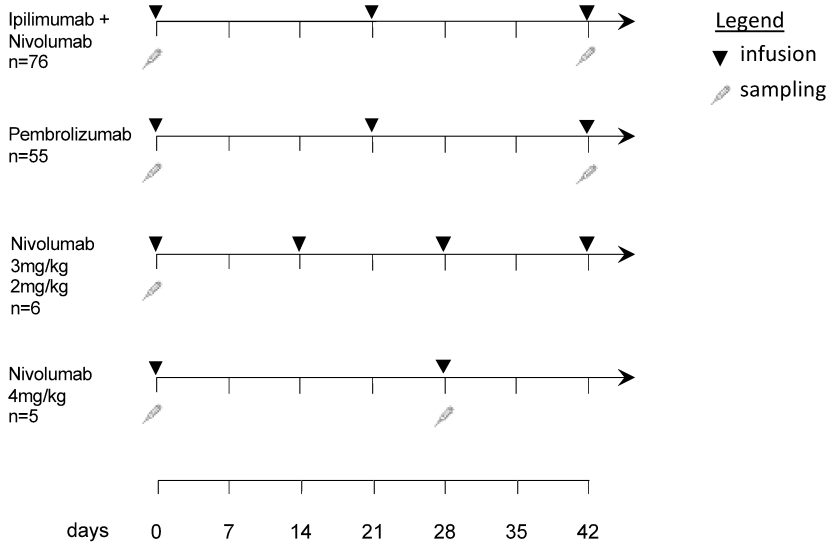

Supplementary Figure 4: Overview of the treatment and sample collection protocol.

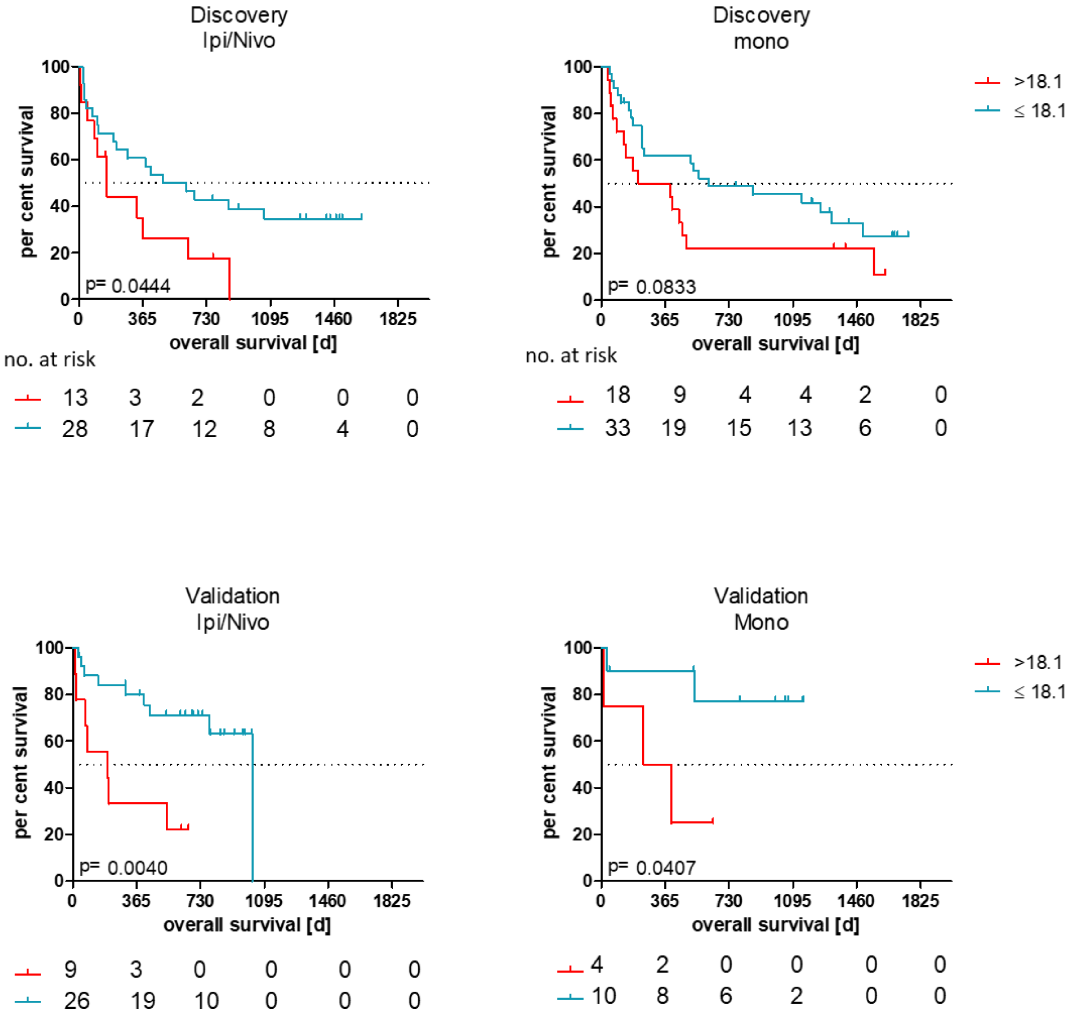

Supplementary Figure 5: Investigation of potential correlations of PD-1 mono (Mono)- versus CTLA-4 combination therapy (Ipi/Nivo) in the discovery (upper panel) and validation cohort (lower panel) with the probability of overall survival using long rank testing.

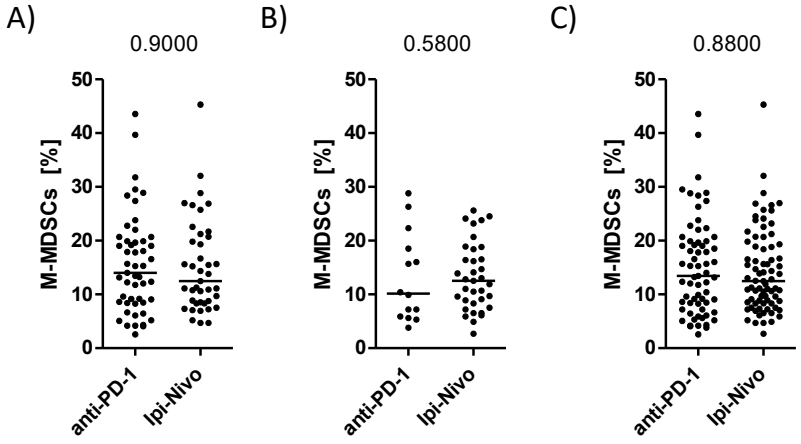

Supplementary Figure 6: Comparison of M-MDSC frequencies between PD-1 mono- (anti-PD-1) and CTLA-4 combination (Ipi-Nivo) therapy in A) the discovery, B) the validation, and C) the combined cohorts, applying Mann-Whitney-U testing. Each dot represents an individual patient and lines indicate the populations median.

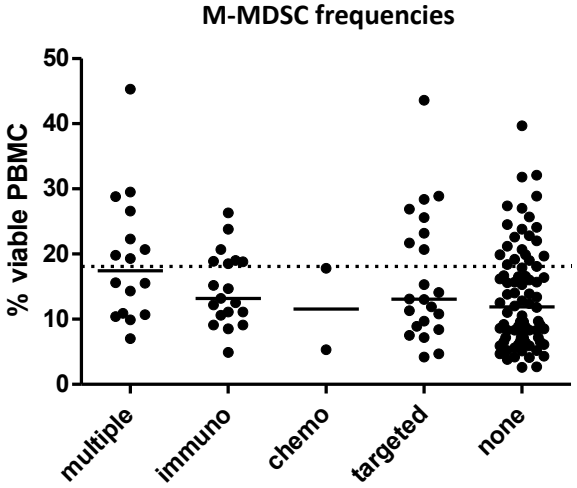

Supplementary Figure 7: Stratification of the M-MDSC frequencies of the patients of both cohorts after previous therapies. Each dot represents the M-MDSC frequency of a single patient and lines indicate the population median. Statistical evaluation using one-way ANOVA testing revealed no significant differences.

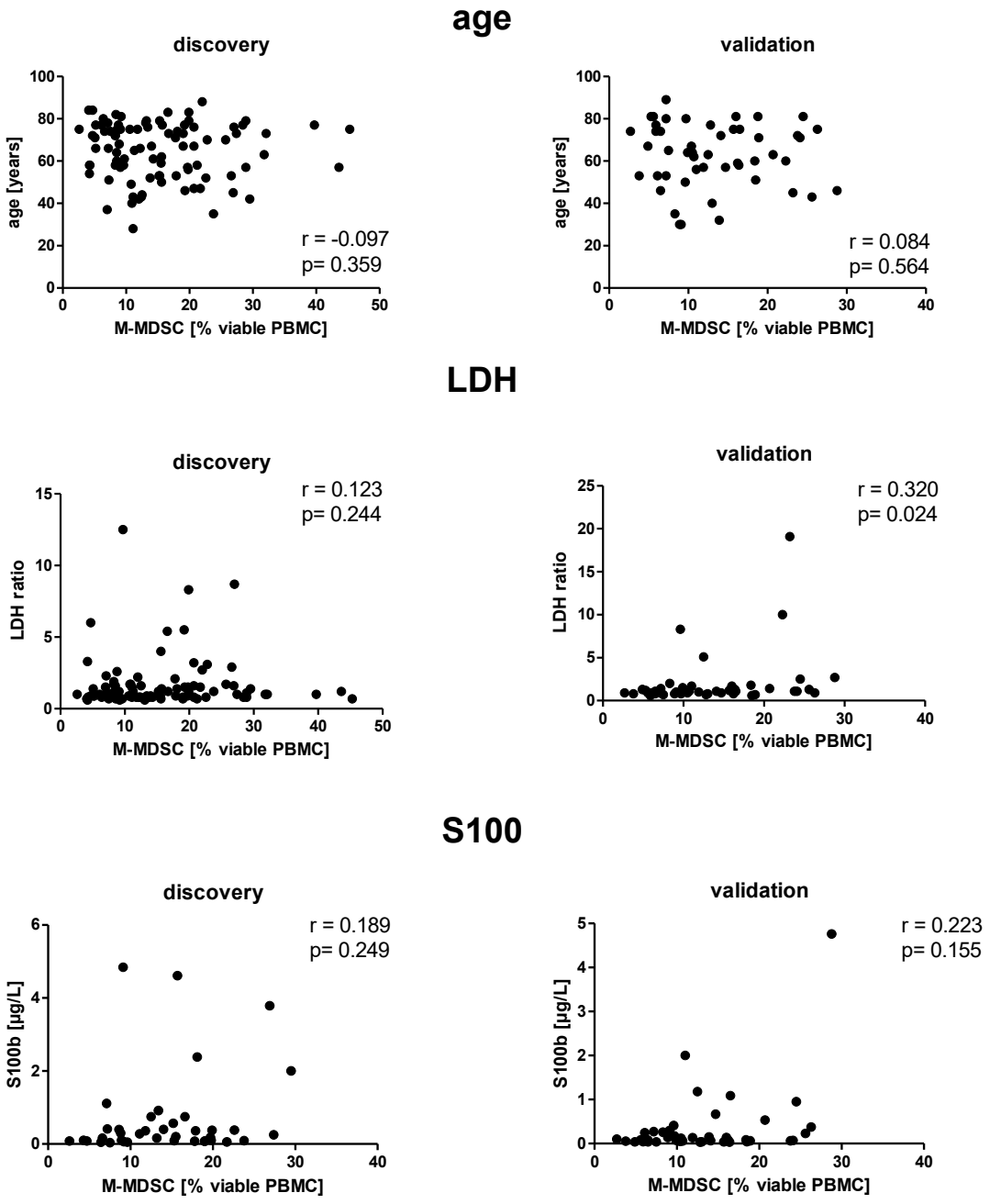

Supplementary Figure 8: Correlations of potentially confounding features of the M-MDSC frequencies in the discovery and validation cohort. Spearman R testing was performed to statistically evaluate potential correlations.

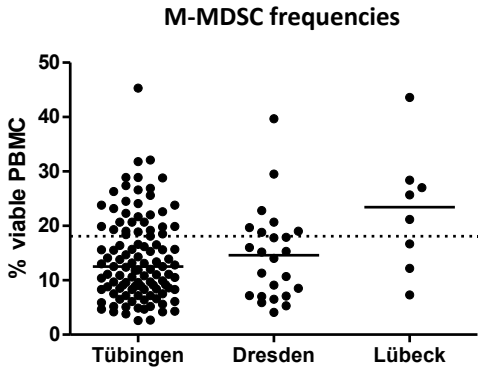

Supplementary Figure 9: Comparison of M-MDSC frequencies between the different centers. Each dot represents one M-MDSC frequency of an individual patient before start of therapy and lines indicate the populations median. One-way ANOVA testing did not reveal significant differences between the three centers.

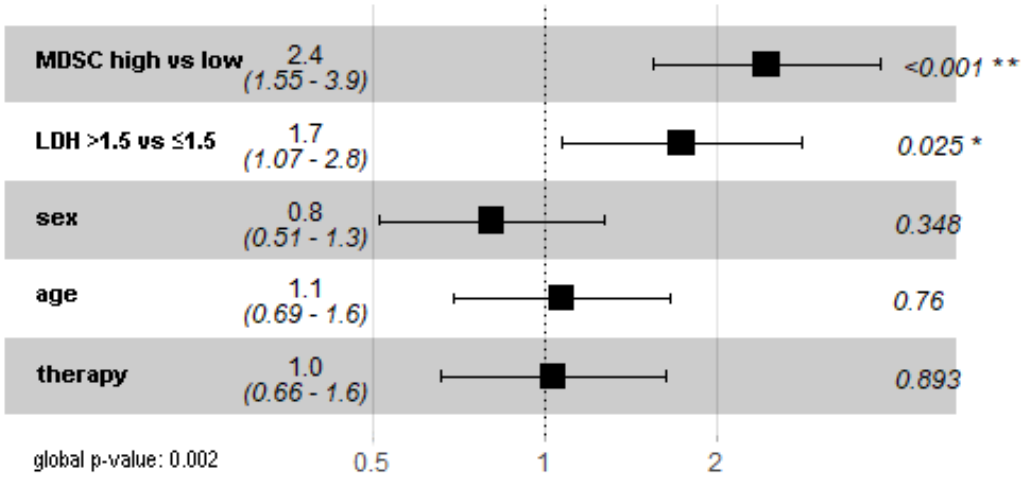

Supplementary Figure 10: Forest Plot summarizing the results of a Cox regression analysis of potential confounding features for the identified predictive characteristic of M-MDSC frequencies before the start of therapy and survival under therapy. Only high M-MDSC frequencies and LDH values correlate independently with OS. PD-1 ± CTLA-4 inhibition was used as separator in the variable “therapy”.

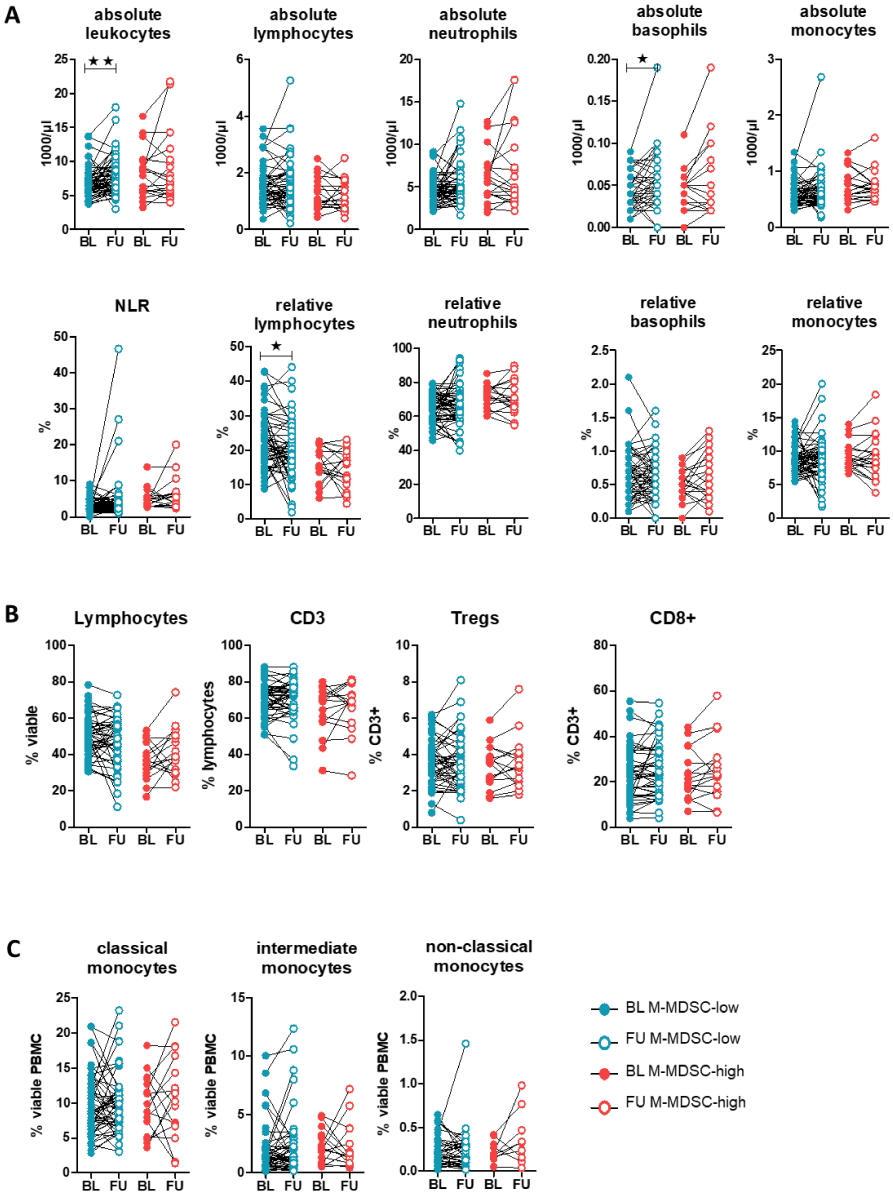

Supplementary Figure 11: Comparison of changes in the abundance of immune cell subsets under immune checkpoint blockade in M-MDSC-high versus M-MDSC-low patients: blood counts (A), lymphocytes (B) and of total myeloid cell frequencies (C). ★p<0.05 ★★p<0.01

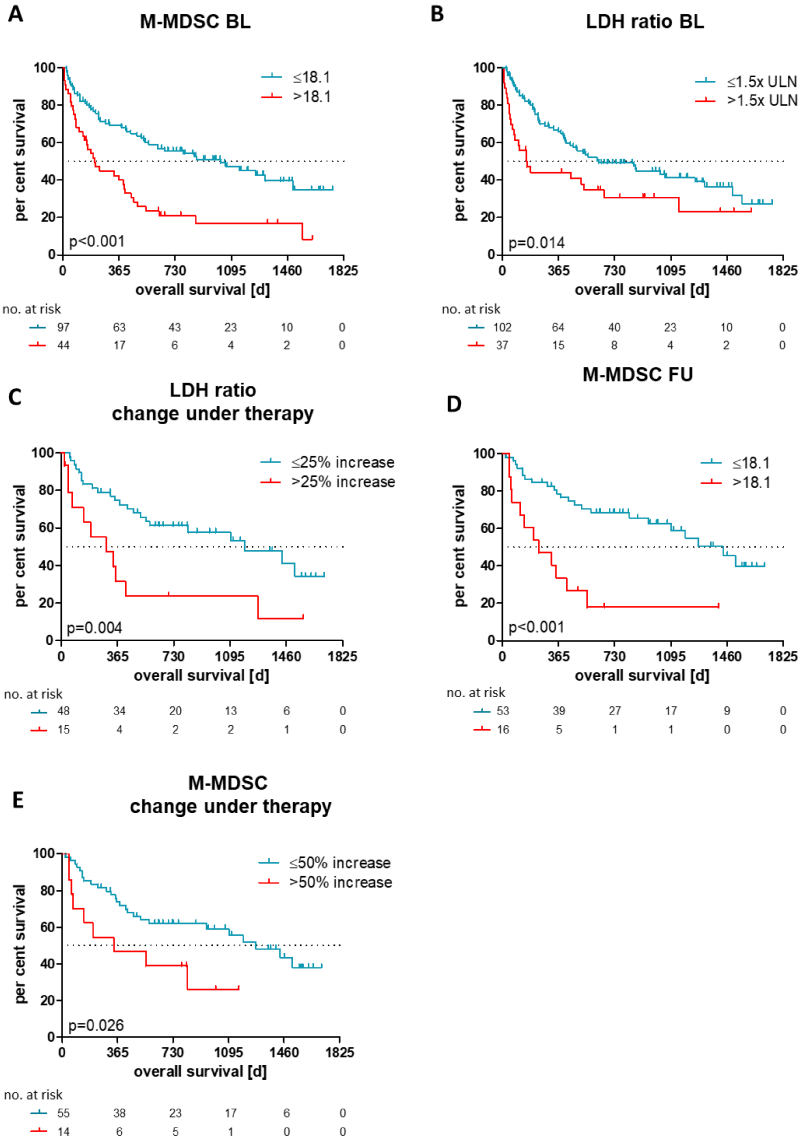

Supplementary Figure 12: Univariate analysis of the combined cohort (discovery + validation) at BL of M-MDSC frequency (A: p<0.001), LDH-ratio at BL (LDH serum level divided by the ULN (250 U/L)) (B: p=0.014) and a general increase >25% of the LDH-ratio under immune checkpoint blockade (C: p=0.004). M-MDSC frequencies at FU (D: p<0.001) and an increase of > 50% M-MDSC frequencies under immune checkpoint blockade (E: p=0.026).

BL = baseline, FU = follow up, LDH = lactate dehydrogenase, ULN= upper limit of normal

Supplementary Tables

Supplementary Table 1: Antibodies used in the myeloid cell and the T cell panel

panel	*marker*	*clone*	*fluorophore*	*vendor*	*cat*
myeloid cells	CD3	OKT3	BV605	Biolegend	317322
	CD19	HIB19	BV605	Biolegend	302244
	CD16	3G8	PacificBlue	Biolegend	302032
	CD11b	ICRF44	APC-fire	Biolegend	301352
	CD14	M5E2	PE-Cy7	Biolegend	301814
	CD33	P67.6	FITC	Biolegend	366620
	HLA-DR	L243	PerCP-Cy5.5	BD	339216
	CD56	HCD56	BV711	Biolegend	318336
	CD56	HCD56	BV605	Biolegend	318334
T cells	CD25	M-A251	PE	BD	555432
	CD127	AO19D5	BV510	Biolegend	351322
	CD8	SK1	APC-fire	Biolegend	344746
	CD8	SK1	APC-Cy7	Biolegend	344714
	CD3	UCHT1	A700	Biolegend	300424
	CD4	SK3	PerCP	BD	345770
	LAG-3	11C3C65	BV421	Biolegend	369314
	PD-1	EH12.2H7	BV711	Biolegend	329928
	TIM-3	7D3	BB515	BD	565568
	FoxP3	259DC7	A647	BD	560045
	Isotype	MOPC-21	BV421	Biolegend	400158
	Isotype	MOPC-22	BV711	Biolegend	400168
	Isotype	X40	BB515	BD	564416

Supplementary Table 2: Summary of Bonferroni corrected p-values from log rank testing of univariate overall survival correlations with blood counts.

			discovery cohort n=92		validation cohort n=49	
factor	**description**	**category**	**log rank p-value**	**Inter-pretation**	**log rank p-value**	**inter-pretation**
leukocytes [1000/µL]	median	≤ 7.05 vs > 7.05	0.867	failed		
	lower cutoff	< 6.11 vs ≥ 6.11	2.661	failed		
	upper cutoff	≤ 7.91 vs > 7.91	0.927	failed		
erythrocytes [1mio/µL]	Median	≤ 4.50 vs > 4.50	0.563	failed		
	lower cutoff	< 4.26 vs ≥ 4.26	0.135	failed		
	upper cutoff	≤ 4.75 vs > 4.75	2.145	failed		
thrombocytes [1000/µL]	Median	≤ 268.50 vs > 268.50	0.797	failed		
	lower cutoff	< 239.00 vs ≥ 239.00	1.926	failed		
	upper cutoff	≤ 296.00 vs > 296.00	2.787	failed		
abs. neutrophiles [1000/µL]	Median	≤ 4.66 vs > 4.66	2.268	failed		
	lower cutoff	< 4.20 vs ≥ 4.20	1.815	failed		
	upper cutoff	≤ 6.3 vs > 6.3	0.333	failed		
rel. neutros [%]	Median	≤ 70.30 vs > 70.30	2.827	failed		
	lower cutoff	< 66.00 vs ≥ 66.00	2.067	failed		
	upper cutoff	≤ 73.60 vs > 73.60	2.772	failed		
abs. eosinophile [1000/µL]	Median	≤ 0.10 vs > 1.10	2.710	failed		
	lower cutoff	< 0.11 vs ≥ 0.11	2.709	failed		
	upper cutoff	≤ 0.22 vs > 0.22	0.051	failed		
rel. eosinophile [%]	Median	≤ 1.50 vs > 1.50	1.469	failed		
	lower cutoff	< 1.40 vs ≥ 1.40	0.576	failed		
	upper cutoff	≤ 2.70 vs > 2.70	0.882	failed		
abs. basophile [1000/µL]	Median	≤ 0.04 vs > 0.04	2.290	failed		
	lower cutoff	< 0.04 vs ≥ 0.04	2.349	failed		
	upper cutoff	≤ 0.07 vs > 0.07	<0.001	candidate	0.627	failed
rel. basophile [%]	Median	≤ 0.50 vs > 0.50	1.805	failed		
	lower cutoff	< 0.50 vs ≥ 0.50	1.736	failed		
	upper cutoff	≤ 0.80 vs > 0.80	0.513	failed		
abs. monocytes [1000/µL]	Median	≤ 0.61 vs > 0.61	0.123	failed		
	lower cutoff	< 0.52 vs ≥ 0.52	0.549	failed		
	upper cutoff	≤ 0.76 vs > 0.76	0.051	failed		
rel. monocytes [%]	Median	≤ 8.55 vs > 8.55	1.724	failed		
	lower cutoff	< 8.00 vs ≥ 8.00	2.085	failed		
	upper cutoff	≤ 10.00 vs > 10.00	0.285	failed		
abs. lymphozyten [1000/µL]	Median	≤ 1.32 vs > 1.32	1.649	failed		
	lower cutoff	< 1.07 vs ≥ 1.07	1.095	failed		
	upper cutoff	≤ 1.69 vs > 1.69	2.190	failed		
rel. lymphozyten [%]	Median	≤ 18.05 vs > 18.05	1.555	failed		
	lower cutoff	< 15.40 vs ≥ 15.40	2.019	failed		
	upper cutoff	≤ 22.70 vs > 22.70	1.086	failed		
NLR	Median	≤ 3.80 vs > 3.80	1.119	failed		
	lower cutoff	< 3.20 vs ≥ 3.20	1.104	failed		
	upper cutoff	≤ 5.10 vs > 5.10	2.655	failed		

Supplementary Table 3: Summary of Bonferroni corrected p-values from log rank testing of univariate overall survival correlations with T cell populations assed by flow cytometry.

			discovery cohort n=92		validation cohort n=49	
factor	**description**	**category**	**log rank p-value**	**inter-pretation**	**log rank p-value**	**inter-pretation**
Lymphocytes	median	≤ 50.6 vs > 50.6	0.771	failed		
	lower cutoff	< 42.3 vs ≥ 42.3	2.661	failed		
	upper cutoff	≤ 53.4 vs > 53.4	2.286	failed		
CD3 [%Lymphocytes]	Median	≤ 68.5 vs > 68.5	2.260	failed		
	lower cutoff	< 61.2 vs ≥ 61.2	2.994	failed		
	upper cutoff	≤ 74.9 vs > 74.9	0.141	failed		
Tregs [%CD3]	median	≤ 3.6 vs > 3.6	0.491	failed		
	lower cutoff	< 3.1 vs ≥ 3.1	0.129	failed		
	upper cutoff	≤ 74.9 vs > 74.9	0.306	failed		
LAG3 [%Tregs]	median	≤ 1.4 vs > 1.4	2.438	failed		
	lower cutoff	< 1.2 vs ≥ 1.2	2.010	failed		
	upper cutoff	≤ 2 vs > 2	2.406	failed		
PD1 [%Tregs]	median	≤ 15.8 vs > 15.8	1.733	failed		
	lower cutoff	< 13.5 vs ≥ 13.5	2.091	failed		
	upper cutoff	≤ 17.9 vs > 17.9	1.308	failed		
TIM3 [%Tregs]	median	≤ 10.9 vs > 10.9	2.852	failed		
	lower cutoff	< 9 vs ≥ 9	1.371	failed		
	upper cutoff	≤ 13.4 vs > 13.4	0.396	failed		
CD4 without Tregs [%CD3]	median	≤ 61 vs > 61	1.785	failed		
	lower cutoff	< 54.1 vs ≥ 54.1	1.677	failed		
	upper cutoff	≤ 66.5 vs > 66.5	2.595	failed		
LAG3 [%CD4 without Tregs]	median	≤0.3 vs > 0.3	2.669	failed		
	lower cutoff	< 0.4 vs ≥ 0.4	2.670	failed		
	upper cutoff	≤ 0.9 vs > 0.9	0.231	failed		
PD1[%CD4 without Tregs]	median	≤ 11.1 vs > 11.1	1.516	failed		
	lower cutoff	< 8.6 vs ≥ 8.6	0.903	failed		
	upper cutoff	≤ 14.7 vs > 14.7	2.637	failed		
TIM3[%CD4 without Tregs]	median	≤ 5.7 vs > 5.7	0.763	failed		
	lower cutoff	< 4.6 vs ≥ 4.6	2.820	failed		
	upper cutoff	≤ 7.8 vs > 7.8	2.307	failed		
CD8 [%CD3]	median	≤ 20.0 vs > 20.0	2.806	failed		
	lower cutoff	< 16.9 vs ≥ 16.9	2.013	failed		
	upper cutoff	≤ 25.2 vs > 25.2	2.454	failed		
CD25 [%CD8]	median	≤ 7.0 vs > 7.0	2.955	failed		
	lower cutoff	< 5.6 vs ≥ 5.6	2.451	failed		
	upper cutoff	≤ 12.9 vs > 12.9	1.974	failed		
LAG3 [%CD8]	median	≤ 0.5 vs > 0.5	2.108	failed		
	lower cutoff	< 0.9 vs ≥ 0.9	0.561	failed		
	upper cutoff	≤ 1.7 vs > 1.7	1.545	failed		
PD1 [%CD8]	median	≤ 18.1 vs > 18.1	1.721	failed		
	lower cutoff	< 13.9 vs ≥ 13.9	2.898	failed		
	upper cutoff	≤ 25.9 vs > 25.9	0.657	failed		
TIM3 [%CD8]	median	≤ 14.8 vs > 14.8	0.869	failed		
	lower cutoff	< 11.9 vs ≥ 11.9	1.263	failed		
	upper cutoff	≤ 21.0 vs > 21.0	2.154	failed		

Supplementary Table 4: Summary of Bonferroni corrected p-values from log rank testing of univariate overall survival correlations with myeloid cell populations assed by flow cytometry.

			discovery cohort n=92		validation cohort n=49	
factor	**description**	**category**	**log rank p-value**	**inter-pretation**	**log rank p-value**	**inter-pretation**
M-MDSC	median	≤ 13.8 vs > 13.8	2.179	failed		
	lower cutoff	< 10.8 vs ≥ 10.8	1.211	failed		
	upper cutoff	**≤ 18.1 vs > 18.1**	**0.030**	**candidate**	**<0.001**	**confirmed**
classical monocytes	median	≤ 8.7 vs > 8.7	1.264	failed		
	lower cutoff	< 6.6 vs ≥ 6.6	0.719	failed		
	upper cutoff	≤ 10.8 vs > 10.8	1.925	failed		
intermediate monocytes	median	≤ 1.2 vs > 1.2	2.031	failed		
	lower cutoff	< 1.4 vs ≥ 1.4	1.853	failed		
	upper cutoff	≤ 3.0 vs > 3.0	2.327	failed		
non-classical monocytes	median	≤ 0.2 vs > 0.2	2.081	failed		
	lower cutoff	< 0.2 vs ≥ 0.2	0.819	failed		
	upper cutoff	≤ 3.0 vs > 3.0	0.179	failed		

Supplementary Table 5: Summary of median frequencies, counts, interquartile range (IQR) of the investigated cell populations in patients in the M-MDSC-low versus M-MDSC-high group. P-values have been determined using Mann-Whitney U testing.

			M-MDSC low		M-MDSC high	
	cell population	p	median	IQR	median	IQR
serum blood parameters	leukocytes [1000/µL]	**0.015**	6.8	2.7	8.2	4.0
	erythrocytes[1mio/µL]	0.817	4.5	0.7	4.5	0.8
	thrombocytes [1000/µL]	0.161	252	85.3	280.5	79.8
	abs. neutrophils [1000/µL]	**0.001**	4.4	2.5	6.0	3
	rel. neutrophils [%]	**<0.001**	66	12.3	75	9.5
	abs. eosinophils [1000/µL]	**0.044**	0.1	0.1	0.1	0.1
	rel. eosinophils [%]	**0.005**	1.9	1.7	1	1.4
	abs. basophils [1000/µL]	0.973	<0.1	<0.1	<0.1	0.1
	rel. basophils [%]	0.127	0.6	0.4	0.4	0.4
	abs. monocytes [1000/µL]	**0.001**	0.6	0.3	0.7	0.3
	rel. monocytes [%]	0.131	8.5	2.6	9	2.6
	abs. lymphocytes [1000/µL]	**<0.001**	1.5	0.8	1.0	0.7
	rel. lymphocytes [%]	**<0.001**	21.8	11.1	14.4	6.5
	NLR	**<0.001**	3.0	2.2	5.1	4.1
flow cytometry	lymphocytes	**<0.001**	51.4	17.5	32.6	13.5
	CD3+ [lymphocytes]	**0.015**	72	10.6	68.0	18.4
	Tregs [CD3]	0.378	3.8	1.7	4.0	1.9
	LAG-3+Tregs	0.981	1.1	1.3	1.2	1.3
	PD-1+Tregs	**0.025**	12.5	9.7	14.1	7.1
	TIM-3+Tregs	0.761	8.5	7.5	8.7	6.7
	CD4+ [CD3]	0.338	61	17.6	60.2	21
	LAG-3+CD4	0.554	0.3	0.3	0.3	0.4
	PD-1+CD4	0.131	10.2	8.7	10.5	9.4
	TIM-3+CD4	0.988	4.5	4.0	5.0	4.7
	CD8+ [CD3]	0.759	21.5	14.4	20.6	19.1
	CD25+CD8	0.655	7.5	13.2	6.3	7.7
	LAG-3+CD8	0.511	0.5	1.2	0.75	1.4
	PD-1+CD8	0.146	15.4	12.5	18.3	20.2
	TIM-3+CD8	0.251	10.9	12.0	11.5	15.4
	classical monocytes [viable PBMCs]	0.101	8.7	5.8	10.0	6.8
	intermediate monocytes [viable PBMC]	**0.031**	1.1	1.4	1.4	2.1
	non-classical monocytes [viable PBMC]	0.389	0.2	0.2	0.1	0.2